MODULATION OF SONIC HEDGEHOG SIGNALING ALTERS CEREBELLAR DEVELOPMENT AND MEDULLOBLASTOMA FORMATION

By

Frances Yun Cheng

Dissertation

Submitted to the Faculty of the

Graduate School of Vanderbilt University

in partial fulfillment of the requirements

for the degree of

DOCTOR OF PHILOSOPHY

in

Cellular and Developmental Biology

December 2013

Nashville, Tennessee

Committee Members:

Professor Chin Chiang

Professor Christopher V.E. Wright

Professor Bruce D. Carter

Professor Robert J. Coffey

Professor Ethan Lee

To my parents and sister

To my husband and baby boy

ACKNOWLEDGEMENTS

The work presented here was made possible by Public Health Service award T32 GM07347 from the National Institute of General Medical Studies for the Vanderbilt Medical-Scientist Training Program (MSTP), and the National Institute Of Neurological Disorders And Stroke of the National Institutes of Health under Award Number F31NS074638.

I would like to thank my advisor, Dr. Chin Chiang, who has always challenged, focused, and supported me. His scientific perception, intuitive curiosity, and preciseness have had a huge impact on my scientific training, and I will always feel grateful.

I would like to thank other faculty members who aided in my scientific growth while at Vanderbilt University, particularly my committee chair, Dr. Chris Wright, who has shown incredible support and care for my scientific training, and my committee members: Dr. Robert Coffey, Dr. Bruce Carter and Dr. Ethan Lee. They have all continually provided guidance and encouragement for my research progress and career development.

The Vanderbilt MSTP program has been a steady and consistent source of support and the strongest advocates for my success. I am thankful to Dr. Terry Dermody for initially recruiting me into the program and for continual inspiration, as well as Dr. Michelle Grundy, Dr. Jim Bills, Dr. Larry Swift and Melissa Krasnove for their continual support. Thanks also to my MSTP mentor Dr. Pampee Young, who has been supportive and provided me with personal and professional advice. The Vanderbilt Cell and Developmental Biology department has been instrumental to my success in graduate school and I'd like to thank the following members for their help: Elaine Caine, Kim Kane, Dr. Anthony Tharp, Mark Wozniak, Ian McCullough.

Current and former members of the Chiang lab have been invaluable as friends and colleagues, both in the lab and outside of it. Dr. Ying Litingtung has been full of

scientific knowledge, ideas, and encouragement. My thanks particularly go out to Jonathan Fleming, Kaitlyn Ryan, and Xi Huang (former member) for their support and discussions on a daily basis both scientifically and personally, and who taught me many of the things I know. This work would not be possible without them. I thank Jiang Liu, Tatiana Ketova, and Annabelle Williams who were great colleagues. I thank former mentors, Dr. Nenad Sestan, Dr. Mladen-Roko Rasin, and Dr. Vsevolod Gurevich who guided and supported me.

I am certain I have the best MSTP class, whom I consider my family here in Nashville, particularly Elizabeth, Eric, Tanner, John, Brian, Caroline, and Courtney. Additionally, my friends from around the world have been there for me in the best and worst of times and for their support and prayers I am eternally grateful: Emely, Victoria, Jenny, Amy, Crissaris, Vanessa, Anna, Karen, Nana, Lynne, Connie, and many more.

I have been blessed with the most wonderful family. My husband, Johnny Lu, has been by my side as a source of love and support from the moment I embarked on this journey. I couldn't have done any of this without him. Our greatest blessing, baby Thomas, has given me so much joy and happiness. My dad (Ying), mom (Shirley), sister (Diana) have always been an inspiration to me and my strongest supporters. I strive to be more like them each day. Above all, I am thankful to my God for filling me with strength, love, hope, and purpose (Isaiah 40:28-31).

TABLE OF CONTENTS

Page

ACKNOWLEDGEMENTS……iv

LIST OF TABLES……..…..vii

LIST OF FIGURES…… viii

CHAPTER

I. INTRODUCTION……..……...……... 1

Cerebellar structure…… 1
Embryonic and early postnatal cerebellar development……..…… 3
Sonic hedgehog signaling……..…… 12
Sonic hedgehog signaling in the cerebellum……..…. 15
Sonic hedgehog signaling and medulloblastoma…….. 17
Novel findings as elucidated by modulation of Shh signaling…..…. 23

II. WIDESPREAD CONTRIBUTION OF GDF7 LINEAGE TO CEREBELLAR CELL TYPES AND IMPLICATIONS FOR HEDGEHOG-DRIVEN MEDULLOBLASTOMA……...……... 26

Introduction……..……..…… 26
Results……..……..…… 29
Discussion……..……..…… 44
Materials and Methods……...…. 52
Acknowledgements……..…….. 54

III. GLIAL SONIC HEDGEHOG SIGNALING ACTIVITY IS REQUIRED FOR PROPER CORTICAL EXPANSION AND CEREBELLAR ARCHITECTURE…… 55

Introduction……..…… 55
Results……..……..…… 58
Discussion……..…… 88
Materials and Methods……..…. 94
Acknowledgements……..…….. 96

IV. ANTAGONISM OF THE HEDGEHOG PATHWAY AT THE LEVEL OF GLI TRANSCRIPTION BY SMALL MOLECULE 5-AMINOIMIDAZOLE-4-CARBOXAMIDE-1-ß-4-RIBOFURANOSIDE (AICAR)…… 98

Introduction……..…… 98
Results……..……..…… 101
Discussion……..……..…… 122
Materials and Methods……..... 127
Acknowledgements……..…….. 130

V. GENERAL DISCUSSION……..…….. 131

Summary……..…… 131
Implications……..…..…… 135
Future Directions……..…….…… 141

REFERENCES…….. 150

LIST OF TABLES

Table		Page
1.	Medulloblastoma subgroups……	20

LIST OF FIGURES

Figure.		Page
1.1	Cerebellar structure……..…….……..	3
1.2	Early cerebellar development……	7
1.3	Shh signaling pathway……..	12
2.1	Shh pathway activation in Gdf7-lineage cells leads to cerebellar hyperplasia……..	30
2.2	*Gdf7$^{Cre/}$;SmoM2* mice develop medulloblastoma with CGNP features……..	32
2.3	A subset of Gdf7-lineage cells express neural stem cell markers……..	34
2.4	Roof plate cells give rise to a distinct population of cerebellar vermal radial glia cells……	39
2.5	Gdf7-lineage cells in the cerebellar rhombic lip are Lmx1a+ neural progenitor cells that give rise to CGNPs……	42
2.6	Gdf7-lineage cells contribute to an extensive array of mature cerebellar cell types……..	44
2.7	*In situ* hybridization for *Gdf7* expression……	48
3.1	TNC-YFP-expressing cells are Bergmann glia. ……	61
3.2	*TNC$^{YFP-CreER}$;Smo$^{F/-}$* (Smo^{BG}) mutants display a hypoplastic cerebellum. ….	63
3.3	Mutant EGL is largely agranular due to severely reduced CGNP proliferation. ……	64
3.4	Loss of Shh signaling is profound in CGNPs despite normal PC Shh production…….	67
3.5	Resident astroglial cells in the EGL do not contribute significantly to the granular neuron population..……	72
3.6	Smo^{BG} mutants display altered BG arrangement and cytoarchitecture……..	78
3.7	Smo^{BG} mutants have disrupted alignment and dendritic arborization of PCs……	81
3.8	Smo^{BG} mutants exhibit aberrant Wnt signaling……..	86

4.1 AICAR antagonizes Hedgehog (Hh) pathway activity in fibroblasts and CGNPs…….. 103

4.2 AICAR inhibits CGNP proliferation and growth of primary medulloblastoma cells……... 107

4.3 AICAR downregulates Shh signaling independently of the GSK3ß, cholesterol, PKA, sirtuin, and mTOR pathways……. 111

4.4 AICAR downregulates Shh signaling independently of the AMPK pathway. 112

4.5 AICAR acts downstream of Smoothened to inhibit Shh pathway activity….. 115

4.6 AICAR regulates *Gli1* transcription…….. 117

4.7 AICAR acts on human medulloblastoma cells to alter cell fate…..……. 120

CHAPTER I

GENERAL INTRODUCTION

Development of the cerebellar cortex proceeds in a remarkably controlled fashion, with the intersection of complex signaling pathways governing the coordinated generation of its laminar structure. While it has long been appreciated that the role of the cerebellum is to control balance and sensorimotor coordination (Ito 2006; Roussel and Hatten 2011), as well as take part in the vestibular ocular reflex, recent studies have revealed an even wider range of cognitive actions, including sensory-motor learning, speech, and spatial memory (De Zeeuw and Yeo 2005; Schmahmann et al. 1999; Koziol et al. 2013). Despite its complex functions, the cerebellum's relatively simple architecture makes it an attractive model to study CNS development, neuronal connectivity, and disease. Sonic Hedgehog (Shh) signaling has been recognized as a critical regulator in many aspects of development including cerebellar morphogenesis. As a morphogen, it is secreted and can act over both short and long distances to affect the growth, proliferation, or differentiation of its receiving cell. The focus of my thesis work is to elucidate novel mechanisms of Shh signaling in embryonic and postnatal development of the cerebellum, as well as its implications for the cerebellar tumor medulloblastoma.

Cerebellar Structure

The mammalian cerebellum (Figure 1A) has a distinct, well-organized architecture. Through a series of dramatic cellular movements, the early cerebellar primordium is transformed from a smooth embryonic structure into one with complex lobules and folia by postnatal day 14 (P14) (Sudarov and Joyner 2007). On a gross anatomical level, the cerebellum is separated on the mediolateral axis into three broad

regions. The most medial region is called the vermis and is surrounded on either side by a hemisphere (Figure 1B). The anterior-posterior axis is divided into ten morphological folds known as lobules (Figure 1C). Each of the ten lobules is further divided into secondary and tertiary sublobules on the basis of species (Schmahmann et al. 1999; Larsell 1947). On a cellular level, the cerebellar cortex has three layers that surround an inner core of white matter and deep cerebellar nuclei (Sillitoe and Joyner 2007). The innermost layer is the internal granular layer (IGL), which largely consists of small granular neurons but also includes Golgi, Lugaro, and unipolar brush cells. The outermost layer is the molecular layer (ML), a mostly acellular layer consisting of granule cell axons (called parallel fibers), climbing fiber terminals, Purkinje cell (PC) dendrites, and stellate and basket cells. Between these two layers is the Purkinje cell monolayer (PCL), which consists of Purkinje cells and specialized glial cells called Bergmann glia (BG), which are sandwiched between the PCs. In much lower numbers, candelabrum cells are also present in the PCL (Figure 1C).

Ramon j Cajal, working over a century ago, elucidated the basic circuitry of the cerebellum (Cajal 1911). The central cell type around which other cerebellar synapses are organized is the PC. Excitatory inputs to PCs are derived from two sources—the first are climbing fibers, which are axonal projections from brainstem neurons. In addition, PCs receive excitatory input from granule cells that are transmitting input from mossy fibers originating in over two-dozen brainstem and spinal cord nuclei (Fu et al. 2011). Modulation of granule neuronal input to PCs is mediated by inhibitory signals from stellate and basket cells (Konnerth, Llano, and Armstrong 1990). PCs integrate the excitatory and inhibitory inputs to control the output of cerebellar and vestibular nuclei neurons. Thus, PCs can sensitively respond to incoming signals that can then be communicated to the brain and spinal cord.

Figure 1.1

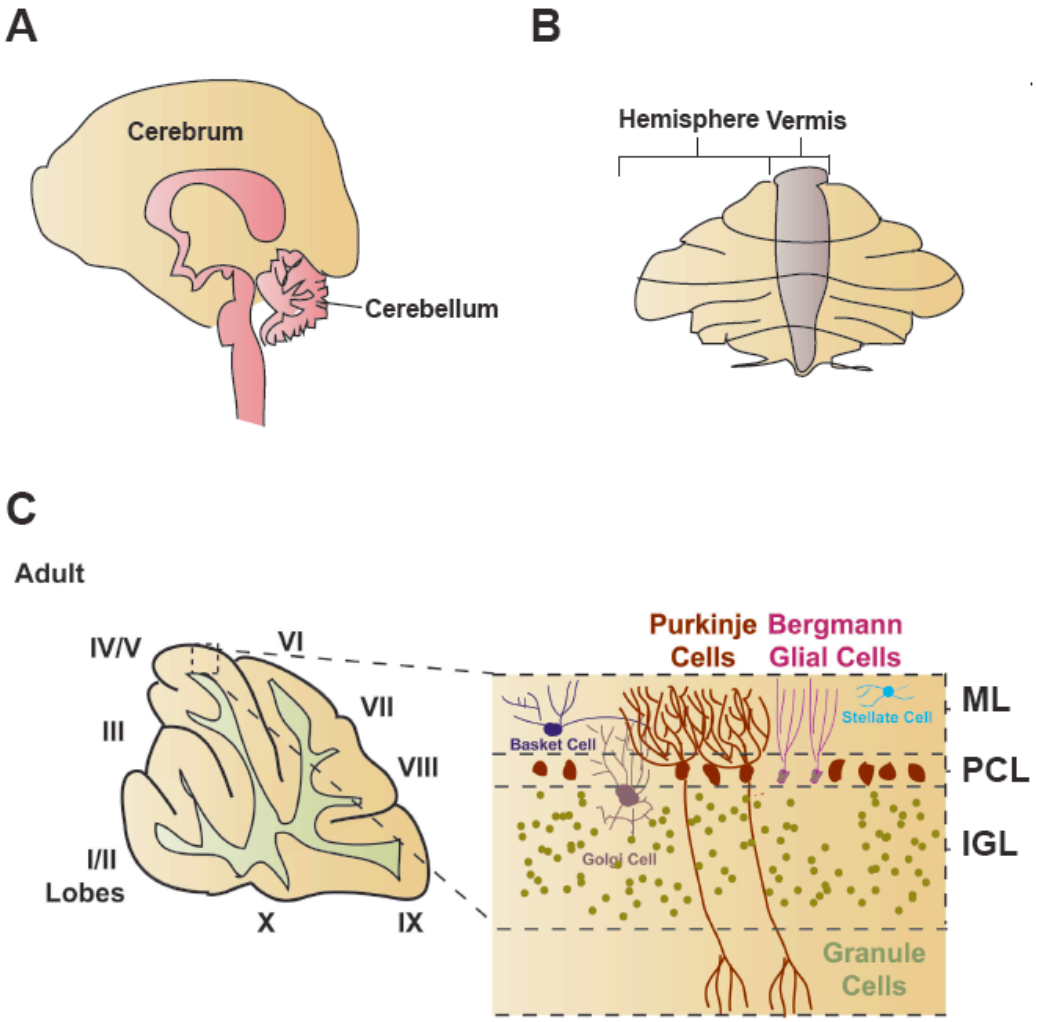

Figure 1.1. Cerebellar structure.

Embryonic and Early Postnatal Cerebellar Development

The early cerebellar anlage arises in the mouse around embryonic day 8.5 (E8.5) to E9.5 from a region that initially encompasses the boundary between the

mesencephalon and metencephalon of the neural tube (Wingate and Hatten 1999; Hallonet, Teillet, and Le Douarin 1990; Millet et al. 1996). An isthmus separating these two embryonic vesicles acts as an inductive signaling center responsible for regulating both cerebellum and midbrain development (Lumsden and Krumlauf 1996) (Figure 2A). Fate mapping studies established that the anterior boundary of the cerebellar anlage is delineated by Otx2 (Millet et al. 1996) and posterior boundary marked by Gbx2 (Millet et al. 1996). In the later embryo, this domain, which comprises the most anterior aspect of the hindbrain, resolves to a single defined neuromere designated as rhombomere (r) 1 (Zervas et al. 2004).

Around E10.5, a specialized group of cells, known as the roof plate, acts as an additional signaling center to regulate cellular positioning and proliferation of the entire cerebellar anlage (Chizhikov et al. 2006). The roof plate domain differentiates shortly after neural tube closure to form a distinct narrow strip of cells along the dorsal midline and is molecularly defined as the *Lmx1a*+/*Gdf7*+ dorsal domain throughout the anterior-posterior extent of r1 (Chizhikov et al. 2006) (Figure 2B). Roof plate-derived inductive signals, such as Bmp6, Bmp7, Gdf7 (Bmp12), and Wnt1 (Chizhikov and Millen 2004; K. Lee, Dietrich, and Jessell 2000; K. J. Lee, Mendelsohn, and Jessell 1998), are important for directing differentiation of dorsal neuronal cell types (Chizhikov and Millen 2004; Lee, Dietrich, and Jessell 2000; Lee, Mendelsohn, and Jessell 1998; Chizhikov et al. 2006). In the spinal cord and telencephalon, roof plate cells not only regulate development of neighboring tissues through the secretion of growth factors, but also have the capacity to generate different cell types. However, previous fate-mapping studies have indicated that the hindbrain roof plate is uniquely restricted in lineage potential and its contributions are mostly limited to non-neural hindbrain choroid plexus epithelial (hChPe) cells (Chizhikov et al. 2006; Currle et al. 2005; Hunter and Dymecki 2007; Landsberg et al. 2005; Chizhikov et al. 2010). *Hence, the capacity for hindbrain roof plate cells to*

contribute to specific cell types in the cerebellum has not been shown. In Chapter II of this work, we demonstrate that hindbrain roof plate cells can contribute to diverse cell types in the cerebellum.

Secreted Wnt and Fgf family members, including Wnt1, Fgf8, and Fgf15, control expression of transcription factors delineating r1 as well as of genes required to establish cerebellar territory (Roussel and Hatten 2011; McMahon and Bradley 1990; Chi 2003; Crossley, Martinez, and Martin 1996; Martinez et al. 1999; Joyner, Liu, and Millet 2000), homeobox genes En1 and Pax2/5/8 (Joyner 1996; Joyner, Skarnes, and Rossant 1989). Between embryonic day 9 (E9) in the mouse and E12, a 90-degree rotation converts the anterior-posterior axis of the dorsal neural tube to the medial-lateral axis of the cerebellar priomordium, which takes on the characteristic bilateral, wing-like morphology of the cerebellum that persists into adulthood (Sillitoe and Joyner 2007; Sgaier et al. 2005).

During cerebellar histogenesis, carefully orchestrated cellular movements and complex neurogenesis generate the cortical structure and cerebellar nuclei (Hatten and Heintz 1995; Morales and Hatten 2006). All cerebellar neurons originate from multipotent radial glial progenitor cells situated in one of two germinal zones (Anthony et al. 2004; Mori et al. 2006). First, the dorsomedial ventricular zone (VZ) along the fourth ventricle gives rise to inhibitory GABAergic neurons which include Purkinje cells (PC), the principal output neuron of the cerebellar cortex, as well as cerebellar interneurons including Golgi, stellate, and basket cells and neurons of the cerebellar nuclei (Dino et al. 2000; Laine and Axelrad 2002). Second, a germinal zone forms along the anterior region of the rhombic lip, which is located at the interface between the dorsal neural tube and the widened portion of the fourth ventricle roof plate in the most posterior region of r1 (Wingate 2001). The rhombic lip is responsible for the generation of excitatory glutamatergic neurons called cerebellar granular neurons, the most abundant neuron in

the brain, and a subpopulation of neurons of the cerebellar and precerebellar nuclei (Dymecki and Tomasiewicz 1998; Machold and Fishell 2005; Wingate and Hatten 1999; Wingate 2001) (Figure 2C).

Proliferation of VZ progenitor cells requires expression of Shh, which, although not endogenous to the cerebellum prior to E16 in the mouse, is delivered to the cerebellum by the cerebrospinal fluid of the fourth ventricle (Huang, Liu, et al. 2010). Studies have revealed that neurons of the cerebellar VZ are generated in three sequential but overlapping waves (Morales and Hatten 2006). Around E10.25, the earliest cerebellar progenitors exit the cell cycle to generate neurons of the deep cerebellar nuclei (Morales and Hatten 2006). By E11, these progenitors migrate radially along a nascent glial fiber system to form a superficial zone across the dorsal surface of the cerebellar anlage. They eventually settle in the white matter beneath internal granular neurons (Morales and Hatten 2006). Between E11 and E14, precursors of the Purkinje neuron, identified by the LIM transcription factors LHX1 and LHX5 (Morales and Hatten 2006), become postmitotic and migrate from the VZ along radial glial fibers to form symmetrical clusters (Morales and Hatten 2006; Oberdick et al. 1993; Miyata et al. 2010). These clusters are multilayered and are situated between migrating cerebellar nuclei cells; they can be detected by gene expression starting at E14 in mice. Last, a third population of neurons, which include GABAergic interneurons of the DCN, stellate, basket, Lugaro, and Golgi cells, is generated during late embryonic development (starting at E14.5) and into early postnatal stages (Roussel and Hatten 2011).

Figure 1.2.

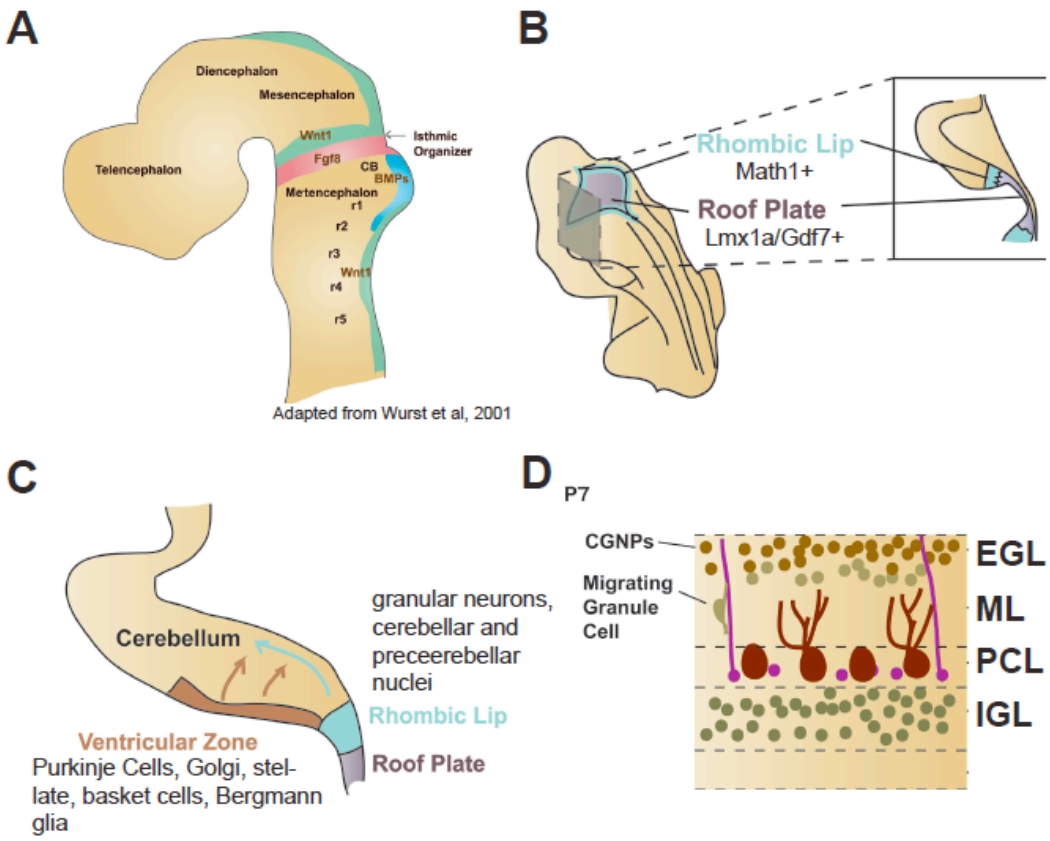

Figure 1.2. Early cerebellar development.

The second germinal zone of cerebellar progenitors appears by E12.5 in the mouse along the anterior rhombic lip. Studies have shown that specification of the cerebellar rhombic lip and its derivative fates is entirely dependent on the r1 roof plate (Machold and Fishell 2005; Wang and Zoghbi 2001). Previous genetic analyses of the cerebellar rhombic lip have suggested that the basic helix-loop-helix transcription factor Mouse atonal homolog 1 (Math1) molecularly defines this region (Machold and Fishell 2005; Wang and Zoghbi 2001). However, more recent investigation has shown the rhombic lip to be molecularly heterogeneous with Lmx1a expression representing at least one Math1-independent rhombic lip gene (Chizhikov et al. 2010). *Thus, the extent and contribution of Math1-negative cell types residing in the rhombic lip has yet to be elucidated. Our studies as detailed in Chapter II show that roof plate-lineage cells in the rhombic lip are Math1-negative neural progenitor cells. These findings support studies suggesting molecular heterogeneity within rhombic lip progenitors* (Chizhikov et al. 2010) *rather than the classical definition of the rhombic lip as a homogenous Math1+ progenitor population* (Rob Machold and Fishell 2005; V. Wang, Rose, and Zoghbi 2005).

Around E14.5 in the mouse, the vast majority of rhombic lip derivatives begin to migrate outwards onto the dorsal surface and spread across the cerebellar anlage to form the external granular layer (EGL). The EGL consists of proliferative cerebellar granular cell precursors (CGNPs) that generate the granular neuron, a cell type that constitutes nearly half of all neurons in the human brain (45 billion granular neurons out of 110 billion neurons) (Figure 2D). As CGNPs begin migrating out of the rhombic lip, Math1-positive postmitotic cerebellar nuclei precursors migrate towards the rostral aspect of the cerebellar anlage. This migration continues until E15.5, and cerebellar

nuclei progenitors occupy a position beneath the emerging zone of the PC precursors to form the DCN (Morales and Hatten 2006; V. Wang, Rose, and Zoghbi 2005). Last, the anterior rhombic lip also generates neuronal precursors of the lateral pontine nucleus, cochlear nucleus, and hindbrain nuclei of the “cerebellar system”.

In mice, the EGL forms by E15 and CGNPs within the EGL continue to proliferate until two weeks after birth (Sillitoe and Joyner 2007). CGNPs reach their peak of proliferation between postnatal day 6 (P6) and P8. At approximately P0, some CGNPs begin to exit the cell cycle and differentiate into mature GCs as they simultaneously extend axons and begin tangential migration within the deep layer of the EGL. As CGNPs exit the cell cycle, they down regulate expression of Math1 and upregulate expression of NeuroD1 (J. K. Lee et al. 2000), Zic1,3 (Aruga et al. 1996; Aruga 2004), and the tumor suppressor cyclin-dependent kinase inhibitory protein p27Kip1 . As they migrate into deeper layers of the EGL, their extending axons express the GPI-linked axonal glycoprotein TAG1. TAG1 expression peaks during the first 3 days after CGNPs exit the cell cyle and decrease dramatically as their parallel fibers form synapses with PC dendrites. CGNPs then migrate radially along Bergmann glial fibers (Rakic 1971) into the developing cerebellar cortex past the developing PCs to occupy their final position in the internal granular layer (Wang and Zoghbi 2001). Their migration and maturation are complete by P20, several days after the disappearance of the EGL.

Many developmental signal transduction pathways important in the regulation of CGNP proliferation and differentiation have been identified. The Shh pathway, has been discovered as the master player triggering expansion of the pool of CGNPs. Shh ligand is secreted from Purkinje cells to signal to the EGL (Hynes et al. 1995; Vogel, Sunter, and Herrup 1989), and regulates CGNP proliferation through several mechanisms. First, Shh regulates expression of cell cycle regulators cyclin D1, cyclin D2, and cyclin E. Mice lacking cyclin D1 have slowed proliferation of CGNPs and impaired cerebellar growth

(Kenney and Rowitch 2000). Second, Shh activity upregulates expression of the protooncogene N-myc that when overexpressed, promotes cell autonomous upregulation of cyclin D1 mRNA and protein independently of Shh signaling (Kenney and Rowitch 2000). This mechanism involves other members of the Myc/Max/Mad family of basic helix–loop–helix leucine zipper (bHLHZ) DNA binding proteins, such as Mad3 protein which has been shown to play a crucial role in CGNP proliferation (Yun et al. 2007). Other targets of Shh mitogenic signaling in CGNPs include YAP1 (Fernandez et al. 2010), the microRNA miR17/92, and members of the insulin signaling pathway such as IRS1 (Parathath et al. 2008).

N-myc is required for rapid expansion of CGNPs and inhibition of neuronal differentiation. Mice lacking N-myc in neural precursor populations have increased expression of cyclin-dependent kinase inhibitory proteins p27kip1 and p18Ink4c in the cerebellum (Knoepfler, Cheng, and Eisenman 2002) whereas engineered disruption of these inhibitory proteins in N-myc-null cerebella partially rescues the defects in CGNP proliferation and cerebellar foliation (Zindy et al. 2006). In addition, a synergistic effect of the Shh pathway and the phosphoinositide-3-kinase (PI3K) pathway on CGNP proliferation has been described, converging on N-myc. While Shh signaling drives expression of N-myc mRNA, the PI3K pathway stabilizes N-myc protein by inhibiting GSK3-dependent phosphorylation and degradation of N-myc. The PI3K agonist, insulin-like growth factor, mimics the effects of PI3K activity (Kenney, Widlund, and Rowitch 2004). Negative regulators of CGNP proliferation, ones that promote cell cycle exit and differentiation, include FGF (Fogarty et al. 2007) and BMP family members (Roussel and Hatten 2011; Rios et al. 2004; Zhao et al. 2008). Bmp2 and Bmp4 are expressed in postmitotic, differentiating CGNPs in the EGL and can inhibit Shh-induced CGNP proliferation in vitro via the Smad signaling pathway (Rios et al. 2004; Zhao et al. 2008). Bmp4 acts by inducing rapid posttranscriptional turnover of Math1 (Zhao et al. 2008).

Although radial glia play integral roles in the development of the cerebellar neurogenesis and circuitry, relatively little attention has been given to the function of neuron-glial interactions. At the time of PC specification around E11 in the mouse, cerebellar radial glia project smooth fibers from the VZ to the pia mater where endfeet are formed (Kettenmann and Verkhratsky 2011). As PCs migrate through the cerebellar anlage, radial glial soma migrate in a synchronous fashion behind PC soma. At this stage, the developing Bergmann glia retain a descending process through the granular layer which can reach as far as the white matter (Sommer, Lagenaur, and Schachner 1981). While postmitotic GCs migrate from the EGL to the IGL along radial Bergmann glial fibers, the PC dendritic tree elaborates in the opposite direction (Yamada et al. 2000; Lordkipanidze and Dunaevsky 2005). As synapses form in the molecular layer, the Bergmann glial fibers begin to transform from the rod-like process to elaborate, leaf-like projections which ensheath newly developing synapses on PC dendrites (Yamada et al. 2000). From P1 to P21, Bergmann glia proliferate in the PCL to attain a final ratio of 8:1 Bergmann glia to PCs (Shiga, Ichikawa, and Hirata 1983; Reichenbach et al. 1995). The cellular maturation of BG, which involves process extension and transformation, is highly dependent on diffusible factors like neuregulin (Huang and Mei 2001) and neuronal cell surface contacts (Oomman et al. 2006; Hatten 1987). Activation of the Notch receptor on Bergmann glia by the Delta/Notch-like EGF-related receptor (DNER) ligand found on PC dendrites also appears to play a role in driving Bergmann glial cell maturation (Eiraku et al. 2005), as does caspase-3 (Oomman et al. 2006). By P21, neuronal migration, synaptogenesis, and differentiation of Bergmann glia into their characteristic adult form are complete (Bellamy 2006).

Mice with BG defects during development exhibit severe cerebellar abnormalities, including altered cerebellar layering, neuronal migration, synaptic connectivity, and a disrupted pial membrane (Belvindrah et al. 2006; Graus-Porta et al.

2001; Wang et al. 2011; Eiraku et al. 2005; Komine et al. 2007; Weller et al. 2006). However, whether BG interactions with CGNPs influence CGNP proliferation has not yet been determined. In addition, genetic studies of BG function utilize either the human GFAP-Cre, Nestin-Cre, or Engrailed1-Cre lines (Corrales et al. 2004; Yu et al. 2011), which also induce widespread recombination in neuronal precursors (Zimmerman et al. 1994; Graus-Porta et al. 2001). *Thus investigations of the postnatal function of BG without affecting the vast majority of the neuronal population have not yet been performed. In Chapter III, we describe experiments in which we spatially and temporally alter Shh signaling activity specifically in postnatal BG and uncover a novel role for the BG-CGNP interaction in promoting CGNP precursor proliferation.*

Shh Signaling

Shh is a member of the Hedgehog (Hh) family of secreted signaling proteins. It has diverse functions in vertebrates, playing an essential role in the development of many organs including the brain, bone, skin, GI tract, gonads, and lungs (Ruiz i Altaba 1998; di Magliano and Hebrok 2003). Humans or mice lacking Shh develop holoprosencephaly and cyclopia due to failure of the forebrain lobes to separate (Roessler et al. 1996; S. A. Brown et al. 1998; Chiang et al. 1996), highlighting the requirement of proper Shh signaling for the development of the neural tube.

Shh ligand is released from secreting cells following cholesterol and palmitate modifications, which are essential for the proper activity and distribution of the ligand (Zeng, Jia, and Liu 2010; Ryan and Chiang 2012). The Shh receptor, Patched1 (Ptc), is a 12-pass transmembrane protein with homology to the RND family of bacterial transporter proteins. In the absence of Shh ligand (Figure 3A), Ptc localizes to the primary cilium and inhibits the Shh signal transducer, seven-pass transmembrane protein Smoothened (Smo). Smo is maintained in an inactive conformation such that it

cannot enter the cilium (Rohatgi and Scott 2007). Although the mechanism of Ptc inhibition of Smo remains elusive, it is speculated that Ptc may regulate molecules that activate or inhibit Smo, a theory that is supported by the susceptibility of Smo to modulation by small molecules such as the steroidal alkaloid cyclopamine (Cooper et al. 2003; Taipale et al. 2002; Chen 2002) and the fact that Ptc bears sequence similarities to the RND family of bacterial transporter proteins (Cooper et al. 2003; Taipale et al. 2002; Chen 2002).

The zinc finger-containing Gli family of transcription factors, which are the principal effectors of Shh signaling, are proteolytically processed from their full-length form (Gli-FL) into a truncated, N-terminal transcriptional repressor form (Gli-R). Vertebrates possess three Gli family members, Gli1-3. Gli2 and Gli3 can function as both transcriptional activators and repressors, whereas Gli1 exists only as an activator. Several proteins are necessary for efficient processing of Gli-FL into Gli-R forms. At the base of the primary cilium, protein kinase A (PKA) and Kif7 promote proteolytic processing of Gli3-FL into Gli3-R, and PKA also prohibits accumulation of Gli2-FL in the cilium. Suppressor of Fused (Sufu) stabilizes Gli2-FL and Gli3-FL and sequesters the proteins in the cytosol to prevent their nuclear translocation and activation (Wilson and Chuang 2010; Humke et al. 2010; Tukachinsky, Lopez, and Salic 2010; C. Wang, Pan, and Wang 2010). Sufu also promotes phosphorylation of Gli-FL by PKA, thus priming Gli-FL for further phosphorylation by GSK3β and CK1α. Phosphorylated Gli-FL is then ubiquitylated at the C-terminus by the E3 ubiquitin ligase β-TrCP and subsequently degraded to generate Gli-R. Although both Gli2 and Gli3 undergo proteolytic processing to repressor forms, degradation of Gli3 is more efficient than that of Gli2 (Pan et al. 2006), thus Gli3-R serves as the main transcriptional repressor of Hh signaling whereas Gli2 functions as the principal activator when Hh ligand is present (Hui et al. 1994). Thus the Shh pathway is silenced in the absence of ligand.

Figure 1.3.

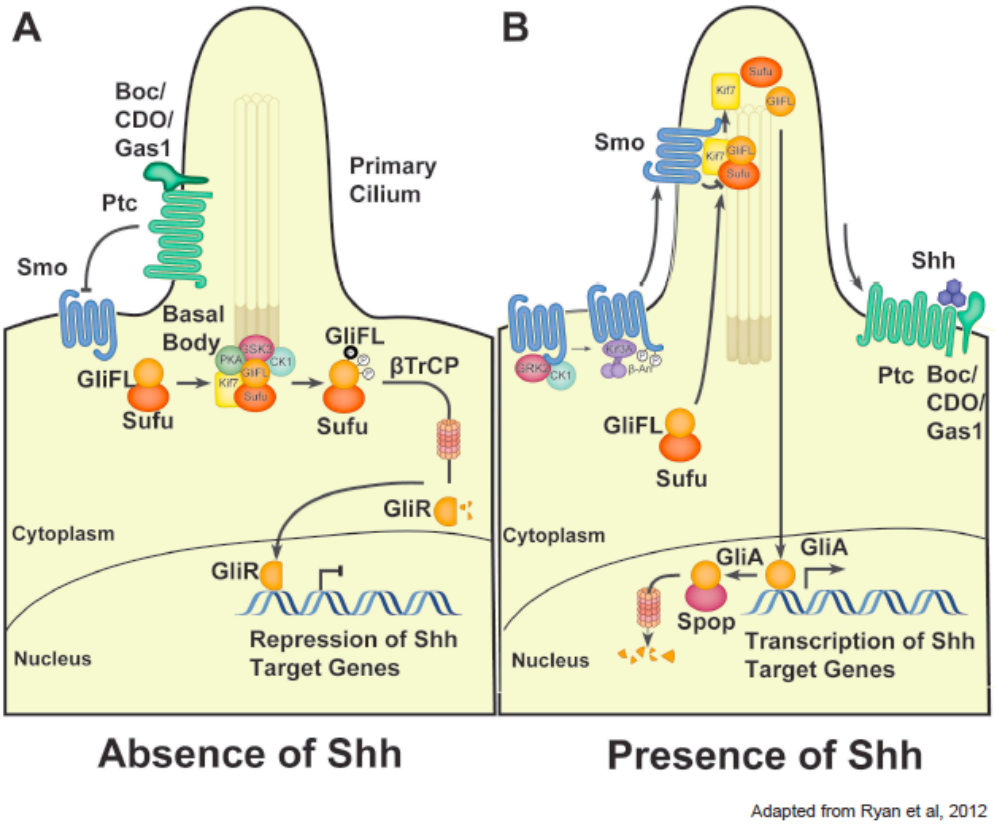

Adapted from Ryan et al, 2012

Figure 1.3. Shh signaling pathway.

In the presence of Shh ligand (Figure 3B), Ptc inhibition of Smo is relieved, allowing for activation of Smo. Ptc reception of Shh is enhanced by co-receptors Cdo, Boc, and Gas1 (Allen et al. 2011; Izzi et al. 2011; Beachy et al. 2010) which, if removed, result in a tissue-specific decrease in Shh pathway activity (Allen et al. 2011; Beachy et al. 2010; Izzi et al. 2011). Smo activation involves phosphorylation of its C-terminus by CKα1 and GRK2, which induces conformational changes, recruitment of β-arrestin and the kinesin-2 motor subunit Kif3a, and its subsequent translocation into the primary cilium (Ryan and Chiang 2012; Chen et al. 2011; Chen 2004; Kovacs et al. 2008). Smo accumulates in the ciliary membrane through both lateral transport and secretory pathways (Nozawa, Lin, and Chuang 2013). Smo then is able to inhibit Gli-FL processing into repressor forms, likely by promoting the disassembly of Sufu-Gli complexes that accumulate in the tip of the cilium following pathway activation (Humke et al. 2010; Wang, Pan, and Wang 2010; Tukachinsky, Lopez, and Salic 2010; Zeng, Jia, and Liu 2010). Accumulation of Gli2/3 at the ciliary tip is associated with production of Gli activators. The Gli activators then translocate to the nucleus enabling activation of Hh target genes including Gli1, negative Hh pathway regulators Ptc and Hhip1, and other, cell-type specific genes involved in proliferation, differentiation, and cell-survival.

Shh Signaling in the Cerebellum

Shh is indispensable for proper early neural tube formation, and subsequently functions in various ways to direct formation of CNS regions including the cerebellum (Dahmane and Ruiz i Altaba 1999; Wallace 1999; Wechsler-Reya and Scott 1999), neocortex, tectum (Dahmane et al. 2001), hippocampus (Dahmane et al. 2001; Lai et al. 2002; Robert Machold et al. 2003), and other areas including the amygdala and septum (Dahmane and Ruiz i Altaba 1999; Lai et al. 2002).

In the cerebellum, Shh plays several important roles. First, it is now well-established that Shh is produced by PCs and regulates CGNP proliferation. Shh signaling inhibition *in vivo* results in a marked decrease of proliferation in the EGL (Dahmane and Altaba 1999; Wallace 1999; Wechsler-Reya and Scott 1999). In fact, a widely used assay for studying the proliferation of CGNPs involves their isolation and purification from postnatal cerebella. Addition of Shh induces their proliferation, thus allowing cell-cycle associated phenomena to be studied *in vitro* (Dahmane and Altaba 1999; Kenney and Rowitch 2000; Kenney, Cole, and Rowitch 2003; Wechsler-Reya and Scott 1999; Fernandez-L et al. 2009; Leung et al. 2004). Second, blocking Shh signaling *in vivo* leads to development of a hypoplastic cerebellum with abnormal foliation, a disorganized PCL, and impaired CGNP proliferation (Dahmane and Altaba 1999; Lewis et al. 2004). Subsequent experiments using conditional mutagenesis showed that a graded series of Shh signaling levels generated varying degrees of fissure formation in the cerebellum, showing a correlation between the levels of Shh signaling and the extent of cerebellar foliation (Corrales et al. 2006). Third, recent work in our laboratory has demonstrated its role in the expansion of VZ-derived GABAergic progenitors of the cerebellum (Huang, Liu, et al. 2010). Surprisingly, the source of Shh is not derived from the cerebellum but is rather delivered from the cerebrospinal fluid of the fourth ventricle (Huang, Liu, et al. 2010). Fourth, our laboratory has shown that PC-derived Shh signaling is required for proliferation of white matter progenitor cells and specification of late-born GABAergic interneurons and astrocytes (Fleming et al.) (submitted). Last, it has been observed that Shh signaling induces the glial differentiation of immature postnatal mouse astroglia *in vitro* (Dahmane and Altaba 1999). In addition, inhibition of Shh activity using 5E1 hybridoma cells injected into chick embryos at early stages resulted in massive perturbations of cerebellar development, including a concomitant reduction in BLBP+ BG (Dahmane and Altaba 1999), leading to the speculation that Shh

induces differentiation of Bergmann glia. However, these studies did not use *in vivo* glial specific reduction of Shh signaling (Dahmane and Altaba 1999) but rather ablated Shh signaling at an early embryonic stage when Shh also plays essential roles in development of the neural tube. *Thus the role of Shh signaling activity in BG in vivo and its consequences for cerebellar development are not well understood. In Chapter III, we provide genetic evidence that Shh signaling in Bergmann glia is required for proper CGNP proliferation and subsequent cortical expansion.*

All three Gli genes are expressed in the developing cerebellum in the PCL and EGL (Corrales et al. 2004) although levels of Gli3 are low. Shh acts at a distance from its source—it is produced in the PCL and it diffuses several cell layers away to regulate proliferation of cells in the EGL. Modulation of the mitogenic effect of Shh has been demonstrated by several interacting pathways, including FGF (Wechsler-Reya and Scott 1999) and IRS1. Shh is still expressed in the PCL of the adult brain well after the EGL disappears (Traiffort et al. 1999; Wallace 1999), although its function at that time is unknown. Notably, BG retain the ability to respond to PC-derived Shh into adulthood (Corrales et al. 2004; Corrales et al. 2006). It is possible that it plays a role related to survival and neurotrophic activities in other contexts (Thibert et al. 2003).

Shh Signaling and Medulloblastoma

Defects in Shh signaling have been linked to a wide variety of CNS disorders, including the malignancies medulloblastoma (Scales and de Sauvage 2009), glioblastoma (Dahmane et al. 2001; Bar et al. 2007; Clement et al. 2007; Ehtesham et al. 2007), and pituitary adenomas (Vila 2005; Vila 2004), as well as Parkinson's, Alzheimer's, depression, anxiety, traumatic and ischemic brain injury, and the demyelinating disorder multiple sclerosis (Traiffort, Angot, and Ruat 2010). Specifically in the cerebellum, mutations causing overactive Shh signaling occur in 25-30% of human

medulloblastomas (Gilbertson and Ellison 2008; Raffel 2000; Reifenberger et al. 1998), the most common malignant pediatric brain tumor. Activating mutations of the Shh pathway occurring in human medulloblastomas (Gilbertson and Ellison 2008; Reifenberger et al. 1998; Raffel 2000) was a phenomenon that was first identified in Gorlin's Syndrome patients (Gorlin 1987). These patients have loss-of-function mutations in the Shh inhibitory receptor complex PTC or SUFU (Raffel 2000; Gilbertson and Ellison 2008; Brugieres et al. 2012), predisposing them to develop medulloblastomas, basal cell carcinomas, and skeletal abnormalities. On the other hand, cerebellar hypoplasia has been linked to reductions in Shh delivery in the cerebellum (Roper et al. 2006; Tam 2013; Heine et al. 2010).

Medulloblastoma is the most common malignant pediatric brain tumor with about 1000 new cases every year worldwide and a mean age between 3 and 7 years (Northcott et al. 2012). It accounts for over 20% of all CNS tumors in children (Dhall 2009; Jozwiak, Grajkowska, and Wlodarski 2007). The current WHO classification recognizes four classes of medulloblastoma--classic MB, desmoplastic/nodular MB, MB with extensive nodularity, large cell MB, and anaplastic MB (Fuller 2008). The majority of medulloblastomas arise in the vermis of the cerebellum while some occupy the fourth ventricle and brainstem (Ellison et al. 2003; Gibson et al. 2010; Gilbertson and Ellison 2008).

Advances in genome analysis have very recently accelerated our understanding of the molecular basis of medulloblastoma. Transcriptional profiling of messenger mRNAs (Kool et al. 2012; Thompson et al. 2006; Kool et al. 2008) in human medulloblastoma have identified four molecularly distinct subgroups, each characterized by discrete clinical presentation, prognosis, demographics, expression profiling, and genomic abnormalities (Table 1). These subgroups are WNT, Sonic Hedgehog (SHH), Group 3, and Group 4 (Jones et al. 2012; Northcott et al. 2012; Pugh et al. 2012;

Robinson et al. 2012; Taylor et al. 2011). WNT-associated tumors, which occur in children, teenagers, and adults, are associated with disrupted WNT signaling genes including activating mutations in β-catenin and inactivating mutations in the negative regulator adenomatous polyposis coli (APC) gene (Hamilton et al. 1995). WNT MBs often have classic histology and have favorable outcomes compared to other subgroups of MB (Clifford et al. 2006; Ellison et al. 2003). SHH-associated MB can result from inactivating mutations PTC or SUFU, activating mutations in SMO, or amplification of GLI2 (Taylor et al. 2011; Brugieres et al. 2012). Many SHH-associated MBs have desmoplastic/nodular histology (Taylor et al. 2011) and often occurs in infants, where the prognosis is favorable, as well as in adults, where the prognosis is more variable (Kool et al. 2012). Group 3 MB often exhibit MYC overexpression or amplification whereas Group 4 tumors often exhibit amplification of CDK-6 or MYCN or duplication of the Parkinson's Disease-associated gene synuclein alpha interacting protein (SNCAIP) (Northcott et al. 2012; Taylor et al. 2011). The majority of Group 3 MB is found in children and is often associated with metastasis; it has the poorest prognosis among all subtypes of MB. Group 4 MB can be found in both children and adults and has more variable prognosis.

Table 1.1. Medulloblastoma subgroups. Adapted from Taylor et al, 2012.

		WNT	SHH	Group 3	Group 4
Demographics	Age Group	Children, adults	Mostly infants and adults, some children	Infants, children	All ages, mostly children
	Gender (Male: Female)	1:1	1:1	2:1	2:1
Clinical Features	Histology	Classic, rarely LCA	Demoplastic/ nodular, classic, LCA	Classic, LCA	Classic, LCA
	Metastasis	Rarely M+	Uncommonly M+	Very frequently M+	Frequently M+
	Prognosis	Very good	Infants good, others intermediate	Poor	Intermediate
	Genetics	*CTNBB1* mutation	*PTC/SMO/ SUFU* mutation *GLI2* amplification *MYCN* amplification	*MYC* amplification	*CDK6* amplification *MYCN* amplification
	Gene Expression	WNT signaling	SHH signaling	Photoreceptor/ GABAergic	Neuronal/ Glutamatergic

As with many pediatric malignancies, medulloblastoma is thought to arise from progenitor cells that experience anomalies in growth- and development-associated genes and proteins. WNT medulloblastomas arise in lower rhombic lip progenitors of the dorsal brainstem and have been modeled in mice with an activated b-catenin allele and compounded by p53 deletion (Gibson et al. 2010). In contrast, the SHH subgroup of medulloblastoma has been shown to originate from CGNPs in the EGL (Behesti and Marino 2009; Gilbertson and Ellison 2008; Schüller, Heine, et al. 2008). Accordingly, several mouse models have been generated to phenocopy hedgehog-driven medulloblastomas. A well-established model is a mouse heterozygous for *Patched*, in which 10-15% develop spontaneous medulloblastomas within one year (Johnson et al. 1996; Goodrich et al. 1997; Hahn et al. 1996; Berman et al. 2002). When crossed with $p53^{-/-}$ mice, the incidence of medulloblastoma rises to >95% before three months of age (Wetmore, Eberhart, and Curran 2001). Other established mouse models drive expression of a constitutively active Smoothened allele, SmoM2 or SmoA1, and when crossed with an appropriate Cre driver for example *Math1-Cre, Nestin-Cre, or GFAP-Cre*, can result in 100% medulloblastoma incidence with an average survival of 33-41 days (Schüller, Heine, et al. 2008). Notably, the majority of these Shh-driven mouse models involve transformation of a large number of neural stem cells (GFAP) (Yang et al. 2008), neural progenitors (Nestin) (Rao et al. 2003; Rao et al. 2004) or CGNPs (Math1) (Schüller, Heine, et al. 2008). *To date there have been few distinct subsets of CGNPs identified which can be transformed to initiate medulloblastoma formation, with the exception of Olig2- and Tlx3-expressing precursors* (Schüller, Heine, et al. 2008). *In Chapter II, we demonstrate that a small subset of CGNPs, identified as Gdf7-lineage cells, can be oncogenically transformed by deregulated Shh signaling; our investigation demonstrates how remarkably few cells are sufficient for oncogenic transformation and*

tumor formation. Further identification of the cellular origins of medulloblastoma may help to better understand early developmental pathways involved in tumorigenesis and focus treatment on cell types responsible for tumor initiation.

Therapy for Medulloblastoma

Current treatments for medulloblastoma typically involve surgical resection coupled with chemotherapy and radiation regardless of molecular subgroup, leading to a five-year survival of almost 90% in average-risk patients and 70% in high-risk patients (Gajjar et al. 2006). However, five-year disease-free survival remains low, at 36%, for patients with dissemination and prognosis remains poor for patients with recurrent medulloblastoma (Packer et al. 2006). In addition, a majority of survivors exhibit long-term cognitive and endocrine deficits as a complication of therapy (Mulhern 2005; Ribi et al. 2005), underscoring the desperate need for improved therapies.

Recent advances in the understanding of Shh signaling have led to the discovery and development of small molecule inhibitors of the pathway. Several small molecule inhibitors of Smoothened function have worked remarkably well to suppress medulloblastoma in allografts and mouse models (Berman et al. 2002; Justyna Romer and Curran 2005), and some have even been tested in clinical trials. One promising therapeutic, Visomegib, was reported in one patient to cause almost complete remission of the disease only to have it return at a later time with a mutation in Smo that made tumor cells insensitive to the drug (Rudin et al. 2009; Rudin 2012; Yauch et al. 2012). Thus there is great need for novel targets as well as small molecule antagonists to the Shh pathway that may be used in combination treatments with Smo inhibitors. Current studies are being directed at targeting Gli, and few Gli-level inhibitors have been identified, including arsenic trioxide, GANT58, and GANT61 (Lauth et al. 2007; Kim et al. 2010). *Small molecule inhibitors of the Shh pathway that act downstream of Smo have*

the advantage of being active against MBs in which Smo is mutated and hold great potential as future therapeutics for medulloblastoma. *In Chapter IV of this work, we identify a small molecule as a novel and potent inhibitor of Shh signaling at the level of Gli1 transcription.*

Novels findings as elucidated by modulation of Shh signaling

In this work, we have modulated Shh signaling through genetic mouse models to reveal novel findings regarding its role in cerebellar development and medulloblastoma.

First, in Chapter II we demonstrate that focal activation of Shh signaling in a distinct subset of CGNPs, specifically derived from hindbrain roof plate cells expressing growth differentiation factor-7 (Gdf7), is sufficient to promote cerebellar tumorigenesis. This is accomplished by utilizing a $Gdf7^{Cre/+}$ line to drive constitutive activation of the Shh pathway activator Smoothened (SmoM2). $Gdf7^{Cre/+};SmoM2$ (GM2) mutant mice were observed to display stunted growth, cranial bulging, and impaired motor coordination; all GM2 mice died within three weeks of birth. Analysis of mutant cerebellar architecture revealed severe hyperplasia suggestive of tumor formation. Tumors from both GM2 and established medulloblastoma model $Patched^{LacZ/+}$ mice displayed strong expression of CGNP, neural progenitor, and proliferative markers. In addition, cultured GM2 cerebellar cells expressed multiple stem cell markers and were clonogenic and multipotent. Collectively, these data indicate that targeting constitutively active Shh signaling to the Gdf7-lineage leads to formation of medulloblastoma. Detailed fate-mapping was performed of the Gdf7 lineage which revealed that surprisingly, Gdf7-lineage cells contribute to a small subset of proliferating CGNPs. In addition, Gdf7-lineage cells also contribute to an extensive array of mature cerebellar cell types. The GM2 medulloblastoma mouse model demonstrates how remarkably few cells are sufficient for oncogenic transformation and tumor formation. Thus hindbrain roof plate cells are

established as a novel source of diverse neural cell types in the cerebellum that is also susceptible to oncogenic transformation by deregulated Shh signaling. This work is published in *PlosOne* (April 2012) (Cheng et al. 2012).

Second, in Chapter III we use a tamoxifen-inducible *Tenascin-CreER* line to spatially and temporally alter Shh signaling activity specifically in postnatal BG. Mice in which Shh activator Smoothened (Smo) is postnatally ablated in BG demonstrate an obvious reduction in cerebellar size within two days of ablation of Shh signaling. Surprisingly, mutant CGNPs exhibit severely reduced proliferation and increased differentiation accompanied by a loss of Shh activity, suggesting a novel role for the BG-CGNP interaction in promoting CGNP precursor proliferation. Interestingly, Wnt signaling is ectopically elevated in TNC mutant CGNPs concomitant with a reduction in EGL area, suggesting that this pathway is involved in cross-talk with the Shh pathway in regulating CGNP proliferation. In addition, loss of Shh signaling in BGs leads to disrupted PC laminar organization and dendritic arborization as well as BG fiber morphology, indicating that BG-Shh signaling activity contributes to the maintenance of proper cerebellar laminar formation. Collectively, these data show a previously unappreciated role for BG Shh signaling activity in the proliferation of CGNPs and preservation of cerebellar architecture, thus leading to a new level of understanding of the neuronal-glial relationship in the cerebellum. This work is to be submitted for publication by early 2014.

In Chapter IV of this work, we identify AICAR as a potent Hh pathway antagonist in multiple cell types, including Hh-responsive human medulloblastoma cells. Importantly, we show that AICAR acts downstream of Smo and regulates *Gli1* transcription in a proteasome-independent manner. Sufu stabilizes the Gli proteins from AICAR inhibition, as downregulation of Shh pathway activity was more efficient in Sufu-null MEFs. Last, we find that although AICAR activates AMPK in these cell lines, inhibition of the Hh pathway by AICAR is AMPK-independent. Our findings establish AICAR as a modulator

of Shh signaling in both a developmentally relevant cell type as well as medulloblastoma cells, providing an encouraging basis to further explore its full potential as an antagonist in Shh-associated tumors. This work represents a collaboration between myself and a colleague in the Chiang lab, Jiang Liu, Ph.D. My contributions encompassed the studies in CGNPs and human medulloblastoma cells, as well as the written document. This work will be submitted for publication following completion of *in vivo* studies of AICAR effects on Shh-driven tumors.

Although seemingly disparate projects, each of these chapters is connected to understanding the function of Shh signaling in a developmental context of the cerebellum in order to elucidate consequences of aberrant Shh signaling in the context of disease. A central focus of our studies is the origin and proliferative capacity of the CGNP, which is the cell-of-origin for hedgehog driven medulloblastomas (Yang et al. 2008; Schüller, Heine, et al. 2008). In Chapter II, we examine the developmental origins of CGNPS and find that hindbrain roof plate cells can give rise to this cell type, thereby revealing a novel source of cerebellar cells. In Chapter III, we focus on factors regulating the proliferation of CGNPs, and establish the specialized glial cell Bergmann glia as a previously unidentified regulator of these cells. And in Chapter IV, we extend studies of factors regulating CGNPs and identify a small molecule as a novel Shh pathway activity inhibitor with consequences on proliferation of not only CGNPs but on hedgehog-driven medulloblastoma cells. Thus, our studies collectively elucidate cellular mechanisms involved in CGNP proliferation, with implications for medulloblastoma. It is our hope that understanding Shh-dependent signaling in the cerebellum during normal development and disease can provide insight into cellular relationships integral to brain growth as well as inform development of targeted therapies for disease processes resulting from deregulated signaling.

CHAPTER II

WIDESPREAD CONTRIBUTION OF GDF7 LINEAGE TO CEREBELLAR CELL TYPES AND IMPLICATIONS FOR HEDGEHOG-DRIVEN MEDULLOBLASTOMA FORMATION

INTRODUCTION

The roof plate is a transient embryonic dorsal midline epithelial tissue spanning the entire developing central nervous system (CNS). The LIM-homeodomain transcription factor Lmx1a is a central regulator of roof plate development, as loss of Lmx1a resulted in a major absence of roof plate cells during early embryogenesis (Chizhikov and Millen 2004; Millonig, Millen, and Hatten 2000). The roof plate consists of a distinct strip of the most dorsal-lateral neuroectodermal cells that collectively function as an essential organizing center regulating development of neighboring tissues. Roof plate-derived inductive signals, such as Bmp6, Bmp7, Gdf7 (Bmp12), and Wnt1 (Chizhikov and Millen 2004; Lee, Dietrich, and Jessell 2000; Lee, Mendelsohn, and Jessell 1998), are important for directing differentiation of dorsal neuronal cell types (Chizhikov and Millen 2004; Lee, Dietrich, and Jessell 2000; Lee, Mendelsohn, and Jessell 1998; Chizhikov et al. 2006). While regulating the development of neighboring tissues by secreted growth factors, the roof plate cells also have the capacity to generate different cell types. For example, in the spinal cord region, Gdf7-expressing roof plate progenitors give rise to dorsal interneurons and neural crest-derived sensory neurons and glia (Lee et al. 2000; Lo, Dormand, and Anderson 2005). In the telencephalon, roof plate progenitor cells have been implicated as a source of marginal zone neurons (Monuki, Porter, and Walsh 2001). Although the roof plate varies in its differentiation potential along the rostral-caudal axis of the neural tube (Awatramani et al. 2003; Currle et al. 2005; Hunter and Dymecki 2007), previous fate-mapping studies have indicated that the hindbrain roof

plate is uniquely restricted in lineage potential and its contributions are mostly limited to non-neural hindbrain choroid plexus epithelial (hChPe) cells (Chizhikov et al. 2006; Currle et al. 2005; Hunter and Dymecki 2007; Landsberg et al. 2005; Chizhikov et al. 2010). Hence, the capacity for hindbrain roof plate Gdf7-expressing cells to contribute to specific cell types in the cerebellum has not been shown.

Adjacent to the hindbrain roof plate is the cerebellar rhombic lip, which is a source of migratory neurons that primarily stream towards the cerebellar anlage to form multiple cell types. Rhombic lip derivatives include neurons of the deep cerebellar nuclei, granule neuron progenitors, and unipolar brush cells, each arising within a specific developmental time window. Previous genetic analyses of the cerebellar rhombic lip have suggested that the basic helix-loop-helix transcription factor Mouse atonal homolog 1 (Math1) molecularly defines the region of the rhombic lip (Machold and Fishell 2005; Wang, Rose, and Zoghbi 2005). However, more recent investigation has shown the rhombic lip to be molecularly heterogeneous with Lmx1a expression representing at least one Math1-independent rhombic lip gene (Chizhikov et al. 2010). Thus, the extent and contribution of Math1-negative cell types residing in the rhombic lip has yet to be elucidated.

Medulloblastoma, the most common malignant brain tumor in children, is characterized by its rapid progression and tendency to spread along the entire brain-spinal axis with poor clinical outcome. Recent integrative transcriptional profiling studies have showed that medulloblastoma comprises a collection of four clinically and molecularly diverse subgroups (Thompson et al. 2006; Kool et al. 2008; Northcott, Korshunov, et al. 2011; Taylor et al. 2011; Kool et al. 2012; Cho et al. 2011). Two of these subgroups, molecularly defined by overactivated WNT or SHH signaling, consistently demonstrate distinct genetic profiles and recently were found to arise from different cellular origins (Gibson et al. 2010). It is now well established that Sonic

hedgehog (Shh) signaling stimulates proliferation of cerebellar granule neuron precursors (CGNPs) during cerebellar development (Wechsler-Reya and Scott 1999; Wallace 1999; Sillitoe and Joyner 2007; Dahmane and Ruiz i Altaba 1999). Numerous studies using mouse models in which the Shh pathway is constitutively activated have linked Shh signaling to medulloblastoma and CGNPs as a cellular origin (Gilbertson and Ellison 2008; Yang et al. 2008; Schüller, Heine, et al. 2008). Notably, the majority of Shh-driven mouse models involve transformation of a large number of neural stem cells (GFAP) (Z. Yang et al. 2008), neural progenitors (Nestin) (Rao et al. 2003; Rao et al. 2004) or CGNPs (Math1) (Schüller, Heine, et al. 2008). To date there have been few distinct subsets of CGNPs identified which can be transformed to initiate medulloblastoma formation, with the exception of Olig2- and Tlx3-expressing precursors (Schüller, Heine, et al. 2008). Further identification of the cellular origins of medulloblastoma may help to better understand early developmental pathways involved in tumorigenesis and focus treatment on cell types responsible for tumor initiation.

In our previous study, we observed that *Gdf7*$^{Cre/+}$*;SmoM2* mutant mice, in addition to demonstrating enhanced proliferation of the hindbrain choroid plexus epithelial progenitor cells, are runted and exhibit neurological defects (Huang et al. 2009). Here we show that ectopic Shh signaling in the *Gdf7*-lineage cells invariably led to formation of medulloblastoma with CGNP features, indicating that focal activation of the Shh signaling pathway in the Gdf7-lineage cells is sufficient to promote cerebellar tumorigenesis. This result is at odds with previous findings that hindbrain roof plate may only contribute to non-neural choroid plexus epithelium. Using lineage tracing analysis, we demonstrate that in addition to their contribution to the choroid plexus epithelium, *Gdf7*-expressing cells are a source of distinct progenitor populations in the rhombic lip and dorsal midline cerebellar ventricular zone. These populations contribute to multiple cerebellar neuronal and glial cell types, including CGNPs, the presumed cell of origin for

hedgehog-driven medulloblastoma. Our findings uncover a broad contribution of Gdf7-lineage to the cerebellum and suggest that medulloblastoma can stem from progenitor populations that were previously thought to be restricted to the choroid plexus lineage.

RESULTS

Targeted activation of Shh signaling pathway in Gdf7-lineage leads to rapid cerebellar hyperplasia

We recently reported that the hChPe cells robustly express Shh and Shh signaling defines a discrete hChPe progenitor domain close to the lower rhombic lip (Huang et al. 2009). To support a crucial proliferative role for Shh signaling during hChPe development, we generated *Gdf7$^{Cre/+}$;SmoM2* mutants in which *Gdf7^{Cre}* drives constitutively active Shh signaling in a ligand-independent manner due to a point mutation in the Smo allele (Xie et al. 1998; Jeong et al. 2004). In line with the regulation of Shh signaling in the biogenesis of the hChP, we observed enlarged hChP in the gain-of-function *Gdf7$^{Cre/+}$;SmoM2* mutant mice. Notably, *Gdf7$^{Cre/+}$;SmoM2* mice displayed stunted growth, cranial bulging in the hindbrain region, and impaired motor coordination (Huang et al. 2009). As reported in our previous study, all of the *Gdf7$^{Cre/+}$;SmoM2* mice died within three weeks of birth with a median survival of 13.5 days (Huang et al. 2009). Dissected *Gdf7$^{Cre/+}$;SmoM2* cerebella often lacked visible foliations, suggesting that the spaces between cerebellar lobules were filled with cellular material. Examination of hindbrain histology in surviving pups prior to P10 revealed proper development of all cerebellar layers and relatively normal architecture (Figure 2.1A-B'). However, hematoxylin and eosin staining of tissue sections from mice surviving beyond P14 revealed tumors within

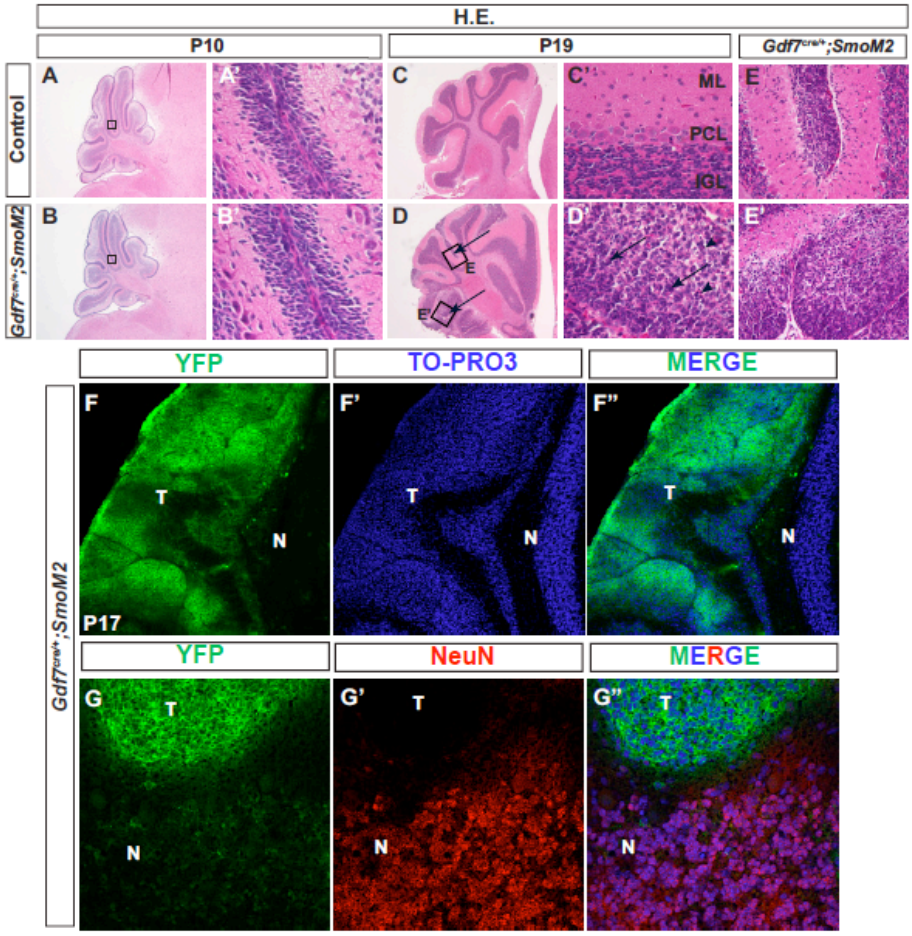

Figure 2.1. Shh pathway activation in Gdf7-lineage cells leads to cerebellar hyperplasia

Gdf7$^{Cre/+}$*;SmoM2* gain-of-function mutant mice exhibit cerebellar defects. (A-B') Hematoxylin-eosin staining of wild-type and *Gdf7*$^{Cre/+}$*;SmoM2* mutants. Prior to P10 histological sections of mutants are similar to control. (C-E') *Gdf7*$^{Cre/+}$*;SmoM2* mutants over 14 days old develop ectopic foci of densely packed cells within the molecular layer of their cerebella. Higher magnification view of these foci reveals no discernible layer organization and resemblance to neoplastic lesions. Arrows in (D) indicate regions of hypercellularity. Boxed regions E and E" are magnified and shown in the right adjacent panels. Arrows in D' indicate nuclear molding. Arrowheads in D' indicate apoptotic nuclei. (F-F") The ectopic foci consist of cells of the Gdf7-lineage as indicated by their expression of SmoM2-YFP. (G-G") Ectopic foci do not express differentiated neuronal marker NeuN. Abbreviations: EGL, external granular layer. ML, molecular layer. IGL, internal granular layer. T, tumor region. N, normal cerebellum.

the cerebellar parenchyma and leptomeninges (Figure 2.1C-E', arrows). The cells were pleomorphic with a high nuclear-to-cytoplasmic ratio. Nuclear molding was a common feature (Figure 2.1D', arrows), as was the presence of apoptotic cells (Figure 2.1D', arrowheads). In the parenchymal lesions, areas of relatively preserved molecular layer architecture with hypercellularity were suggestive of persistence of the external granule layer (EGL) (Figure 2.1E-E'). As the membrane-localized SmoM2 protein is fused with a YFP reporter protein (Xie et al. 1998; Jeong et al. 2004), we determined that the medulloblastoma cells were all YFP-positive (Figure 2.1F-F"). Furthermore, YFP expression covering most of the cerebellar surface in the *Gdf7$^{Cre/+}$;SmoM2* mice suggests that the tumor cells are derived from Gdf7-expressing progenitor cells. Importantly, YFP-positive cells do not express the differentiated neuronal marker NeuN (Figure 2.1G-G"). Collectively, these data indicate that targeting constitutively active Shh signaling to the Gdf7-lineage leads to the formation of medulloblastoma.

Gdf7$^{Cre/+}$;SmoM2 medulloblastomas display cerebellar granule neuron precursor features and similar molecular phenotypes to medulloblastomas in _Patched$^{LacZ/+}$_ mice

Consistent with the fact that constitutively active SmoM2 was expressed in Gdf7-lineage cells and the tumor cells are marked by YFP, we detected a high level of Shh signaling, as evidenced by robust expression of pathway target genes *Gli1* and *Ptch1* in *Gdf7$^{Cre/+}$;SmoM2* medulloblastomas (Figure 2.2B and 2B'). In contrast, moderate levels of *Gli1* and *Ptch1* were detected only in putative Bergmann glial cells of control cerebella (Figure 2.2A and A'). Emerging evidence suggests that Nmyc is an essential oncogenic mediator for Shh-dependent medulloblastoma (Kenney, Widlund, and Rowitch 2004; Hatton et al. 2006; Kenney, Cole, and Rowitch 2003; Thomas et al. 2009). More importantly, a recent study demonstrated that Nmyc promotes progression from

Figure 2.2.

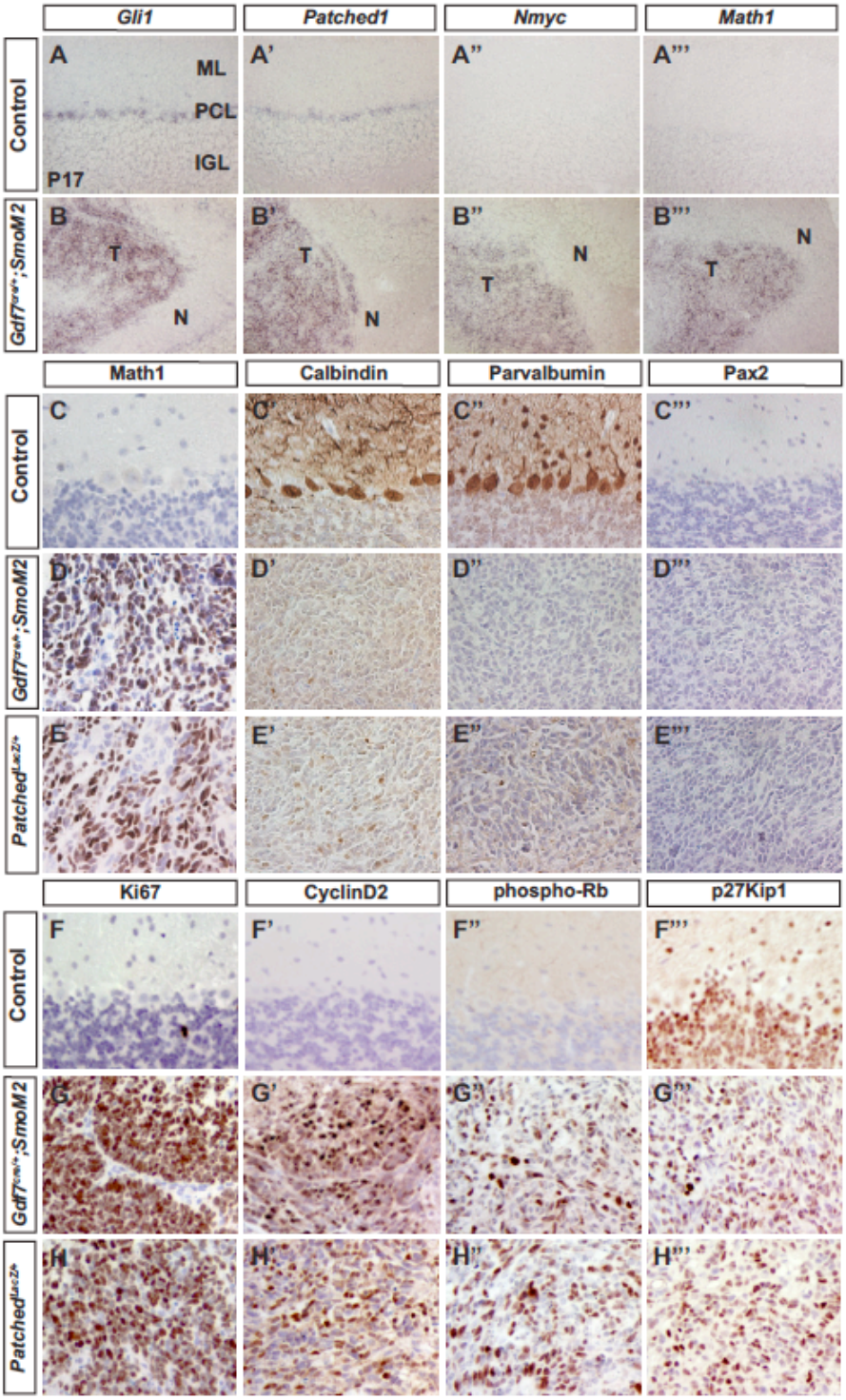
Gli1
Patched1
Nmyc
Math1
Control
A
ML
PCL
IGL
P17
A'
A''
A'''
Gdf7cre/+;SmoM2
B
T
N
B'
T
N
B''
T
N
B'''
T
N
Math1
Calbindin
Parvalbumin
Pax2
Control
C
C'
C''
C'''
Gdf7cre/+;SmoM2
D
D'
D''
D'''
PatchedlacZ/+
E
E'
E''
E'''
Ki67
CyclinD2
phospho-Rb
p27Kip1
Control
F
F'
F''
F'''
Gdf7cre/+;SmoM2
G
G'
G''
G'''
PatchedlacZ/+
H
H'
H''
H'''

Figure 2.2. *Gdf7$^{Cre/}$;SmoM2* mice develop medulloblastoma with CGNP features
(A-B"') In situ hybridization of wild-type and *Gdf7$^{Cre/+}$;SmoM2* mutants. The aberrant tissue foci of *Gdf7$^{Cre/+}$;SmoM2* cerebella display high level Shh signaling as determined by *Gli1* and *Ptch1* expression, and *Nmyc* and *Math1* expression. (C-H"') *Gdf7$^{Cre/+}$;SmoM2* mice develop medulloblastoma consisting of cells of the CGNP fate. Tumors in *Gdf7$^{Cre/+}$;SmoM2* mice and adult *Patched1$^{LacZ/+}$;SmoM2* mice appear very similar. Abbreviations: ML, molecular layer. PCL, Purkinje cell layer. IGL, internal granular layer. T, tumor region. N, normal cerebellum.

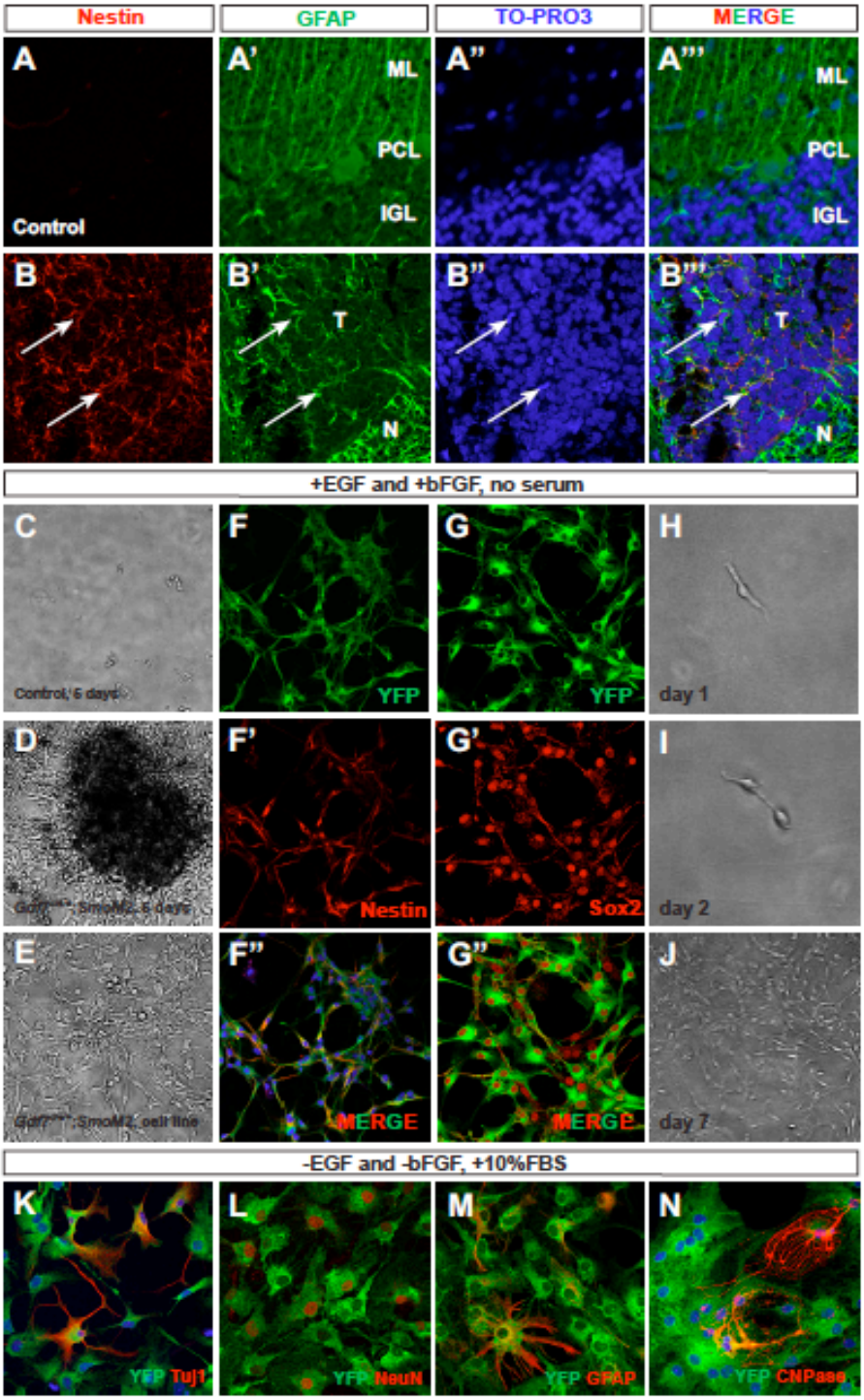
Nestin
GFAP
TO-PRO3
MERGE
A
A'
A''
A'''
ML
PCL
IGL
Control
B
B'
B''
B'''
T
N
+EGF and +bFGF, no serum
C
F
G
H
Control, 6 days
YFP
YFP
day 1
D
F'
G'
I
Nestin
Sox2
day 2
E
F''
G''
J
MERGE
MERGE
day 7
-EGF and -bFGF, +10%FBS
K
L
M
N
YFP Tuj1
YFP NeuN
YFP GFAP
YFP CNPase

Figure 2.3. A subset of Gdf7-lineage cells express neural stem cell markers
(A-B"') Many cells within the tumor tissue of *Gdf7$^{Cre/+}$;SmoM2* mice coexpress neural stem cell marker Nestin (red) and glial marker GFAP (green). Arrows indicate co-localization. (C-E) Tumor cell lines can be invariably established from *Gdf7$^{Cre/+}$;SmoM2* cerebella. (F-G") These cells highly express multiple neural stem cell markers Nestin and Sox2 and can undergo serial passages. (H-J) Here, one representative colony is shown when cultured for 3 and 6 days. (K-N) *Gdf7$^{Cre/+}$;SmoM2* cultured cells can differentiate into mature cerebellar cell types upon switching to culture media containing 10% FBS.

preneoplastic lesions to medulloblastoma (Kessler et al. 2009). While *Nmyc* expression was not detectable in the cerebella of control mice older than 2 weeks, robust expression was measured in *Gdf7$^{Cre/+}$;SmoM2* medulloblastoma cells (Figure 2.2A" and 2B"), consistent with oncogenic transformation. Previous studies have shown that acquisition of CGNP fate is a prerequisite for medullollastoma formation (Yang et al. 2008; Schüller, Heine, et al. 2008). As oncogenic transformation of CGNPs has been faithfully modeled in the *Patched$^{LacZ/+}$* mice (Johnson et al. 1996; Berman et al. 2002), we compared medulloblastomas in these mice to those in the *Gdf7$^{Cre/+}$;SmoM2* mice. Notably, tumors from both *Gdf7$^{Cre/+}$;SmoM2* and *Patched$^{LacZ/+}$* mice displayed strong expression of Math1, a marker of cells of the CGNP fate (Figure 2.2C, 2D, 2E), comparably low expression of calbindin-positive Purkinje neurons and parvalbumin-positive GABAergic interneurons, and absence of Pax2-positive GABAergic interneuron progenitors (Figure 2.2C-E"'). Similar to *Patched$^{LacZ/+}$* tumors, *Gdf7$^{Cre/+}$;SmoM2* medulloblastomas expressed the neural progenitor marker Nestin and were highly proliferative as indicated by strong expression of Ki67, CyclinD2, and phosphorylated Rb and partial loss of differentiation marker p27Kip1 (Figure 2.2F-H"'**)**. Taken together, these data demonstrate that *Gdf7$^{Cre/+}$;SmoM2* and *Patched$^{LacZ/+}$* mice develop medulloblastomas with similar cellular and molecular phenotypes and CGNP identity.

A subset of Gdf7-lineage tumor cells are multipotent

A recent report has shown that a subset of medulloblastoma cells from *Patched1$^{LacZ/+}$* mice are multipotent progenitors and capable of differentiating into glial and neuronal lineages (Ward et al. 2009). To determine whether the medulloblastoma cells in *Gdf7$^{Cre/+}$;SmoM2* mice possessed similar properties, we assayed for the presence of potential cancer stem-cell like markers. Consistently, we were able to detect Nestin+ and GFAP+ cells in *Gdf7$^{Cre/+}$;SmoM2* tumor foci, suggestive of a tumor stem cell immunophenotype (Figure 2.3A-B"', arrows). We then dissected the cerebella from

Gdf7$^{Cre/+}$*;SmoM2* mice older than 14 days and from age-matched control mice. Cerebellar cells were dissociated and cultured in neural stem cell medium. While we did not observe appreciable colony formation by the dissociated control cerebellar cells, we observed the formation of numerous highly proliferative colonies within days from every mutant cerebellum analyzed (Figure 2.3C-E). These cells expressed the neural stem cell markers Nestin, Sox2, and GFAP, sustained multiple serial passages (over 50) and were clonogenic at a plating density of 100 cells per mL culture medium (Figure 2.3F-J). Under stem cell culture conditions, the YFP+ cells from *Gdf7*$^{Cre/+}$*;SmoM2* medulloblastomas were small and bipolar with large nuclei and scant cytoplasm (Figure 2.3I). Upon switching to medium supplemented with 10% fetal bovine serum, the YFP+ cells displayed dramatically altered morphology within 5-7 days, withdrew from the cell cycle, and differentiated into Tuj1+ or NeuN+ neurons, GFAP+ astrocytes or CNPase+ oligodendrocytes, highlighting their multi-potency (Figure 2.3K-N). These data suggest that a subset of Gdf7-lineage cells in the *Gdf7*$^{Cre/+}$*;SmoM2* tumors express multiple stem cell markers and are clonogenic and multipotent, reported characteristics for the medulloblastoma-propagating cells of the *Patched*$^{LacZ/+}$ mouse model (Ward et al. 2009).

Distinct Gdf7-expressing cells of the cerebellar vermal ventricular zone are radial glial cells

The unexpected finding that *Gdf7*$^{Cre/+}$*;SmoM2* mice displayed cerebellar oncogenic transformation prompted us to ask whether the Gdf7-lineage cells only differentiate into mature hChPe cells as previously recognized, or contribute to other cerebellar cell types including CGNPs that are susceptible to oncogenic transformation by aberrant Shh signaling. Therefore, we performed detailed fate-mapping of the Gdf7 lineage in *Gdf7*$^{Cre/+}$*;ROSA26*^{LacZ} and *Gdf7*$^{Cre/+}$*;ROSA26*^{eYFP} mice, where LacZ or enhanced YFP indelibly marks cells that are, or once were, expressing Gdf7. As expected, Gdf7-lineage

cells were distributed at the dorsal midline along the entire cranio-spinal axis (Figure 2.4A, 4B). In this hindbrain region, Gdf7-lineage cells emanated from the lateral edge to occupy the medial portion of the roof plate, a migratory pattern similar to the reported *Ttr*-expressing primitive hChPe cells (Figure 2.4B) (Hunter and Dymecki 2007). We observed a streak of Gdf7-lineage cells in the midline vermal cerebellar tissue where the two hemispheres meet (Figure 2.4C). This observation is consistent with the fact that we detected restricted *Gdf7*-expressing cells in the cerebellar midline tissue (Figure 2.4E), which persisted into E16.5 embryos (Figure 2.7). Interestingly, *Msx1*, a Bmp signaling target gene, was highly expressed in this cerebellar midline domain and suggestive of local signaling (Figure 2.4F). Furthermore, we observed that at embryonic day 14.5 (E14.5), all Gdf7-lineage cells localized to the vermal ventricular zone expressed radial glial cell markers BLBP and Sox2 (Figure 2.4G-H'). Radial glial cells have been shown to be multipotent neural stem cells during embryogenesis (Anthony et al. 2004). These data suggested that the Gdf7-expressing cerebellar vermal cells are a distinct sub-population of multipotent radial glial cells. As radial glial cells are rapidly proliferating during embryonic stages, we asked whether Gdf7 could act as a proliferative signal. The lack of apparent Gdf7 and Msx1 expression in the Math1+ tumor tissue of *Gdf7$^{Cre/+}$;SmoM2* mice argues against this possibility (Figure 2.4I-K).

Figure 2.4.

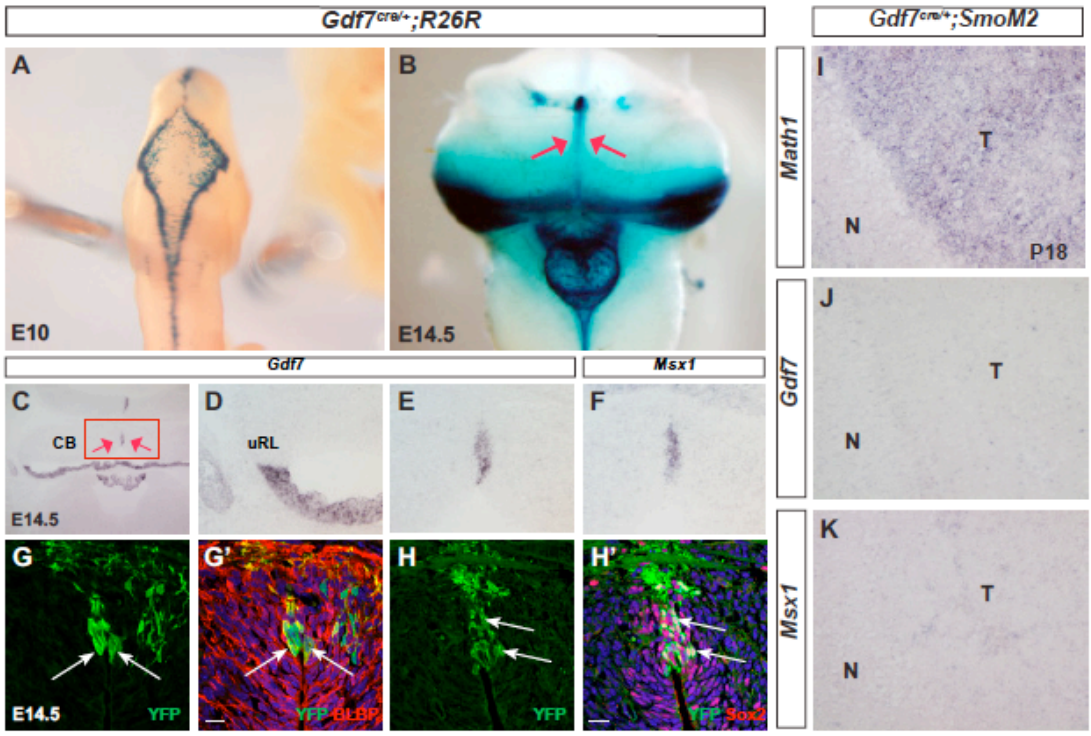

Figure 2.4. Roof plate cells give rise to a distinct population of cerebellar vermal radial glia cells

(A) Whole mount X-gal staining for ß-galactosidase in *Gdf7*$^{Cre/+}$;*ROSA*^{lacZ} embryos shows that Gdf7 lineage is present in the hindbrain roof plate at E10. (B) At E14.5, in addition to hindbrain choroid plexus, Gdf7 lineage also contributes to the ventricular zone of cerebellar vermis (red arrows). (C-F) In situ hybridization at E14.5 showing *Gdf7* and its transcriptional target *Msx1* are expressed in the cerebellar vermis. (G-H') Fate-mapping of the Gdf7-lineage in *Gdf7*$^{Cre/+}$;*ROSA*^{eYFP} cerebella indicates that Gdf7 is present at E14.5 in a distinct population of vermal radial glia cells as highlighted by coexpression of YFP and BLBP (G-G') or Sox2 (H-H') Arrows indicate colocalization. (I-K) In situ hybridization at P18 shows that the *Math1*+ *Gdf7*$^{Cre/+}$;*SmoM2* tumor tissue does not express *Gdf7* or *Msx1.* Abbreviations: N, normal cerebellar tissue. T, tumor tissue. CB, cerebellum. uRL, upper rhombic lip.

Gdf7-lineage cells of the cerebellar rhombic lip are Lmx1a+ neural progenitor cells that likely give rise to CGNPs

As expected, at stage E14.5 a second population of Gdf7-lineage cells was present in the laterally positioned roof plates adjacent to the choroid plexus. Surprisingly, several Gdf7-lineage cells delaminated from the clustered roof plate cells to enter the rhombic lip (Figure 2.5A). The number of delaminating Gdf7-lineage cells was few but distinct, amounting to no more than 20-30 cells per embryo at E14.5. In order to determine the identity of these cells, we sought to co-localize them with Math1, a molecular marker of the rhombic lip (Machold and Fishell 2005). Using *Gdf7$^{Cre/+}$;ROSA26^{LacZ};Math1$^{GFP/GFP}$* in which GFP marks cells expressing Math1 and β-gal labels cells that once were or are expressing Gdf7, we found that the Gdf7-lineage cells in the rhombic lip were Math1-negative, corroborating recent evidence that molecular heterogeneity exists within the cerebellar RL (Figure 2.5A-A") (Chizhikov et al. 2010). Accordingly, the cells were negative for Pax6, a marker for CGNPs (Figure 2.5C-C"). However, Gdf7-lineage cells retain the capacity to express Math1 as they migrate into the EGL (Figure 2.5B-B"). Because Lmx1a is currently the only known Math1-independent rhombic lip gene (Chizhikov et al. 2010), we sought to colocalize the Gdf7-expressing progeny with Lmx1a and found that they were indeed Lmx1a-positive (Figure 2.5D-D"). To further characterize the identity of the delaminated Gdf7-lineage cells in the rhombic lip, we determined their expression of Sox2, a marker for neural progenitor cells (Figure 2.5E-E") and also found that they are BLBP-negative (Figure 2.5F-F"). Some GFP-positive cells co-labeled with Tbr2 (Figure 2.5G-G", arrows), a marker for unipolar brush cells (UBC) which also originate from the rhombic lip (Sotelo and Dusart 2009; Corrales et al. 2004), suggesting that Gdf7-lineage cells can also contribute to the UBC population. We then analyzed the fate of Gdf7- lineage cells at postnatal stages. Consistent with the Math1+ YFP cells at E14.5, we detected apparent YFP signal in the EGL and other

tissue layers of the P6 cerebellum (Figure 2.5H, 5I, data not shown). The YFP positive cells in the EGL were Ki67 positive, indicating that they are cycling, proliferative CGNPs (Figure 2.5H-I"). These findings strongly suggest that progeny of Gdf7-expressing cells can enter the rhombic lip and eventually the EGL to become Math1+ CGNPs. Additionally, we observed YFP positive cells in the IGL that were also Tbr2 positive, demonstrating that Gdf7 lineage cells can become mature UBCs (Figure 2.5J-J").

Gdf7-lineage cells contribute to an extensive array of mature cerebellar cell types

In line with their widespread distribution in P6 cerebellum, we found that the Gdf7-lineage cells contribute extensively to various mature cerebellar cell types. In *Gdf7$^{Cre/+}$;ROSA26^{eYFP}* cerebella from adult mice, YFP-marked cells co-expressed granule neuron marker NeuN (~3.5%), Purkinje neuron marker calbindin (~0.1%), GABAergic interneuron marker parvalbumin (<0.1%), Bergmann glia marker Sox2 (~0.2%), and white matter astrocyte cell marker GFAP (<0.1%) (Figure 2.6A-F"). It is interesting to note that granule neurons were the predominant cellular derivatives. A similar situation has been reported indicating that Gdf7-expressing roof plate cells of the spinal cord region preferentially become sensory neurons, a process suggested to be mediated by the function of Gdf7 itself (Lo, Dormand, and Anderson 2005). Granule neurons derived from the Gdf7-lineage were not uniformly distributed among the cerebellar lobes, with higher numbers found in Lobes III-V and IX (Figure 2.6G, 6H).

Figure 2.5.

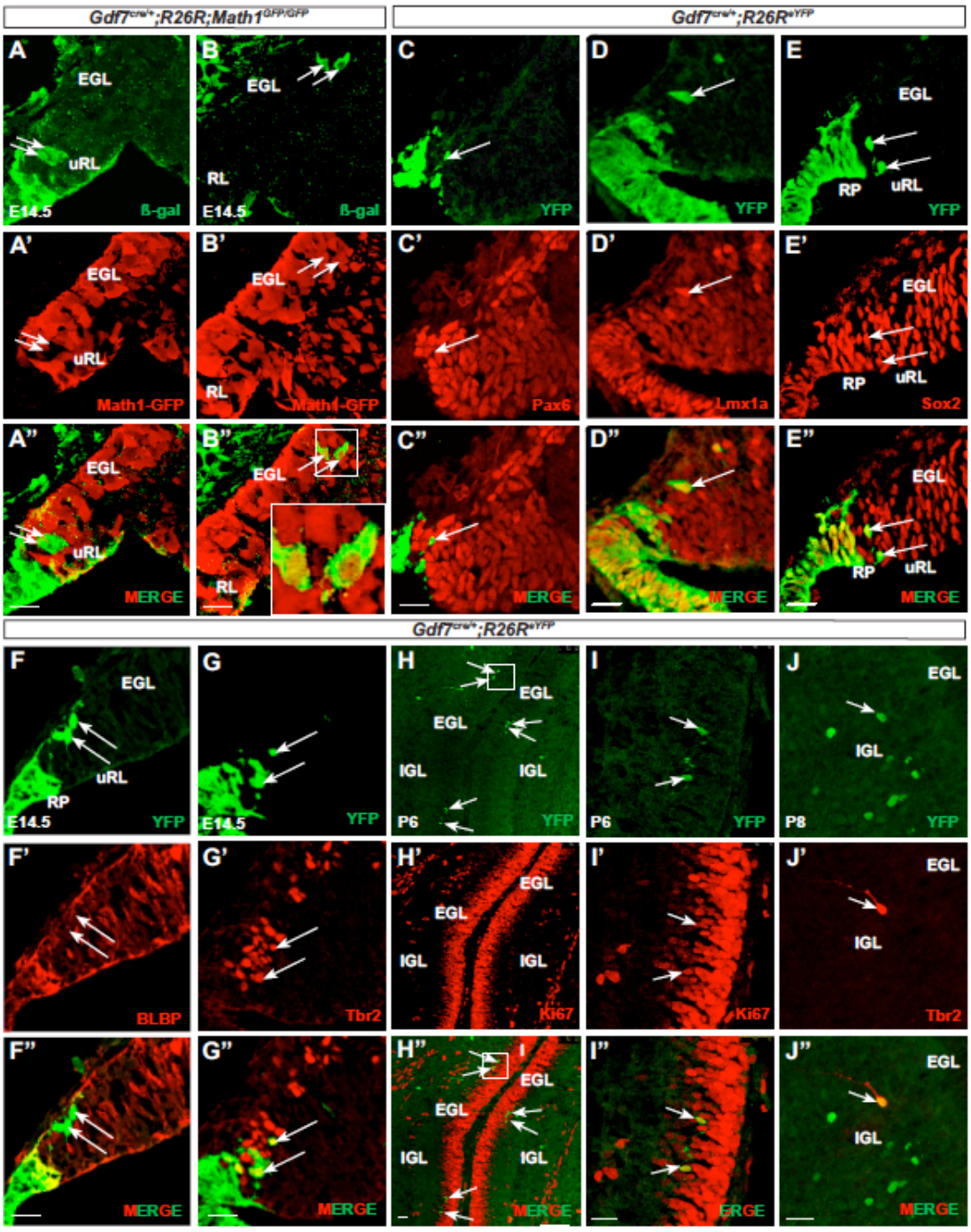
Gdf7cre/+;R26R;Math1GFP/GFP
Gdf7cre/+;R26ReYFP
A
EGL
uRL
E14.5
ß-gal
B
EGL
RL
E14.5
ß-gal
C
YFP
D
YFP
E
EGL
RP
uRL
YFP
A'
EGL
uRL
Math1-GFP
B'
EGL
RL
Math1-GFP
C'
Pax6
D'
Lmx1a
E'
EGL
RP
uRL
Sox2
A"
EGL
uRL
MERGE
B"
EGL
RL
C"
MERGE
D"
MERGE
E"
EGL
RP
uRL
MERGE
Gdf7cre/+;R26ReYFP
F
EGL
uRL
RP
E14.5
YFP
G
E14.5
YFP
H
EGL
EGL
IGL
IGL
P6
YFP
I
P6
YFP
J
EGL
IGL
P8
YFP
F'
BLBP
G'
Tbr2
H'
EGL
EGL
IGL
IGL
Ki67
I'
Ki67
J'
EGL
IGL
Tbr2
F"
MERGE
G"
MERGE
H"
I
EGL
EGL
IGL
IGL
MERGE
I"
ERGE
J"
EGL
IGL
MERGE

Figure 2.5. Gdf7-lineage cells in the cerebellar rhombic lip are Lmx1a+ neural progenitor cells that give rise to CGNPs

(A-B") Fate-mapping studies in *Gdf7$^{Cre/+}$;ROSA26^{eYFP};Math1$^{GFP/GFP}$* at E14.5 show that Gdf7-lineage cells (as indicated by b-gal, green) are Math1-negative (as indicated by GFP) in sagittal sections of the upper rhombic lip. However these cells retain the capacity to express Math1 in the EGL. Arrows indicate delaminating Gdf7-lineage cells from the upper rhombic lip en route to the EGL. (C-F") Fate-mapping studies in *Gdf7$^{Cre/}$;ROSA26^{eYFP}* mice at E14.5 show that delaminating Gdf7-lineage cells (green, arrows) are present in sagittal sections of the cerebellar rhombic lip and are Pax6- (C", red), Lmx1a+ (D", red), Sox2+ (E", red), and BLBP- (F", red). (G-G") Some delaminating cells are also Tbr2+. Arrows indicate delaminating YFP-positive cells. (H-I") Fate-mapping studies in P6 sagittal sections show co-localization of YFP and Ki67 (red), demonstrating that Gdf7-lineage cells contribute to proliferating cells in the EGL. Arrows indicate double-positive cells. Rectangle in (H) indicates enlarged area in (I). (J-J") Tbr2-immunostaining at P8 demonstrates that Gdf7-lineage cells can also contribute to the cerebellar population of unipolar brush cells. Abbreviations: EGL, external granular layer. uRL, upper rhombic lip. RP, roof plate. Scale bar, 20 μm.

Figure 2.6.

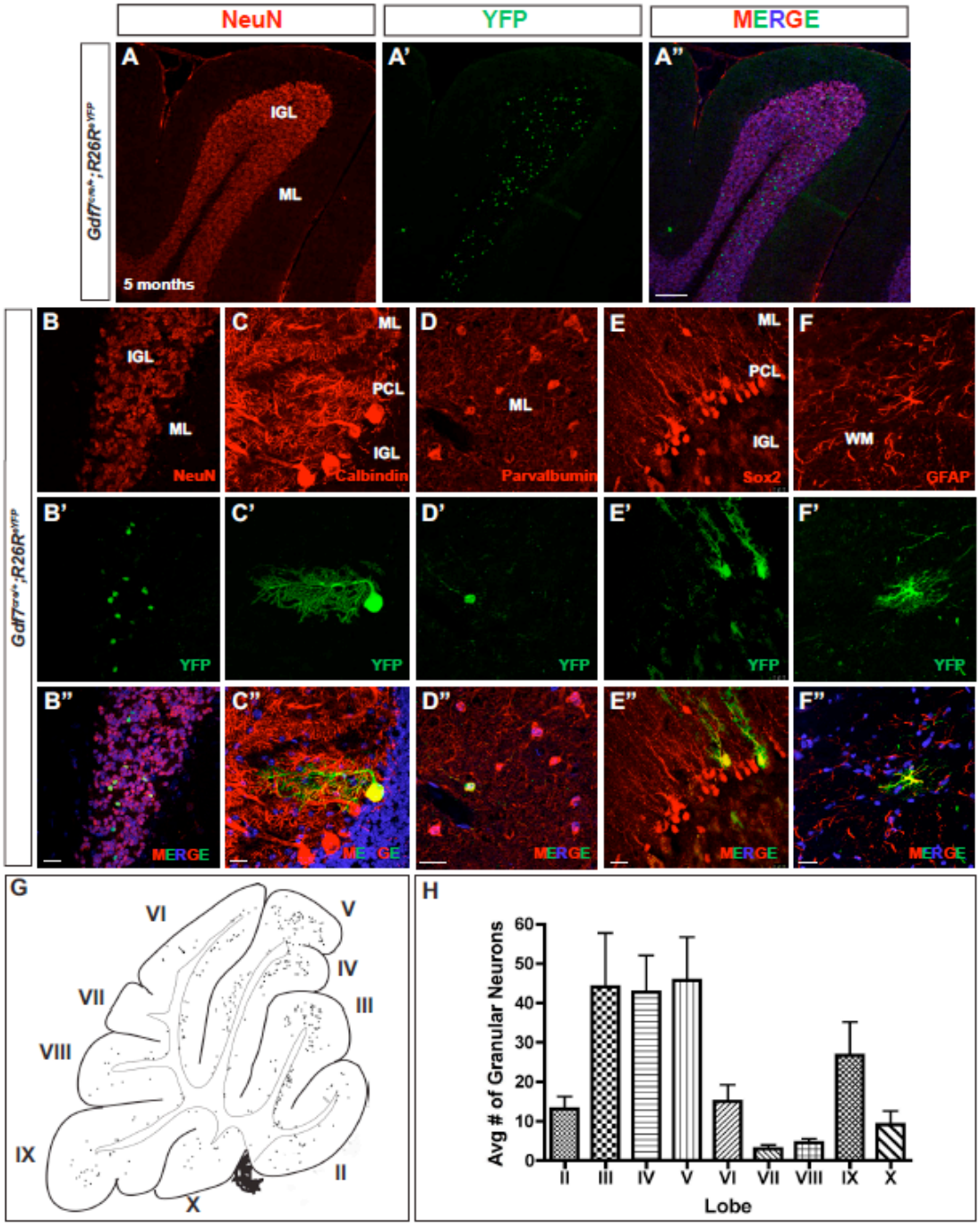
NeuN
YFP
MERGE
A
A'
A"
IGL
ML
5 months
B
C
D
E
F
PCL
WM
NeuN
Calbindin
Parvalbumin
Sox2
GFAP
B'
C'
D'
E'
F'
YFP
B"
C"
D"
E"
F"
MERGE
G
VI
V
IV
III
VII
VIII
IX
II
X
H
Avg # of Granular Neurons
60
50
40
30
20
10
0
II
III
IV
V
VI
VII
VIII
IX
X
Lobe

Figure 2.6. Gdf7-lineage cells contribute to an extensive array of mature cerebellar cell types

(A-F") Fate-mapping studies in *Gdf7*$^{Cre/+}$*;ROSA26*^{eYFP} adult mice (age 5 months) show that Gdf7-lineage cells distribute to all the mature cerebellar tissue layers and contribute to granule neurons (A-B"), Purkinje neurons (C-C"), GABAergic interneurons (D-D"), Bergmann glia (E-E"), white matter astrocytes (F-F"), as well as non-neural hindbrain choroid plexus epithelial cells (data not shown). (G) Representative image of distribution of Gdf7-lineage cells in the adult mouse cerebellum (age 5 months). The locations of Gdf7-lineage cell nuclei (dots) were mapped by tracing from digital images of sagittal sections. Thick lines indicate the cerebellar surface; thin lines indicate the boundary between cerebellar cortex and white matter. Gdf7-lineage cells were located mainly in the internal granular layer with fewer in the PCL and ML. Cells in the IGL were concentrated in lobules III-V and IX. Roman numerals indicate lobules of the vermis. (H) Quantification of YFP+ granule neurons in the IGL per lobule. Data are mean of n = 10 sagittal sections of *Gdf7*$^{Cre/+}$*;ROSA26*^{eYFP} age 5 months. Abbreviations: EGL, external granular layer. ML, molecular layer. IGL, internal granular layer. WM, white matter. Scale bar, 100 μm.

DISCUSSION

In this study we have discovered that Gdf7 lineage cells contribute to diverse cell types in the cerebellum. This observation is surprising given that previous studies using the same *Gdf7*$^{Cre/+}$ driver line reported that Gdf7 lineage cells do not contribute to the cerebellum (Lee, Dietrich, and Jessell 2000; Chizhikov et al. 2010). The contribution of Gdf7 lineage cells constitutes a minor percentage of each cerebellar cell type (<0.1% to ~3.5%), which likely explains the discrepancy in findings. Indeed, the cerebellar oncogenic transformation that we observed in *Gdf7*$^{Cre/+}$*;SmoM2* mice served as a sensitive method for uncovering the important and broader lineage potential of hindbrain roof plate cells. Our studies indicate that the cerebellar cell types derived from Gdf7 lineage include both neuronal and non-neuronal cells that originate from two distinct Gdf7-expressing domains within rhombomere 1 (rh1). The first domain is located in the midline of the cerebellar ventricular zone and consists of a small cluster of cells expressing radial glial markers. As radial glial cells are multipotent progenitors that contribute to different cell types in the cerebellum (Anthony et al. 2004; Zhang et al. 2010), and the cerebellar ventricular zone is the sole source of Purkinje cells and other GABAergic cell types including interneurons (Sillitoe and Joyner 2007), these midline cells are likely the progenitors for Purkinje cells, GABAergic interneurons, Bergman glia, and astrocytes that we observed in our Gdf7-lineage analysis. Our data provides evidence that, similar to the cortex, midbrain, and spinal cord (Lee, Dietrich, and Jessell 2000; Monuki, Porter, and Walsh 2001; Dymecki and Tomasiewicz 1998), the hindbrain roof plate has a conserved role in the generation of neurons and other cell types. This region can be molecularly defined by the expression of *Gdf7* and *Msx1* (Figure 2.4). We propose that this cerebellar vermal region is a previously undescribed source of neurons

that is continuous with and extends beyond the cerebellar ventricular zone.

Gdf7, along with other Bmps, has been shown to be capable of inducing CGNP marker expression in cultured neural tissue (Alder et al. 1999). In addition, genetic ablation of Gdf7-expressing cells using diptheria toxin results in complete loss of Math1+ cells and reduced numbers of Ptf1a, Lhx1/5, and Lmx1a-expressing cells and their improper positioning in the developing cerebellar anlage (Chizhikov et al. 2006). The fact that both *Gdf7* and *Msx1*, a readout of the Bmp signaling pathway, are expressed in this central vermal region (Figure 2.4) suggests that continuous local signaling is occurring. Thus there is a strong possibility that Gdf7 is involved in providing local and perhaps even autocrine signals for specification of cerebellar cellular subtypes originating from this vermal ventricular zone, in a manner consistent with its role in the differentiation of dorsal interneurons in the spinal cord (Lee, Mendelsohn, and Jessell 1998) and in regulating the number of cortical ventricular zone progenitors in the developing telencephalon (Monuki, Porter, and Walsh 2001). Indeed, *Gdf7* is present in the hindbrain dorsal midline beginning at E10.5 (Chizhikov et al. 2006) until at least E16.5 (Figure 2.4, Supplementary Figure 2.1); *Msx1* expression is present at least until E14.5 (Figure 2.4). Purkinje precursor cells continue to proliferate in the cerebellar ventricular zone from E10 to E13 (Sillitoe and Joyner 2007; Inouye and Murakami 1980), after which they begin radial migration to form a monolayer in the adult cerebellum.

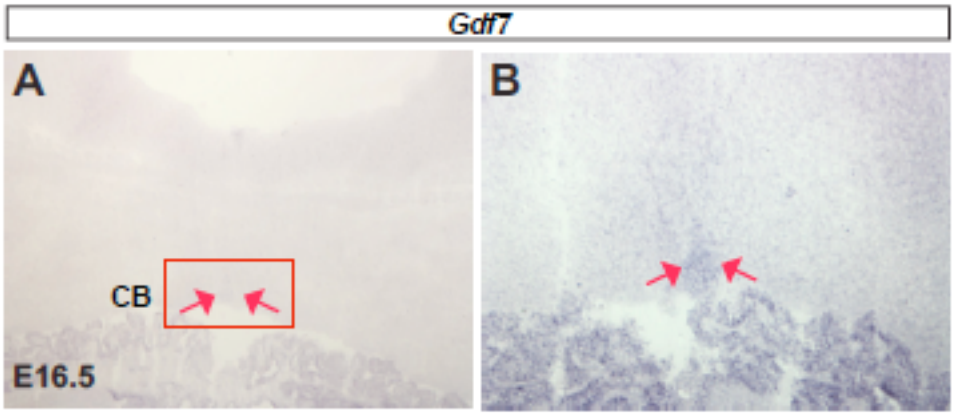

Figure 2.7. (A-B) In situ hybridization at E16.5 shows *Gdf7* expression persists in the cerebellar vermis.

The other domain of Gdf7 expression occurs distal to the upper rhombic lip, in the hindbrain roof plate epithelial (hRPe) cells and incipient choroid plexus (Chizhikov et al. 2010; Hunter and Dymecki 2007) (Figure 2.4). Recent fate mapping studies showed that Lmx1a activity is required to prevent Gdf7-expressing hRPe cells from acquiring upper rhombic lip-derived neuronal lineages including CGNPs (Chizhikov et al. 2010). However, Lmx1a progenitors themselves also contribute to the neuronal lineage in the cerebellum (Chizhikov et al. 2010). Moreover, in contrast to posterior rhombomere-derived hRPe cells that express choroid plexus markers upon their emergence from the Gdf7+ lineage at E9.5, the rh1-derived hRPe cells remain molecularly naïve and do not begin to differentiate into hChPe until E13 (Hunter and Dymecki 2007). This observation suggests that Gdf7+ progenitors distal to the upper rhombic lip are not necessarily restricted to the choroid plexus lineage. Indeed, we found delaminating Gdf7-lineage cells beyond the clustered roof plate cells in the rhombic lip as well as in the EGL. These lineage tracing studies provide evidence that hRPe cells normally give rise to CGNPs.

Our studies show that delaminating Gdf7-lineage cells in the rhombic lip are Math1-/Lmx1a+/Sox2+ neural progenitor cells. These findings support previous studies

suggesting molecular heterogeneity within rhombic lip progenitors (Hunter and Dymecki 2007) rather than the classical definition of the rhombic lip as a homogenous Math1+ progenitor population (Machold and Fishell 2005; Wang, Rose, and Zoghbi 2005). These cells however retain the capacity to express Math1 and eventually contribute to the Math1 lineage (Figure 2.5). A previous inducible genetic fate mapping study showed that RL progenitors born early (E13.5) give rise to granule cells that will populate the anterior lobes, whereas later born RL progenitors (E15.5 to E18.5) give rise to granule cells that will populate the posterior lobes (Machold and Fishell 2005). Interestingly, we found Gdf7-lineage contribution to granule cells in all lobes with the majority being in the anterior lobes III-V and posterior lobe IX, suggesting that Gdf7-lineage CGNPs are generated unevenly throughout the duration of rhombic lip CGNP production. Another low-represented precursor type similar to Gdf7-lineage CGNPs is Olig2 precursor cells (Schüller, Ruiter, et al. 2008). Olig2 lineage cells populate lateral caudal folia (lobes IX and X) and *Olig2-Cre;SmoM2* tumors correspondingly have a posterior lateral location. The factors responsible for induction of CGNP fate from hRPe progenitors requires further study.

CGNP cells originate from the upper rhombic lip and migrate tangentially to transiently occupy the EGL, and are the cell-of-origin for Shh-dependent medulloblastoma (Yang et al. 2012; Schüller, Heine, et al. 2008). The Shh-dependent mouse medulloblastomas harbor molecular signatures associated with CGNPs. While several hedgehog-driven medulloblastoma mouse models have been generated and use Nestin, GFAP, or Math1 as driver lines for constitutive Shh pathway activity (Yang et al. 2008; Schüller, Heine, et al. 2008; Rao et al. 2003; Rao et al. 2004), our *Gdf7$^{Cre/+}$;SmoM2* medulloblastoma mouse model demonstrates how remarkably few cells are sufficient for oncogenic transformation and tumor formation. Gdf7-lineage cells contribute to approximately 3.5% of granule neurons in the mature cerebellum; the

number of delaminating Gdf7-lineage neural progenitor cells in the rhombic lip is far fewer, amounting to no more than 20-30 cells per embryo at E14.5. Furthermore, our study shows that Gdf7+ lineage cells originating from hRPe are also susceptible to oncogenic transformation in response to deregulated Shh pathway activation. Of note, we emphasize that the transformed cells are Gdf7+ lineage cells and not Gdf7+ expressing cells. Our mouse studies demonstrate that Gdf7 is not expressed in Shh MBs (Figure 2.4J); it is therefore unlikely that human SHH-MBs would express GDF7. Indeed, this observation was corroborated by an online database search that revealed no Gdf7 upregulation in human MBs across all molecular subgroups (Kool et al. 2008; Northcott, Korshunov, et al. 2011; Taylor et al. 2007; Welte 2004; Northcott, Hielscher, et al. 2011; Thompson et al. 2006) though this does not exclude the possibility that Gdf7 is expressed in a rare subset of MBs.

The multi-lineage nature of hRPe progenitors suggests that medulloblastoma originating from hRPe can be associated with aberrant choroid plexus function. Previously we have shown that Shh signaling is essential to promote hChPe expansion and that constitutive Shh pathway activation in the Gdf7 lineage can lead to an expanded choroid plexus (Huang et al. 2009). It is estimated that about 15% children diagnosed with medulloblastoma also suffer from hydrocephalus (Lang et al. 2011). While tumor obstruction of the fourth ventricle may account for some of the cases, a significant portion of patients continue to suffer from hydrocephalus after tumor resection (Toslashnnessen and Helseth 2007). Interestingly we found that overactivation of Shh pathway in the choroid plexus, while leading to an expanded proliferative domain, did not result in choroid plexus tumor formation (this study and (Huang et al. 2009)). However other signaling pathways, most notably the Notch pathway, have been implicated in the formation of choroid plexus neoplasias, as *Gdf7-Cre* driven expression of the activated ligand $Notch_{ICD}$ (Hunter and Dymecki 2007) led to persistent proliferation of hChPe cells

and retrovirus-driven expression of the ligand Notch3 (Dang et al. 2006) resulted in choroid plexus papillomas. As choroid plexus dysfunction is often linked to hydrocephalus (Fujimura et al. 2004; Filippidis, Kalani, and Rekate 2010), it is tempting to speculate that a subset of medulloblastoma patients may have defective choroid plexus function (Banka, Walsh, and Brundler 2006) and thus, a common pathological pathway and cellular origin of these diseases.

MATERIALS AND METHODS

Ethics Statement. All animal experiments were carried in accordance to protocols (M09-222 and M09-160) approved by the Vanderbilt University Animal Care and Use committee.

Mouse strains. The generation of *Gdf7*$^{Cre/+}$ mice was described previously (Lee, Dietrich, and Jessell 2000). *SmoM2* (Jeong et al. 2004), *ROSA26*^{LacZ} (Soriano 1999), and *ROSA26*^{eYFP} (Srinivas et al. 2001) mice were obtained from the Jackson Laboratory. *Gdf7*$^{Cre/+}$*;SmoM2* mice were identified by their smaller size, bulging cranium and confirmed by genotyping. *Math1*$^{GFP/GFP}$ mice were obtained from Jane Johnson, University of Texas-Southwestern. Fate-mapping studies were performed on *Gdf7*$^{Cre/+}$*; ROSA26*^{LacZ} and *Gdf7*$^{Cre/+}$*; ROSA26*^{eYFP} mice. At least three animals from control and mutants were used for each morphological/molecular analysis shown in each figure.

Histological analyses, immunohistochemistry and immunocytochemistry. Standard hematoxylin and eosin stainings were performed to compare the histological features of control and mutant mice. All immunohistochemical analyses were performed on sections collected from OCT- or paraffin-embedded tissues. Twenty minutes of antigen retrieval at 95C^{o} with citrate buffer (pH 6.0) were included for all stainings on paraffin sections. The primary antibodies used were rabbit anti-GFP, (Molecular Probe, 1:500), chicken anti-GFP, (Aves Labs, 1:200), rabbit anti-Sox2, (Millipore, 1:400), rabbit anti-BLBP, (Millipore, 1:1000), rabbit anti-Pax6, (Covance, 1:500), mouse anti-NeuN, (Millipore, 1:200), mouse anti-Nestin, (Developmental Studies Hybridoma Bank, DSHB, 1:50), mouse anti-Calbindin, (Swant, 1:500), mouse anti-Parvalbumin, (Sigma, 1:200), rabbit anti-Math1 (gift of Jane Johnson, 1:400), rabbit anti-Ki67 (NeoMarkers, 1:400), rabbit anti-GFAP (Neuromics, 1:500), mouse anti-GFAP (Neuromics, 1:200), mouse anti-Cyclin

D2 (NeoMarkers, 1:500), rabbit-anti-phospho-Rb (Ser807/811) (Cell Signaling, 1:300), mouse-anti-p27Kip1 (Transduction Laboratories, 1:1000), chicken anti-Tbr2 (Millipore, 1:100), and rabbit anti-Lmx1a (gift of Michael German, University of California-San Francisco, 1:200**)**. Immunocytochemical stainings were performed on primary *Gdf7$^{Cre/+}$;SmoM2* tumor cells (see below under Medulloblastoma cell culture) grown for 48 hours on gelatinized glass coverslips. The primary antibodies were rabbit anti-GFP, (Molecular Probes, 1:2000), mouse anti-Nestin, (DSHB, 1:500), mouse anti-Sox2, (Millipore, 1:500) mouse anti-Tuj1, (Sigma, 1:1000), mouse anti-NeuN, (Millipore, 1:1000), mouse anti-GFAP, (Neuromics, 1:1000) and mouse anti-CNPase, (Sigma, 1:1000). All fluorescent images were taken using Zeiss LSM 510 confocal microscope. Independent stainings were performed on at least three animals for each marker and representative images are shown.

X-gal staining and transcript detection. X-gal staining for ß-galactosidase was performed according to standard protocol. Section *in situ* hybridizations were performed on 20 micron frozen sections as previously described (Litingtung and Chiang 2000). The following cDNAs were used as templates for synthesizing digoxygenin-labeled riboprobes: *Gdf7* (Tom Jessell, Columbia University)*, Gli1* (C-C Hui, University of Toronto)*, Patched1* (Matthew Scott, Stanford University)*, Nmyc* (Mary E. Palko, NCI)*, Math1* (ATCC, I.M.A.G.E. No. 6530849)*.*

Medulloblastoma cell culture. Medulloblastoma tissue dissociation and tumor cell culturing were performed essentially as previously described (Huang, Ketova, et al. 2010). Specifically, tumor-bearing cerebella in *Gdf7$^{Cre/+}$;SmoM2* mice over 14 days old were dissected in sterile, ice-cold PBS, minced with 50% Accutase in PBS for 5 minutes followed by repetitive pipeting with Pipetman (P1000) for 3 minutes, then cell pellets

were collected after brief centrifugation. Pelleted cells were then resuspended in neural stem cell culture medium and plated in a gelatinized 60mm tissue culture dish. The stem cell culture medium is composed of Neurobasal medium with glutamine, N2, B27, 25 ng/ml human EGF and 25 ng/mL basic FGF. Unattached cells were removed by changing medium on the following day after initial seeding, then medium was changed every four days. All experiments using primary mouse MB cells were performed within 3 passages. For differentiation conditions, EGF and bFGF were withdrawn and 10% FBS added for 5-7 days.

ACKNOWLEDGEMENTS

I would like to thank Xi Huang for his contributions and discussions to this project. We are grateful to Tom Jessell and Jane Dodd for providing the *Gdf7*$^{Cre/+}$ mice, and to Jane Johnson and Trish Savage for providing the *Math1*$^{GFP/GFP}$ mice. We are also grateful to Michael German for providing the rabbit anti-Lmx1a antibody. We thank Ty Abel for expert review of medulloblastoma pathology. We acknowledge Sean Schaffer at the Vanderbilt University Cell Imaging Shared Resource for use of the confocal microscope.

CHAPTER III

GLIAL SONIC HEDGEHOG SIGNALING ACTIVITY IS REQUIRED FOR PROPER CORTICAL EXPANSION AND CEREBELLAR ARCHITECTURE

INTRODUCTION

Cerebellar development proceeds in a tightly regulated manner, requiring the proper balance of neural progenitor cell expansion and differentiation to form a characteristically organized structure. However, our understanding of the cellular relationships and signaling pathways that contribute to this balance is incomplete. A cell type integral to development of the cerebellum is the cerebellar granular neuron precursor (CGNP), which occupies a transient layer on the outer surface of the cerebellum from embryonic day 14 to two weeks postnatally in mice. CGNPs proliferate in response to Sonic hedgehog (Shh) ligand, which is secreted by neighboring Purkinje cells (PC). The Shh signal is transduced in CGNPs by the Smoothened (Smo) transmembrane protein to initiate production of activator forms of the Gli transcription factors (Goodrich et al. 1996; Ingham and McMahon 2001; Marigo et al. 1996; Varjosalo and Taipale 2008; Fuse et al. 1999). After exiting mitosis, differentiated granular neurons migrate inward, past the PC layer, where they populate the internal granular layer (IGL). CGNPs are the presumed cell-of-origin for the Shh-driven subset of the malignant pediatric brain tumor medulloblastoma; thus understanding the cellular and molecular factors that govern their proliferation is critical.

Neuronal progenitors including CGNPs are often in close contact with glial cells (Shiga, Ichikawa, and Hirata 1983; Buffo and Rossi 2013), however relatively little attention has been given to the function of neuron-glial interactions in the cerebellum. Specialized, unipolar astrocytes called Bergmann glia (BG) are present in the

cerebellum and originate from radial glia of the cerebellar ventricular zone. As early postnatal cerebellar development proceeds, BGs migrate behind PCs, ultimately aligning their cell bodies in the same single-celled layer. Their characterized functions in the cerebellum are three-fold. First, BG radial fibers extend to the pial surface shortly after birth where their endfeet contact the basement membrane (Rakic 1971; Yamada et al. 2000). The endfeet adhere to one another to form a glia limitans over the cerebellum (Das 1976), providing structural support as the cerebellar plate expands (Hausmann and Sievers 1985; Sievers and Pehlemann 1986; Sievers et al. 1981). Second, as granular neurons differentiate and begin to migrate inwards to form the internal granular layer, BG radial fibers function as guides to the closely aligned CGNP cell bodies (Palma et al. 2005; Ruiz i Altaba 1998). And last, BG radial fibers synapse on PC dendrites; it has been proposed that BGs contribute to PC dendritic elaboration (Zecca, Basler, and Struhl 1995; Mullor et al. 1997) and stabilization of neuronal synaptic connections (Iino 2001; Yue 2005).

BGs belong to a select group of specialized astroglia that retain radial glial-like morphology postnatally and into adulthood; members of this group include BGs, Muller cells in the retina, and tanycytes of the hypothalamus (Rakic 2003). Importantly, while both Muller cells and tanycytes have been demonstrated to have neurogenic potential and contribute to neurogenesis in their respective regions (Haan et al. 2013; Surzenko et al. 2013; Robins et al. 2013), BGs have not been found to display such features. Rather, mice with BG defects during development exhibit altered cerebellar layering, neuronal migration, synaptic connectivity, and a disrupted pial membrane (Belvindrah et al. 2006; Graus-Porta et al. 2001; Wang et al. 2011; Eiraku et al. 2005; Komine et al. 2007; Weller et al. 2006). The contribution of BGs to neuronal specification and proliferation in the cerebellum has not been extensively studied.

Many signaling pathways are important for the formation and maintenance of BGs. Genetic studies using mice that lack Notch pathway components have demonstrated the pathway to be integral for BG specification, maturation, and monolayer formation (Eiraku et al. 2005; Komine et al. 2007; Weller et al. 2006). Other studies have shown that PTEN and integrin-linked kinase play roles in BG differentiation (Yue 2005; Belvindrah et al. 2006), whereas APC maintains BG morphology (Wang et al. 2011) and the guanine nucleotide exchange factor Ric-8a regulates BG basement membrane adhesion (Ma, Kwon, and Huang 2012). A recent single-cell transcriptional profiling study of BGs also identified the Wnt and TGFß signaling pathways as developmentally upregulated in BG though their function in BG has yet to be identified (Koirala and Corfas 2010). Interestingly, BGs have been shown to be capable of responding to Purkinje-derived Shh signals in postnatal stages through adulthood (Corrales et al. 2004; Corrales et al. 2006). It has been observed that Shh signaling induces the glial differentiation of immature postnatal mouse astroglia *in vitro* (Dahmane and Ruiz i Altaba 1999). In addition, inhibition of Shh activity using 5E1 hybridoma cells injected into chick embryos at early stages resulted in massive perturbations of cerebellar development, including a concomitant reduction in BLBP+ BG (Dahmane and Ruiz i Altaba 1999) (Dahmane and Ruiz i Altaba 1999). However the role of Shh signaling activity in BG *in vivo* and its consequences for cerebellar development are not well understood. Understanding how Bergmann glia contribute to CGNP proliferation and thus overall architecture of the cerebellum can shed light on basic developmental processes and have implications for cerebellar diseases that derive from aberrant Shh signaling and neuronal-glial relationships.

In this study, we spatially and temporally alter Shh signaling activity specifically in postnatal BG. Mice in which Shh activator Smoothened (Smo) is postnatally ablated in BG demonstrate an obvious reduction in cerebellar size within two days of ablation of

Shh signaling. Surprisingly, mutant CGNPs exhibit severely reduced proliferation and increased differentiation accompanied by a loss of Shh activity, suggesting a novel role for the BG-CGNP interaction in promoting CGNP precursor proliferation. Interestingly, Wnt signaling is ectopically elevated in TNC mutant CGNPs concomitant with a reduction in EGL area, suggesting that this pathway is involved in cross-talk with the Shh pathway in regulating CGNP proliferation. In addition, loss of Shh signaling in BGs leads to disrupted PC laminar organization and dendritic arborization as well as BG fiber morphology, indicating that BG-Shh signaling activity contributes to the maintenance of proper cerebellar laminar formation. Collectively, these data show a previously unappreciated role for BG Shh signaling activity in the proliferation of CGNPs and preservation of cerebellar architecture, thus leading to a new level of understanding of the neuronal-glial relationship in the cerebellum.

RESULTS

Smo^{BG} mutants display a hypoplastic cerebellum

In our experiments, we used a tamoxifen-inducible Cre line *Tenascin* $C^{YFP\text{-}CreER}$ ($TNC^{YFP\text{-}CreER}$) in order to ablate Shh signaling in BG. $TNC^{YFP\text{-}CreER}$ mice express CreER and YFP as a bicistronic message from the endogenous Tenascin C (TNC) locus (Fleming et al.), submitted); thus YFP can be used to mark TNC expressing cells. We first wanted to verify that TNC-YFP+ was indeed localized to BG cells, as previously described (Bartsch et al. 1992; Yuasa 1996). Using antibodies against YFP and radial glial markers Sox2 and Blbp (Feng, Hatten, and Heintz 1994; Yamada et al. 2000) at postnatal day 1, we confirmed that TNC-YFP was expressed by Sox2+, Blbp+ BG (Figure 3.1A-D), whose cell bodies are seen in the developing cerebellar cortex with radial processes extending towards the pia matter. Notably, these TNC-expressing cells were proliferative as many of them expressed proliferative marker Ki67 (Figure 3.1E, inset and arrowheads).

In order to determine the role for Shh signaling in BG, we crossed *TNC*$^{YFP\text{-}CreER}$ mice with *Smo*$^{F/-}$ mice to generate *TNC*$^{YFP\text{-}CreER}$*; Smo*$^{F/-}$ (Smo^{BG} mutant) mice in which Shh effector protein Smoothened (Smo) is removed from TNC-expressing BG cells (Yuasa 1996). We chose to affect the time period when BG are closely apposed to their final destination between PC bodies, thus we injected one dose each of tamoxifen at P1 and P2 (Yuasa et al. 1991)**.** We began our analysis of tamoxifen-injected animals at P3 and also analyzed later stages at P4, P5, P7 and P30 (Figure 3.2A).

Interestingly, Smo^{BG} mutant mice at P5 revealed a noticeably hypoplastic cerebellum, a phenotype which was observed in an obviously more severe manner at P30 (Figure 3.2B). H&E staining of sagittal sections demonstrated a reduction in cerebellar area and folia size (Figure 3.2C). By P7, a 35.8% (n = 3, p = 0.0282) reduction in cerebellar area was observed (Figure 3.2C, E). At P30, the smaller cerebellar size was accompanied by a profound decrease in internal granular layer (IGL) density (Figure 3.2C).

We note that the phenotype is not as severe as other mutants with aberrant cerebellar Shh signaling, *L7*^{Cre}*;Shh*$^{F/-}$ (Lewis et al. 2004) mice, in which Shh ligand is deleted from PCs, and *Math1*^{CreER}*; Smo*$^{F/-}$ mice in which Smo is temporally ablated in CGNPs using tamoxifen at P1 and P2 (Machold and Fishell 2005). As shown in Figure 3.2D-E at P7, both the *L7*^{Cre}*;Shh*$^{F/-}$ and the *Math1*^{CreER}*;Smo*$^{F/-}$ mutants displayed a more severe cerebellar hypoplasia as compared to Smo^{BG} mutants, with a 49.7% (n = 3, p = 0.0033) and 49.8% decrease (n = 3, p = 0.0008) in cerebellar size compared to wild-type littermates, respectively. In addition, *L7*^{Cre}*; Shh*$^{F/-}$ and *Math1*^{CreER}*; Smo*$^{F/-}$ mutants lacked an EGL as would be expected since Shh signaling is required for expansion of CGNPs (Figure 3.2D) (Dahmane and Ruiz i Altaba 1999; Wechsler-Reya and Scott 1999; Kenney and Rowitch 2000). Taken together, these studies demonstrate that ablation of

Shh signaling in the TNC-expressing BG cell population results in severe reduction of cerebellar size.

Figure 3.1.

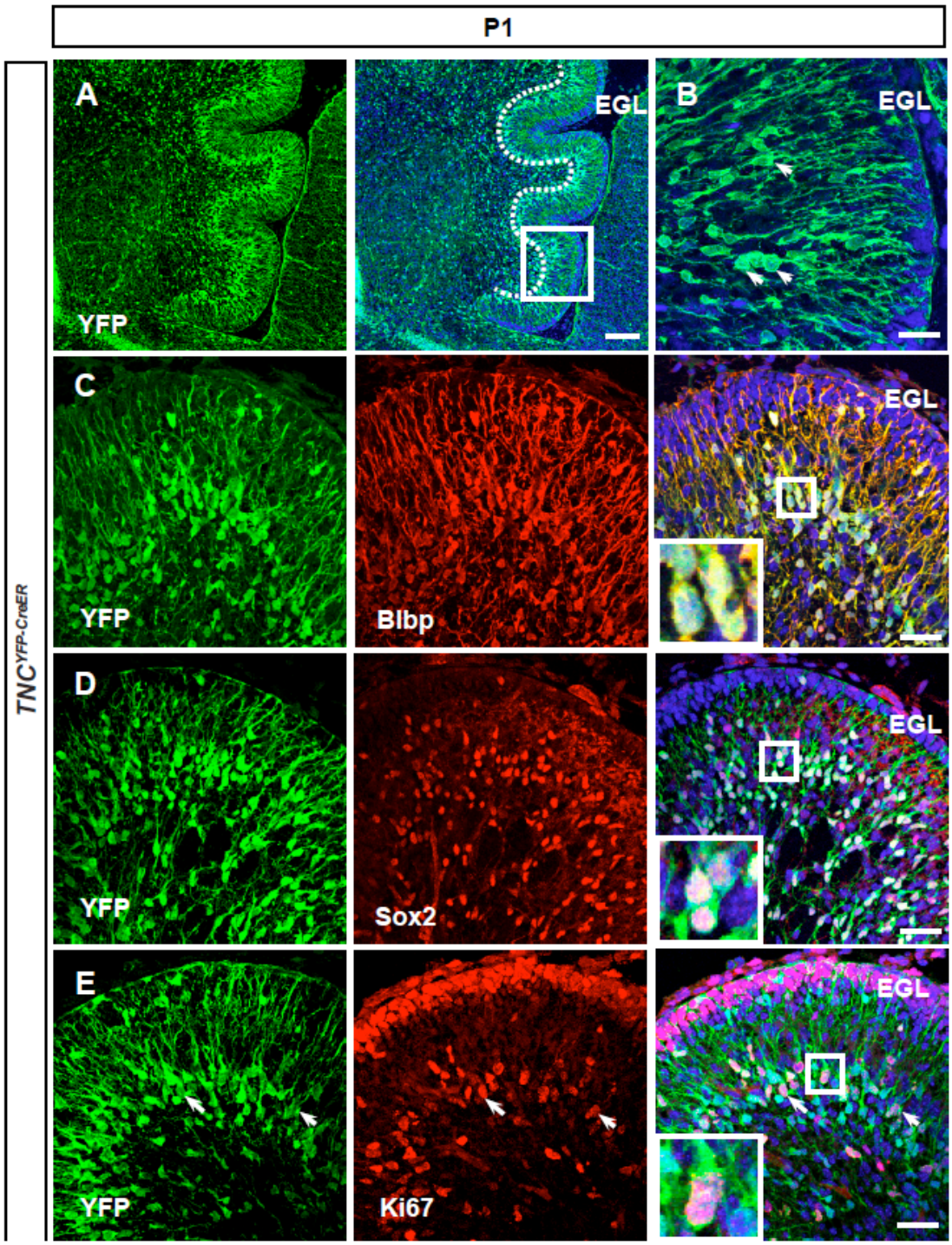
P1
TNC^YFP-CreER
A
YFP
EGL
B
EGL
C
YFP
Blbp
EGL
D
YFP
Sox2
EGL
E
YFP
Ki67
EGL

Figure 3.1. TNC-YFP-expressing cells are Bergmann glia.
(A) YFP immunohistochemistry on sagittal sections demonstrates pattern of TNC expressing cells. Boxed region denotes enlarged area in (B). Scale bar: 100 μm. (B) TNC-YFP expression is observed in cells that extend long processes to the pial surface. (C-D) TNC-YFP expressing cells are Blbp+ and Sox2+, indicating that they express astroglial markers. Inset shows example of co-labeled cell. (E) TNC-YFP expressing cells are ki67+, indicating that they are proliferative. Inset shows example of co-labeled cell. Abbreviation: EGL, external granular layer. Scale bar: 100 μm and 20 μm.

Figure 3.2

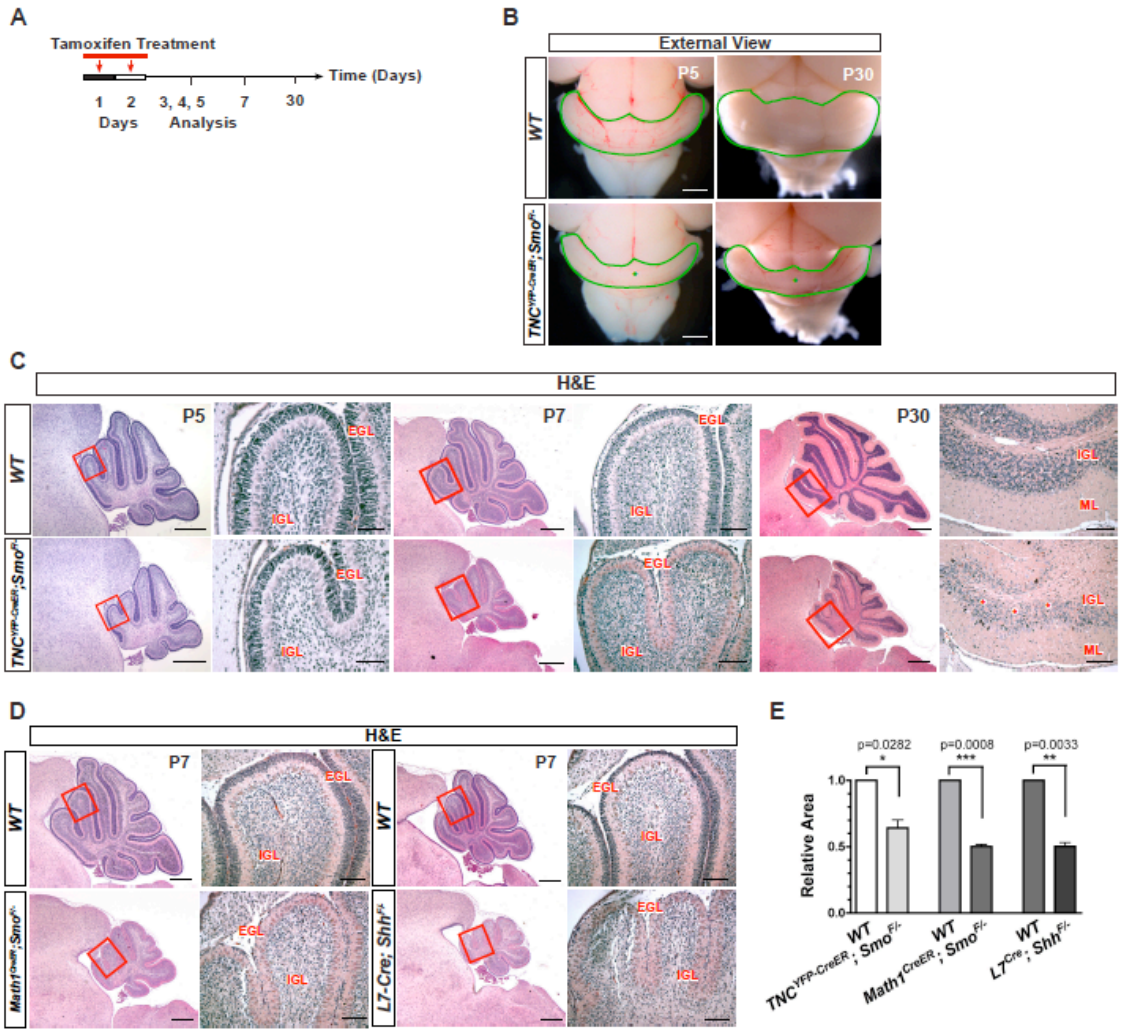
A
Tamoxifen Treatment
Time (Days)
1 2 3, 4, 5 7 30
Days Analysis
B
External View
P5
P30
WT
C
H&E
P5
P7
P30
EGL
IGL
ML
D
H&E
P7
Math1CreER; Smo
L7-Cre; Shh
E
p=0.0282
p=0.0008
p=0.0033
Relative Area
1.0
0.5
0.0
WT
TNCYFP-CreER; SmoFl-
Math1CreER; SmoFl-
L7Cre; ShhFl-

Figure 3.2. *TNC*$^{YFP\text{-}CreER}$*;Smo*$^{F/-}$ (Smo^{BG}) mutants display a hypoplastic cerebellum. (A) Tamoxifen injection scheme in Smo^{BG} mutant mice. Tamoxifen was injected at P1 and P2 in wild-type and Smo^{BG} mutants. Mice were analyzed as early as P3 and as late as P30. (B) External view of Smo mutants and wild-type littermates at P5 and P30 demonstrates the reduction in overall cerebellar size. (C) H&E staining of sagittal sections of Smo mutants and wild-type littermates at P5, P7, and P30 demonstrates that mutants have significant cerebellar hypoplasia. Boxed region shows enlarged region in adjacent panel. (D) H&E staining of sagittal sections of *Math1*^{CreER}*;Smo*$^{F/-}$ and *L7*^{Cre}*;Shh*$^{F/-}$ mutants at P7 demonstrates cerebellar hypoplasia. (E) Quantification of cerebellar area of wild-type littermates and Smo mutants, *Math1*^{CreER}*;Smo*$^{F/-}$ mutants, and *L7*^{Cre}*;Shh*$^{F/-}$ mutants. Data are mean of n=3 wild-type and littermate pairs for each genotype. Abbreviations: EGL, external granular layer. ML, molecular layer. PCL. Purkinje cell layer. IGL, internal granular layer. Scale bar: 20 μm.

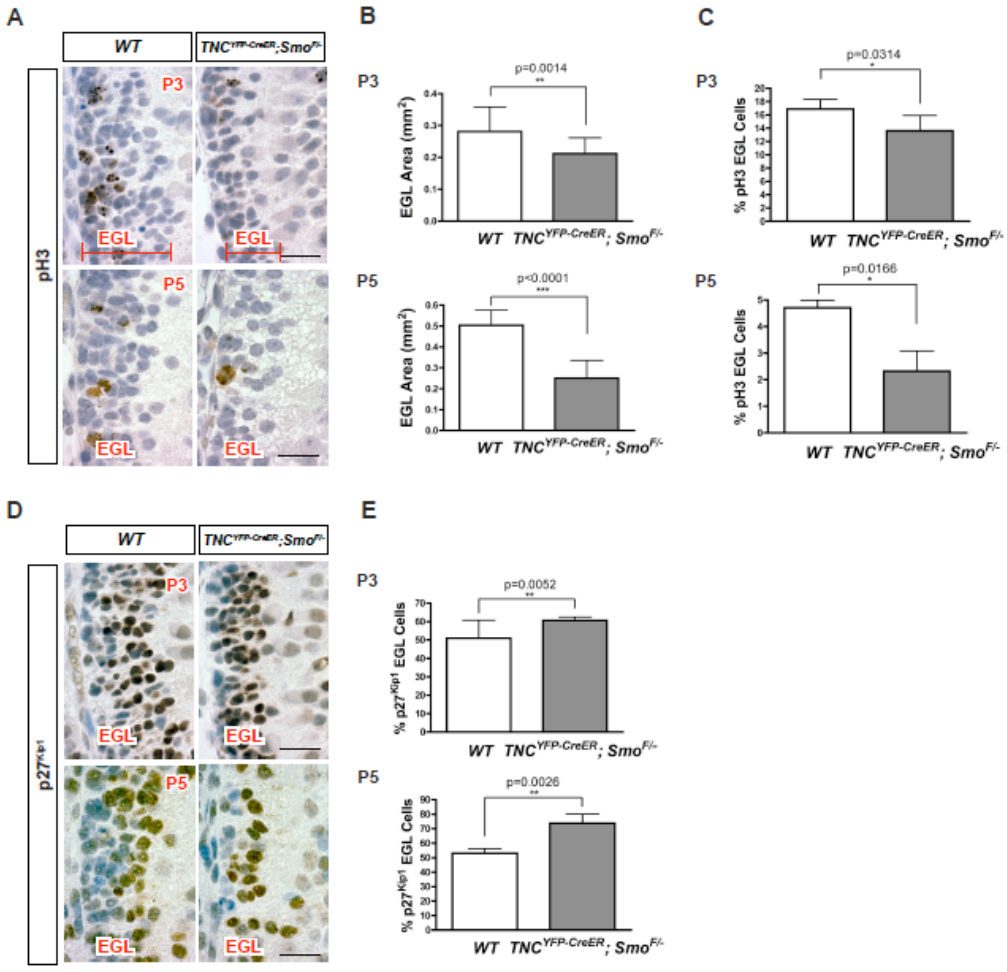

Figure 3.3. Mutant EGL is largely agranular due to severely reduced CGNP proliferation.
(A) Immunohistochemistry for pH3 at P3 and P5 in wild-type and Smo^{BG} mutants. (B) Quantification of EGL area at P3 and P5 revealed a significant reduction in mutants compared to wild-type littermates at both stages. At P3, the Smo^{BG} mutant EGL was significantly reduced in area by 24.8% (n=3, p=0.0014) and at P5, the reduction in EGL area was 50.3% (n=3, p<0.0001). (C) Quantification of pH3 staining as a percentage of total EGL cells. At P3, a 19.5% decrease (n=3, p=0.0314) in pH3 was observed. At P5, a 51.1% decrease in pH3 (n=3, p=0.0166) was observed. (D) Immunohistochemistry for $p27^{Kip1}$ at P3 and P5 in wild-type and Smo^{BG} mutants. (E) Quantification of $p27^{Kip1}$ staining as a percentage of total EGL cells. At P3, an 18.9% increase (n=3, p=0.0052) in $p27^{Kip1}$-positive cells was observed. At P5, a 39.2% increase (n=3, p=0.0026) in $p27^{Kip1}$-positive cells was observed. Abbreviations: EGL, external granular layer. Scale bar: 20 μm.

Mutant EGL is largely agranular due to severely reduced CGNP proliferation

One striking feature noted in the Smo^{BG} mutant was that, despite all cortical layers being present at early postnatal stages, the external granular layer (EGL) was noticeably reduced in thickness at P7 (Figure 3.2C). In order to determine the earliest time point at which EGL area reduction could be observed, we collected Smo^{BG} mutants at P3 and P5 and quantified the area of the EGL. At P3, the Smo^{BG} mutant EGL was significantly reduced in area by 24.8% ($n = 3$, $p = 0.0014$) (Figure 3.3A, B). By P5, the reduction in EGL area was 50.3% ($n = 3$, $p<0.0001$) (Figure 3.3A, B).

In order to determine whether the reduction in EGL thickness was due to changes in proliferation, differentiation, or apoptosis of cerebellar granular neuron precursors (CGNPs), we performed immunohistochemistry of mitotic marker phospho-histone H3 (pH3), differentiated neural marker p27Kip1, and cleaved caspase 3, respectively. At P3, we observed a 19.5% decrease ($n = 3$, $p = 0.0314$) in pH3 (Figure 3.3A, C) and an 18.9% increase ($n = 3$, $p = 0.0052$) in p27Kip1-positive cells (Figure 3.3D, E). At P5, we observed a 51.1% decrease in pH3 ($n = 3$, $p = 0.0166$) (Figure 3.3A, C) and a 39.2% increase ($n = 3$, $p = 0.0026$) in p27Kip1-positive cells (Figure 3.3D, E). No changes in apoptotic marker cleaved-caspase 3 were observed (data not shown). These results suggest that ablation of Shh signaling in BG surprisingly results in a profound reduction in CGNP proliferation with a concomitant increase in differentiation. As the current understanding of BG function during early postnatal development has been limited to their roles in CGNP migration and PC synaptogenesis (Rakic 1971; Yamada et al. 2000; Lordkipanidze and Dunaevsky 2005), these findings represent a novel role for BG in the regulation of CGNP proliferation. In addition, they demonstrate that Shh signaling in BG has a previously unappreciated role in maintaining the proliferative capacity of CGNPs.

Loss of Shh signaling is profound in CGNPs despite normal PC Shh production

It is now well-established that CGNP expansion in the EGL relies on Shh signaling activity from PCs as a proliferative signal (Dahmane et al. 1997; Wallace 1999; Wechsler-Reya and Scott 1999; Kenney and Rowitch 2000; Pons et al. 2001). In the absence of Shh signal, CGNPs stop proliferation, withdraw from the cell cycle, and differentiate (Dahmane and Ruiz i Altaba 1999; Wallace 1999; Wechsler-Reya and Scott 1999). As Smo^{BG} mutants display a profound reduction in CGNP proliferation in the EGL and an increase in differentiation (Figure 3.3), we next sought to determine whether Shh signaling activity was affected. Therefore, we crossed Smo^{BG} mutant and wild-type mice with the *Gli1*^{nlacZ} knock-in mouse (Bai et al. 2002). In wild-type animals, X-gal staining was localized to the EGL and PC layer as previously reported (Corrales et al. 2004; Lewis et al. 2004) (Figure 3.4A), indicating the presence of Shh responsive cell types in those layers. As expected, in Smo^{BG} mutants, X-gal staining was reduced in the PC layer, indicating a decrease in Shh signaling in BG (Figure 3.4A). In addition, X-gal staining was noticeably reduced in the EGL (Figure 3.4A) at P4. Likewise, ß-gal antibody staining was visibly reduced in CGNPs in the EGL in addition to the BG (Figure 3.4B). We corroborated these results by isolating fresh CGNPs from the cerebellum and blotting for Gli1 protein levels. We found that CGNPs isolated from Smo^{BG} mutant cerebella demonstrated a decrease in Gli1 and Gli2 levels as compared with those from WT cerebella (Figure 3.4C). Smo^{BG} mutant cerebellar lysates also demonstrated a decrease in Gli1 levels compared to WT cerebellar lysates (Figure 3.4D), indicating an

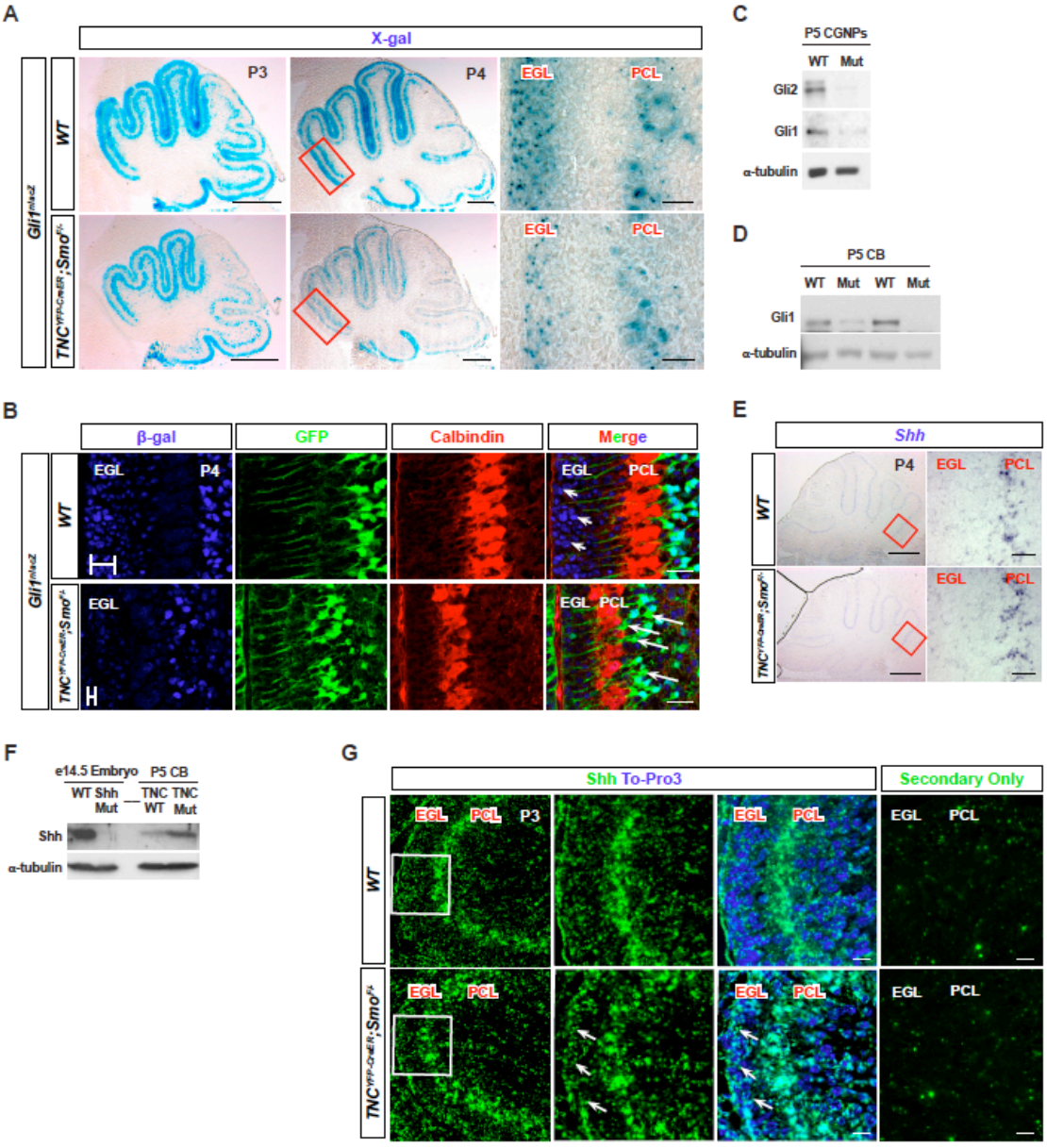
A
X-gal
P3
P4
EGL
PCL
WT
C
P5 CGNPs
WT Mut
Gli2
Gli1
α-tubulin
D
P5 CB
WT Mut WT Mut
Gli1
α-tubulin
B
β-gal
GFP
Calbindin
Merge
E
Shh
F
e14.5 Embryo
P5 CB
WT Shh Mut
TNC WT
TNC Mut
Shh
α-tubulin
G
Shh To-Pro3
Secondary Only

Figure 3.4. Loss of Shh signaling is profound in CGNPs despite normal PC Shh production

(A) X-gal staining for ß-galactosidase in *Gli1*^{lacZ} and *TNC*$^{YFP\text{-}CreER}$;*Smo*$^{F/-}$;*Gli1*^{lacZ} mutants shows that X-gal is reduced in the PCL and EGL of mutants at P3 and P4. Rectangular region in P4 panel shows enlarged area in adjacent panel. (B) Western blotting of P5 wild-type and mutant CGNPs shows a decrease in Gli1 and Gli2 protein levels in the mutant. (C) Western blotting of P5 cerebellar lysates shows a reduction in Gli2 protein levels in the mutant. (D) ß-galactosidase immunohistochemistry in wild-type and mutants reveals a decrease in antibody staining in the mutant EGL at P4. GFP and Calbindin staining demonstrates location of BGs and PCs, respectively. Arrowheads indicate presence of ß-gal+ cells in wild-type EGL, note that ß-gal expression is absent in the mutant EGL. Arrows indicate GFP+ BGs that no longer express ß-gal+, indicating a reduction in Gli1 expression in the mutant. (E) *In situ* hybridization at P4 showing *Shh* is similarly expressed in wild-type and mutant. Boxed region shows enlarged region in adjacent panel. (F) Western blotting for Shh in E14.5 wild-type and Shh-null embryos demonstrates the antibody specificity for Shh. Probing for Shh in P5 cerebellar lysates shows expression in both the wild-type and the mutant. (G) Shh immunohistochemistry (green) demonstrates Shh expression in both the wild-type and mutant EGL. Arrows indicate Shh localization to outer EGL in mutant cerebella. Secondary-only immunohistochemistry is shown as a negative control. Abbreviations: EGL, external granular layer. PCL. Purkinje cell layer. CGNPs, cerebellar granular neuron precursors. CB, cerebellum. Scale bar: 100 µm and 20 µm.

overall reduction in Shh signaling in mutant cerebella. These results demonstrate that reduction in proliferation of the EGL and subsequent differentiation of CGNPs in Smo^{BG} mutants occurs as a result of attenuated Shh signaling activity.

Given the reduction of Shh responsiveness in the EGL, we next sought to determine whether Shh production was occurring normally, and whether Shh ligand was properly reaching the EGL. Using *in situ* hybridization, we found that localization and intensity of Shh mRNA was unchanged in the PCL where the ligand is produced (Figure 3.4E). Shh ligand is made as a precursor peptide that subsequently undergoes autocatalytic cleavage and two covalent modifications to generate a 19 kDa N-terminal signaling fragment called ShhN (Porter, Young, and Beachy 1996). This fragment is the mature fragment that is released from the producing cell and can travel long distances to reach its target (Varjosalo and Taipale 2008). In order to determine whether the mature, processed fragment was produced in Smo^{BG} mutants, we harvested P5 cerebellar lysates for Western blotting and assayed for ShhN protein. The specificity of the antibody for Shh-N was verified using E14.5 WT and Shh-mutant embryos. As demonstrated in Figure 3.4F, Shh-N was present in both WT and mutant cerebellar lysates. An increase in Shh-N protein level was observed in the mutant, likely due to the fact that a higher density of Shh secreting PCs are present in a smaller cerebellum (See Figure 3.6A), thus increasing the concentration of the protein. Collectively, these results demonstrate that proper production of Shh ligand occurs in PCs of Smo^{BG} mutant cerebella.

In order to determine whether Shh ligand was reaching the EGL, we performed immunohistochemistry against Shh on both wild-type and mutant sections at P3. We found that Shh was localized to the PC layer in the wild-type and mutant, as expected (Figure 3.4G). Shh ligand was also localized to the EGL in the wild-type animals as previously reported (Lewis et al. 2004). Interestingly, we found no difference in Shh

ligand localization to the EGL in mutant animals. Our results suggest that Shh ligand is made and localized properly in the mutant cerebellum.

Resident astroglial cells in the EGL do not contribute significantly to the granular neuron population

In our characterization of the *TNC*$^{YFP\text{-}CreER}$ mouse, we observed a small subset of sparsely dispersed TNC-YFP expressing cells in the EGL (Figure 3.5A). In order to investigate their identity, we used Sox2 and Blbp to determine if they were astroglial cells because a small subset of astroglia have been described in the external granular layer (EGL) that express Sox2 and Blbp and are capable of giving rise CGNPs (Silbereis et al. 2010; Sievers et al. 1981). We found the TNC-YFP-expressing EGL cells to be both Sox2+ and Blbp+ (Figure 3.5A), suggesting that TNC-YFP marks these previously described astroglial cells (Silbereis et al. 2010).

We next determined whether these cells, in addition to BG, were Shh signaling-responsive, because if so, these cells would also undergo deletion of Smo, and could explain the reduction of CGNPs in our mutants. Using β-gal and YFP double immunohistochemistry in *TNC*$^{YFP\text{-}CreER}$;*Gli1*^{lacZ} mice at P5, we found that YFP-expressing BG located in the PC monolayer co-labeled with β-gal (Figure 3.5B), as has been previously described (Corrales et al. 2004). In addition, YFP-expressing astroglial cells in the EGL co-labeled with β-gal (Figure 3.5B), indicating that both subsets are capable of responding to Shh signaling.

Figure 3.5.

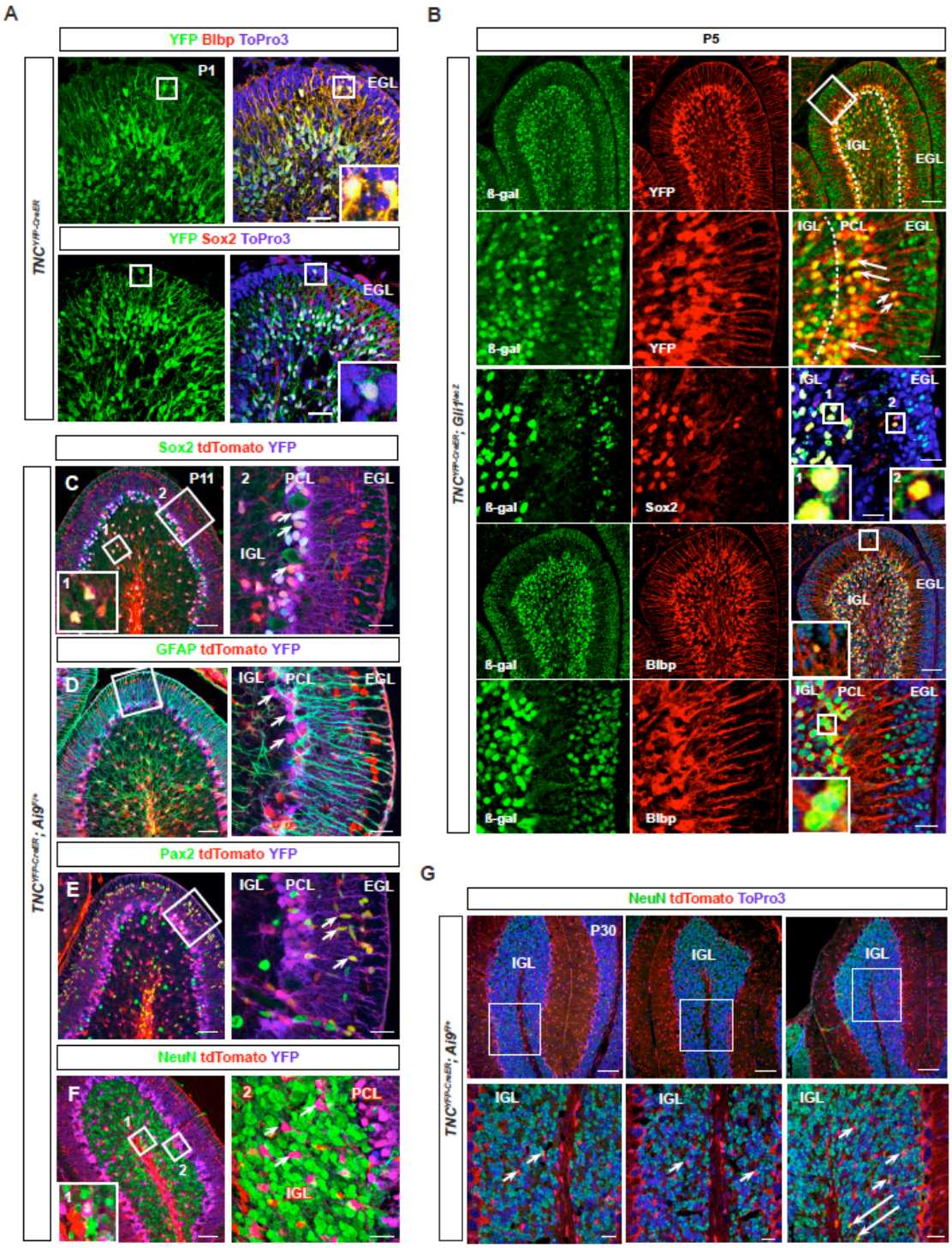
A
YFP Blbp ToPro3
P1
EGL
YFP Sox2 ToPro3
EGL
Sox2 tdTomato YFP
C
P11
2
1
PCL
EGL
IGL
GFAP tdTomato YFP
D
IGL
PCL
EGL
Pax2 tdTomato YFP
E
IGL
PCL
EGL
NeuN tdTomato YFP
F
1
2
PCL
IGL
TNC^YFP-CreER; Ai9^fl/+
B
P5
ß-gal
YFP
IGL
EGL
PCL
Sox2
Blbp
TNC^YFP-CreER; Gli1^lacZ
G
NeuN tdTomato ToPro3
P30
IGL
TNC^YFP-CreER; Ai9^fl/+

Figure 3.5. Resident astroglial cells in the EGL do not contribute significantly to the granular neuron population.
(A) YFP immunohistochemistry of *TNC*$^{YFP\text{-}CreER}$ at P1 on sagittal sections demonstrates ß-gal+-expressing cells in the EGL. These are Blbp+ and Sox2+, indicating that they express astroglial markers. Inset shows example of co-labeled cell. (B) ß-galactosidase immunohistochemistry of *TNC*$^{YFP\text{-}CreER}$*; Gli1*^{lacZ} sagittal sections at P5 demonstrates that YFP+ cells in the EGL and PCL are ß-gal+. Arrows and arrowheads indicate cells that are co-labeled with YFP and ß-gal in the PCL and EGL, respectively. ß-gal+ cells in the PCL and EGL are Sox2+ and Blbp+. Boxed regions indicate examples of co-labeled cells. (C-F) Lineage tracing using *TNC*$^{YFP\text{-}CreER}$*; tdTomato* sagittal sections at P11. (C) The majority of tdTomato+ cells are in the PCL and are Sox2+. Boxed region labeled “1” demonstrates example of Sox2+ TNC-lineage cell in IGL. Boxed region labeled “2” shows enlarged region in adjacent panel. Arrowheads indicate co-labeled cells in PCL, indicating that TNC-lineage cells are BGs. (D) The tdTomato+ cells in the EGL show GFAP+ fibers, boxed region shows enlarged region in adjacent panel. Arrowheads indicate tdTomato+ BGs associated with GFAP+ fibers. (E) Pax2 immunohistochemistry demonstrates that TNC-lineage cells found adjacent to the EGL are immature GABAergic interneurons. Arrowheads indicate co-labeled cells. (F) NeuN immunohistochemistry demonstrates that the majority of TNC-lineage cells are not tdTomato+, indicating that TNC-lineage cells do not contribute significantly to the granular neuron population. Boxed region labeled “1” shows the only example of co-labeled cell. Boxed region labeled “2” shows enlarged region in adjacent panel, and arrowheads indicate tdTomato+ cells that are not NeuN+. (G) Lineage tracing using *TNC*$^{YFP\text{-}CreER}$*; tdTomato* sagittal sections at P30 supports the data at P11 and shows that TNC-lineage cells do not contribute significantly to the granular neuron population. Arrowheads indicate tdTomato+ cells that are not NeuN+ and arrows indicate the only two examples of co-labeled cells that were observed in three lobes. Abbreviations: EGL, external granular layer. IGL, internal granular layer. PCL. Purkinje cell layer. Scale bar: Scale bar: 100 μm and 20 μm.

Because the major defect observed in Smo^{BG} mutants was reduced CGNP proliferation, we wanted to determine whether the TNC-YFP+ population residing in the EGL could contribute significantly to CGNPs, similar to what has been reported (Silbereis et al. 2010). Fate-mapping of the TNC lineage using *$TNC^{YFP\text{-}CreER}$; tdTomato* mice indicated that the majority of tdTomato+ cells in the P11 cerebellum were largely confined to Sox2+ BG (Figure 3.5C) with GFAP+ fibers (Figure 3.5D). There was a subset of Pax2+, tdTomato+ cells apposed to the EGL (Figure 3.5E), which were immature GABAergic interneurons that have not yet begun to express Parvalbumin. In order to determine whether tdTomato+ cells contributed to the mature granular neuron population, we co-labeled with granular neuron marker NeuN (Figure 3.5F). Approximately one or two cells per lobe co-labeled with NeuN, demonstrating that TNC-expressing cells can contribute to the granular neuron population, this number remained very small (no more than 1-2 per lobe, or <0.1% of total NeuN+ cells). In fact, the majority of tdTomato+ cells in the IGL were Sox2+ glial cells (Figure 3.5C). These results were corroborated by NeuN, tdTomato double immunohistochemistry in *$TNC^{YFP\text{-}CreER}$; tdTomato* mice at P30, a stage when the EGL has completely disappeared. In all lobes examined, no more than 2 NeuN, tdTomato double positive cells could be found (Figure 3.5G, arrows), and the majority of tdTomato cells in the IGL were NeuN-negative (Figure 3.5G, arrowheads). These results demonstrate that TNC-lineage cells do not contribute significantly to the adult granular neuron population. Therefore it is unlikely that the Smo^{BG} mutant EGL phenotype occurs as a consequence of attenuated Shh signaling in the EGL astroglial population rather than in BG.

Smo^{BG} mutants display altered BG arrangement and cytoarchitecture

In order to further study whether loss of Shh signaling in BG affected the cytoarchitecture of BG and other cerebellar cell types, we analyzed PC and BG arrangement, density, and morphology. At P7, Calbindin+ PCs in WT cerebella formed the single-celled layer in between the molecular layer and internal granular layer that is characteristic of normal cerebellar architecture, but, in P7 Smo^{BG} mutant cerebella, PC soma localization was disrupted with many bodies out of alignment from the single-cell layer (Figure 3.6A, starred). BG fibers form a well-organized scaffold and extend processes towards the pial membrane where their endfeet contact the pial surface, and cell bodies of BG are uniformly arranged between PC bodies in the PC monolayer. We observed that BG cell soma size, as labeled by BG cell marker Sox2, were similar between WT and mutant; however positioning of cell bodies in Smo^{BG} mutants was irregular and aberrantly disorganized such that there was a significantly increased number of Sox2+ BG per mm of PCL (68.4%, n = 3, p = 0.0339) (Figure 3.6A, arrows and graph). Rather than being localized in between PC soma, mutant BG cell bodies were displaced behind PC soma.

In order to more extensively study Smo^{BG} mutant BG fibers, we used immunohistochemistry against BLBP, GFAP, and 3-phosphoglycerate dehydrogenase (3-PGDH) (Furuya) to label BG at P3, P5, and P7. BLBP is strongly expressed in BG cell bodies and fibers at early postnatal stages and is increasingly downregulated into adulthood (Feng, Hatten, and Heintz 1994). On the other hand, GFAP expression cannot be detected in BG fibers until P5 (Piper et al. 2011) and is upregulated throughout the next two weeks as BG mature (Giménez Y Ribotta et al. 2000). The enzyme 3-phosphoglycerate dehydrogenase (3-PGDH) strongly labels BG soma and fibers throughout postnatal development and adulthood (Furuya et al. 2000).

Mutant BG were positive for Blbp (Figure 3.6B), indicating that differentiation along a glial lineage was preserved in the mutant. However, beginning at P5 we

observed an expansion of the endfeet upon contact with the pial surface, which was particularly pronounced at the fissures in BG lacking Shh signaling (Figure 3.6B, arrows). In addition, in wild-type cerebella, BG fibers were uniformly rod-like and parallel to one another as they stretched from cell body to pial surface. However in the mutant the rod-like domain was severely disrupted and tortuous with an increase in lateral branching and complexity (Figure 3.6B). 3-PGDH and GFAP expression likewise demonstrated an increased complexity of BG fibers and expansion of endfeet at the pial surface (Figure 3.6C, D, arrows), which increased in severity over time.

Because CGNPs inwardly migrate along BG fibers to form the IGL (Rakic 1971), and we observed fiber morphology differences in BG fibers in Smo^{BG} mutants, we wanted to determine whether Smo^{BG} mutants had granular migration defects. We examined mutants and wild-type cerebella at P30, a stage when the EGL has completely disappeared, using immunohistochemistry for mature granular neuron marker NeuN. We discovered that while the majority of NeuN-positive mature granular neurons in the Smo^{BG} mutant were localized to their proper location in the IGL, the molecular layer (ML) retained small ectopic clusters of cells (Figure 3.6E, arrows), indicating that some mature granular neurons had failed to migrate properly past the PC layer to the IGL. This suggests a granular neuron migration defect in the Smo^{BG} mutant. As BG fibers provide a scaffold for inwardly migrating granular neurons (Rakic 1971), this migration defect is likely due to aberrant morphological BG fibers.

Of note, the ectopic clusters were scattered throughout the ML of anterior (lobes I-IV), while the ML of central lobes (lobes V-VIII) retained fewer granular neuron clusters (Figure 3.6E). This variable phenotype by lobe is consistent with the variable expression of Shh signaling, as *Shh* mRNA and Gli1-lacZ expression are stronger in the anterior and posterior-most lobes compared to central lobes ((Corrales et al. 2004), see Fig. 4A).

Defects in BG fibers are also associated with aberrant formation or maintenance of the meningeal basement membrane, as has been demonstrated in several genetic mouse mutants with BG fiber defects (Belvindrah et al. 2006; Graus-Porta et al. 2001). Therefore we assayed for laminin expression, which revealed in wild-type cerebella that the cerebellar cortex was covered with a continuous laminin+ layer that separated cerebellar folia (Figure 3.6F). We did not see any differences in laminin staining in Smo^{BG} mutants, indicating the basement membrane of mutant cerebella is intact (Figure 3.6F).

Smo^{BG} mutants have disrupted alignment and dendritic arborization of PCs

As the radial processes of BG provide a scaffold for the directed vertical growth of PC dendrites (Lordkipanidze and Dunaevsky 2005), we examined PC morphology and dendritogenesis using immunohistochemistry for the PC-cell specific marker Calbindin (Lordkipanidze and Dunaevsky 2005). At P3, the earliest timepoint collected, we did not see a difference in PC morphology, layering, or dendritogenesis (Figure 3.7A). However as mentioned above, at P7, Calbindin+ PC soma localization was disrupted (Figure 3.6A and 7B, starred). During early postnatal cerebellar development, clustered PCs disperse into the characteristic monolayer seen in the adult cerebellum in response to Reelin secreted by the EGL (Miyata et al. 1997; Miyata et al. 1996; Schiffmann, Bernier, and Goffinet 1997). As the EGL is severely disrupted in Smo^{BG} mutants, PC soma mislocalization is likely due to a consequence of loss of CGNPs and subsequently reduced CGNP-derived Reelin signaling. Consistent with this, we found that the absolute number of Calbindin+ PCs were comparable between the WT and mutant (Figure 3.7C), however there was a significant increase in the number of PCs per mm of PCL in Smo^{BG} mutants (28.3%, $n = 3$, $p = 0.0027$) (Figure 3.7C).

Figure 3.6.

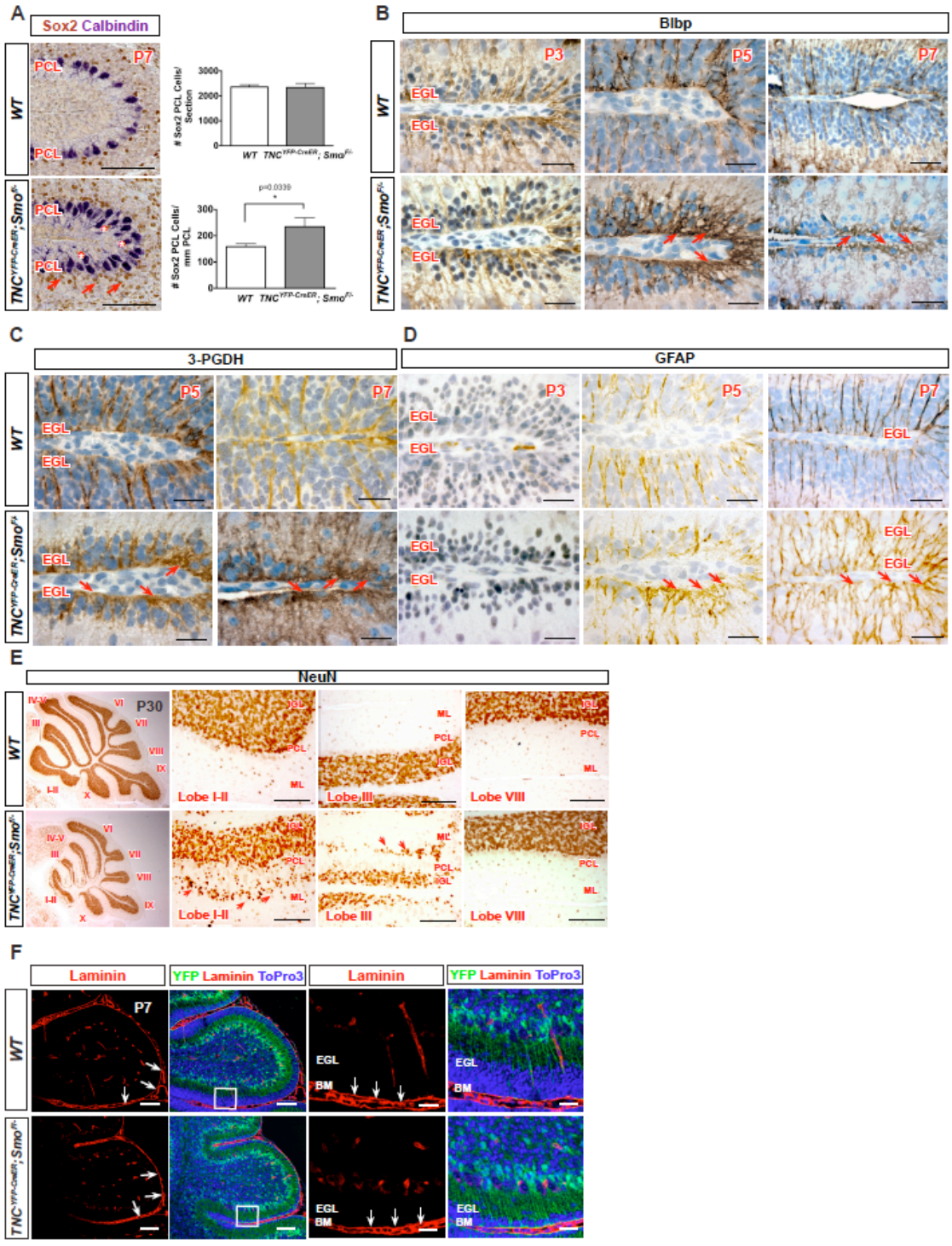
A
Sox2 Calbindin
WT
TNC^YFP-CreER;Smo^F/-
P7
PCL
# Sox2 PCL Cells/ Section
# Sox2 PCL Cells/ mm PCL
p=0.0339
WT TNC^YFP-CreER; Smo^F/-
B
Blbp
P3
P5
P7
EGL
C
3-PGDH
D
GFAP
E
NeuN
P30
Lobe I-II
Lobe III
Lobe VIII
ML
PCL
IGL
F
Laminin
YFP Laminin ToPro3
BM

Figure 3.6. Smo^{BG} mutants display altered BG arrangement and cytoarchitecture
(A) Sox2 labeling in P7 Smo^{BG} mutants demonstrate positioning of BG cell bodies in Smo^{BG} mutants is irregular and aberrantly disorganized (arrowheads). Calbindin labeling indicates disrupted PC soma localization (starred). Graph shows a significantly increased number of Sox2+ BG per mm of PCL and absolute numbers of BG are not different. Data are mean of n = 3 wild-type and littermate pairs for each genotype. (B-D) Blbp, 3-PGDH, and GFAP staining at P3, P5, and P7 demonstrate an increased complexity of BG fibers and expansion of endfeet at the pial surface starting at P5 that increased in severity at P7. (E) NeuN staining at P30 in Smo^{BG} mutants demonstrates ectopic clusters of mature granular neurons in the ML (arrowheads), suggesting a granular neuron migration defect. The ectopic clusters were scattered throughout the ML of anterior (lobes I-IV), while the ML of central lobes (lobes V-VIII) retained fewer granular neuron clusters. (F) Laminin staining for the basement membrane did not reveal any differences Smo^{BG} mutants, indicating the basement membrane of mutant cerebella is intact. Abbreviations: EGL, external granular layer. ML, molecular layer. IGL, internal granular layer. Scale bar, 100 μm and 20 μm.

While PC dendritic arborization is immature at P7 (Sotelo and Dusart 2009), dendritic tips have begun to ascend vertically and enter the base of the EGL (Yamada et al. 2000), which was observed in our wild-type cerebella (Figure 3.7B). In contrast, mutant PCs had a severely disrupted fiber network, with stunted, thinned dendrites and poorly branched arbors (Figure 3.7B, arrowheads). PC dendritic outgrowth depends on electrical activity (Schilling et al. 1991; Baptista et al. 1994) and neurotrophins secreted from CGNPs, including thyroid hormone (Heuer and Mason 2003), neurotrophin-3 (Lindholm et al. 1993), and BDNF (Shimada, Mason, and Morrison 1998). Thus, the disruption in PC arborization seen in Smo^{BG} mutants could be attributed to the loss of EGL.

However, neuron dendritogenesis can also depend on factors derived from glial cells (Martin, Brown, and Balkowiec 2012; Procko and Shaham 2010), and it has been proposed that BGs contribute to PC dendritic elaboration (Lippman et al. 2008; Yamada et al. 2000). Therefore a possibility remained that BG-Shh signaling may play a role in PC dendrite formation that was unable to be appreciated due to the severity of the reduction in EGL area in Smo^{BG} mutants. In order to investigate BG Shh signaling contribution to PC dendritogenesis independent of CGNP proliferative effects, we ablated Shh signaling in BG at later developmental stages by injecting one dose each of tamoxifen at P5 and P6 and analyzed at P8 (Figure 3.7D). This later time point enabled us to examine the cerebellar phenotype after the first wave of CGNP proliferation has taken place. Changes in cerebellar size and EGL area were less severe when BG Shh signaling was ablated at P5 and P6 compared to ablation at P1 and P2 (Figure 3.7E). Notably, the PC dendrites still lacked secondary branching structures as revealed by Calbindin immunohistochemistry (Figure 3.7F, arrows), though a BG fiber defect was not observed as determined by GFAP immunohistochemistry (Figure 3.7F). Because we

continue to observe a PC dendrite defect in the absence of a severe EGL phenotype or BG fiber morphology defects, and in the absence of severe cerebellar hypoplasia, our results suggest that proper outgrowth of PC dendrites depends on Shh signaling activity to BG.

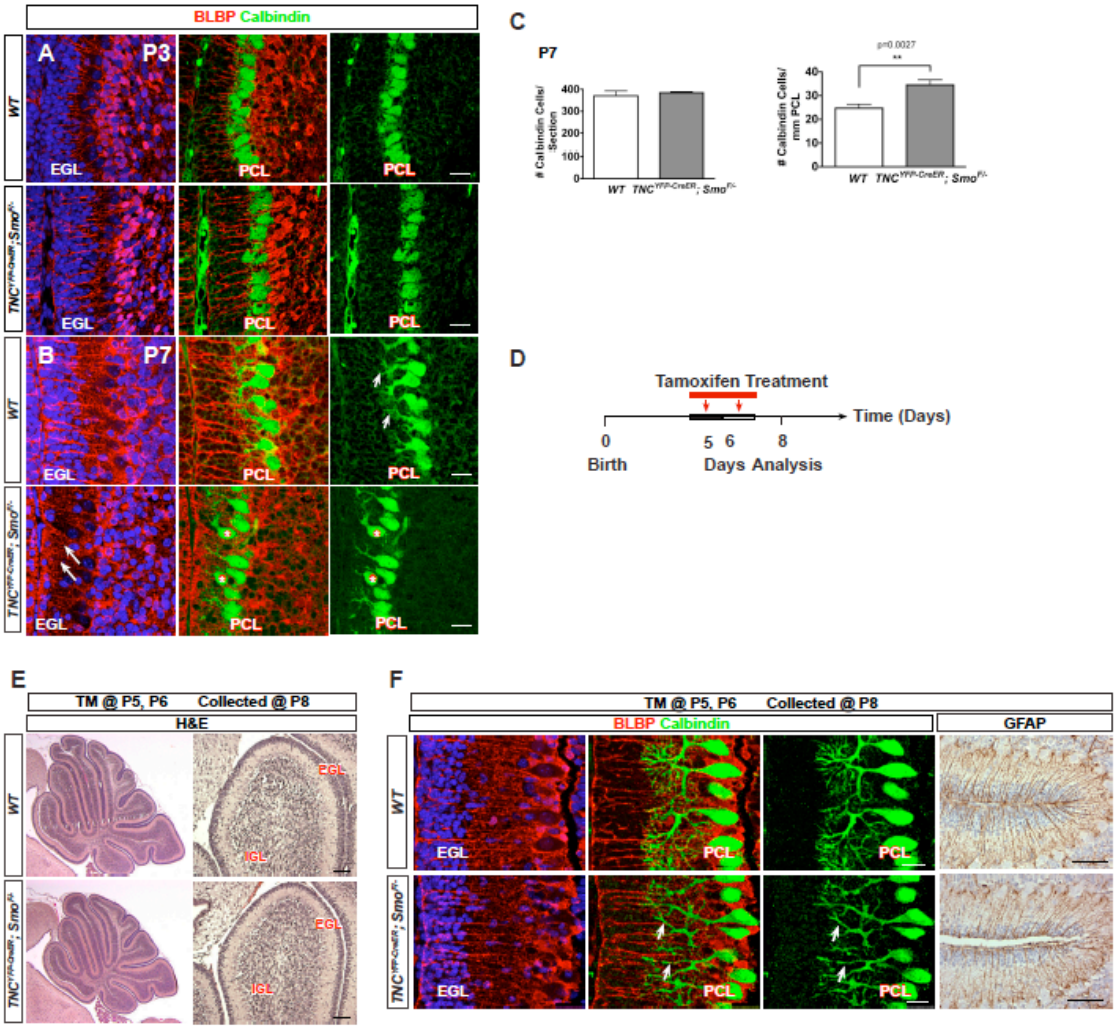

Figure 3.7. Smo^{BG} mutants have disrupted alignment and dendritic arborization of PCs

(A) At P3, Calbindin immunohistochemistry shows no difference in Smo^{BG} mutant PC morphology, layering, or dendritogenesis. (B) At P7, Calbindin immunohistochemistry shows that PC soma localization is disrupted and have a severely disrupted fiber network, with stunted, thinned dendrites and poorly branched arbors. (C) The absolute number of Calbindin+ PCs were comparable between the WT and mutant. There was a significant increase in the number of PCs per mm of PCL in Smo^{BG} mutants. Data are mean of n = 3 wild-type and littermate pairs for each genotype. (D) Tamoxifen injection scheme in Smo^{BG} mutant at later timepoints. One dose of tamoxifen was injected at P5 and P6 in wild-type and Smo^{BG} mutants. Mice were analyzed at P8. (E) H&E staining shows that changes in cerebellar size and EGL area were less severe when BG Shh signaling was ablated at P5 and P6 compared to ablation at P1 and P2. (F) PC dendrites in later timepoint-injected Smo^{BG} mutants lacked secondary branching structures as revealed by Calbindin immunohistochemistry (arrowheads) and no appreciable differences in BG fibers can be observed using Blbp and GFAP immunohistochemistry. Abbreviations: EGL, external granular layer. IGL, internal granular layer. PCL. Purkinje cell layer. Scale bar: 100 μm and 20 μm.

Smo^{BG} mutants exhibit aberrant Wnt signaling

Next we wished to determine downstream signaling pathways that could be aberrantly regulated by depletion of BG-Shh signaling in mutant cerebella, leading to the reduction in CGNP proliferation. Several studies have implicated that antagonism of the Wnt pathway is important for the maintenance and proliferation of CGNPs. First, Wnt signaling is active in the rhombic lip and early migratory CGNPs at E14.5 but not in later stages of CGNP development (Fiacco and McCarthy 2006; Perea and Araque 2007; Pascual 2005). However, while it is not detected in the EGL, Wnt signaling is active postnatally in the PC layer in S100β+ BG cells (Selvadurai and Mason 2011) and at least one Wnt ligand, Wnt3, is expressed by BGs (GENSAT Mouse Brain Atlas). Additionally, CGNP-specific deletion of Wnt inhibitor APC resulted in severely inhibited CGNP proliferation and premature differentiation (Lorenz et al. 2011) and conditional activation of Wnt signaling using a dominant active form of β-catenin in neural precursors impaired CGNP proliferation (Pöschl et al. 2013). These studies suggest that ectopic Wnt signaling to the EGL may inhibit CGNP proliferation.

Since we observed impaired CGNP proliferation in Smo^{BG} mutants, we hypothesized that Wnt signaling could be ectopically activated in the EGL. To test this hypothesis, we used a *BAT-Gal* transgenic reporter strain that expresses a lacZ gene under the control of β-catenin/T-cell factor responsive elements (Maretto et al., 2003) and has been widely used as a general reporter of Wnt/β-catenin activity. By crossing these mice with our mutants to obtain $TNC^{YFP\text{-}CreER}$; $Smo^{F/-}$; *BAT-Gal* mice, Wnt signaling activity could be examined in the EGL. In wild-type mice examined at P4, we observed very few cells expressing β-gal positivity, corroborating studies demonstrating that Wnt signaling is not normally active in CGNPs at that stage (Selvadurai and Mason 2011).

However, in the Smo^{BG} mutant we observed the presence of ectopic β-gal+ cells in the EGL of mutant mice (Figure 3.8A, arrows). These results indicate that Smo^{BG} mutant mice have enhanced Wnt signaling in CGNPs, suggesting that BG-derived Shh signaling may regulate Wnt signaling activity to the EGL.

As several extracellular modulators of the Wnt pathway are expressed in BG and CGNPs, including Wnt-inhibitory factor 1 (Wif1) and Shh target gene secreted frizzled receptor protein-1 (Sfrp1), we hypothesized that the enhanced Wnt signaling observed in Smo^{BG} mutants may be due to reduced levels of Wnt antagonist expression. Sfrp1 is a 30-kDa secreted glycoprotein that acts as an antagonist of Wnt signaling (Finch et al. 1997). It has been identified as a Shh signaling target gene, frequently upregulated in Hh-activated tumors (Romer et al. 2004), and suggested to serve as a molecular link for Shh-mediated Wnt inhibition (Katoh and Katoh 2006). Therefore we examined gene expression of *Sfrp1* in Smo^{BG} mutant cerebella using *in situ* hybridization. As seen in Figure 3.8B, *Sfrp1* is localized to the EGL in the P4 wild-type cerebellum. In TNC mutants, there was a striking decrease in *Sfrp1* expression (Figure 3.8B), a finding we confirmed by probing lysates of freshly isolated CGNPs via Western blotting (Figure 3.8C). This data indicates a downregulation of Sfrp1 expression in the EGL of TNC mutants, suggesting one possible downstream target of BG-derived Shh signaling activation. The *Drosophila* homologue of Wif1, shifted, is required for normal Shh signaling in the wing imaginal disc and has been suggested to bind *Drosophila* co-receptors of the Shh pathway, the BOC/CDO family members Ihog and Boi (Avanesov et al. 2012). This suggests that in addition to antagonizing the Wnt pathway, Wif1 may be involved in Shh signaling activation. Consistent with this hypothesis, *Wif1* mRNA is expressed in the PCL of the cerebellum (Allen Brain Atlas). Thus it is also possible that BG-derived Wif1 expression may be normally required to inhibit Wnt activity to CGNPs and allow for full activation of Shh signaling. Collectively, our data demonstrates that

ablation of BG Shh signaling in Smo^{BG} mutants results in ectopic Wnt activity in CGNPs and suggest that inhibition of the Wnt pathway is a downstream target of BG Shh signaling.

Figure 3.8.

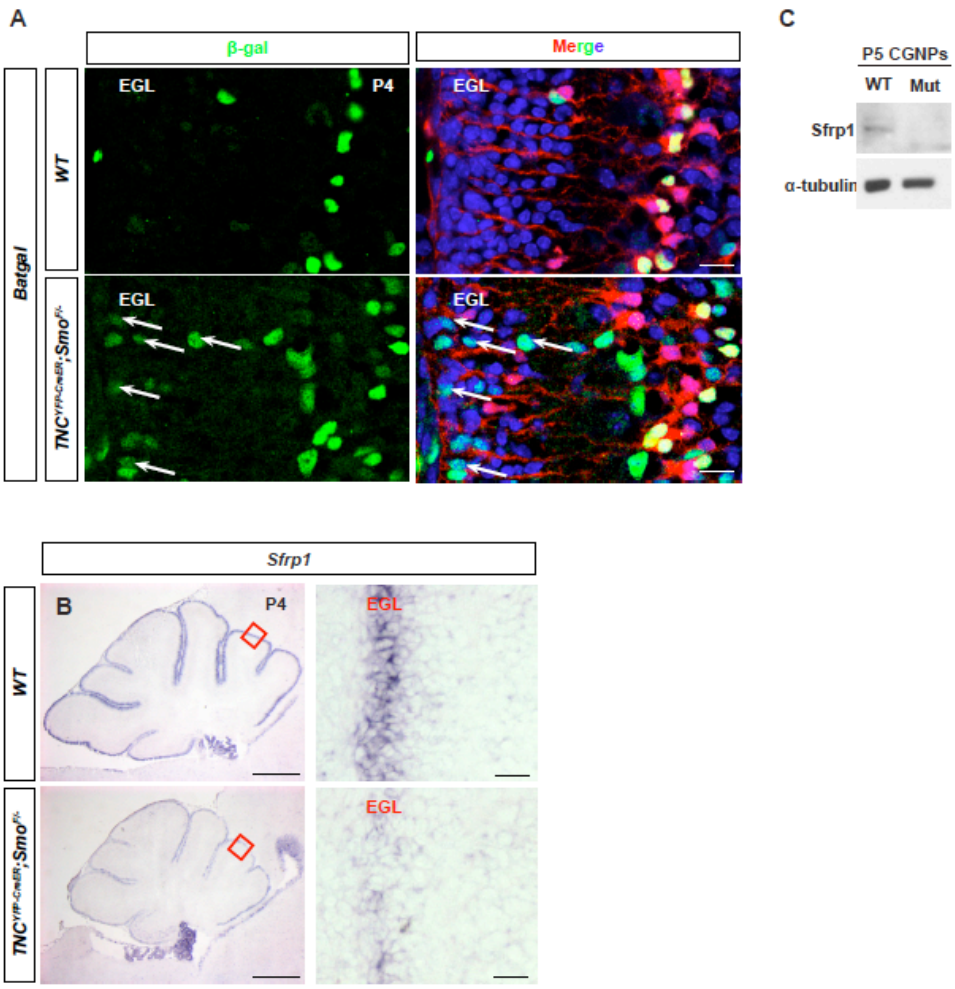
A
β-gal
Merge
Batgal
WT
TNC^YFP-CreER;Smo^F/-
EGL
P4
C
P5 CGNPs
WT
Mut
Sfrp1
α-tubulin
Sfrp1
B
WT
TNC^YFP-CreER;Smo^F/-
P4
EGL

Figure 3.8. Smo^{BG} mutants exhibit aberrant Wnt signaling
(A) ß-galactosidase immunohistochemistry in P4 *$TNC^{YFP\text{-}CreER}$; $Smo^{F/-}$; BAT-Gal* mice shows the presence of ectopic β-gal+ cells in the EGL of mutant mice (arrows), indicating that Smo^{BG} mutant mice have enhanced Wnt signaling in CGNPs. (B) *In situ* hybridization for *Sfrp1* in Smo^{BG} mutants at P4 indicates a downregulation of the mRNA in the EGL. (C) Western blotting of lysates of freshly isolated CGNPs indicates a downregulation of Sfrp1 expression. Abbreviations: EGL, external granular layer. CGNPs, cerebellar granular neuron precursors. Scale bar, 200 μm and 20 μm.

DISCUSSION

In this study, we provide genetic evidence that Shh signaling in Bergmann glia is required for proper CGNP proliferation and subsequent cortical expansion. Our study therefore provides a novel role for Shh signaling in the cerebellum—that is the non-cell-autonomous regulation of CGNP proliferation by Bergmann glia. Interestingly, Smo mutants have profound reductions in EGL area that can be observed starting 24 hours after the last tamoxifen injection (Figure 3.3A, C) and prior to observable defects in BG fiber formation (Figure 3.6). This rapid timecourse from initiation of Cre-mediated recombination to EGL size reduction in mutants demonstrates the remarkable sensitivity of CGNP proliferation to BG-Shh activity, underscoring its relevance for the maintenance of overall cerebellar size and architecture.

BGs belong to a select group of astroglia—they are astrocytic derivatives of radial glia that retain radial-glial like morphology into adulthood. While the other members of this group, retinal Muller cells and hypothalamic tanycytes, have been found to be neurogenic (Haan et al. 2013; Surzenko et al. 2013; Robins et al. 2013), BGs have not been described as such and our lineage tracing studies demonstrate that TNC-YFP cells contribute very minimally to the granular neuron population (Figure 3.5C, D). Thus it is unlikely that BG-derived neurogenesis plays a significant role during normal development. Rather, our study indicates that, in addition to their well-characterized role in providing guidance cues for the inward migration of CGNPs (Rakic 1971), BGs have a previously undescribed postnatal function in modulating proliferation of the cerebellar neuronal precursor population. This is consistent with a role for astrocytes in providing factors that support neuronal growth (Vernadakis 1988) and adds to our understanding of the neuronal-glial relationship in the cerebellum.

Although a select few other Shh-responsive cell types express TNC-YFP in the cerebellum, we conclude that the phenotype we observe is due to Shh signaling ablation in BG. Several lines of evidence support this conclusion. First, our lineage tracing studies in *TNC$^{YFP\text{-}CreER}$; tdTomato* mice indicate that the contribution of TNC-expressing cells to the granular neuron population in the IGL is insignificant, with no more than one or two per lobe in the cerebellum at P30 (Figure 3.5C, D). Thus, while the small TNC-expressing Sox2+/Blbp+ astroglial population in the EGL has been demonstrated to contribute to CGNPs (Silbereis et al. 2010) and is Shh responsive (Figure 3.5B), their contribution to the total number of granular neurons is too small to cause the severe phenotype we observe in Smo mutants. We cannot, however, exclude the possibility that these Sox2+/Blbp+ EGL cells are secreting an inhibitory factor that modulates CGNP responsiveness to Shh ligand. The difficulty of studying these cells in isolation of other radial glial cells limits our ability to draw conclusions regarding this hypothesis, as currently there is no specific marker for this cell population and their function is unknown. Nevertheless, our lineage tracing studies and the sheer number of BG cells compared to these sparsely populated EGL cells, as well as the ability of the BG fiber to reach to the pial surface and contact all CGNPs, all support our conclusion that BG Shh signaling ablation is responsible for the phenotype of Smo mutants. Additionally, the small population of TNC-expressing astroglial cells in the white matter have not been demonstrated to contact cells in the EGL.

It has been speculated that Shh signaling provides differentiation capacity for Bergmann glia (Dahmane and Ruiz i Altaba 1999). These studies were performed *in vitro* and also through the use of blocking antibodies *in vivo* at early stages in the chick embryo when Shh is important in development of the entire neural tube. Thus it has been difficult to distinguish between Shh regulation of radial glial cells and Shh signaling regulation of BG development without a BG-specific knockdown of Shh signaling. Using

the *TNC*$^{YFP\text{-}CreER}$ driver line to ablate Shh signaling in postnatal BG cells, we demonstrate that BG cell number is unchanged between the wild-type and mutant (Figure 3.6A). Indeed, BG mitotic activity peaks between P1 and P6 (Yuasa 1996) and our analysis following tamoxifen injection at P1 and P2 showed no difference in absolute numbers of BG at P7. Our findings suggest that Shh signaling in BG is not necessary for their postnatal differentiation but do not rule out the possibility that Shh signaling regulates their specification prior to birth.

There are several possibilities for how BG-Shh signaling alters CGNP Shh responsiveness. One possibility is that BG fibers are responsible for delivery of Shh ligand to the outer EGL where the bulk of CGNP proliferation takes place. PC dendrites reach only to the most superficial part of the ML, whereas BG fibers extend to the pial surface (Yamada et al. 2000). Conceivably, proteins on the surface of BG fibers could facilitate the transfer of secreted Shh ligand to CGNPs. However, our data indicate that the processed Shh ligand is produced normally by PCs in Smo mutants and is able to localize to the outer EGL. While it is possible that the dosage and concentration of Shh ligand is reduced in Smo mutants at a level that cannot be assessed by immunohistochemistry, our results suggest that Shh delivery to CGNPs does not depend on BG-Shh signaling.

Another more likely possibility is that BG Shh signaling serves to modulate levels of inhibitory secreted factors, allowing for full activation of the Shh pathway in CGNPs. Several signaling pathways have been identified that are antagonistic to Shh signaling in regulating CGNP proliferation. For example, extracellular matrix glycoproteins (Pons et al. 2001) and FGFs (Wechsler-Reya and Scott 1999) are able to differentially modulate but not completely suppress Shh-mediated proliferation of CGNPs. We however did not find differences in gene expression of FGF transcriptional target *Etv5* in Smo mutants compared to wild-type cerebella (data not shown), suggesting that FGF signaling does

not occur downstream of Shh signaling in BG. BMP2 and BMP4 significantly reduce CGNP proliferation in organotypic slice cultures (Rios et al. 2004) via the Smad signaling pathway (Zhao et al. 2008), however we did not find differences in protein localization and intensity of BMP signaling readout phospho-Smad1 (Ser463/465) (data not shown), suggesting that this pathway is also not regulated by Shh signaling in BG.

Notably, our data using *BAT-gal* reporter mice demonstrate that Wnt signaling activity is upregulated in the EGL of Smo mutants (Figure 3.8A), concomitant with a reduction in EGL area (Figure 3.3B). While we cannot rule out the possibility that the upregulation in Wnt activity is a consequence rather than a cause of BG-Shh signaling ablation, several studies have implicated that antagonism of the Wnt pathway is important for the maintenance and proliferation of CGNPs. First, Wnt signaling is active in the rhombic lip and early migratory CGNPs at E14.5 but not in later stages of CGNP development (Selvadurai and Mason 2011). Additionally, CGNP-specific deletion of Wnt inhibitor APC resulted in severely inhibited CGNP proliferation and premature differentiation (Lorenz et al. 2011) and conditional activation of Wnt signaling using a dominant active form of ß-catenin in neural precursors impaired CGNP proliferation (Pöschl et al. 2013). Interestingly, the latter study observed a comparably severe cerebellar phenotype in their mutant mice as that seen when blocking Shh *in vivo* (Dahmane et al. 1997), with cerebellar hypoplasia with a thinned EGL, abnormally positioned Purkinje cells, and reduced Bergmann glia (Pöschl et al. 2013). Thus Wnt signaling to the EGL is likely inhibited during normal cerebellar development to allow for complete Shh pathway activation. Our results indicate that BG Shh signaling is involved in Wnt signaling antagonism. The source of the Wnt signal to the EGL may very well be BGs as Wnt3 is expressed in BG (Gensat Brain Atlas). While we do not find differences in Wnt3 gene expression in Smo mutants (data not shown), several extracellular modulators of the Wnt pathway are expressed in BG and CGNPs, including Wif1 and

Shh target gene Sfrp1. Notably, we detect a substantial downregulation of EGL *Sfrp1* expression in Smo mutants, suggesting at least one possible mediator of Wnt inhibition that may be downstream of BG-Shh signaling.

Our study of BG fiber morphology demonstrates that Shh signaling in BG is required for proper BG fiber expansion, as BGs of Smo mutants display expanded endfeet and increased lateral branching (Figure 3.6B-D). However, an EGL area reduction is observed prior to detection of BG fiber defects, which are noticeable at P5. Thus we conclude that the aberrant growth of BG fibers is secondary to the reduction in EGL area and subsequent hypoplasia. Consistent with this hypothesis, we observe a similar increase in BG lateral branching and thickening of fibers in $Math1^{CreER};Smo^{F/-}$ mice which lack an EGL (Figure 3.7D).

Our results also indicate that Shh signaling in BG is necessary for proper PC soma localization and dendritic arborization. Post-mitotic PCs migrate from the ventricular zone to form clusters in the postnatal cerebellum, and cluster dispersal depends on CGNP-derived Reelin signaling. As the EGL in our mutants is severely reduced, the disorganization of PC cell bodies is most likely due to the secondary effect of decreased Reelin secretion. These results are corroborated by similarly disrupted PC soma localization in $L7^{Cre};Shh^{F/-}$ and $Math1^{CreER};Smo^{F/-}$ mutants where the EGL is completely absent. PC dendritogenesis is a dynamic process, with constant restructuring, retraction, and regrowth of fibers. It is speculated that PC dendrites eventually use BG fibers as a guide for synaptogenesis and subsequent arborization (Wang et al. 2011; Lordkipanidze and Dunaevsky 2005; Yue 2005). We find that PC dendrite arborization in Smo mutants is reduced compared to PCs in wild-type mice (Figure 3.7A). While the PC dendrite phenotype we observe could be a consequence of disrupted BG fiber morphology, a second possibility is that PC dendritic arborization is dependent on BG Shh signaling directly. Our studies in mutant animals with later stage

tamoxifen injections indicate that the latter explanation is more likely. In these mutants, we find that cerebellar hypoplasia, EGL reduction, and BG fiber morphology are comparable to WT, whereas PC dendritic arborization defects are strikingly apparent (Figure 3.7G, H) indicating that this PC phenotype precedes the observed disruption of BG fiber morphology. The mechanism by which Shh signaling in BG regulates PC dendritogenesis requires further study.

Because CGNPs are the presumed cell of origin of MB, determining factors that inhibit their proliferation are central to the investigation of MB development and may elucidate pathways that can be exploited in the development of future therapies. Our study suggests that BG play a role in providing modulatory factors, likely involving Wnt signaling, that positively regulate Shh signaling in the postnatal EGL. Thus their potential contribution to medulloblastoma pathogenesis should not be ignored. Further studies are needed to determine the molecular mechanism by which this regulation of CGNP proliferation occurs. In addition, as Shh signaling is still active in the BG in the adult (Corrales et al. 2004), its function in BG in the adult may be very different from its early postnatal role of regulating proliferation and subsequent migration of CGNPs and needs additional investigation. Nevertheless, our mutant mouse model specifically demonstrates a requirement for Shh signaling in Bergmann glia for proper proliferation of CGNPs and multiple aspects of cerebellar architecture and lamination and therefore sheds light on the importance of neuron-glia communication in the cerebellum.

MATERIALS AND METHODS

Animals and Tamoxifen Administration. Mice of the following genetic lines, of either sex, were used in the study: *Gli1*^{nlacZ} (Bai et al. 2002), *TNC*$^{YFP\text{-}CreER}$ (gift of Wenjuan He, University of California-San Francisco, San Francisco, CA and Chuanming Hao, Fudan University, Shanghai, China), *Smo*$^{F/F}$ (Long et al. 2001), *Bat-gal* (Maretto et al. 2003), *Math1*^{CreER} (Rob Machold and Fishell 2005), *R26R*^{eYFP} (Srinivas et al. 2001), *tdTomato* (Madisen et al. 2009), *L7*^{Cre} (Lewis et al. 2004) and *Shh*$^{F/F}$ (Lewis et al. 2001). Tamoxifen (Sigma) was dissolved to a final concentration of 2 mg/ ml in corn oil (Sigma). Postnatal *TNC*$^{YFP\text{-}CreER}$*; tdTomato*, *TNC*$^{YFP\text{-}CreER}$*; R26R*^{eYFP}*, TNC*$^{YFP\text{-}CreER}$*; Smo*$^{F/-}$ (Smo^{BG}), *Math1*^{CreER}*; Smo*$^{F/-}$, and wild-type littermates received 50 µL of tamoxifen by intraperitoneal injection on P1 and P2 or on P4 and P5 where noted.

Tissue processing and Immunohistochemistry. For animals younger than P30, brains were dissected and fixed in 4% paraformaldehyde for either 4-6 hours or O/N at 4^{o} C. Animals P30 and older received 50 µL intraperitoneal injections of Ketamine and received ice-cold PBS via transcardial perfusion followed by 4% paraformaldehyde. Brains were collected and submersion fixed in 4% paraformaldehyde O/N at 4^{o}C. These tissues were either processed for frozen embedding in OCT compound or processed for paraffin embedding. Frozen tissues were sectioned on a Leica cryostat at 10 µm, paraffin embedded tissues were cut at 5 µm. Immunohistochemistry were performed as previously described (Huang et al. 2009; Huang, Liu, et al. 2010). The following primary antibodies were used on frozen and/or paraffin tissue sections: chicken α-β-Gal (ICL), rabbit α-β-Gal (ICL), rabbit α-BLBP (Abcam), rabbit α-GFAP (Abcam), chicken α-GFP (Aves), guinea pig α-Gli2 (Qin et al., 2011), rabbit α-Calbindin (Swant), rabbit α-phospho-Histone-3 (Upstate Cell Signaling), mouse α-NeuN (Millipore), mouse α-

Parvalbumin (Sigma), rabbit α-3-PGDH (Thermo-Scientific), rabbit α-Sox2 (Millipore), mouse α-Laminin (Thermo-Scientific), rabbit α-$p27^{Kip1}$ (BD Transduction Labs). For bright-field staining, species-specific HRP-conjugated secondary antibodies (Invitrogen) were used followed by incubation in DAB reaction (Invitrogen) or alkaline-phosphatase (Invitrogen). Double-labeling fluorescence immunohistochemistry was performed using species-specific, AlexaFluor-tagged secondary antibodies Alexa 488, Alexa 568, and Alexa 647 (Invitrogen) followed by counterstaining with To-pro3 iodide (Invitrogen).

X-Gal and In Situ Hybridization. X-Gal staining for β-Galactosidase activity was performed on post-fixed, frozen sections according to standard protocols. Section *in situ* hybridizations were performed using digoxygenin-labeled riboprobes as previously described (Y. Li et al. 2006; Y. Li et al. 2008). Riboprobes were synthesized using the digoxygenin RNA labeling kit (Roche). The following cDNAs were used as templates for synthesizing digoxygenin-labeled riboprobes: *Shh* and *Sfrp1 (*gift of Paula Bovolenta, Centro de Biologia Molecular Universidad Autonoma Madrid, Madrid, Spain).

GCP and Cerebellar Isolation and Western Blotting. For GCP isolation, P4 or P5 cerebella from CD1 or Smo^{BG} mice were dissected into calcium-free Hanks buffered saline solution (Mediatech) supplemented with 6 g/L D-glucose. The meninges were stripped and pooled cerebella dissociated with Accutase (Gibco) and trituration. Cells were pelleted and resuspended in Neurobasal A-medium containing 250 μM KCl, 500 μL 100X GlutaMAX I, 500μL 100X penicillin-streptomycin, and 10% FBS. Cells were passed through a 70 μm filter and incubated for two times 20 minutes on poly-d-lysine coated plates. Following the settling step, the cells remaining in the media were considered the GCP fraction and were collected, pelleted, and ready for lysis. For cerebellar isolation,

P4 or P5 cerebella from CD1 or Smo^{BG} mice were dissected and tissue mechanically dissociated by trituration. Cell or tissue lysis was performed in RIPA buffer containing 2.5 mM EDTA, 1 mM PMSF, 10 mM NEM, 0.1 mM sodium orthovanadate, 0.2 mM sodium fluoride, and EDTA-free complete mini protease inhibitor tablets (Roche), for thirty minutes, followed by boiling in SDS, and resolution on 10% SDS-polyacrylamide gels. For cerebellar Shh ligand detection, P4 or P5 cerebella from CD1 or Smo^{BG} mice were dissected and immediately boiled in SDS for 5 minutes.

Primary antibodies used for Western blotting were mouse α-Sfrp1 (Abcam, 1:500), rabbit α-Gli1 (Cell Signaling Technology #2534, 1:2000), guinea pig α-Gli2 (gift of Jonathan Eggenschwiler, 1:500), rabbit α-Shh (H160) (Santa Cruz Biotechnology, 1:500), mouse anti-α-tubulin (Hybridoma Bank, 1:10,000), mouse α-β-actin (ThermoScientific BA3R, 1:10,000).

Quantification and statistical analyses. Stained slides for quantification were scanned with the Leica SCN400 Slide Scanner and quantification was performed using the Leica Ariol Software. Statistical analyses were performed using Prism software (GraphPad).

ACKNOWLEDGEMENTS

We thank the following individuals for their contributions: Jonathan Fleming for his contributions and discussions for this project, Wenjuan He (University of California-San Francisco, San Francisco, CA) and Chuanming Hao (Fudan University, Shanghai, China) for the gift of the $TNC^{YFP\text{-}CreER}$ mouse, Jonathan Eggenschwiler, PhD (University of Georgia, Atlanta, GA) for the generous gift of polyclonal antibodies against Gli2 and Paula Bovolenta, PhD (Centro de Biologia Molecular Universidad Autonoma Madrid, Madrid, Spain) for the generous gift of the *Sfrp1* probe. For their insightful feedback and

discussion we thank members of the Chiang laboratory. Additionally, we are grateful to Joseph Roland and the Vanderbilt University Medical Center Epithelial Biology Digital Histology Shared Resource for assistance with slide scanning and quantification, and Sean Schaffer and the Vanderbilt University Cell Imaging Shared Resource for assistance with confocal imaging. We thank the DSHB that was developed with support from the NIH. This work is supported by National Institutes of Health (NIH) T32 GM007347, National Institute Of Neurological Disorders And Stroke of the National Institutes of Health under Award Number F31NS074638, and NIH NS 042205.

CHAPTER IV

ANTAGONISM OF THE HEDGEHOG PATHWAY AT THE LEVEL OF GLI TRANSCRIPTION BY THE SMALL MOLECULE 5-AMINOIMIDAZOLE-4-CARBOXAMIDE-1-ß-4-RIBOFURANOSIDE (AICAR)

INTRODUCTION

The Hedgehog signaling pathway is essential for embryonic development (Varjosalo and Taipale 2008) and has been implicated in many cancers such as basal cell carcinoma, medulloblastoma, Ewing sarcoma, and rhabdoid tumors (Teglund and Toftgård 2010). As aberrant Hh signaling is involved in the initiation and maintenance of tumor progenitor cells for a broad variety of cancers, including ones of both sporadic and heritable origins, multiple pharmaceutical companies have begun large scale drug discovery and clinical trial efforts to develop Hh pathway antagonists for therapeutic use(Ajeawung, Wang, and Kamnasaran 2013).

Hh pathway activity occurs when mature Hh protein binds its membrane receptor Patched (Ptch). Patched releases its inhibitory effect on the 7-pass transmembrane protein Smoothened (Smo) (Jiang and Hui 2008), which then accumulates in the primary cilium (Corbit et al. 2005; Kim, Kato, and Beachy 2009; Rohatgi and Scott 2007). Activation of Smo promotes the dissociation of a Suppressor of Fused (Sufu)-Gli protein complex, derepressing the Gli family of transcription factors and allowing the activated Gli proteins to enter the nucleus. The Gli proteins bind to Hh signaling target genes, including Ptch and Gli1.

Recent clinical trials have identified several promising small molecule inhibitors of the Shh pathway (Ajeawung, Wang, and Kamnasaran 2013). For example, GDC-0449 (Vismodegib), an inhibitor of the Smoothened receptor, was recently approved by the

Food and Drug Administration for the treatment of metastatic and surgically unresectable advanced basal cell carcinomas (Guha 2012). Other inhibitors currently in clinical trials include additional derivatives of the plant alkaloid cyclopamine (Heretsch, Tzagkaroulaki, and Giannis 2010; Ma, Li, and Zhang 2013) and the anti-fungal agent itraconazole (Antonarakis et al. 2013). However, the current arsenal of therapeutics in clinical trials targeting the Hedgehog pathway is limited to Smo inhibition. It is becoming apparent that a major pitfall of these inhibitors is the development of acquired resistance, as has been documented with Vismodegib among patients (Ajeawung et al. 2012; Metcalfe and de Sauvage 2011; Yauch et al. 2012). Among others, cancer cell resistance mechanisms include de novo mutations in the Smo receptor that hinder drug-binding (Yauch et al. 2012) or gene duplications of Gli2 or Shh target gene cyclin D1 that bypass the requirement of Smo to inappropriately maintain Hh pathway activity (Buonamici et al. 2010). Therefore, elucidation and development of Shh signaling inhibitors downstream of Smo can expand the current treatment arsenal to target the significant fraction of tumors that possess downstream pathway activation.

Several Gli inhibitors have been identified thus far through large-scale screens of compound libraries. GANT58 and GANT61 are two molecules (Lauth et al. 2007) with similar IC50 to cyclopamine and suppress xenografts of Gli1-positive human prostate cancer. In addition, arsenic trioxide (ATO) acts at the level of Gli transcription, either by blocking Gli2 accumulation in primary cilia and reducing Gli2 protein levels (Kim et al. 2010) or by directly binding to Gli1 and inhibiting its transcriptional activity (Beauchamp et al. 2011), resulting in inhibition of medulloblastoma growth in mouse models (Kim et al. 2010; Beauchamp and Üren 2012). ATO holds promise as a potential therapeutic agent as it is already in clinical use against acute promyelocytic leukemia. Identifying and targeting Gli modulators may thus provide strong support for the use of combined therapy to treat tumors that have developed resistance to Smo antagonists.

The adenosine analog 5-aminoimidazole-4-carboxamide-1-ß-D-ribofuranoside (AICAR) is a natural metabolic intermediate of purine biosynthesis that is present in all organisms. It has been widely used as a small molecule agonist of the heterotrimeric metabolic sensor AMP-activated protein kinase (AMPK) (Sullivan et al. 1994; Bergeron et al. 2001; Song et al. 2002; Buhl et al. 2002; Sriwijitkamol and Musi 2008b). AICAR is taken up by cells, where it is phosphorylated to AICAR-monophosphate (ZMP) and mimics an increase in AMP intracellular levels (Rattan 2005). ZMP enters the de novo synthesis pathway for adenosine synthesis to inhibit adenosine deaminase and causes an increase in ATP and adenosine levels (Rattan 2005). Downstream effectors of AMPK include important cell cycle progression factors and tumor suppressors Tuberous Sclerosis Complex (TSC2) and the mammalian target of Rapamycin (mTOR) (Kemp et al. 2003). As a potential cancer therapeutic, studies are increasingly demonstrating AICAR's effectiveness in inhibiting proliferation and inducing apoptosis of various cancer cell types, including multiple myeloma (Baumann et al. 2007), neuroblastoma (Garcia-Gil et al. 2003), glioblastoma (Guo et al. 2009), childhood acute lymphoblastic leukemia (ALL) (Sengupta et al. 2007), colon cancer (Su et al. 2007), prostate cancer (Swinnen et al. 2005), and retinoblastoma (Theodoropoulou et al. 2010). In addition, AICAR has low or no apparent toxicity in humans and has been shown to act as an *in vivo* exercise mimetic (Narkar et al. 2008). However, its AMPK-independent effects have largely remained unexplored, as well as its role in hedgehog-driven tumors including the pediatric malignant tumor medulloblastoma.

In this study we identify AICAR as a potent Hh pathway antagonist in multiple cell types, including Hh-responsive human medulloblastoma cells. Importantly, we show that AICAR acts downstream of Smo and regulates *Gli1* transcription in a proteasome-independent manner. Sufu stabilizes the Gli proteins from AICAR inhibition, as

downregulation of Shh pathway activity was more efficient in Sufu-null MEFs. Last, we find that although AICAR activates AMPK in these cell lines, inhibition of the Hh pathway by AICAR is AMPK-independent. Our findings establish AICAR as a modulator of Shh signaling in both a developmentally relevant cell type as well as medulloblastoma cells, providing an encouraging basis to further explore its full potential as an antagonist in Shh-associated tumors.

RESULTS

AICAR antagonizes Hedgehog (Hh) pathway activity in fibroblasts and CGNPs

The effect of AICAR on Shh signaling activity was assayed using the well-established Gli-dependent luciferase reporter assay. NIH-3T3 fibroblasts were transfected with a Gli-luciferase reporter and luciferase activity measured when Shh pathway agonist, Smoothened agonist (SAG) (Chen 2002), and other Hh pathway modulators were added. Cells were incubated with 50 nM SAG with or without 1 mM AICAR for 24 hours. As NIH-3T3 fibroblasts are Shh-responsive, we expectedly observed a significant increase in luciferase activity in the presence of SAG (Figure 4.1A). However, addition of 1 mM AICAR significantly downregulated luciferase activity to 15-20% of the maximum level (Figure 4.1A). As AICAR is best characterized as an AMPK agonist, we also wanted to look at effects of other known AMPK activators. Thus we assayed for the effect of 2-DG and metformin on Shh signaling activity and found that both similarly downregulated Gli-dependent luciferase activity (Figure 4.1A).

In order to determine whether AICAR downregulation of Gli1-mediated transcriptional activity was dose-dependent, we treated cells with vehicle or 0.1 mM, 0.3 mM, 0.6 mM, or 1 mM of AICAR for 24 hours. AICAR was able to inhibit Gli1 transcriptional activity in a dose-dependent manner compared to vehicle control, with an IC_{50} of 0.16 mM (Figure 4.1B). Cell viability was also evaluated in parallel to luciferase

reporters at matching doses. We did not observe any reduction in cell viability at doses up to 1 mM AICAR and concluded that reduction in luciferase activity was not mediated by cytotoxicity. In order to determine whether AICAR can downregulate Gli1 protein levels, we treated wild-type mouse embryonic fibroblasts (MEFs) with 1mM AICAR and harvested them for Western blotting at 1 hr, 3 hr, 6 hr, 9 hr, and 12 hr intervals. We observed a downregulation of Gli1 protein levels as early as 6 hrs (Figure 4.1C). Taken together, these results demonstrate that AICAR is capable of opposing Shh pathway activity in a dose- and time-dependent manner.

Next we wished to determine whether AICAR had an effect on a developmentally relevant cell population normally responsive to Shh signaling. Cerebellar granular cell precursors (CGNPs) are the proposed cell-of-origin for medulloblastoma (Z. Yang et al. 2008; Schüller, Heine, et al. 2008) and depend heavily on Hh signaling as a proliferative signal (Dahmane and Ruiz i Altaba 1999; Anna Kenney and Rowitch 2000; Wechsler-Reya and Scott 1999). Primary cultures of isolated CGNPs treated with SAG are a widely used tool to recapitulate Shh mitogenic signaling (Dahmane and Ruiz i Altaba 1999; Kenney and Rowitch 2000; Wechsler-Reya and Scott 1999; Leung et al. 2004; Kenney, Cole, and Rowitch 2003). As shown in Figure 4.1D, untreated primary CGNPs and those treated with AICAR alone show a low level of Gli1 and cyclin D1. However, 1 mM AICAR was able to potently downregulate Hh signaling in SAG-induced CGNPs as demonstrated by significantly reduced levels of Shh target genes Gli1 and cyclin D1 in a similar manner to KAAD-cyclopamine. We then wished to determine the timecourse of Gli1 downregulation by AICAR in CGNPs. Thus we treated CGNPs with AICAR and harvested them for Western blotting at 6 hr, 12 hr, and 24 hr intervals. Similar to the timecourse of downregulation in WT MEFs, we observed a downregulation of Gli1 protein levels as early as 6 hrs (Figure 4.1D).

Figure 4.1

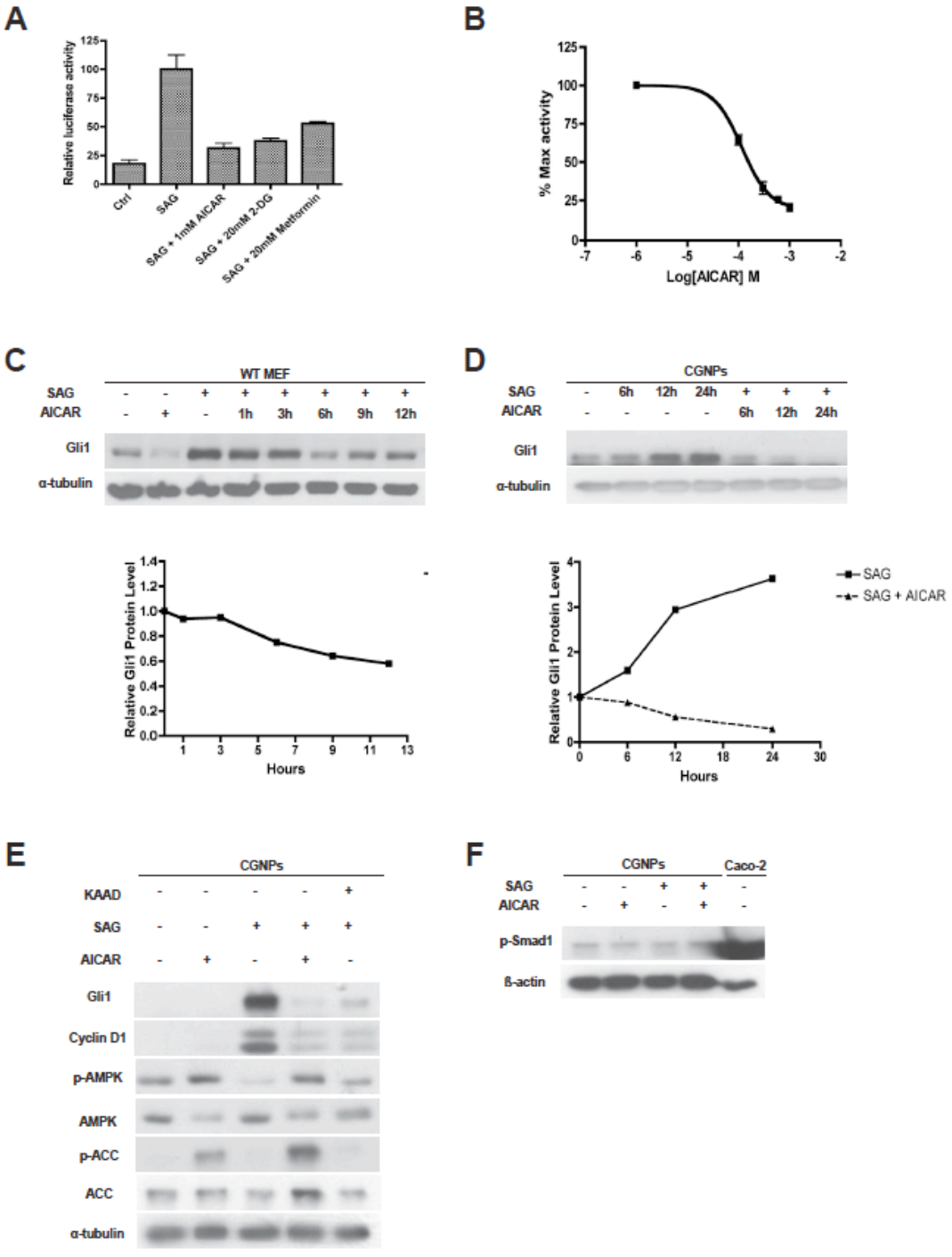
A
Relative luciferase activity
125
100
75
50
25
0
Ctrl
SAG
SAG + 1mM AICAR
SAG + 20mM 2-DG
SAG + 20mM Metformin
B
% Max activity
125
100
75
50
25
0
-7
-6
-5
-4
-3
-2
Log[AICAR] M
C
WT MEF
SAG - - + + + + + +
AICAR - + - 1h 3h 6h 9h 12h
Gli1
α-tubulin
D
CGNPs
SAG - 6h 12h 24h + + +
AICAR - - - - 6h 12h 24h
Gli1
α-tubulin
Relative Gli1 Protein Level
1.4
1.2
1.0
0.8
0.6
0.4
0.2
0.0
1
3
5
7
9
11
13
Hours
Relative Gli1 Protein Level
4
3
2
1
0
0
6
12
18
24
30
Hours
SAG
SAG + AICAR
E
CGNPs
KAAD - - - - +
SAG - - + + +
AICAR - + - + -
Gli1
Cyclin D1
p-AMPK
AMPK
p-ACC
ACC
α-tubulin
F
CGNPs
Caco-2
SAG - - + + -
AICAR - + - + -
p-Smad1
ß-actin

Figure 4.1. AICAR antagonizes Hedgehog (Hh) pathway activity in fibroblasts and CGNPs

(A) Effects of vehicle or SAG (100 nM), AICAR (1 mM), 2-deoxyglucose (2-DG) (20 mM), or metformin (20 mM)-treated on NIH-3T3 cells were assessed by relative Gli-luciferase activity. Cells were plated at ~90% confluency and treated with SAG at 10 nM for 15 hr. We observed significant increase in reporter activity in the presence of SAG. Addition of AICAR, 2-DG, or metformin significantly downregulated luciferase activity to 15-20% of the maximum level. Data represent mean of triplicates ± SD. (B) Effect of the addition of increasing doses of AICAR on NIH-3T3 cells transfected with Gli-luciferase. (C) Timecourse of SAG ± AICAR addition in wild-type MEFs of Gli1 protein levels. SAG and AICAR were added concurrently for 15 hours. (D) Timecourse of SAG ± AICAR addition in CGNPs of Gli1 protein levels. SAG (10 nM) was added for 24 hours followed by AICAR (1 mM) addition for 12 hours. (E) CGNPs were treated with SAG, AICAR, or KAAD (4 μM) and cell lysates subject to SDS-PAGE followed by immunoblotting with indicated antibodies. (F) CGNPs were treated with SAG and AICAR as in (D). Lysates and Caco-2 cell lysates (right lane) were subject to SDS-PAGE followed by immunoblotting with indicated antibodies.

AICAR is widely used as an activator of AMPK (Corton et al. 1995), which is primarily dependent on the phosphorylation of threonine-172 on the α-subunit by the upstream tumor suppressor LKB1 (Hawley et al. 2003; Woods 2003). Upon binding to AMPK, AMP or in the case of AICAR addition, ZMP, activates the enzyme up to 5-fold and enhances LKB1-dependent AMPK phosphorylation (Davies et al. 1995; Towler and Hardie 2007). In order to determine whether AICAR was capable of activating AMPK in CGNP cultures, we blotted for phosphorylated AMPK (Thr-172) (p-AMPK) and its direct substrate phosphorylated acetyl-coA carboxylase (p-ACC). We found that addition of 1 mM AICAR upregulated both p-AMPK and p-ACC (Figure 4.1E).

BMP signaling has been shown to inhibit CGNP proliferation and antagonize Shh signaling (Zhao et al. 2008), thus to examine the specificity of AICAR action, we assayed for the effects of AICAR on the BMP pathway in CGNPs. We found that 1 mM AICAR, a concentration that fully blocks SAG response, for 12 hours did not inhibit phosphorylated-Smad1 (Ser263/265) protein levels (Figure 4.1F). The human epithelial colorectal adenocarcinoma (Caco-2) cell line, which expresses high levels of BMP signaling (Wang, Davidow, et al. 2012), was used as a positive control for the α-phosphorylated-Smad1 antibody. These results exclude a general suppressive effect on signal-dependent transcriptional events as the basis for AICAR inhibition of Hh pathway response.

AICAR inhibits CGNP proliferation and growth of primary medulloblastoma cells

To determine if AICAR inhibits CGNP proliferation, we used the mitotic marker phosphorylated Histone H3 (pH3). As CGNP proliferation is SAG-dependent, expectedly SAG treatment significantly increased the number of pH3-positive cells whereas AICAR alone had no effect on CGNP proliferation. However, AICAR significantly reduced

proliferation in SAG-treated samples (Figure 4.2A, B). In addition, we performed flow cytometric analysis of PI fluorescence in order to determine cell cycle phase distribution. As shown in Figure 4.2C, approximately 11.8% of cells were in S-phase in SAG treated cultures. However in AICAR treated samples, 8.2% of cells were in S-phase, suggesting an inhibition of Shh signaling in CGNPs. When we performed immunohistochemistry for apoptotic marker cleaved caspase-3 on AICAR-treated CGNPs, we observed a slight, but insignificant, increase compared to SAG-treated CGNPs (Figure 4.2A, B). Together, these results indicate an anti-proliferative effect of AICAR on CGNPs and that AICAR does not play a significant role in inducing programmed cell death of CGNPs.

To determine if AICAR inhibits Shh signaling in a tumor context, we isolated primary medulloblastoma cells from freshly dissociated *GFAP$^{Cre/+}$;SmoM2* tumors. *GFAP$^{Cre/+}$;SmoM2* mice express the constitutively active, ligand-independent Smoothened allele (SmoM2) under control of the human GFAP-promoter; 100% of the mice develop medulloblastoma with an average survival of 33 days (Schüller, Heine, et al. 2008). Parallel to our findings in CGNPs, AICAR significantly reduced Gli1 and Gli2 protein levels (Figure 4.2F) and caused a reduction in cell proliferation as indicated by pH3 staining from 10.19% in untreated tumor cells to 6.89% in AICAR-treated tumor cells ($p = 0.012$) (Figure 4.2D, E). In addition, we observed a significant increase in cleaved caspase-3 positive cells in tumor cells treated with AICAR, from 6.86% CC3 positive in untreated tumor cells to 20.55% in AICAR treated cells ($p = 0.002$) (Figure 4.2D, E). Collectively, these results suggest that AICAR has profound effects on tumor growth and survival.

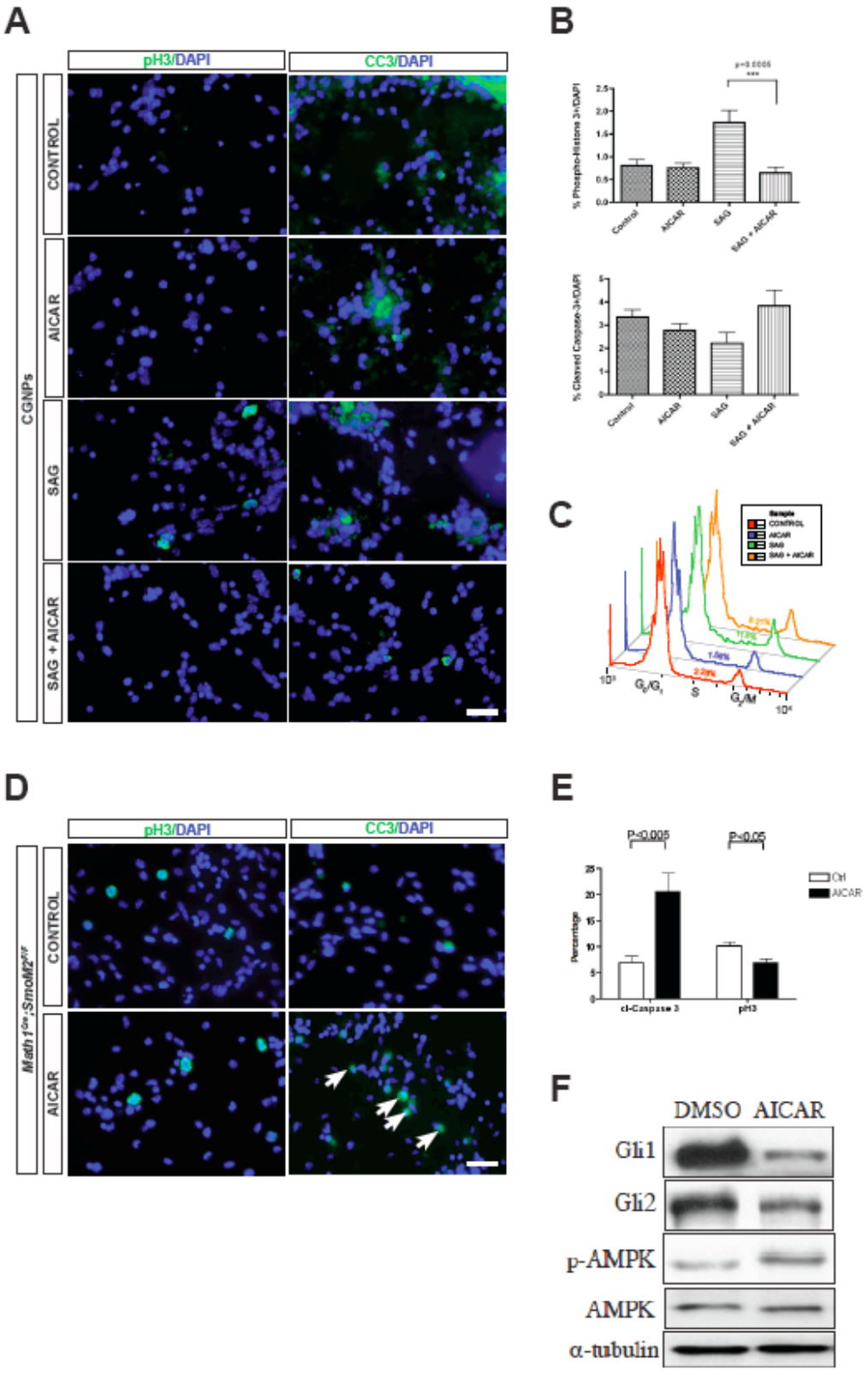
A
pH3/DAPI
CC3/DAPI
CGNPs
CONTROL
AICAR
SAG
SAG + AICAR
B
% Phospho-Histone 3+/DAPI
Control
AICAR
SAG
SAG + AICAR
% Cleaved Caspase-3+/DAPI
C
Sample
CONTROL
AICAR
SAG
SAG + AICAR
G0/G1
S
G2/M
D
pH3/DAPI
CC3/DAPI
Math1Cre;SmoM2fl/fl
CONTROL
AICAR
E
P<0.005
P<0.05
Ctrl
AICAR
Percentage
cl-Caspase 3
pH3
F
DMSO
AICAR
Gli1
Gli2
p-AMPK
AMPK
α-tubulin

Figure 4.2. AICAR inhibits CGNP proliferation and growth of primary medulloblastoma cells

(A) CGNPs treated with SAG ± AICAR were fixed and immunostained with pH3 and cleaved caspase 3. (B) Quantification of percentage of pH3-positive and cleaved-caspase 3-positive cells out of total DAPI+ cells demonstrates a significant decrease in pH3-positive cells in SAG and AICAR-treated samples compared to SAG-treated samples ($n = 10$, $p = 0.0006$) but no significant difference in cleaved caspase-positive samples. (C) CGNPS treated with SAG ± AICAR labeled with propidium iodide and subjected to flow cytometric cell cycle analysis demonstrates a decrease in S phase in SAG and AICAR-treated samples compared to SAG treated samples. (D) Primary medulloblastoma cells from *Math1^{Cre};SmoM2* mice were treated with 1 mM AICAR for 12 hours, then fixed and immunostained for pH3 and cleaved-caspase 3. (E) Quantification of percentage of pH3-positive and cleaved-caspase 3-positive cells out of total DAPI+ cells demonstrates a significant decrease in pH3-positive cells in SAG and AICAR-treated samples compared to SAG-treated samples ($n = 10$, $p < 0.05$) and a significant increase in cleaved caspase-3 cells ($n = 10$, $p < 0.005$). (F) Lysates from *Math1^{Cre};SmoM2* primary medulloblastoma cells treated with AICAR were subjected to SDS-PAGE followed by immunoblotting with indicated antibodies. Scale Bar, 20 μm.

AICAR downregulates Shh signaling in an AMPK-independent manner

In order to determine the mechanism through which AICAR acts to downregulate Shh signaling, we tested the GSK3ß (Horike et al. 2008; King, Song, and Jope 2006), cholesterol (Wang et al. 2008; Namgaladze et al. 2013), PKA (Hallows et al. 2009), and sirtuin (Bai et al. 2012; Velasquez et al. 2011) pathways which have been shown to be activated by AICAR. We applied inhibitors for these pathways to determine whether they are required for AICAR inhibition of Shh response. We found that AICAR inhibition was sustained in the presence of GSK3ß inhibitor CH99021, cholesterol synthesis inhibitor simvastatin, PKA inhibitors KT5720 and H89, and sirtuin inhibitors sirtinol and salermide (Figure 4.3A-D), thus ruling out these pathways as mediators of AICAR action on Shh signal response. In addition, AICAR has been postulated to mediate its anti-growth effects primarily through AMPK inhibition of mTOR signaling (Guo, Chien, and Shyy 2007; Inoki, Zhu, and Guan 2003; Gleason et al. 2007). Administration of AICAR has been shown to cause mTOR inhibition *in vitro* and *in vivo* in retinoblastoma tumor xenografts (Theodoropoulou et al. 2013; Theodoropoulou et al. 2010), and mTORC1 is directly inhibited by phosphorylation of raptor as a consequence of activation of the AMPK (Bolster 2002). Thus we also asked whether mTOR inhibition using the drug Rapamycin could downregulate Gli1 levels in a manner similar to AICAR. We found that although phosphorylated-S6 levels were decreased in both AICAR and Rapamycin-treated samples, suggesting that mTOR pathway activity was inhibited, Gli1 levels were not reduced to the same level in Rapamycin treated samples as compared to AICAR-treated samples (Figure 4.3E). These results suggest that AICAR does not function through mTOR inhibition to affect Shh pathway activity.

We then turned to the heterotrimeric metabolic enzyme 5'-Amp-activated protein kinase (AMPK). AICAR has a widely documented role as an activator of AMPK (Sullivan et al. 1994; Bergeron et al. 2001; Song et al. 2002; Buhl et al. 2002; Sriwijitkamol and Musi 2008b) although signaling through AMPK-independent mechanisms have been reported (Santidrian et al. 2010; Jacobs et al. 2006). As shown in previous figures, AICAR induces the phosphorylation of AMPK in several cell types including CGNPs (Figure 4.1D) and primary medulloblastoma cells (Figure 4.2F), as well as its direct substrate ACC, suggesting its ability to activate AMPK when added to culture media. To determine whether AICAR acts through AMPK to downregulate Shh signaling activity, we added the pyrazolopyrimidine compound Compound C, which functions as an ATP-competitive inhibitor of AMPK and other protein kinases (Bain et al. 2007), to SAG and AICAR-treated samples in the Gli-dependent luciferase assay. As compound C inhibits AMPK function, we would expect a rescue of luciferase activity in AICAR-treated cells if AICAR acted through AMPK to downregulate Shh signaling activity. However, we failed to observe rescue of AICAR-mediated inhibition of Gli-luciferase (Figure 4.4A). We corroborated these observations by using AMPKa-null fibroblasts (Laderoute et al. 2006; Jørgensen et al. 2004), and found that addition of AICAR was still able to inhibit Gli1 levels over time in the absence of AMPK (Figure 4.1C and 4C). Collectively, these studies indicate that AICAR-induced Shh pathway antagonism occurs in a manner independent of AMPK signaling.

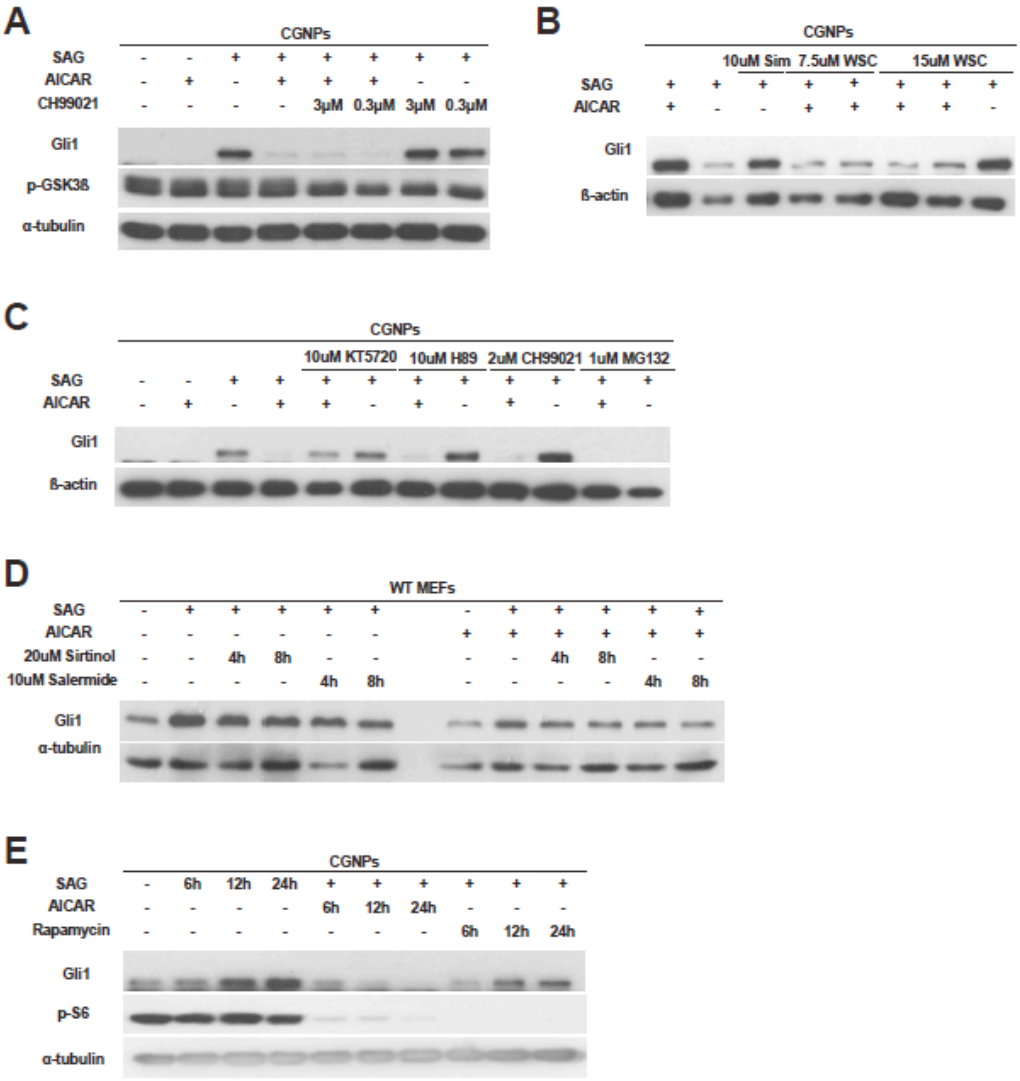

Figure 4.3. AICAR downregulates Shh signaling independently of the GSK3ß, cholesterol, PKA, sirtuin, and mTOR pathways
(A-C) CGNPs were treated with SAG, AICAR, and/or inhibitors of pathways shown to be activated by AICAR. AICAR inhibition was sustained in the presence of GSK3ß inhibitor CH99021, cholesterol synthesis inhibitor simvastatin, PKA inhibitors KT5720 and H89, suggesting AICAR action on Shh signal response is not mediated through these pathways. (D) Wild-type MEFs were treated with SAG, AICAR, and/or sirtuin inhibitors sirtinol and salermide. AICAR does not mediate its effects on Shh signaling through the sirtuin pathway. (E) AICAR does not work through the mTOR signaling pathway, since addition of rapamycin (inhibitor of mTOR) is not able to downregulate Gli1 protein levels to the same extent as with AICAR.

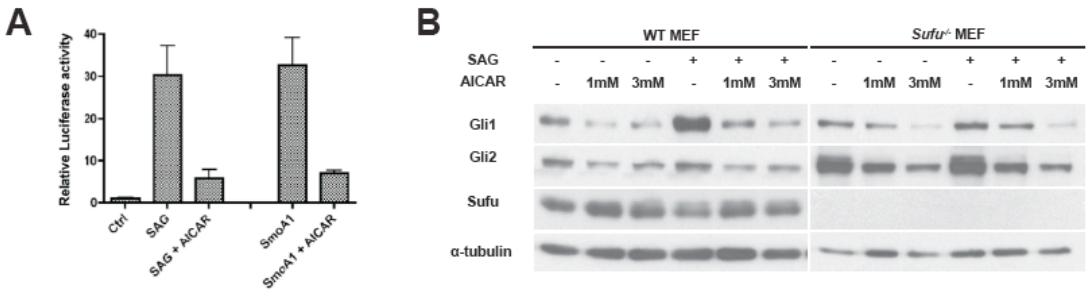

Figure 4.4. AICAR downregulates Shh signaling independently of the AMPK pathway

(A) Effects of AMPK inhibitor Compound C (1 and 3 μM) were evaluated in NIH-3T3 cells by relative Gli-luciferase activity. Compound C was unable to rescue AICAR mediated downregulation of Gli-luciferase activity. (B) Timecourse of SAG ± AICAR addition in AMPK-/- MEFs shows that AICAR is still able to downregulate Gli1 levels, similar to those in WT MEFs (see Figure 1C), suggesting an AMPK-independent mechanism for AICAR-mediated downregulation of Gli protein.

AICAR acts downstream of Smoothened to inhibit Shh pathway activity

Since we had determined that AICAR acts through an AMPK-independent mechanism to inhibit Shh pathway activity, we wanted to assess where in the Shh pathway AICAR acts. Shh pathway activation is critically dependent on Smoothened activation, and we first sought to determine whether AICAR inhibits Smo activity. We assessed the ability of AICAR to inhibit Shh signaling induced by constitutively active Smo (SmoA1) in NIH-3T3 transfected with Gli-luciferase. SmoA1 is a mutation found in sporadic basal cell carncinomas and has a leucine substitution at tryptophan 535, rendering the protein constitutively active (Xie et al. 1998). If AICAR inhibited Shh activity by impairing the ability of Smo to activate Gli, we would expect that Shh signaling would not be reduced in the presence of SmoA1. As shown in Figure 4.5A, AICAR significantly inhibited Gli-luciferase activity induced by SmoA1, comparable to the reduction observed in SAG and AICAR treated samples. This finding suggests that AICAR acts downstream of or parallel to Smo in the Shh signaling pathway.

Next we sought to determine whether AICAR depends on the Shh negative regulator Sufu to inhibit signaling activity. In the absence of Shh ligand, Sufu controls the level of Gli2 and Gli3 proteins by binding and stabilizing them in the cytoplasm (Wilson and Chuang 2010; Humke et al. 2010; Tukachinsky, Lopez, and Salic 2010; Wang, Pan, and Wang 2010). Shh signaling stimulates dissociation of the Sufu/Gli2 and Gli3 complexes, permitting full activity of Gli2 (Bai et al. 2002). Thus in the absence of Sufu, the Shh pathway is constitutively active although Gli2 and Gli3 become more labile (Wilson and Chuang 2010; Humke et al. 2010; Tukachinsky, Lopez, and Salic 2010; Wang, Pan, and Wang 2010). If AICAR inhibits Shh signaling by modulating Sufu function, for example by preventing Sufu-Gli disassembly in the presence of Shh, we would expect the effects of AICAR to be diminished in cells lacking Sufu. We assessed Gli1 and Gli2 protein levels in Sufu-/- MEFs (Svärd et al. 2006) and compared protein

levels to those in wild-type MEFs. As shown in Figure 4.5.5B, in WT cells, 1 mM AICAR treatment for 12 hours reduced basal levels of Gli1 and Gli2; however, higher concentrations of AICAR did not appreciably reduce their levels further. 100 nM SAG treatment alone significantly upregulated Gli1 but Gli2 level remained unchanged, consistent with previous studies that Shh signaling regulates Gli2 primarily at the post-transcriptional level by modulating its activity partly through its interaction with Sufu (Wilson and Chuang 2010; Humke et al. 2010; Tukachinsky, Lopez, and Salic 2010; Wang et al. 2010). As expected, addition of SAG had little or no effect on Gli1 and Gli2 levels in the absence of Sufu (Figure 4.5C), consistent with near full Shh pathway activation in Sufu-/- MEFs. Addition of AICAR significantly reduced SAG-induced Gli1 and Gli2 protein levels (Figure 4.5B). Given that AICAR reduces Shh signaling in Sufu-/- MEFs, in which Gli is constitutively activated in the nucleus, we propose that AICAR inhibits Shh signaling at the level of the Gli transcription factors, either by regulating Gli protein stability or Gli transcription.

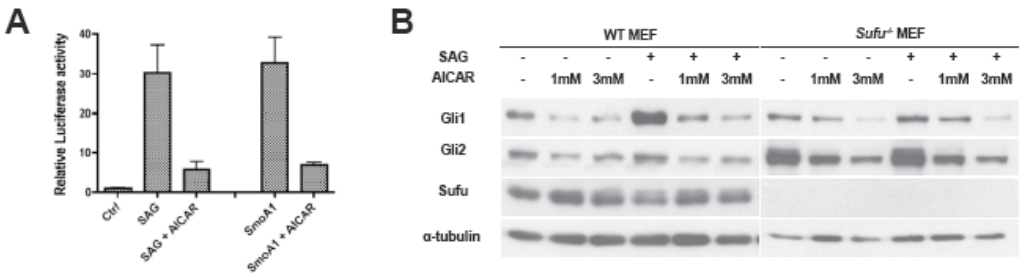

Figure 4.5. AICAR acts downstream of Smoothened to inhibit Shh pathway activity
(A) The ability of AICAR to inhibit Shh signaling induced by constitutively active Smo (SmoA1) was assessed in NIH-3T3 cells transfected with Gli-luciferase. AICAR significantly inhibited Gli-luciferase activity induced by SmoA1, comparable to the reduction observed in SAG and AICAR treated samples, suggesting that AICAR acts downstream of or parallel to Smo in the Shh signaling pathway. Data represent mean of triplicates ± SD. (B) 100 nM SAG ± 1 or 3 mM AICAR treatment for 12 hours in WT MEFs reveals that 1 mM AICAR reduces basal levels of Gli1 and Gli2 and 3 mM AICAR does not appreciably reduce levels further. In the absence of Sufu (Sufu-/- MEFs), SAG had little or no effect on Gli1 and Gli2 levels, whereas addition of AICAR significantly reduced SAG-induced Gli1 and Gli2 protein levels.

AICAR regulates *Gli1* transcription

To determine whether AICAR regulation of Gli protein levels is proteasome-mediated, we treated WT fibroblasts with AICAR in the presence of proteasome inhibitor MG132. We did not observe a rescue of Gli1 or Gli2 protein levels in AICAR-treated samples in the presence of 10 μM MG132 in WT (Figure 4.6A) for 2.5 hrs or Sufu-/- MEFs treated with MG132 for 3 or 6 hrs (Figure 4.6A). Consistent with previously published results, MG132 stabilized Gli2 in Sufu-/- cells in the absence of AICAR (Humke et al. 2010) (Figure 4.6A). This indicates that AICAR does not inhibit the Shh pathway by promoting proteolytic destruction of Gli and thus does not regulate Gli protein stability.

As we determined that AICAR acts downstream of Sufu to affect Gli protein levels, we next wished to determine whether AICAR regulates Gli transcription. Therefore we treated MEFs with SAG and/or AICAR for 12 hours and performed qRT-PCR to determine mRNA levels. As shown in Figure 4.6B, we observed no significant changes in *Gli2* and *Gli3* mRNA levels with different treatment conditions, whereas SAG-induced *Gli1* mRNA levels were reduced by nearly 40% in the presence of AICAR (from relative mRNA level 43 to 26). Next, we examined effects of AICAR on Gli3 protein levels in WT MEFs. Gli3-R serves as the principal transcriptional repressor of Shh signaling in the absence of ligand (Ryan and Chiang 2012); Shh pathway activation blocks Gli3 repressor formation and destabilizes full-length Gli3. Thus if AICAR inhibits the Shh pathway by stabilizing Gli3 protein or Gli3 repressor formation, we would expect an increase in Gli3R in AICAR treated cells. However, we found that addition of AICAR had no significant effect on Gli3 full-length or repressor (Figure 4.6C), suggesting that AICAR does not regulate Gli3 protein levels. Since AICAR does not appreciably decrease Gli2 or Gli3 protein levels but is able to substantially downregulate Shh

transcriptional target *Gli1*, these results suggest that AICAR acts at the level of the Gli transcriptional effectors.

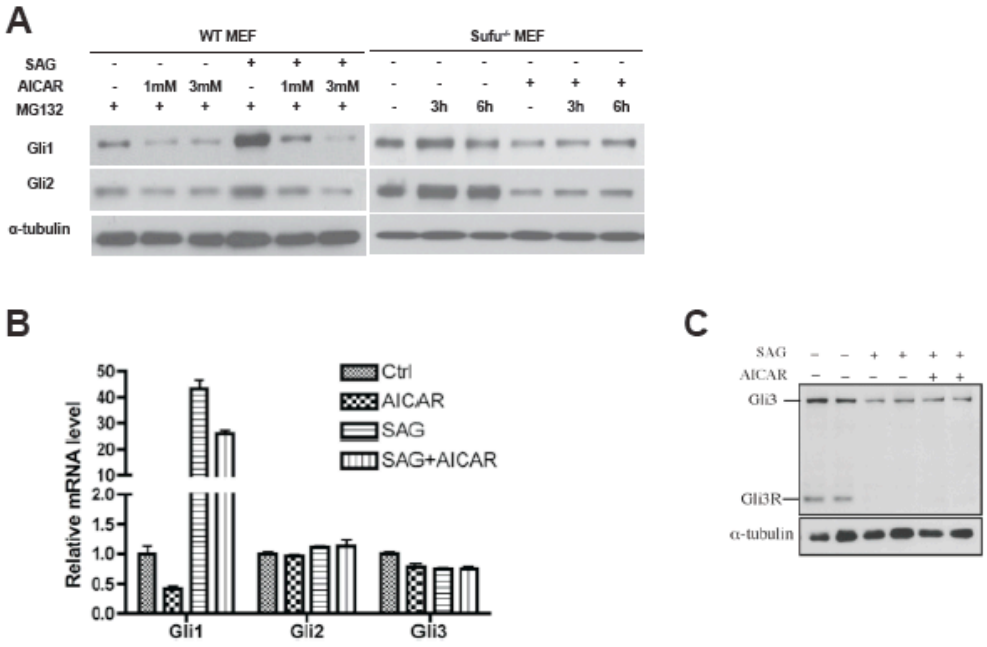

Figure 4.6. AICAR regulates *Gli1* transcription
(A) WT MEFs were treated with SAG ± AICAR were treated with proteasome inhibitor MG132 (10 μM) for 2.5 hours. Sufu-/- MEFs were treated with MG132 for 3 or 6 hours. A rescue of Gli1 and Gli2 protein levels was not observed suggesting that AICAR does not regulate Gli protein stability. (B) WT MEFs were treated with SAG ± AICAR for 12 hours and qRT-PCR performed to determine mRNA levels. No significant changes in *Gli2* and *Gli3* mRNA levels were observed with different treatment conditions, whereas SAG-induced *Gli1* mRNA levels were reduced by nearly 40% in the presence of AICAR (from relative mRNA level 43 to 26). (C) Effects of AICAR on Gli3 protein levels were examined in WT MEFs. Addition of AICAR had no significant effect on Gli3 full-length or repressor, suggesting that AICAR does not regulate Gli3 protein levels.

AICAR acts on human medulloblastoma cells to alter cell fate

Since we had observed a decrease in Shh signaling activity by AICAR in CGNPs and in mouse medulloblastoma cells, we sought to determine whether AICAR could affect proliferation of primary human medulloblastoma cells. We obtained a frozen human medulloblastoma sample, dissociated the tissue, and established a cell line. We determined first that the primary medulloblastoma cells were responsive to Shh signaling, as evidenced by an upregulation of Gli1 upon addition of 50 nM SAG (Figure 4.7B) for 24 hours. Next we assayed whether AICAR addition affected tumor cell morphology and Gli1 protein levels. Upon addition of 3 mM AICAR to both SAG-treated and untreated samples, we observed distinct morphological changes. Cells in control or SAG-treated wells were pleomorphic, undifferentiated cells. Upon addition of AICAR, the morphology changed to triangular shaped cells with extensive neurite outgrowth. Processes exhibited numerous bulbous protuberances along their course (Figure 4.7A, arrowheads). Using Western blotting, we determined that Gli1 levels were significantly downregulated upon addition of AICAR (Figure 4.7B). Interestingly, Gli1 levels were downregulated to a greater extent in SAG-treated samples upon addition of AICAR compared to untreated samples, suggesting that AICAR has a preferential effect on cells treated with SAG. These experiments demonstrate that AICAR is able to antagonize Shh signaling in human medulloblastoma cells, and that AICAR addition to these cells results in a change in fate.

In order to determine whether AMPK affected proliferation, differentiation, or apoptosis of the tumor cells, we used immunocytochemistry (Figure 4.7C). We found a decrease in pH3 staining, indicating that AICAR affects proliferation (Figure 4.7C, arrowheads). Immunocytochemistry with apoptotic marker cleaved caspase-3 revealed an increase in AICAR treated cells. An increase was observed in neuronal marker Tuj1,

suggesting that AICAR-treated cells acquire a neuronal cell fate and that AICAR may promote neuronal differentiation in tumor cells. Sox2 is a transcription factor localized to both the nuclei and cytoplasm in neural progenitor cells and their progeny (Wegner and Stolt 2005); it shuttles between the two subcellular compartments and its nuclear localization regulates its transcriptional activity (Li et al. 2007). Increased expression of Sox2 has been reported in many tumors, particularly in highly aggressive central nervous system neoplasms including both glioblastoma and medulloblastoma (Sutter et al. 2010; Ben-Porath et al. 2008; Annovazzi et al. 2011; Leis et al. 2011). Sox2 immunocytochemistry in control and SAG-treated cells revealed robust expression in the cytoplasm and nucleus, indicating a neural stem-cell-like fate. Interestingly, however, Sox2 expression was limited to the cytoplasm with addition of AICAR, regardless of SAG treatment (Figure 4.7C, arrowheads). This suggests AICAR inhibits Sox2 nuclear localization, preventing Sox2 transcriptional activity from occurring. As Sox2 inhibition leads to premature cell cycle exit and neuronal differentiation (Wegner and Stolt 2005), this suggests AICAR-treated cells have initiated a differentiation program. Taken together, our results demonstrate that AICAR antagonizes Shh signaling and promotes apoptosis and neuronal differentiation in cultured primary medulloblastoma cells.

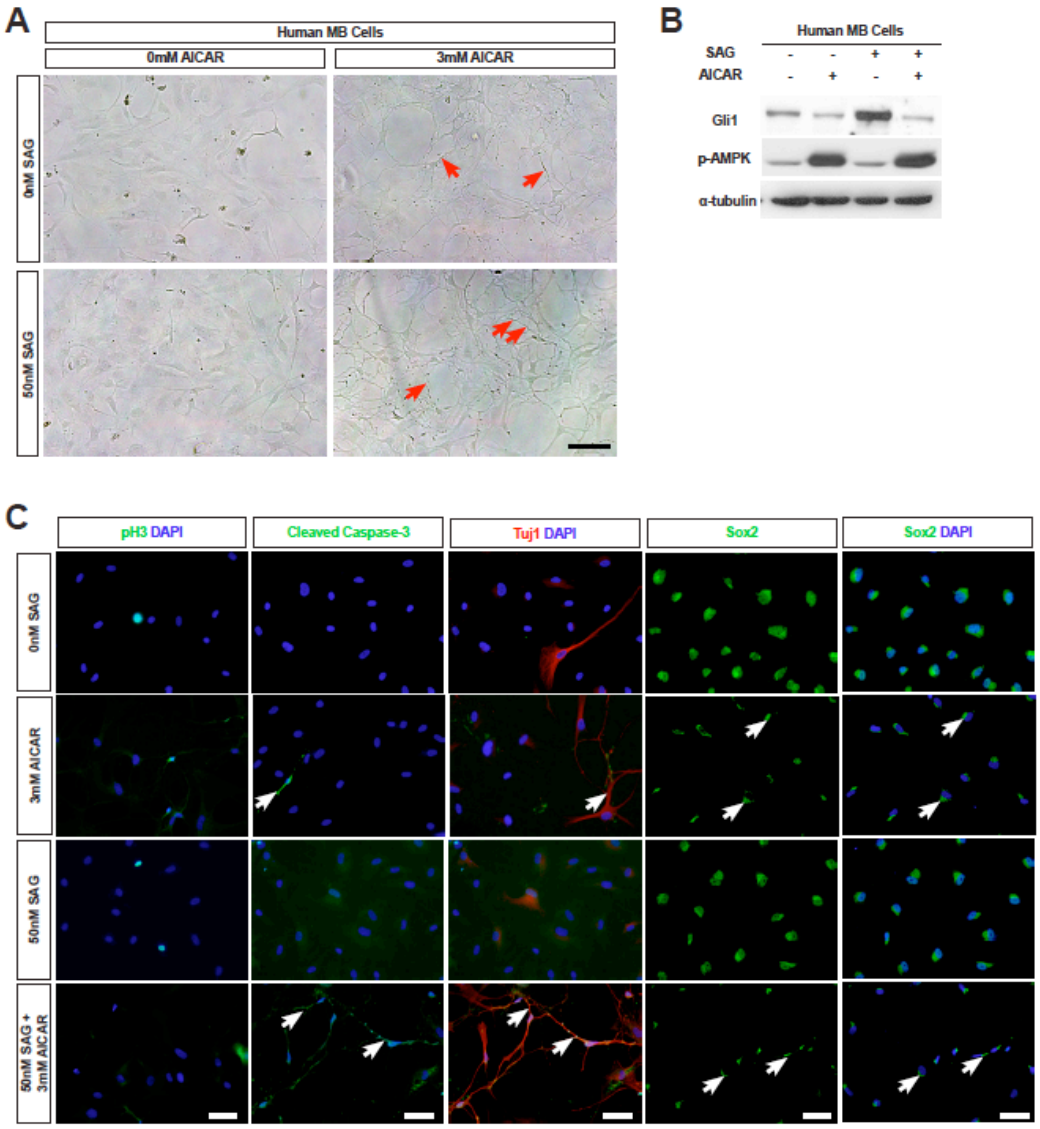
A
Human MB Cells
0mM AICAR
3mM AICAR
0nM SAG
50nM SAG
B
Human MB Cells
SAG - - + +
AICAR - + - +
Gli1
p-AMPK
α-tubulin
C
pH3 DAPI
Cleaved Caspase-3
Tuj1 DAPI
Sox2
Sox2 DAPI
0nM SAG
3mM AICAR
50nM SAG
50nM SAG + 3mM AICAR

Figure 4.7. AICAR acts on human medulloblastoma cells to alter cell fate
(A) A primary human medulloblastoma cell line was treated with 50 nM SAG ± 3 mM AICAR for 24 hours. Brightfield images of cells reveal distinct morphological changes. Cells in AICAR treated wells change morphology to triangular shaped cells with extensive neurite outgrowth. Processes exhibited numerous bulbous protuberances along their course (arrowheads). (B) Western blotting on lysates collected from cells with treatment as in (A) shows Gli1 downregulation upon addition of AICAR. Interestingly, Gli1 levels were downregulated to a greater extent in SAG-treated samples upon addition of AICAR compared to untreated samples, suggesting that AICAR has a preferential effect on cells treated with SAG. (C) Immunocytochemistry of the human medulloblastoma cell line reveals a decrease in pH3 staining, increase in caspase-3, increase in neuronal marker Tuj1, and differential localization of Sox2 in AICAR treated samples. The increase in Tuj1 suggests that AICAR-treated cells acquire a neuronal cell fate and that AICAR may promote neuronal differentiation in tumor cells. Sox2 immunocytochemistry in control and SAG-treated cells revealed robust expression in the cytoplasm and nucleus, indicating a neural stem-cell-like fate. Interestingly, however, Sox2 expression was limited to the cytoplasm with addition of AICAR, regardless of SAG treatment (arrowheads), suggests AICAR inhibits Sox2 nuclear localization. Scale Bar, 20 μm.

DISCUSSION

In this study we show that AICAR is able to downregulate Shh pathway activity and potently inhibits proliferation in multiple cell lines. To date, no study has demonstrated the effects of AICAR on Shh pathway activity. We find that AICAR modulates the Shh pathway by downregulating *Gli1* transcription in a manner that is independent of AMPK activation. Identifying novel inhibitors of the Shh pathway that act at the level of the Gli transcriptional effectors has great clinical potential for treatments of Shh-driven tumors, given the recent discoveries involving tumor resistance to Smoothened inhibitors.

Our results demonstrate that AICAR regulates Shh pathway activity downstream of pathway mediators Smoothened and Sufu. We find that while both Gli1 protein and transcript levels are downregulated by AICAR addition, Gli2 and Gli3 protein and transcript levels are not affected by AICAR addition (Figure 4.5A). These observations, together with the fact that AICAR-mediated Gli1 protein down-regulation occurs as early as six hours in both MEFs and GCPs (Figure 4.1C, D), suggests that AICAR targets *Gli1* via a transcription-dependent mechanism. The mechanism by which AICAR targets *Gli1* transcription requires further study. Gli2 protein functions as an upstream regulator of *Gli1* transcription (Sasaki, Kurisu, and Kengaku 2010), and Gli2-activator levels are regulated by proteasomal degradation of Gli2-full length protein (Pan et al. 2006). Experiments using proteasomal inhibitor MG132 suggest that AICAR is unlikely to affect Gli2 protein stability. Thus AICAR may act by regulating Gli2 post-translational modification, protein translation, or activation. Specifically AICAR may affect translocation of Gli2 to the cilium, accumulation in the nucleus, or its phosphorylation status, all of which are necessary for its activation (Chen et al. 2009; Kim, Kato, and Beachy 2009). Alternatively, AICAR may affect Gli2 transcriptional activity, either by inhibiting binding of Gli2 to promoter regions of its transcriptional targets or by inhibiting the recruitment of as

yet undetermined cofactors necessary for Gli2 DNA binding. It is also possible that AICAR promotes the proteasomal-independent degradation of Gli. Indeed, AICAR is able to induce autophagy in a p53-dependent manner in MEFs and HCT116 colon cancer cells (Buzzai et al. 2007). Thus one conceivable mechanism by which AICAR may act to regulate *Gli1* transcriptional levels may be through the lysosomal degradation of cofactors required for Gli binding to DNA.

Interestingly, our study is not the first example of a small molecule affecting Shh signaling at the level of Gli transcription. Arsenic trioxide (ATO), an FDA-approved drug used for the treatment of acute promyelocytic leukemia, has recently been discovered to target the Gli transcriptional effectors (Beauchamp et al. 2011; Kim et al. 2010), either by blocking Shh-induced ciliary accumulation of Gli2 (Kim et al. 2010) or by binding directly to Gli1 protein to inhibit its transcriptional activity (Beauchamp et al. 2011). While several other compounds, including the GANT family of inhibitors (Lauth et al. 2007), natural products zerumbone and physalin F and B (Hosoya et al. 2008), and HPI-1 and HPI-2 (Hyman et al. 2009) have also been shown to inhibit Gli transcriptional activity, their precise mechanism of action is unknown. These studies and ours may potentially be used as a tool for understanding events surrounding Gli transcriptional activation, which remains an open field of investigation. Although the activated form of Gli is believed to be phosphorylated (Humke et al. 2010), little else is known about additional post-transcriptional modifications that regulate nuclear entry or transcriptional activity of Gli. In addition, inhibitors targeting the Shh pathway at the level of Gli hold great promise as adjunctive therapeutics in Shh-driven tumors, since current therapies specifically targeting the Shh pathway act at the level Smo. Smoothened antagonists are not expected to be effective for the treatment of malignancies arising from downstream mutations in the Shh pathway (Robarge et al. 2009; Tremblay et al. 2009; Miller-Moslin et al. 2009; Peukert and Miller-Moslin 2010; Roberts et al. 1989; Khatib et al. 1993;

Zwerner et al. 2007; Beauchamp and Üren 2012) and resistant Smo mutations have been documented in at least in one human medulloblastoma patient treated with the cyclopamine-derivative GDC-0449 (Vismodegib) (Rudin et al. 2009; Rudin 2012; Yauch et al. 2012). Of note, the combined effect of Gli antagonist ATO and cyclopamine in cultured cell-signaling assays permitted equivalent or more potent pathway inhibition at lower drug concentrations of both drugs (Kim et al. 2010), providing an encouraging rationale for combination strategies utilizing both Smo and Gli inhibitors. Such therapies may not only provide multi-level targeting of the pathway but also allow for lower drug levels and hence reduced toxic effects. Further studies are needed to determine whether AICAR may similarly be effective in combination with cyclopamine mimics.

AICAR is a potent agonist of AMPK, thus it has primarily been used to study AMPK-dependent metabolic regulation (Sullivan et al. 1994; Bergeron et al. 2001; Song et al. 2002; Buhl et al. 2002; Sriwijitkamol and Musi 2008a). In the present study, we find that although AMPK phosphorylation is upregulated in all cell types treated with AICAR, the effects of AICAR on Shh signaling are AMPK-independent as AICAR is still able to downregulate Shh signaling in AMPK-/- cells. Thus the AMPK-independent effects of AICAR may have profound consequences on Shh-driven cancer cell proliferation and survival. At present, little is known about the AMPK-independent effects of AICAR. In CLL cells, AICAR induces apoptosis in an AMPK-independent manner by upregulating gene expression of BCL-2 family members BIM, NOXA, and PUMA in the mitochondrial apoptotic pathway (Santidrian et al. 2010). Furthermore, AICAR regulates key enzymes involved in phospholipid biosynthesis in hepatic cells independently of AMPK activation through an unknown mechanism (Jacobs et al. 2006). In a select few cases, direct binding of AICAR to specific proteins has been reported. These include phosphofructokinase (PFK) and fructose-1,6-biphosphatase (F1,6-BPase) which are inhibited *in vitro* by AICAR (Guigas et al. 2006; Javaux et al. 1995; Vincent, Bontemps,

and Van den Berghe 1992), and heat-shock protein Hsp90, whose client proteins were found to be destabilized in the presence of AICAR *in vivo* (Meli et al. 2006). As both PFK and Hsp90 contribute to important functions for tumor growth (reviewed in (Yalcin et al. 2009; Siegelin 2013), it remains possible that AMPK-independent anti-proliferative effects of AICAR in cancer cells, including those cell lines used in our study, may be mediated through these proteins. These investigations and ours demonstrate that AICAR targets multiple pathways, including the Shh signaling pathway, unrelated to its ability to activate AMPK. The mechanism of action of AMPK agonists in cancer treatment and their true molecular targets requires further study.

Our results demonstrate that AICAR inhibits proliferation in CGNPs, mouse medulloblastoma cells, and a human primary medulloblastoma cell line as well as promotes apoptosis in both mouse and medulloblastoma cells. AICAR has been known to exert various effects on cell growth, including regulation of the pro-inflammatory response (Hoogendijk et al. 2013), cytokine production (Katerelos et al. 2010), cell proliferation (Theodoropoulou et al. 2010), and apoptosis (González-Gironès et al. 2013). AICAR has also been shown to inhibit proliferation and protect from apoptosis in many types of cancer, including multiple myeloma (Baumann et al. 2007), neuroblastoma (Garcia-Gil et al. 2003), glioblastoma (Guo et al. 2009), childhood ALL (Sengupta et al. 2007), retinoblastoma (Theodoropoulou et al. 2010) and colon cancer (Su et al. 2007), by various mechanisms. However, ours is the first study to link the anti-proliferative and pro-apoptotic effects of AICAR to its actions on Shh signaling, therefore identifying a novel mechanism of action by which AICAR mediates its effects on tumor growth.

Differentiation therapy describes the enforced differentiation of primary tumors with therapeutic compounds, and has been used successfully to achieve remission in patients with acute promyelocytic leukemia (Weis et al. 1994; Tallman et al. 2002).

Significantly, we observed that AICAR addition to the human medulloblastoma cells induced differentiation and neurite outgrowth (Figure 4.7A, C). Our findings corroborate recent evidence that AICAR induces astroglial differentiation in neural stem cells derived from postnatal rat hippocampus and embryonic cortex (Zang et al. 2008). Notably, the ability of AICAR to promote differentiation in these cells was determined to be independent of AMPK, and was mediated through the JAK/STAT pathway (Zang et al. 2008). As differentiation status of tumors has been shown to have a strong correlation with metastatic potential (Bloom and Richardson 1957; Contesso et al. 1987; Kouros-Mehr et al. 2008), where well-differentiated tumors tend to have a low capacity for metastasis formation and poorly differentiated tumors have a high capacity for metastasis, compounds that induce differentiation of tumor cells, such as AICAR, justify further investigation.

A final note on the potential clinical utility of AICAR is that though it is not yet FDA-approved, AICAR has been used in clinical trials since the 1980s (Leung et al. 1994; Bosselaar et al. 2013; Babraj et al. 2009; Cuthbertson et al. 2007; Mangano 1997) for its effects on reducing myocardial ischemic injury as well as in B-CLL patients, and has recently entered into Phase II clinical trials (Santidrian et al. 2010). While it is currently on the banned substances list of the World Anti-Doping Agency, investigating the potential for AICAR to treat cancers holds great promise because it is a natural metabolic intermediate normally present in the body. The penetration of AICAR across the blood brain barrier into medulloblastomas and other CNS tumors such as gliomas is not well understood (Marangos et al. 1990; Guo et al. 2009). Nevertheless, given our current findings, future studies involving AICAR or more potent derivatives of the compound in the treatment of Shh-driven cancers are warranted.

MATERIALS AND METHODS

Animals and Reagents. AICAR, 2-DG, metformin, rapamycin, compound C, and MG132 (all from Sigma) were dissolved in DMSO and SAG was dissolved in MeOH (Gift of Dr. Michael Cooper) for *in vitro* experiments. *Math1*$^{Cre/+}$ (Helms et al. 2000) and *SmoM2* (Mao et al. 2006) mice were obtained from Jackson Laboratory. Mice were housed in an animal facility and were maintained in a temperature-controlled and light-controlled environment with an alternating 12-hour light/dark cycle. All protocols have been approved by the Vanderbilt Institutional Animal Care and Use Committee.

Gli-Luciferase Assay. Gli1 and SmoA1 constructs were transfected in NIH-3T3 cells along with a firefly luciferase reporter construct. Luciferase assays were performed as previously described (Huang, Liu, et al. 2010) using the Promega Dual Luciferase Reporter Assay system (Promega, WI). All reporter assays were normalized using Renilla luciferase as an internal control. Each data point represents the mean of triplicate wells with error bar representing the standard deviation (SD). Cells were treated with 50 nM SAG or 50 nM SAG and AICAR for 24 hours before being lysed in Passive Lysis Buffer at room temperature.

Cell lines, primary human and mouse MB cell derivation, and culture. NIH-3T3 cells, wild-type MEFs, AMPK-/- MEFs, and Sufu-/- MEFs were grown in DMEM with 10% FBS and 1X penicillin-streptomycin. Primary human MB cells were derived from patients admitted to Vanderbilt University Medical Center (VUMC). MB specimens from patients treated at the VUMC were obtained in accordance with the Institutional Review Board's approval. Tumor samples were dissociated with StemPro Accutase (Invitrogen) and plated in DMEM/F12, 10% FBS, and 1X penicillin–streptomycin. Cells from one patient,

REDCAP number 15289, were successfully maintained in DMEM with 10% FBS and propagated using standard tissue culture protocols. Primary mouse medulloblastoma cells were isolated from *Math1$^{Cre/+}$;SmoM2* mice as previously described (X. Huang, Liu, et al. 2010).

Immunocytochemistry. All immunocytochemistry analyses were performed on cells that were fixed for 20min in 4% PFA on ice. Cells were washed three times in PBS, blocked for 20 mins with 10% goat serum, and incubated with primary antibody for 90 minutes. Cells were then washed three times in PBS, incubated with secondary antibody for 30 minutes, and counterstained with DAPI or ToPro-3. Primary antibodies were rabbit anti-phosphorylated Histone H3 (Millipore, 1:1000), rabbit anti-cleaved caspase-3 (Cell Signaling Technology #9661, 1:1000), mouse anti-Tuj1 (Sigma, 1:1000), and mouse anti-Sox2 (Millipore, 1:1000).

CGNP Isolation. P4 or P5 cerebella from CD1 mice mice were dissected into calcium-free Hanks buffered saline solution (Mediatech) supplemented with 6g/L D-glucose. The meninges were stripped and pooled cerebellar dissociated with Accutase (Gibco) and trituration. Cells were pelleted and resuspended in Neurobasal A-medium containing 250 µM KCl, 500µL 100X GlutaMAX I, 500 µL 100X penicillin-streptomycin, and 10% FBS. Cells were passed through a 70 µm filter and incubated for two times 20 minutes on poly-d-lysine coated plates. Following the settling step, the cells remaining in the media were collected, pelleted, and resuspended in Neurobasal A-medium containing 1mL 50X B-27 serum-free supplement (Invitrogen), 250 µM KCl, 500 µL 100X GlutaMAX I, 500 µL 100X penicillin-streptomycin. Cells were plated at a density of 3 million cells/mL onto poly-D-ornithine coated plates or glass coverslips. After 24 hours incubation at 37C, 10 nM SAG was added to fresh serum-free media. 1 mM AICAR or DMSO was added

following 24 hour incubation in 10 nM SAG for 12 hours. Cells were then ready for harvesting for Western blotting or fixation for immunocytochemistry.

Western Blotting. For western analysis, cells were lysed in RIPA buffer containing 2.5 mM EDTA, 1 mM PMSF, 10 mM NEM, 1 mM sodium orthovanadate, 1 mM sodium fluoride, and EDTA-free complete mini protease inhibitor tablets (Roche), boiled in SDS, and resolved on 10% SDS-polyacrylamide gels. Primary antibodies used for Western blotting were mouse anti-cyclin D1 (BD Pharminogen #556470, 1:500), rabbit anti-Gli1 (Cell Signaling Technology #2534, 1:2000), guinea pig anti-Gli2 (gift of Jonathan Eggenschwiler), rabbit anti-phosphorylated-AMPKα (Thr172) (Cell Signaling Technology #2535, 1:1000), rabbit anti-AMPKα (Cell Signaling Technology #2532, 1:1000), mouse anti-α-tubulin (Hybridoma Bank, 1:10,000), mouse anti-b-actin (ThermoScientific BA3R, 1:5000), rabbit anti-phosphorylated-S6 (Cell Signaling Technology, 1:1000), rabbit anti-phosphorylated-ACC (Ser79) (Cell Signaling Technology #3661, 1:1000), rabbit anti-ACC (Cell Signaling Technology, 1:1000), and rabbit anti-Sufu (Cell Signaling Technology #2522, 1:1000), rabbit anti-Gli3 (1:500).

RT-PCR. RT-PCR was performed as previously described (Huang 2010 PNAS). Primers used were as follows: GAPDH (5′TTCACCACCATGGAGAAGGC3′F; 5′GGCATGGACTGTGGTCATGA3′R), Gli1 (5′CTGGAGAACCTTAGGCTGGA3′F; 5′CGGCTGACTGTGTAAGCAGA3′R); Gli2 (For: CTTTGCCGATTGACATGAGA; REV: CATATGGGGGTTCACGTAGG); Gli3 (FOR:GCAATCACTATGCAGCCTCA; REV: TGGCATCAATTGGTACAGGA)

Flow cytometry. Cellular DNA content was determined by flow cytometry. CGNPs were harvested and washed in ice-cold PBS, resuspended in 70% ethanol, and fixed for 2

hours at -20C. Cells were washed again once in PBS and resuspended in propidium iodide. PI fluorescence was determined by flow cytometry using a FACScan (BD Biosciences) and Cellquest software (Becton Dickinson) for acquisition. FlowJo was used for quantifying cell cycle phase distribution.

ACKNOWLEDGEMENTS

We thank Jiang Liu for his contributions and discussions for this project, and members of the Chiang laboratory for helpful and stimulating discussion. We would like to acknowledge the following individuals: Juan Gerardo Valadez and Michael Cooper, Vanderbilt University, for the human medulloblastoma samples and SAG, Danyvid Olivares-Villagomez, Vanderbilt University, for assistance with flow cytometry, and Jonathan Eggenschwiler, University of Georgia, for the guinea pig anti-Gli2 antibody. This work is supported by National Institutes of Health (NIH) T32 GM007347, National Institute Of Neurological Disorders And Stroke of the National Institutes of Health under Award Number F31NS074638, and NIH NS 042205.

CHAPTER V

GENERAL DISCUSSION

Cerebellar development is a complex process involving the tightly regulated proliferation, specification, migration, and connectivity of thousands of neurons and glia. Perturbations in signaling pathways important for any of these processes can have drastic consequences, including the formation of malignancies such as medulloblastoma. In this dissertation work I have focused on Shh signaling and its role in cerebellar development and formation of medulloblastoma. Our studies have identified a novel contribution of a particular cell type, the multipotent hindbrain roof plate cell, to diverse lineages in the cerebellum. Importantly, the roof plate cell is susceptible to oncogenic transformation as activation of constitutive Shh signaling in this cell type leads to the formation of medulloblastoma. In addition, we have determined a previously unappreciated role for Shh signaling in specialized cerebellar glial cells, which functions to sustain proliferation of neighboring neuronal precursors. We find that Shh signaling in this neuronal-glial relationship is critical for maintenance of cerebellar size and architecture. Last, we identify a small molecule as a novel and potent Hh pathway antagonist in multiple cell types, including Hh-responsive medulloblastoma cells. My work therefore offers insight into the diverse roles of Shh activity in the cerebellum and provides the basis for interesting questions that may be addressed in the future.

SUMMARY

Widespread contribution of Gdf7 lineage to cerebellar cell types and implications for Sonic hedgehog-driven medulloblastoma

Medulloblastomas can arise from CGNPs with aberrant Shh signaling. However, the molecular mechanism by which Shh pathway-mediated proliferation and transformation of CGNPs occurs is poorly understood. Prior to this work, few distinct subsets of CGNPs were identified which could be transformed to initiate medulloblastoma formation. In Chapter II, we demonstrated that focal activation of Shh signaling in a distinct subset of CGNPs, specifically derived from hindbrain roof plate cells expressing Gdf7, was sufficient to promote cerebellar tumorigenesis. This was accomplished by using a *Gdf7*$^{Cre/+}$ line to drive a constitutively active allele of Smoothened, SmoM2. We found that *Gdf7*$^{Cre/+}$*;SmoM2* (GM2) mutant mice displayed stunted growth, cranial bulging, and impaired motor coordination; all GM2 mice died within three weeks of birth. Analysis of mutant cerebellar architecture revealed severe hyperplasia suggestive of tumor formation. Tumors from both GM2 and established medulloblastoma model *Patched*$^{LacZ/+}$ mice displayed strong expression of CGNP, neural progenitor, and proliferative markers. In addition, cultured GM2 cerebellar cells expressed multiple stem cell markers and were clonogenic and multipotent. Collectively, these data indicated that targeting constitutively active Shh signaling to the Gdf7-lineage led to formation of medulloblastoma.

Hindbrain roof plate cells expressing Gdf7 had previously been shown through fate-mapping studies to contribute mostly to non-neural choroid plexus epithelium. Our data provides evidence that, similar to the cortex, midbrain, and spinal cord (K. Lee, Dietrich, and Jessell 2000; Monuki, Porter, and Walsh 2001; Dymecki and Tomasiewicz 1998), the hindbrain roof plate has a conserved role in the generation of neurons and other cell types. In our study, detailed fate-mapping was performed of the Gdf7 lineage which revealed that surprisingly, Gdf7-lineage cells contribute to a small subset of proliferating CGNPs. These were found beyond the clustered roof plate cells in the rhombic lip as well as the EGL. In addition, Gdf7-lineage cells also contribute to an extensive array of mature cerebellar cell types. These cells arise from the midline of the

cerebellar ventricular zone and consists of a small cluster of cells expressing radial glial markers, and can be molecularly defined by the expression of Gdf7 and Msx1 (Figure 2.4). We proposed that this cerebellar vermal region is a previously undescribed source of neurons that is continuous with and extends beyond the cerebellar ventricular zone. The GM2 medulloblastoma mouse model demonstrates how remarkably few cells are sufficient for oncogenic transformation and tumor formation. Thus hindbrain roof plate cells are established as a novel source of diverse neural cell types in the cerebellum that is also susceptible to oncogenic transformation by deregulated Sonic hedgehog signaling.

Glial Sonic hedgehog signaling activity is required for proper cortical expansion and cerebellar architecture

While the role of BG in providing structural support for inwardly migrating granular cells is well known, the contribution of BGs to neuronal specification and proliferation in the cerebellum has not been extensively studied. In addition, genetic studies of BG function utilize either the human GFAP-Cre, Nestin-Cre, or Engrailed1-Cre lines (Corrales et al. 2004; Yu et al. 2011), which also induce widespread recombination in neuronal precursors (Zimmerman et al. 1994; Graus-Porta et al. 2001). Thus investigations of the postnatal function of BG without vastly affecting the neuronal population have not yet been completed. Our study as detailed in Chapter III is the first to examine BG function using a spatially and temporally controlled genetic system by utilizing the *TNC*$^{CreER\text{-}YFP}$ mouse. Furthermore, our investigation is the first to reveal functions of Shh signaling in BG. We found that mice in which Shh activator Smoothened (Smo) is postnatally ablated in BG demonstrate an obvious cerebellar hypoplasia within two days of ablation of Shh signaling, indicating that BG-Shh signaling is integral to formation of proper cerebellar structure. Perhaps most surprisingly, Smo

mutants exhibit severely reduced CGNP proliferation and increased differentiation accompanied by a loss of Shh activity, suggesting a novel role for the BG-CGNP interaction in promoting CGNP precursor proliferation. These profound reductions in EGL area can be observed starting 24 hours after the last tamoxifen injection (Figure 3.3A, C) and prior to observable defects in BG fiber formation (Figure 3.6), a rapid timecourse that demonstrates the remarkable sensitivity of CGNP proliferation to BG-Shh activity and underscores its relevance for the maintenance of overall cerebellar size and architecture. Interestingly, Wnt signaling is ectopically elevated in Smo mutant CGNPs concomitant with a reduction in EGL area, suggesting that this pathway is involved in cross-talk with the Shh pathway in regulating CGNP proliferation. In addition, we found that loss of Shh signaling in BGs leads to disrupted PC monolayer formation and dendritic arborization as well as BG fiber morphology, indicating that BG-Shh signaling activity contributes to the maintenance of proper cerebellar laminar formation. Collectively, these data show a previously unappreciated role for BG Shh signaling activity in the proliferation of CGNPs and preservation of cerebellar architecture, thus leading to a new level of understanding of the neuronal-glial relationship in the cerebellum.

Antagonism of the hedgehog pathway at the level of Gli transcription by the small molecule 5-aminoimidazole-4-carboximide-1-ß-4-ribofuranoside (AICAR)

In Chapter IV of this work, we identify AICAR as a potent Hh pathway antagonist in multiple cell types, including Hh-responsive medulloblastoma cells. Importantly, we show that AICAR acts downstream of Smo and regulates *Gli1* transcription in a proteasome-independent manner. Sufu stabilizes the Gli proteins from AICAR inhibition, as downregulation of Shh pathway activity was more efficient in Sufu-null MEFs. Last, we find that although AICAR activates AMPK in these cell lines, inhibition of the Hh pathway

by AICAR is AMPK-independent. Our findings establish AICAR as a modulator of Shh signaling in both a developmentally relevant cell type as well as medulloblastoma cells, providing an encouraging basis to further explore its full potential as an antagonist in Shh-associated tumors.

IMPLICATIONS

The overall goals of this work were to 1) advance the understanding of Shh signaling in the cerebellum and 2) determine how aberrant Shh signaling can influence cerebellar disease. The first goal sought to understand functions of Shh signaling in the cerebellum at a cellular level; revealing these processes can increase our appreciation for cell-cell communication within biological systems and signaling processes that govern proper growth of organs. The second goal was to understand how mutations in the Shh pathway can influence cerebellar disease. We and others have found that abnormalities in the Shh pathway can result in medulloblastoma tumorigenesis when cells experience overactive signaling, whereas lack of Shh pathway activity can cause cerebellar hypoplasia. It is our hope that understanding Shh-dependent signaling in the cerebellum during normal development and disease can provide insight into cellular relationships integral to brain growth as well as inform development of targeted therapies for disease processes resulting from deregulated signaling.

Elucidation of roles of Shh signaling in development

Growth control mechanisms in multicellular organisms ensure that organs attain their proper final size, and control of these mechanisms dictates cell fate specification, proliferation, and differentiation. Thus, how distinct signals are emitted and integrated by cells within a growing organ is a major focus of cellular and developmental biology research today. Importantly, the study of the Shh pathway has not only provided

essential and basic paradigms by which cell to cell communication occurs, but has demonstrated how a key mediator of fundamental morphogenetic processes can pattern embryonic growth and development. A notable feature of Shh signaling is that in some contexts, Shh acts as a morphogen in the dose-dependent induction of distinct cell fates (Gritli-Linde et al. 2001; Ko and Eggenschwiler 2011; Ingham and McMahon 2001), whereas in other contexts it acts as a mitogen regulating proliferation of cells or as an inductive factor controlling organ development (Behesti and Marino 2009; Ingham and McMahon 2001). However, the precise mechanisms by which Shh exerts its morphogenetic and mitogenic activities on responsive cells are still being uncovered.

Using a cerebellar BG-specific knockdown of Shh signaling, we demonstrate that ablation of BG Shh signaling results in downregulation of the pathway in neighboring neuronal precursors, with profound implications on proliferation and growth of the organ. The notion that Shh signaling regulates two adjacent but distinct cell populations (ie, BG astroglia and CGNPs) appears to be a unique and novel mechanism by which Shh acts. Although Shh can signal directly to two cell populations in the adult SVZ of the mouse forebrain, the GFAP+ periventricular astrocytes and the more abundant GFAP- early precursors (Palma et al. 2005; Ruiz i Altaba 1998), the former population gives rise to the latter, whereas BGs and CGNPs are not of related lineages and situated in distinct cortical layers. Interestingly, an analogous scenario to that in the cerebellum may occur in *Drosophila,* where Shh employs two different strategies to pattern larval wing imaginal discs: it locally induces a secondary signal (Decapentaplegic [Dpp], the *Drosophila* homolog of vertebrate BMPs), and Shh itself diffuses over several cell diameters to act as a morphogen (Zecca, Basler, and Struhl 1995; Mullor et al. 1997). It is possible that signaling to two neighboring cell populations allows for greater modulatory control of its mitogenic/morphogenetic activities, which may be subject to physiologic fluctuations depending on stressors, injury, etc. Elucidating cellular relationships important for Shh

function in the cerebellum can provide novel insights into fundamental ways in which the pathway signals and thereby, affects processes fundamental for proper development of the organism.

A major thrust of developmental biology is to understand the mechanisms by which Shh signaling and other developmental pathways regulate cell fate decisions; that is how cells know where they are within a tissue and how this information is translated so that they form the appropriate structures for their positions (Barolo 2002; Briscoe et al. 2000). These issues are of particular relevance in early patterning of the cerebellar anlage, where several distinct classes of neurons and glia must be generated at specific timepoints (Hatten et al. 1997; Wingate 2001). Our investigation using mice in which Shh is activated in roof-plate cells illustrates the importance of positional identity for progenitor cells and how this determines subtype identity: we found that roof plate cells not only generate the choroid plexus, as previously known, but also contribute to divergent cerebellar neuronal and glial cell types. The ability of the roof plate cell to generate such diverse lineages must stem from differential integration of molecular and positional cues received by the common progenitor cell. Interestingly, this phenomenon is mirrored in the neighboring lower rhombic lip territory, which, though defined by *Wnt1* expression, is subdivided into molecular subdomains predictive of cell fate (Landsberg et al. 2005). As lower rhombic lip derivatives generate similar cell lineages as those derived from the roof plate and upper rhombic lip, including choroid plexus and Math1+ neurons (Landsberg et al. 2005), parallel molecular mechanisms for the specification of cells may be employed for both regions. For example, in the lower rhombic lip, the homeodomain transcription factor Pax6 is responsible for promoting expression of the *Math1* progenitor cell domain and generation of two neuronal cell types, the precerebellar mossy fiber neurons and climbing fiber neurons (Landsberg et al. 2005). In addition, Pax6 exerts its patterning action through interactions with the BMP signaling pathway in a cell non-

autonomous fashion (Landsberg et al. 2005). As Pax6 expression is exclusive to the hindbrain (Landsberg et al. 2005), and the roof plate and choroid plexus epithelium produce similar sets of BMPs (Chizhikov and Millen 2004), it is possible that the upper rhombic lip similarly depends on Pax6 for regulation of Math1 expression. Determination of how signals are integrated into cellular networks is crucial to our understanding of normal cell behavior and can provide clues into mechanisms by which fate decisions are made to produce the complex cellular specialization needed for a functioning organ.

Elucidation of roles of Shh signaling in disease

A basic tenet in cancer biology is that tumors stem from errors in the carefully regulated balance of cellular processes required to maintain tissue homeostasis. This is exemplified in the case of hedgehog-driven medulloblastoma, where studies in transgenic mouse models have shown that Shh pathway activation must occur in a lineage-specific cellular context to manifest biological effects and cause full malignant transformation (Schüller, Heine, et al. 2008; Yang et al. 2008). We further demonstrate the sensitivity of these cells to oncogenic events through our GM2 mouse model, where the transformation of remarkably few cells was sufficient for tumor formation. Other distinct subsets of CGNPs that can be transformed to initiate medulloblastoma include Olig2- and Tlx3-expressing precursors (Schüller, Heine, et al. 2008), which, consistent with their location within the cerebellum, cause tumorigenesis in posterior cerebellar lobes (Schüller, Heine, et al. 2008). Notably, the notion that tumorigenesis is initiated by transformation of a subset of lineage-restricted progenitor cells can occur in cancers of other organs, including in epithelial ovarian cancer, which can derive from xenoengraftment of fewer than 100 CD44+/CD117+ cells (Zhang et al. 2008). The identification of normal cell populations targeted for transformation will inform future studies directed at understanding how processes important during normal physiological

development become deregulated in tumor initiation and progression. Insight into the cellular context in which neoplastic transformation occurs is critical to the understanding of cancer biology, and will enable development of therapeutic strategies aimed at eliminating these cells in patients.

While cerebellar tumorigenesis can arise from overactive Shh signaling, a depletion of Shh signaling can result in significant reductions in organ size. There is currently increasing awareness that neurodevelopmental disorders are associated with cerebellar deficits and learning impairments (Manto and Jissendi 2012). In fact, the cerebellum is likely to become a major platform for studying how development and learning are associated, because of the modular nature of cerebellar circuits and the marked morphological changes still occurring after birth, allowing for detailed assessment of developmental abnormalities. Moreover, cerebellar development occurs in successive waves of proliferation and migration throughout embryonic and postnatal stages, allowing for the possibility of selectively targeting these developmental waves. Prior to our study, reduced Shh signaling had been linked to cerebellar hypoplasia in a few instances (Roper et al. 2006; Tam 2013; Dehart et al. 1997), including its classic association with Smith–Lemli–Opitz syndrome, an autosomal recessive syndrome that is due to defects in cholesterol homeostasis and results in multiple congenital malformations (Dehart et al. 1997). Other examples of Shh association with cerebellar hypoplasia include the case of glucocorticoid exposure in preterm infants (Haldipur et al. 2011; Manto and Jissendi 2012), as well as a mouse model of Down's syndrome that demonstrates a defective CGNP response to Shh signaling (Roper et al. 2006). Our Smo^{BG} mutants are an example of the important role of Shh signaling in regulating cerebellar size, and we add that a critical component of its ability to impact overall cerebellar growth is through its actions in astroglial cells. The identification of pathways and cell types which are potential targets for novel therapies of neurodevelopmental

disorders is important since these diseases are heterogeneous and in most cases, will span the entire life of patients.

In Chapter IV we show that small molecule AICAR is able to downregulate Shh pathway activity and potently inhibits proliferation in multiple cell lines. Interestingly, our study is not the first example of a small molecule affecting Shh signaling at the level of Gli transcription. Arsenic trioxide (ATO), an FDA-approved drug used for the treatment of acute promyelocytic leukemia, has recently been discovered to target the Gli transcriptional effectors (Beauchamp et al. 2011; Kim et al. 2010), either by blocking Shh-induced ciliary accumulation of Gli2 (Kim et al. 2010) or by binding directly to Gli1 protein to inhibit its transcriptional activity (Beauchamp et al. 2011). While several other compounds, including the GANT family of inhibitors (Lauth et al. 2007), natural products zerumbone and physalin F and B (Hosoya et al. 2008), and HPI-1 and HPI-2 (Hyman et al. 2009) have also been shown to inhibit Gli transcriptional activity, their precise mechanism of action is unknown. These studies and ours may potentially be used as a tool for understanding events surrounding Gli transcriptional activation, which remains an open field of investigation. Although the activated form of Gli is believed to be phosphorylated (Humke et al. 2010), little else is known about additional post-transcriptional modifications that regulate nuclear entry or transcriptional activity of Gli. In addition, inhibitors targeting the Shh pathway at the level of Gli hold great promise as adjunctive therapeutics in Shh-driven tumors, since current therapies specifically targeting the Shh pathway act at the level Smo. Smoothened antagonists are not expected to be effective for the treatment of malignancies arising from downstream mutations in the Shh pathway (Robarge et al. 2009; Tremblay et al. 2009; Miller-Moslin et al. 2009; Peukert and Miller-Moslin 2010; Roberts et al. 1989; Khatib et al. 1993; Zwerner et al. 2007; Beauchamp and Üren 2012) and resistant Smo mutations have been documented in at least in one human medulloblastoma patient treated with the

cyclopamine-derivative GDC-0449 (Vismodegib) (Rudin et al. 2009; Rudin 2012; Yauch et al. 2012). Of note, the combined effect of Gli antagonist ATO and cyclopamine in cultured cell-signaling assays permitted equivalent or more potent pathway inhibition at lower drug concentrations of both drugs (Kim et al. 2010), providing an encouraging rationale for combination strategies utilizing both Smo and Gli inhibitors. Such therapies may not only provide multi-level targeting of the pathway but also allow for lower drug levels and hence reduced toxic effects. The elucidation and development of Shh signaling inhibitors downstream of Smo can expand the current treatment arsenal to target the significant fraction of tumors that possess downstream pathway activation.

FUTURE DIRECTIONS

Investigation of functions of Gdf7-lineage cells

Our lineage tracing results in *Gdf7^{Cre};R26R* mice demonstrate that a subset of Gdf7-lineage cells delaminate from the upper rhombic lip, acquire a CGNP cell fate, and migrate into the external granular layer. Previously it has been shown that the majority of hindbrain roof plate Gdf7-lineage cells contribute to choroid plexus epithelial cells (Currle et al. 2005). Thus, while our study has shed light on the cellular origins of medulloblastoma, we have not identified the factors controlling Gdf7-lineage cell fate; that is, the factors that dictate whether the roof plate cell becomes a choroid plexus epithelial cell or whether it delaminates into the upper rhombic lip to become a cerebellar Math1+ CGNP.

The delaminating Gdf7-lineage cells in the upper rhombic lip are very small in number, with no more than 20-30 per E14.5 embryo (see Discussion, Chapter II), thus it is possible that their ability to escape the choroid plexus fate rests on imprecise molecular boundaries that delineate the roof plate from the rhombic lip. It has recently been shown in chick embryos through a combination of *in ovo* transplantation, co-

culture, and electroporation that both maintenance of a Math1+ rhombic lip and expression of choroid plexus genes in roof plate cells are acutely dependent on the integrity of the rhombic lip/roof plate boundary (Broom et al. 2012). Notably, lack of strict lineage restriction boundaries in other parts of the developing embryo also allow for intermingling of small numbers of derivative cells. For example, in the midbrain/hindbrain junction of the mouse embryo, lack of a strict dorsal posterior mesencephalic lineage boundary allows cells derived from Wnt1-expressing mesencephalic cells to populate the neighboring isthmus (Zervas et al. 2004). Additionally, lineage restriction boundaries between rhombomeres allow approximately 8% of rhombomere cells to freely intermingle with adjacent compartments (Birgbauer and Fraser 1994; M. Fraser et al. 2004). Therefore, the small number of delaminating Gdf7-lineage cells observed in the upper rhombic lip in our study may be a product of an inexact lineage boundary between the roof plate and rhombic lip.

Alternatively, an intriguing possibility is that the delaminating Gdf7-lineage cells in the rhombic lip may have a specific function. One hypothesis is that they may act as multipotent cerebellar progenitor cells. Our lineage studies indicate that the delaminating Gdf7-lineage cells retain multipotency since they express radial glial marker Sox2+ and have the capacity to generate known rhombic lip derivatives CGNPs and Tbr2+ unipolar brush cells (Figure 2.5). Notably, we find that Gdf7-lineage cells also give rise to a small subset of diverse cerebellar cell types, including Bergmann glia, Purkinje neurons, white matter astrocytes, and molecular layer GABAergic interneurons. While we postulated that these cells derive from the midline of the ventricular zone, our studies do not rule out the possibility that some of them may originate from the rhombic lip, which would be consistent with the notion that the rhombic lip possesses a population of Math1-independent cells giving rise to multiple cell types including Bergmann glia and Golgi cells of the IGL (Jensen 2004). Interestingly, recent genetic fate mapping studies have

shown that a class of cells expressing astroglial and neural stem cell markers reside in the external granular layer (EGL) ((Silbereis et al. 2010) and this study, Chapter III). Whether or not the delaminating Gdf7-lineage cells contribute to this astroglial population remains to be tested. In order to investigate this possibility, we can determine whether a subset of Gdf7-lineage cells in the EGL express neural stem cell markers, in addition to those expressing Math1-GFP (Figure 2.5). This would suggest that some delaminating Gdf7-lineage cells in the rhombic lip retain multipotency as they migrate to the EGL. To further study the function of the delaminating Gdf7-lineage cells, we would need to specifically ablate them as they migrate out from the rhombic lip and determine phenotypic differences of the cerebellum. While the developmental contribution of Gdf7-lineage cells to the cerebellum may be small, our investigation demonstrates the importance of these cells in a tumor context, as aberrant Shh signaling in these cells invariably results in medulloblastoma formation. Therefore, further understanding the function of the delaminating Gdf7-lineage rhombic lip cells would not only contribute to our knowledge of hindbrain patterning and subsequent cerebellar development, but to our understanding of the cellular origins of cerebellar disease processes.

A recently published study has noted distinct developmental origins for medulloblastoma subgroups (Gibson et al. 2010) and defined cells of the dorsal brain stem as the cellular origin for the Wnt subgroup of medulloblastoma (Gibson et al. 2010). Interestingly, the dorsal brain stem and the cerebellum have several parallel molecular mechanisms that regulate their development. First, the primary neuronal cell type of both the cerebellum and brain stem derive from Math1+ progenitor cells (Landsberg et al. 2005). Second, these Math1+ progenitor cells are generated in the rhombic lip: the upper rhombic lip for the cerebellum (Chizhikov et al. 2010) and the lower rhombic lip for the brain stem (Landsberg et al. 2005). Third, both the upper and lower rhombic lip regions possess a domain of Gdf7-expressing cells which have been demonstrated to

contribute to the fourth ventricle choroid plexus (Landsberg et al. 2005; Currle et al. 2005; Huang et al. 2009). Although Gdf7-lineage cells in the lower rhombic lip have not been demonstrated to contribute to the dorsal brain stem (Landsberg et al. 2005), it is possible that a few cells escape the choroid-plexus fate and have the capacity to generate multiple cell types, as we found in our investigation of Gdf7-lineage cells in the upper rhombic lip. It is thus interesting to speculate whether mutations in the Wnt signaling pathway in Gdf7-expressing cells may also cause medulloblastoma, this time localized to the dorsal brain stem. Furthermore, additional studies involving mutations in other signaling pathways implicated in medulloblastoma formation such as Notch or Myc, in Gdf7-expressing cells may also be studied, though their cell of origin has not yet been defined. If medulloblastoma formation is observed, this would suggest that different medulloblastoma subtypes, though expressing high levels of distinct signaling pathways, could stem from a common, early progenitor cell. These studies would increase our understanding of the cellular origins of medulloblastoma, in the hopes of finding improved treatments for this disease.

Investigations of Bergmann glial Sonic hedgehog signaling

Mechanistic studies of regulation of CGNP proliferation by Bergmann glial Shh signaling

Our studies using *TNC^{CreER};Smo$^{F/-}$* mice demonstrated that Shh signaling in TNC-expressing cells is critical to the formation of the cerebellum, as mutants display profound cerebellar hypoplasia, reductions in EGL area and CGNP proliferation, defects in BG and PC fiber morphology, and impaired migration of post-mitotic granule cells. The *TNC^{CreER}* driver line is a powerful tool for the study of BGs and their contribution to cerebellum, as it induces recombination specifically in three subsets of cerebellar astroglial cells with the most widespread population by far being BG (Figure 3.1, 3.5).

Notably, other transgenic mouse lines that may target same or similar populations include the *GFAP*^{CreER} mouse line (Silbereis et al. 2010) and *Glast*^{CreER} line (Wang, Rattner, et al. 2012), but have yet to be exploited for the study of BGs. In contrast, previous Cre driver lines used for the study of BGs have affected cells early in cerebellar development and induce widespread recombination not only in astroglial cells but also in all neuronal precursors (Corrales et al. 2006; Zimmerman et al. 1994; Graus-Porta et al. 2001). While we attribute our cerebellar phenotype to ablation of Shh signaling in BGs for reasons stated in the text (Figure 3.5 and Discussion, Chapter 3), we however cannot rule out the possibility that the two other, smaller populations of TNC-expressing astroglia play a role as well. In order to definitively rule them out, we would need to identify a specific marker for BG that is not present in the other populations; this would enable generation of a more specific BG-driven Cre transgenic line than currently available and could be used to study BG function independent of other cerebellar astroglia. Interestingly, studies performed in our lab indicate that BGs and EGL astroglia express high levels of TNC-YFP whereas postnatal white matter progenitor cells express low levels such that flow cytometry can be used to differentiate these two populations (Fleming et al.) (submitted). Gene expression differences can then be determined via microarray or RNAseq experiments.

We demonstrate that in *TNC*$^{CreER\text{-}YFP}$*;Smo*$^{F/-}$ mice, Wnt signaling upregulation is concomitant with a reduction in EGL area. We hypothesize that this link may be through Shh-mediated activation of Wnt inhibitors, or Shh-mediated suppression of Wnt activators. In addition to secreted Wnt inhibitor *Sfrp1,* which we show is downregulated in the EGL of TNC mutants (Figure 3.8), one candidate gene that may be involved in Shh-mediated activation of Wnt inhibitors is Wnt inhibitory factor 1, *Wif1,* which is expressed in the Purkinje cell layer where Bergmann glia reside. The *Drosophila* homologue of Wif1, shifted, is required for normal Shh signaling in the wing imaginal disc

and has been suggested to bind BOC/CDO family members Ihog and Boi (Avanesov et al. 2012). Thus it is possible that Wif1 expression may be required for normal CGNP Shh signaling because of its ability to inhibit Wnt pathway activity. In order to test this hypothesis, we would need to assess for *Wif1* gene expression differences in our mutant and wild-type animals. If expression differences are observed, we could further test the hypothesis using genetic means to knockdown expression of Wif1 in BG and compare the CGNP and cerebellar phenotype to our Smo^{BG} mutants. A floxed Wif1 transgenic mouse is under development at the International Knockout Mouse Consortium. These studies would assist us in elucidating the mechanism by which BG Shh signaling affects CGNP proliferation.

It is important to note that our studies do not rule out the possibility that deregulated Wnt signaling is a consequence of EGL reduction, rather than a cause. While there are several reasons why we believe BG Shh signaling is involved in Wnt antagonism as stated above (Figure 3.8 and Discussion, Chapter 3), further studies are needed to determine whether Wnt signaling is a cause of rather than a secondary effect of EGL size reduction. To determine whether Wnt antagonism plays a role in CGNP proliferation, we can add the Porcupine inhibitor C59 (Proffitt et al. 2013) to slice cultures of mutant cerebella. The membrane-bound O-acyltransferase Porcupine is a key enzyme in Wnt biosynthesis and is required for Wnt secretion and activity (Biechele, Cox, and Rossant 2011). Because of its enyzmatic role in the production of all active Wnts, and the fact that small changes in Porcupine activity can have significant effects on developmental phenotypes (Proffitt et al. 2013; Proffitt and Virshup 2012), Porcupine makes an attractive target for the inhibition of Wnt signaling. We can examine CGNP proliferation and overall EGL thickness using immunohistochemistry of proliferative markers to determine whether the mutant phenotype can be rescued upon Wnt inhibition. Slice culture experiments with small molecule addition have been routinely

used to examine changes in CGNP proliferation in the field (Wechsler-Reya and Scott 1999). In addition, a genetic approach using a floxed allele of Porcupine (Liu et al. 2012) to knockdown expression in BGs with the *TNC*$^{YFP\text{-}CreER}$ line can be used. These studies would assist in clarifying the mechanism through which BG Shh signaling acts on CGNP proliferation. Using a more global approach to determining downstream targets of Shh signaling in BG, TNC-YFP+ BG can be isolated from mutant and wild type cerebella using flow cytometry and analyzed for microarray or RNAseq analysis to determine gene expression differences.

Studies of a potential role for Bergmann glial Shh signaling in Purkinje cell dendritogenesis

Our results demonstrated that, in later time-point injected mutants, PC dendritic arborization may rely upon BG Shh signaling. A more detailed analysis of PC dendrites in both wild-type and mutant animals will help to support this notion and should include analysis of dendritic length, number of branches, and dendritic thickness. In addition, the mechanism by which Shh signaling in BGs regulates PC dendritogenesis requires further investigation. Recent studies have implicated Shh signaling in the guidance of growing axons (Sarnat and Alcalá 1980; Yam et al. 2009) and emerging evidence suggests that it may play a role in dendritogenesis as well (Petralia et al. 2011; Sasaki, Kurisu, and Kengaku 2010). Specifically, Shh has been shown to regulate dendritic spine formation of hippocampal neurons via Tiam1-Rac1-mediated remodeling of the actin cytoskeleton (Sasaki, Kurisu, and Kengaku 2010). Additionally, many studies have demonstrated the dependence of neuronal dendritogenesis on astrocytes or glia in the brain (Martin, Brown, and Balkowiec 2012; Eroglu and Barres 2010; Haber 2006; Nishida and Okabe 2007; Verbich et al. 2012), a regulation that involves several factors including BDNF (Martin, Brown, and Balkowiec 2012), eph-ephrin signaling (Eroglu and

Barres 2010; Nishida and Okabe 2007), and glutamate uptake (Verbich et al. 2012). BG Shh signaling may therefore be involved in activation of these pathways to influence PC dendritic arborization; whether any of these pathways known to affect neuronal dendritogenesis are downstream of BG Shh signaling can be determined by comparing indicators of their expression in mutant and wild-type BGs. Delineating mechanisms by which BGs impact PC dendritic arborization can help understand development of basic cerebellar circuitry and synapse formation, and may increase our knowledge of processes involved in cerebellar-dependent learning.

Studies of Bergmann glial Shh signaling in the adult cerebellum

Our studies in Smo mutant mice demonstrate that early postnatal Shh signaling in BG is required for proper CGNP proliferation with profound consequences on development of cerebellar architecture. This finding adds to our knowledge of early postnatal BG function, as previous understanding has largely been confined to its role in providing migratory cues for postmitotic granule cells as they move inwards to form the IGL (Rakic 1971). Interestingly, Shh responsiveness remains in BG in the adult cerebellum (Garcia et al. 2010), after the EGL has disappeared; however, its function at that stage remains unknown. It is possible that Shh signaling in BG contributes to their survival in a stressed environment, for example during starvation, as it does in cultured rat cerebral astrocytes (Yoshimura, Kawate, and Takeda 2010). Another intriguing possibility is that Shh signaling in BG is responsible for proper synaptic activity and intracellular communication between BG and their neighboring neurons. Consistent with this hypothesis, BGs are increasingly being recognized as critical components of synaptic function (Martínez-Lozada et al. 2013), as they are located close to glutamatergic synapses and participate actively in the recycling of glutamate (Martínez-Lozada et al. 2013). Additionally, astrocytic G-protein-coupled receptor (GPCR)

activation elicits Ca^{2+}-dependent release of various gliotransmitters, including the neuromodulators glutamate, ATP, and D-serine (Fiacco and McCarthy 2006; Perea and Araque 2007; Pascual 2005). Notably, Smoothened was very recently determined to belong to the class F family of GPCRs (Wang et al. 2013) and Shh can increase intracellular Ca^{2+} in mouse embryonic stem cells and rat gastric mucosal cells (Belgacem and Borodinsky 2011). Thus Shh signaling in adult BG may have a normal physiological role in mediating glial-neuronal communication. Our mutant mouse model provides the basis for carrying out such a study, as tamoxifen can be injected at later stages after the EGL has disappeared. In addition to phenotypic analysis, electrophysiological studies can be performed whereby neuronal firing activity is monitored and compared in Smo^{BG} mutant CGNPs and wild-type CGNPs to determine whether their electrical activity is altered in the setting of BG Smo ablation. These studies would improve our understanding of the role of Shh signaling in BG as well as of the contribution of BG to cerebellar function in the adult cerebellum.

REFERENCES

Ajeawung, Norbert F, Hao Y Wang, Peter Gould, and Deepak Kamnasaran. 2012. “Advances in Molecular Targets for the Treatment of Medulloblastomas.” *Clinical & Investigative Medicine* 35 (5): E246–E259.

Ajeawung, Norbert Fonya, Hao Yang Wang, and Deepak Kamnasaran. 2013. “Progress From Clinical Trials and Emerging Non-Conventional Therapies for the Treatment of Medulloblastomas.” *Cancer Letters* 330 (2) (April): 130–140. doi:10.1016/j.canlet.2012.11.039.

Alder, J, KJ Lee, TM Jessell, and ME Hatten. 1999. “Generation of Cerebellar Granule Neurons in Vivo by Transplantation of BMP-Treated Neural Progenitor Cells.” *Nature Neuroscience* 2 (6): 535–540.

Allen, Benjamin L, Jane Y Song, Luisa Izzi, Irene W Althaus, Jong-Sun Kang, Frédéric Charron, Robert S Krauss, and Andrew P McMahon. 2011. “Overlapping Roles and Collective Requirement for the Coreceptors GAS1, CDO, and BOC in SHH Pathway Function.” *Developmental Cell* 20 (6) (June): 775–787. doi:10.1016/j.devcel.2011.04.018.

Annovazzi, Laura, Marta Mellai, Valentina Caldera, Guido Valente, and Davide Schiffer. 2011. “SOX2 Expression and Amplification in Gliomas and Glioma Cell Lines..” *Cancer Genomics & Proteomics* 8 (3) (May): 139–147.

Anthony, Todd E, Corinna Klein, Gord Fishell, and Nathaniel Heintz. 2004. “Radial Glia Serve as Neuronal Progenitors in All Regions of the Central Nervous System..” *Neuron* 41 (6) (March 25): 881–890.

Antonarakis, E S, E I Heath, D C Smith, D Rathkopf, A L Blackford, D C Danila, S King, et al. 2013. “Repurposing Itraconazole as a Treatment for Advanced Prostate Cancer: a Noncomparative Randomized Phase II Trial in Men with Metastatic Castration-Resistant Prostate Cancer.” *The Oncologist* 18 (2) (February 22): 163–173. doi:10.1634/theoncologist.2012-314.

Aruga, J, T Nagai, T Tokuyama, Y Hayashizaki, Y Okazaki, V M Chapman, and K Mikoshiba. 1996. “The Mouse Zic Gene Family: HOMOLOGUES of the DROSOPHILA PAIR-RULE GENE Odd-Paired.” *Journal of Biological Chemistry* 271 (2) (January 12): 1043–1047. doi:10.1074/jbc.271.2.1043.

Aruga, Jun. 2004. “The Role of Zic Genes in Neural Development.” *Molecular and Cellular Neuroscience* 26 (2) (June): 205–221. doi:10.1016/j.mcn.2004.01.004.

Avanesov, Andrei, Shawn M Honeyager, Jarema Malicki, and Seth S Blair. 2012. “The Role of Glypicans in Wnt Inhibitory Factor-1 Activity and the Structural Basis of Wif1'S Effects on Wnt and Hedgehog Signaling.” Edited by Norbert Perrimon. *PLoS Genet* 8 (2) (February 23): e1002503. doi:10.1371/journal.pgen.1002503.g007.

Awatramani, R, P Soriano, C Rodriguez, JJ Mai, and SM Dymecki. 2003. “Cryptic Boundaries in Roof Plate and Choroid Plexus Identified by Intersectional Gene Activation.” *Nature Genetics* 35 (1): 70–75.

Babraj, J A, K Mustard, C Sutherland, M C Towler, S Chen, K Smith, K Green, et al. 2009. “Blunting of AICAR-Induced Human Skeletal Muscle Glucose Uptake in Type 2 Diabetes Is Dependent on Age Rather Than Diabetic Status.” *AJP: Endocrinology and Metabolism* 296 (5) (April 22): E1042–E1048. doi:10.1152/ajpendo.90811.2008.

Bai, B, Y Liang, C Xu, M Y K Lee, A Xu, D Wu, P M Vanhoutte, and Y Wang. 2012. “Cyclin-Dependent Kinase 5-Mediated Hyperphosphorylation of Sirtuin-1 Contributes to the Development of Endothelial Senescence and Atherosclerosis.” *Circulation* 126 (6) (August 6): 729–740. doi:10.1161/CIRCULATIONAHA.112.118778.

Bai, C Brian, Wojtek Auerbach, Joon S Lee, Daniel Stephen, and Alexandra L Joyner. 2002. “Gli2, but Not Gli1, Is Required for Initial Shh Signaling and Ectopic Activation

of the Shh Pathway." *Development* 129 (20) (October 1): 4753–4761.
Bain, Jenny, Lorna Plater, Matt Elliott, Natalia Shpiro, C James Hastie, Hilary Mclauchlan, Iva Klevernic, J Simon C Arthur, Dario R Alessi, and Philip Cohen. 2007. "The Selectivity of Protein Kinase Inhibitors: a Further Update." *The Biochemical Journal* 408 (3) (December 15): 297. doi:10.1042/BJ20070797.
Banka, Siddharth, Richard Walsh, and Marie-Anne Brundler. 2006. "First Report of Occurrence of Choroid Plexus Papilloma and Medulloblastoma in the Same Patient." *Child's Nervous System* 23 (5) (November 15): 587–589. doi:10.1007/s00381-006-0249-6.
Baptista, C A, M E Hatten, R Blazeski, and C A Mason. 1994. "Cell-Cell Interactions Influence Survival and Differentiation of Purified Purkinje Cells in Vitro.." *Neuron* 12 (2) (February): 243–260.
Bar, Eli E, Aneeka Chaudhry, Alex Lin, Xing Fan, Karisa Schreck, William Matsui, Sara Piccirillo, et al. 2007. "Cyclopamine-Mediated Hedgehog Pathway Inhibition Depletes Stem-Like Cancer Cells in Glioblastoma." *Stem Cells* 25 (10) (October): 2524–2533. doi:10.1634/stemcells.2007-0166.
Barolo, S. 2002. "Three Habits of Highly Effective Signaling Pathways: Principles of Transcriptional Control by Developmental Cell Signaling." *Genes & Development* 16 (10) (May 15): 1167–1181. doi:10.1101/gad.976502.
Bartsch, S, U Bartsch, U Dörries, A Faissner, A Weller, P Ekblom, and M Schachner. 1992. "Expression of Tenascin in the Developing and Adult Cerebellar Cortex.." *The Journal of Neuroscience : the Official Journal of the Society for Neuroscience* 12 (3) (March): 736–749.
Baumann, Philipp, Sonja Mandl-Weber, Bertold Emmerich, Christian Straka, and Ralf Schmidmaier. 2007. "Activation of Adenosine Monophosphate Activated Protein Kinase Inhibits Growth of Multiple Myeloma Cells." *Experimental Cell Research* 313 (16) (October): 3592–3603. doi:10.1016/j.yexcr.2007.06.020.
Beachy, P A, S G Hymowitz, R A Lazarus, D J Leahy, and C Siebold. 2010. "Interactions Between Hedgehog Proteins and Their Binding Partners Come Into View." *Genes & Development* 24 (18) (September 15): 2001–2012. doi:10.1101/gad.1951710.
Beauchamp, Elspeth M, and Aykut Üren. 2012. "A New Era for an Ancient Drug." In *Vitamins & Hormones*, 88:333–354. Vitamins & Hormones. Elsevier. doi:10.1016/B978-0-12-394622-5.00015-8.
Beauchamp, Elspeth M, Lymor Ringer, Gülay Bulut, Kamal P Sajwan, Michael D Hall, Yi-Chien Lee, Daniel Peaceman, et al. 2011. "Arsenic Trioxide Inhibits Human Cancer Cell Growth and Tumor Development in Mice by Blocking Hedgehog/GLI Pathway." *Journal of Clinical Investigation* 121 (1) (January 4): 148–160. doi:10.1172/JCI42874DS1.
Behesti, H, and S Marino. 2009. "Cerebellar Granule Cells: Insights Into Proliferation, Differentiation, and Role in Medulloblastoma Pathogenesis." *The International Journal of Biochemistry & Cell Biology* 41 (3): 435–445.
Belgacem, Y H, and L N Borodinsky. 2011. "Sonic Hedgehog Signaling Is Decoded by Calcium Spike Activity in the Developing Spinal Cord." *Proceedings of the National Academy of Sciences* 108 (11) (March 15): 4482–4487. doi:10.1073/pnas.1018217108.
Bellamy, Tomas. 2006. "Interactions Between Purkinje Neurones and Bergmann Glia." *The Cerebellum* 5 (2) (June 1): 116–126. doi:10.1080/14734220600724569.
Belvindrah, Richard, Perihan Nalbant, Sheng Ding, Chuanyue Wu, Gary M Bokoch, and Ulrich Müller. 2006. "Integrin-Linked Kinase Regulates Bergmann Glial Differentiation During Cerebellar Development." *Molecular and Cellular Neuroscience* 33 (2) (October): 109–125. doi:10.1016/j.mcn.2006.06.013.

Ben-Porath, Ittai, Matthew W Thomson, Vincent J Carey, Ruping Ge, George W Bell, Aviv Regev, and Robert A Weinberg. 2008. “An Embryonic Stem Cell-Like Gene Expression Signature in Poorly Differentiated Aggressive Human Tumors..” *Nature Genetics* 40 (5) (May): 499–507. doi:10.1038/ng.127.

Bergeron, Raynald, Stephen F Previs, Gary W Cline, Pascale Perret, Raymond R Russell III, Lawrence H Young, and Gerald I Shulman. 2001. “Effect of 5-Aminoimidazole-4-Carboxamide-1-B-D-Ribofuranoside Infusion on in Vivo Glucose and Lipid Metabolism in Lean and Obese Zucker Rats.” *Diabetes* 50 (5): 1076–1082.

Berman, DM, SS Karhadkar, AR Hallahan, JI Pritchard, CG Eberhart, DN Watkins, JK Chen, MK Cooper, J Taipale, and JM Olson. 2002. “Medulloblastoma Growth Inhibition by Hedgehog Pathway Blockade.” *Science's STKE* 297 (5586): 1559.

Biechele, Steffen, Brian J Cox, and Janet Rossant. 2011. “Porcupine Homolog Is Required for Canonical Wnt Signaling and Gastrulation in Mouse Embryos.” *Developmental Biology* 355 (2) (July): 275–285. doi:10.1016/j.ydbio.2011.04.029.

Birgbauer, E, and S E Fraser. 1994. “Violation of Cell Lineage Restriction Compartments in the Chick Hindbrain..” *Development* 120 (6) (June): 1347–1356.

Bloom, HJG, and W W Richardson. 1957. “Histological Grading and Prognosis in Breast Cancer: a Study of 1409 Cases of Which 359 Have Been Followed for 15 Years.” *British Journal of Cancer* 11 (3): 359.

Bolster, D R. 2002. “AMP-Activated Protein Kinase Suppresses Protein Synthesis in Rat Skeletal Muscle Through Down-Regulated Mammalian Target of Rapamycin (mTOR) Signaling.” *Journal of Biological Chemistry* 277 (27) (May 7): 23977–23980. doi:10.1074/jbc.C200171200.

Bosselaar, Marlies, Paul Smits, Luc J C van Loon, and Cees J Tack. 2013. “Intravenous AICAR During Hyperinsulinemia Induces Systemic Hemodynamic Changes but Has No Local Metabolic Effect.” *The Journal of Clinical Pharmacology* 51 (10) (March 8): 1449–1458. doi:10.1177/0091270010382912.

Briscoe, J, A Pierani, TM Jessell, and J Ericson. 2000. “A Homeodomain Protein Code Specifies Progenitor Cell Identity and Neuronal Fate in the Ventral Neural Tube.” *Cell* 101 (4): 435–445.

Broom, Emma R, Jonathan D Gilthorpe, Thomas Butts, Florent Campo-Paysaa, and Richard J T Wingate. 2012. “The Roof Plate Boundary Is a Bi-Directional Organiser of Dorsal Neural Tube and Choroid Plexus Development..” *Development* 139 (22) (November): 4261–4270. doi:10.1242/dev.082255.

Brown, S A, D Warburton, L Y Brown, C Y Yu, E R Roeder, S Stengel-Rutkowski, R C Hennekam, and M Muenke. 1998. “Holoprosencephaly Due to Mutations in ZIC2, a Homologue of Drosophila Odd-Paired..” *Nature Genetics* 20 (2) (October): 180–183. doi:10.1038/2484.

Brugieres, L, A Remenieras, G Pierron, P Varlet, S Forget, V Byrde, J Bombled, et al. 2012. “High Frequency of Germline SUFU Mutations in Children with Desmoplastic/Nodular Medulloblastoma Younger Than 3 Years of Age.” *Journal of Clinical Oncology* 30 (17) (June 8): 2087–2093. doi:10.1200/JCO.2011.38.7258.

Buffo, Annalisa, and Ferdinando Rossi. 2013. “Origin, Lineage and Function of Cerebellar Glia..” *Progress in Neurobiology* (August 25). doi:10.1016/j.pneurobio.2013.08.001.

Buhl, Esben S, Niels Jessen, Rasmus Pold, Thomas Ledet, Allan Flyvbjerg, Steen B Pedersen, Oluf Pedersen, Ole Schmitz, and Sten Lund. 2002. “Long-Term AICAR Administration Reduces Metabolic Disturbances and Lowers Blood Pressure in Rats Displaying Features of the Insulin Resistance Syndrome.” *Diabetes* 51 (7): 2199–2206.

Buonamici, Silvia, Juliet Williams, Michael Morrissey, Anlai Wang, Ribo Guo, Anthony

Vattay, Kathy Hsiao, Jing Yuan, John Green, and Beatrice Ospina. 2010. “Interfering with Resistance to Smoothened Antagonists by Inhibition of the PI3K Pathway in Medulloblastoma.” *Science Translational Medicine* 2 (51): 51ra70.

Buzzai, M, R G Jones, R K Amaravadi, J J Lum, R J DeBerardinis, F Zhao, B Viollet, and C B Thompson. 2007. “Systemic Treatment with the Antidiabetic Drug Metformin Selectively Impairs P53-Deficient Tumor Cell Growth.” *Cancer Research* 67 (14) (July 15): 6745–6752. doi:10.1158/0008-5472.CAN-06-4447.

Cajal, S. 1911. “Histologie Du Systeme Nerveux De l'Homme Et Des Vertebrates.” *Histologie Du Systdme Nerveux De l'Homme Et Des Vertdbrds* 1.

Chen, J K. 2002. “Inhibition of Hedgehog Signaling by Direct Binding of Cyclopamine to Smoothened.” *Genes & Development* 16 (21) (November 1): 2743–2748. doi:10.1101/gad.1025302.

Chen, M H, C W Wilson, Y J Li, K K L Law, C S Lu, R Gacayan, X Zhang, C-C Hui, and P-T Chuang. 2009. “Cilium-Independent Regulation of Gli Protein Function by Sufu in Hedgehog Signaling Is Evolutionarily Conserved.” *Genes & Development* 23 (16) (August 14): 1910–1928. doi:10.1101/gad.1794109.

Chen, W. 2004. “Activity-Dependent Internalization of Smoothened Mediated by -Arrestin 2 and GRK2.” *Science* 306 (5705) (December 24): 2257–2260. doi:10.1126/science.1104135.

Chen, Yongbin, Noriaki Sasai, Guoqiang Ma, Tao Yue, Jianhang Jia, James Briscoe, and Jin Jiang. 2011. “Sonic Hedgehog Dependent Phosphorylation by CK1α and GRK2 Is Required for Ciliary Accumulation and Activation of Smoothened.” Edited by Konrad Basler. *PLoS Biol* 9 (6) (June 14): e1001083. doi:10.1371/journal.pbio.1001083.s005.

Cheng, Frances Y, Xi Huang, Anuraag Sarangi, Tatiana Ketova, Michael K Cooper, Ying LItingtung, and Chin Chiang. 2012. “Widespread Contribution of Gdf7 Lineage to Cerebellar Cell Types and Implications for Hedgehog-Driven Medulloblastoma Formation.” Edited by Peter Hitchcock. *PLoS ONE* 7 (4) (April 23): e35541. doi:10.1371/journal.pone.0035541.g006.

Chi, C L. 2003. “The Isthmic Organizer Signal FGF8 Is Required for Cell Survival in the Prospective Midbrain and Cerebellum.” *Development* 130 (12) (June 15): 2633–2644. doi:10.1242/dev.00487.

Chiang, C, Y Litingtung, E Lee, K E Young, J L Corden, H Westphal, and P A Beachy. 1996. “Cyclopia and Defective Axial Patterning in Mice Lacking Sonic Hedgehog Gene Function.” *Nature* 383 (6599) (October 3): 407–413. doi:10.1038/383407a0.

Chizhikov, V V, A G Lindgren, Y Mishima, R W Roberts, K A Aldinger, G R Miesegaes, D S Currle, E S Monuki, and K J Millen. 2010. “Lmx1a Regulates Fates and Location of Cells Originating From the Cerebellar Rhombic Lip and Telencephalic Cortical Hem.” *Proceedings of the National Academy of Sciences* 107 (23) (June 8): 10725–10730. doi:10.1073/pnas.0910786107.

Chizhikov, V V, and K J Millen. 2004. “Mechanisms of Roof Plate Formation in the Vertebrate CNS.” *Nature Reviews Neuroscience* 5 (10): 808–812.

Chizhikov, VV, AG Lindgren, DS Currle, MF Rose, ES Monuki, and KJ Millen. 2006. “The Roof Plate Regulates Cerebellar Cell-Type Specification and Proliferation.” *Development* 133 (15): 2793.

Cho, Yoon-Jae, Aviad Tsherniak, Pablo Tamayo, Sandro Santagata, Azra Ligon, Heidi Greulich, Rameen Berhoukim, et al. 2011. “Integrative Genomic Analysis of Medulloblastoma Identifies a Molecular Subgroup That Drives Poor Clinical Outcome..” *Journal of Clinical Oncology* 29 (11) (April 10): 1424–1430. doi:10.1200/JCO.2010.28.5148.

Clement, Virginie, Pilar Sanchez, Nicolas de Tribolet, Ivan Radovanovic, and Ariel Ruiz I

Altaba. 2007. “HEDGEHOG-GLI1 Signaling Regulates Human Glioma Growth, Cancer Stem Cell Self-Renewal, and Tumorigenicity.” *Current Biology* 17 (2) (January): 165–172. doi:10.1016/j.cub.2006.11.033. http://www.sciencedirect.com/science/article/pii/S0960982206025140.

Clifford, Steven C, Meryl E Lusher, Janet C Lindsey, Jacqueline A Langdon, Richard J Gilbertson, Debbie Straughton, and David W Ellison. 2006. “Wnt/Wingless Pathway Activation and Chromosome 6 Loss Characterize a Distinct Molecular Sub-Group of Medulloblastomas Associated with a Favorable Prognosis..” *Cell Cycle* 5 (22) (November): 2666–2670.

Contesso, G, H Mouriesse, S Friedman, J Genin, D Sarrazin, and J Rouesse. 1987. “The Importance of Histologic Grade in Long-Term Prognosis of Breast Cancer: a Study of 1,010 Patients, Uniformly Treated at the Institut Gustave-Roussy..” *Journal of Clinical Oncology : Official Journal of the American Society of Clinical Oncology* 5 (9) (September): 1378–1386.

Cooper, Michael K, Christopher A Wassif, Patrycja A Krakowiak, Jussi Taipale, Ruoyu Gong, Richard I Kelley, Forbes D Porter, and Philip A Beachy. 2003. “A Defective Response to Hedgehog Signaling in Disorders of Cholesterol Biosynthesis.” *Nature Genetics* 33 (4) (April 24): 508–513. doi:10.1038/ng1134.

Corbit, Kevin C, Pia Aanstad, Veena Singla, Andrew R Norman, Didier Y R Stainier, and Jeremy F Reiter. 2005. “Vertebrate Smoothened Functions at the Primary Cilium.” *Nature Cell Biology* 437 (7061) (August 31): 1018–1021. doi:10.1038/nature04117.

Corrales, JMD, GL Rocco, S Blaess, Q Guo, and AL Joyner. 2004. “Spatial Pattern of Sonic Hedgehog Signaling Through Gli Genes During Cerebellum Development.” *Development* 131 (22): 5581.

Corrales, JMD, S Blaess, EM Mahoney, and AL Joyner. 2006. “The Level of Sonic Hedgehog Signaling Regulates the Complexity of Cerebellar Foliation.” *Development-Cambridge-* 133 (9): 1811.

Corton, Julia M, John G Gillespie, Simon A Hawley, and D Grahame Hardie. 1995. “5-Aminoimidazole-4-Carboxamide Ribonucleoside.” *European Journal of Biochemistry* 229 (2): 558–565.

Crossley, P H, S Martinez, and G R Martin. 1996. “Midbrain Development Induced by FGF8 in the Chick Embryo..” *Nature* 380 (6569) (March 7): 66–68. doi:10.1038/380066a0.

Currle, DS, X Cheng, C Hsu, and ES Monuki. 2005. “Direct and Indirect Roles of CNS Dorsal Midline Cells in Choroid Plexus Epithelia Formation.” *Development* 132 (15): 3549.

Cuthbertson, D J, J A Babraj, K J W Mustard, M C Towler, K A Green, H Wackerhage, G P Leese, et al. 2007. “5-Aminoimidazole-4-Carboxamide 1- -D-Ribofuranoside Acutely Stimulates Skeletal Muscle 2-Deoxyglucose Uptake in Healthy Men.” *Diabetes* 56 (8) (August 1): 2078–2084. doi:10.2337/db06-1716.

Dahmane, N, and A Ruiz i Altaba. 1999. “Sonic Hedgehog Regulates the Growth and Patterning of the Cerebellum..” *Development* 126 (14) (June): 3089–3100.

Dahmane, N, J Lee, P Robins, P Heller, and AR i Altaba. 1997. “Activation of the Transcription Factor Gli1 and the Sonic Hedgehog Signalling Pathway in Skin Tumours.” *Nature* 389 (6653): 876–881.

Dahmane, N, P Sanchez, Y Gitton, V Palma, T Sun, M Beyna, H Weiner, and A Ruiz i Altaba. 2001. “The Sonic Hedgehog-Gli Pathway Regulates Dorsal Brain Growth and Tumorigenesis.” *Development* 128 (24): 5201.

Dang, L, X Fan, A Chaudhry, M Wang, N Gaiano, and C G Eberhart. 2006. “Notch3 Signaling Initiates Choroid Plexus Tumor Formation..” *Oncogene* 25 (3) (January 19): 487–491. doi:10.1038/sj.onc.1209074.

Das, G D. 1976. “Differentiation of Bergmann Glia Cells in the Cerebellum: a Golgi Study..” *Brain Research* 110 (2) (July 9): 199–213.

Davies, Stephen P, Nicholas R Helps, Patricia TW Cohen, and D Grahame Hardie. 1995. “5′-AMP Inhibits Dephosphorylation, as Well as Promoting Phosphorylation, of the AMP-Activated Protein Kinase. Studies Using Bacterially Expressed Human Protein Phosphatase-2C A and Native Bovine Protein Phosphatase-2A C.” *FEBS Letters* 377 (3): 421–425.

De Zeeuw, Chris I, and Christopher H Yeo. 2005. “Time and Tide in Cerebellar Memory Formation.” *Current Opinion in Neurobiology* 15 (6) (December): 667–674. doi:10.1016/j.conb.2005.10.008.

Dehart, D B, L Lanoue, G S Tint, and K K Sulik. 1997. “Pathogenesis of Malformations in a Rodent Model for Smith-Lemli-Opitz Syndrome..” *American Journal of Medical Genetics* 68 (3) (January 31): 328–337.

Dhall, G. 2009. “Medulloblastoma.” *Journal of Child Neurology* 24 (11) (October 19): 1418–1430. doi:10.1177/0883073809341668.

di Magliano, Marina Pasca, and Matthias Hebrok. 2003. “Hedgehog Signalling in Cancer Formation and Maintenance.” *Nature Reviews Cancer* 3 (12) (December): 903–911. doi:10.1038/nrc1229.

Dino, M R, R J Schuerger, Y-B Liu, N T Slater, and E Mugnaini. 2000. “Unipolar Brush Cell: a Potential Feedforward Excitatory Interneuron of the Cerebellum.” *Neuroscience* 98 (4): 625–636.

Due-T oslash nnessen, Bernt Johan, and Eirik Helseth. 2007. “Management of Hydrocephalus in Children with Posterior Fossa Tumors: Role of Tumor Surgery.” *Pediatric Neurosurgery* 43 (2): 92–96. doi:10.1159/000098379.

Dymecki, S.M., and H. Tomasiewicz. 1998. “Using Flp-Recombinase to Characterize Expansion ofWnt1-Expressing Neural Progenitors in the Mouse.” *Developmental Biology* 201 (1): 57–65.

Ehtesham, M, A Sarangi, J G Valadez, S Chanthaphaychith, M W Becher, T W Abel, R C Thompson, and M K Cooper. 2007. “Ligand-Dependent Activation of the Hedgehog Pathway in Glioma Progenitor Cells.” *Oncogene* 26 (39) (March 12): 5752–5761. doi:10.1038/sj.onc.1210359.

Eiraku, Mototsugu, Akira Tohgo, Katsuhiko Ono, Megumi Kaneko, Kazuto Fujishima, Tomoo Hirano, and Mineko Kengaku. 2005. “DNER Acts as a Neuron-Specific Notch Ligand During Bergmann Glial Development.” *Nature Neuroscience* 8 (7) (June 19): 873–880. doi:10.1038/nn1492.

Ellison, David W, Steven C Clifford, Amar Gajjar, and Richard J Gilbertson. 2003. “What's New in Neuro-Oncology? Recent Advances in Medulloblastoma.” *European Journal of Paediatric Neurology* 7 (2) (March): 53–66. doi:10.1016/S1090-3798(03)00014-X.

Eroglu, Cagla, and Ben A Barres. 2010. “Regulation of Synaptic Connectivity by Glia.” *Nature* 468 (7321) (November 11): 223–231. doi:10.1038/nature09612.

Feng, L, M E Hatten, and N Heintz. 1994. “Brain Lipid-Binding Protein (BLBP): a Novel Signaling System in the Developing Mammalian CNS..” *Neuron* 12 (4) (April): 895–908.

Fernandez, C, VM Tatard, N Bertrand, and N Dahmane. 2010. “Differential Modulation of Sonic-Hedgehog-Induced Cerebellar Granule Cell Precursor Proliferation by the IGF Signaling Network.” *Developmental Neuroscience* 32 (1): 59–70.

Fernandez-L, A, PA Northcott, J Dalton, C Fraga, D Ellison, S Angers, MD Taylor, and AM Kenney. 2009. “YAP1 Is Amplified and Up-Regulated in Hedgehog-Associated Medulloblastomas and Mediates Sonic Hedgehog-Driven Neural Precursor Proliferation.” *Genes & Development* 23 (23): 2729.

Fiacco, Todd A, and Ken D McCarthy. 2006. “Astrocyte Calcium Elevations: Properties, Propagation, and Effects on Brain Signaling.” *Glia* 54 (7): 676–690. doi:10.1002/glia.20396.

Filippidis, Aristotelis S, M Yashar S Kalani, and Harold L Rekate. 2010. “Hydrocephalus and Aquaporins: Lessons Learned From the Bench.” *Child's Nervous System* 27 (1) (July 13): 27–33. doi:10.1007/s00381-010-1227-6.

Finch, P W, X He, M J Kelley, A Uren, R P Schaudies, N C Popescu, S Rudikoff, S A Aaronson, H E Varmus, and J S Rubin. 1997. “Purification and Molecular Cloning of a Secreted, Frizzled-Related Antagonist of Wnt Action..” *Proceedings of the National Academy of Sciences of the United States of America* 94 (13) (June 24): 6770–6775.

Fleming, Jonathan T, Wenjuan He, Chuanming Hao, Tatiana Ketova, Fong C Pan, Christopher C V Wright, Ying Litingtung, and Chin Chiang. “The Purkinje Neuron Acts as a Central Regulator of Spatially and Functionally Distinct Cerebellar Precursors.”

Fogarty, MP, BA Emmenegger, LL Grasfeder, TG Oliver, and RJ Wechsler-Reya. 2007. “Fibroblast Growth Factor Blocks Sonic Hedgehog Signaling in Neuronal Precursors and Tumor Cells.” *Proceedings of the National Academy of Sciences* 104 (8) (February 13): 2973.

Fraser, MM, X Zhu, CH Kwon, EJ Uhlmann, DH Gutmann, and SJ Baker. 2004. “Pten Loss Causes Hypertrophy and Increased Proliferation of Astrocytes in Vivo.” *Cancer Research* 64 (21): 7773.

Fu, YuHong, Petr Tvrdik, Nadja Makki, George Paxinos, and Charles Watson. 2011. “Precerebellar Cell Groups in the Hindbrain of the Mouse Defined by Retrograde Tracing and Correlated with Cumulative Wnt1-Cre Genetic Labeling.” *The Cerebellum* 10 (3) (April 12): 570–584. doi:10.1007/s12311-011-0266-1.

Fujimura, Miki, Takehide Onuma, Motonobu Kameyama, Osamu Motohashi, Hiroyuki Kon, Katsuya Yamamoto, Kiyoshi Ishii, and Teiji Tominaga. 2004. “Hydrocephalus Due to Cerebrospinal Fluid Overproduction by Bilateral Choroid Plexus Papillomas.” *Child's Nervous System* 20 (7) (February 21). doi:10.1007/s00381-003-0889-8.

Fuller, Gregory N. 2008. “The WHO Classification of Tumours of the Central Nervous System, 4th Edition..” *Archives of Pathology & Laboratory Medicine* 132 (6) (June): 906. doi:10.1043/1543-2165(2008)132[906:TWCOTO]2.0.CO;2.

Furuya, S, T Tabata, J Mitoma, K Yamada, M Yamasaki, A Makino, T Yamamoto, M Watanabe, M Kano, and Y Hirabayashi. 2000. “L-Serine and Glycine Serve as Major Astroglia-Derived Trophic Factors for Cerebellar Purkinje Neurons..” *Proceedings of the National Academy of Sciences of the United States of America* 97 (21) (October 10): 11528–11533. doi:10.1073/pnas.200364497.

Fuse, N, T Maiti, B Wang, JA Porter, TMT Hall, DJ Leahy, and PA Beachy. 1999. “Sonic Hedgehog Protein Signals Not as a Hydrolytic Enzyme but as an Apparent Ligand for Patched.” *Proceedings of the National Academy of Sciences of the United States of America* 96 (20): 10992.

Gajjar, Amar, Murali Chintagumpala, David Ashley, Stewart Kellie, Larry E Kun, Thomas E Merchant, Shaio Woo, et al. 2006. “Risk-Adapted Craniospinal Radiotherapy Followed by High-Dose Chemotherapy and Stem-Cell Rescue in Children with Newly Diagnosed Medulloblastoma (St Jude Medulloblastoma-96): Long-Term Results From a Prospective, Multicentre Trial..” *The Lancet Oncology* 7 (10) (October): 813–820. doi:10.1016/S1470-2045(06)70867-1.

Garcia, A D R, R Petrova, L Eng, and A L Joyner. 2010. “Sonic Hedgehog Regulates Discrete Populations of Astrocytes in the Adult Mouse Forebrain.” *Journal of Neuroscience* 30 (41) (October 13): 13597–13608. doi:10.1523/JNEUROSCI.0830-

10.2010.
Garcia-Gil, M, R Pesi, S Perna, S Allegrini, M Giannecchini, M Camici, and M G Tozzi. 2003. “5′-Aminoimidazole-4-Carboxamide Riboside Induces Apoptosis in Human Neuroblastoma Cells.” *Neuroscience* 117 (4) (April): 811–820. doi:10.1016/S0306-4522(02)00836-9.
Gibson, Paul, Yiai Tong, Giles Robinson, Margaret C Thompson, D Spencer Currle, Christopher Eden, Tanya A Kranenburg, et al. 2010. “Subtypes of Medulloblastoma Have Distinct Developmental Origins.” *Nature* 468 (7327) (December 8): 1–5. doi:10.1038/nature09587.
Gilbertson, RJ, and DW Ellison. 2008. “The Origins of Medulloblastoma Subtypes.”
Giménez Y Ribotta, M, F Langa, V Menet, and A Privat. 2000. “Comparative Anatomy of the Cerebellar Cortex in Mice Lacking Vimentin, GFAP, and Both Vimentin and GFAP..” *Glia* 31 (1) (July): 69–83.
Gleason, C E, D Lu, L A Witters, C B Newgard, and M J Birnbaum. 2007. “The Role of AMPK and mTOR in Nutrient Sensing in Pancreatic Beta-Cells.” *Journal of Biological Chemistry* 282 (14) (February 2): 10341–10351. doi:10.1074/jbc.M610631200.
González-Gironès, Diana M, Cristina Moncunill-Massaguer, Daniel Iglesias-Serret, Ana M Cosialls, Alba Pérez-Perarnau, Claudia M Palmeri, Camila Rubio-Patiño, Andreas Villunger, Gabriel Pons, and Joan Gil. 2013. “AICAR Induces Bax/Bak-Dependent Apoptosis Through Upregulation of the BH3-Only Proteins Bim and Noxa in Mouse Embryonic Fibroblasts..” *Apoptosis : an International Journal on Programmed Cell Death* 18 (8) (August): 1008–1016. doi:10.1007/s10495-013-0850-6.
Goodrich, LV, L Milenkovic, KM Higgins, and MP Scott. 1997. “Altered Neural Cell Fates and Medulloblastoma in Mouse Patched Mutants.” *Science* 277 (5329): 1109.
Goodrich, LV, RL Johnson, L Milenkovic, JA McMahon, and MP Scott. 1996. “Conservation of the Hedgehog/Patched Signaling Pathway From Flies to Mice: Induction of a Mouse Patched Gene by Hedgehog..” *Genes & Development* 10 (3): 301.
Gorlin, RJ. 1987. “Nevoid Basal-Cell Carcinoma Syndrome.” *Medicine* 66 (2): 98.
Graus-Porta, D, S Blaess, M Senften, A Littlewood-Evans, C Damsky, Z Huang, P Orban, R Klein, J C Schittny, and U Müller. 2001. “Beta1-Class Integrins Regulate the Development of Laminae and Folia in the Cerebral and Cerebellar Cortex..” *Neuron* 31 (3) (August 16): 367–379.
Gritli-Linde, Amel, Paula Lewis, Andrew P McMahon, and Anders Linde. 2001. “The Whereabouts of a Morphogen: Direct Evidence for Short- and Graded Long-Range Activity of Hedgehog Signaling Peptides.” *Developmental Biology* 236 (2) (August): 364–386. doi:10.1006/dbio.2001.0336.
Guha, Malini. 2012. “Hedgehog Inhibitor Gets Landmark Skin Cancer Approval, but Questions Remain for Wider Potential.” *Nature Reviews Drug Discovery* 11 (4): 257–258.
Guigas, Bruno, Luc Bertrand, Nellie Taleux, Marc Foretz, Nicolas Wiernsperger, Didier Vertommen, Fabrizio Andreelli, Benoit Viollet, and Louis Hue. 2006. “5-Aminoimidazole-4-Carboxamide-1-Beta-D-Ribofuranoside and Metformin Inhibit Hepatic Glucose Phosphorylation by an AMP-Activated Protein Kinase-Independent Effect on Glucokinase Translocation..” *Diabetes* 55 (4) (April): 865–874.
Guo, D, S Chien, and J Y J Shyy. 2007. “Regulation of Endothelial Cell Cycle by Laminar Versus Oscillatory Flow: Distinct Modes of Interactions of AMP-Activated Protein Kinase and Akt Pathways.” *Circulation Research* 100 (4) (March 2): 564–571. doi:10.1161/01.RES.0000259561.23876.c5.
Guo, Deliang, Isabel J Hildebrandt, Robert M Prins, Horacio Soto, Mary M Mazzotta,

Julie Dang, Johannes Czernin, et al. 2009. “The AMPK Agonist AICAR Inhibits the Growth of EGFRvIII-Expressing Glioblastomas by Inhibiting Lipogenesis..” *Proceedings of the National Academy of Sciences* 106 (31) (August 4): 12932–12937. doi:10.1073/pnas.0906606106.

Haan, N, T Goodman, A Najdi-Samiei, C M Stratford, R Rice, E El Agha, S Bellusci, and M K Hajihosseini. 2013. “Fgf10-Expressing Tanycytes Add New Neurons to the Appetite/Energy-Balance Regulating Centers of the Postnatal and Adult Hypothalamus.” *Journal of Neuroscience* 33 (14) (April 3): 6170–6180. doi:10.1523/JNEUROSCI.2437-12.2013.

Haber, M. 2006. “Cooperative Astrocyte and Dendritic Spine Dynamics at Hippocampal Excitatory Synapses.” *Journal of Neuroscience* 26 (35) (August 30): 8881–8891. doi:10.1523/JNEUROSCI.1302-06.2006.

Hahn, H, J Christiansen, C Wicking, PG Zaphiropoulos, A Chidambaram, B Gerrard, I Vorechovsky, AE Bale, R Toftgard, and M Dean. 1996. “A Mammalian Patched Homolog Is Expressed in Target Tissues of Sonic Hedgehog and Maps to a Region Associated with Developmental Abnormalities.” *Journal of Biological Chemistry* 271 (21): 12125.

Haldipur, Parthiv, Upasna Bharti, Corinne Alberti, Chitra Sarkar, Geetika Gulati, Soumya Iyengar, Pierre Gressens, and Shyamala Mani. 2011. “Preterm Delivery Disrupts the Developmental Program of the Cerebellum.” Edited by Olivier Baud. *PLoS ONE* 6 (8) (August 17): e23449. doi:10.1371/journal.pone.0023449.s010.

Hallonet, M E, M A Teillet, and N M Le Douarin. 1990. “A New Approach to the Development of the Cerebellum Provided by the Quail-Chick Marker System..” *Development* 108 (1) (January): 19–31.

Hallows, K R, R Alzamora, H Li, F Gong, C Smolak, D Neumann, and N M Pastor-Soler. 2009. “AMP-Activated Protein Kinase Inhibits Alkaline pH- and PKA-Induced Apical Vacuolar H+-ATPase Accumulation in Epididymal Clear Cells.” *American Journal of Physiology. Cell Physiology* 296 (4) (February 11): C672–C681. doi:10.1152/ajpcell.00004.2009.

Hamilton, Stanley R, Bo Liu, Ramon E Parsons, Nickolas Papadopoulos, Jin Jen, Steven M Powell, Anne J Krush, Theresa Berk, Zane Cohen, and Bernard Tetu. 1995. “The Molecular Basis of Turcot's Syndrome.” *New England Journal of Medicine* 332 (13): 839–847.

Hatten, M E. 1987. “Neuronal Inhibition of Astroglial Cell Proliferation Is Membrane Mediated..” *The Journal of Cell Biology* 104 (5) (May): 1353–1360.

Hatten, ME, and N Heintz. 1995. “Mechanisms of Neural Patterning and Specification in the Development Cerebellum.” *Annual Review of Neuroscience* 18 (1): 385–408.

Hatten, ME, J Alder, K Zimmerman, and N Heintz. 1997. “Genes Involved in Cerebellar Cell Specification and Differentiation.” *Current Opinion in Neurobiology* 7 (1): 40–47.

Hatton, BA, PS Knoepfler, AM Kenney, DH Rowitch, IM de Alboran, JM Olson, and RN Eisenman. 2006. “N-Myc Is an Essential Downstream Effector of Shh Signaling During Both Normal and Neoplastic Cerebellar Growth.” *Cancer Research* 66 (17): 8655.

Hausmann, B, and J Sievers. 1985. “Cerebellar External Granule Cells Are Attached to the Basal Lamina From the Onset of Migration Up to the End of Their Proliferative Activity..” *The Journal of Comparative Neurology* 241 (1) (November 1): 50–62. doi:10.1002/cne.902410105.

Hawley, Simon A, Jérôme Boudeau, Jennifer L Reid, Kirsty J Mustard, Lina Udd, Tomi P Mäkelä, Dario R Alessi, and D Grahame Hardie. 2003. “Complexes Between the LKB1 Tumor Suppressor, STRAD Alpha/Beta and MO25 Alpha/Beta Are Upstream Kinases in the AMP-Activated Protein Kinase Cascade.” *Journal of Biology* 2 (4): 1–

16. doi:10.1186/1475-4924-2-28.
Heine, V M, M Priller, J LING, D H Rowitch, and U Schuller. 2010. “Dexamethasone Destabilizes Nmyc to Inhibit the Growth of Hedgehog-Associated Medulloblastoma.” *Cancer Research* 70 (13) (July 1): 5220–5225. doi:10.1158/0008-5472.CAN-10-0554.
Helms, Amy W, Andrew L Abney, Nissim Ben-Arie, Huda Y Zoghbi, and Jane E Johnson. 2000. “Autoregulation and Multiple Enhancers Control Math1 Expression in the Developing Nervous System.” *Development* 127 (6): 1185–1196.
Heretsch, Philipp, Lito Tzagkaroulaki, and Athanassios Giannis. 2010. “Cyclopamine and Hedgehog Signaling: Chemistry, Biology, Medical Perspectives.” *Angewandte Chemie International Edition* 49 (20) (April 6): 3418–3427. doi:10.1002/anie.200906967.
Heuer, Heike, and Carol Ann Mason. 2003. “Thyroid Hormone Induces Cerebellar Purkinje Cell Dendritic Development via the Thyroid Hormone Receptor Alpha1..” *Journal of Neuroscience* 23 (33) (November 19): 10604–10612.
Hoogendijk, A J, S S Pinhancos, T van der Poll, and C W Wieland. 2013. “AMP-Activated Protein Kinase Activation by 5-Aminoimidazole-4-Carbox-Amide-1- -D-Ribofuranoside (AICAR) Reduces Lipoteichoic Acid-Induced Lung Inflammation.” *Journal of Biological Chemistry* 288 (10) (March 8): 7047–7052. doi:10.1074/jbc.M112.413138.
Horike, N, H Sakoda, A Kushiyama, H Ono, M Fujishiro, H Kamata, K Nishiyama, et al. 2008. “AMP-Activated Protein Kinase Activation Increases Phosphorylation of Glycogen Synthase Kinase 3 and Thereby Reduces cAMP-Responsive Element Transcriptional Activity and Phosphoenolpyruvate Carboxykinase C Gene Expression in the Liver.” *Journal of Biological Chemistry* 283 (49) (August 12): 33902–33910. doi:10.1074/jbc.M802537200.
Hosoya, Takahiro, Midori A Arai, Takashi Koyano, Thaworn Kowithayakorn, and Masami Ishibashi. 2008. “Naturally Occurring Small-Molecule Inhibitors of Hedgehog/GLI-Mediated Transcription.” *ChemBioChem* 9 (7) (May 5): 1082–1092. doi:10.1002/cbic.200700511.
Huang, X, J Liu, T Ketova, J T Fleming, V K Grover, M K Cooper, Y Litingtung, and C Chiang. 2010. “Transventricular Delivery of Sonic Hedgehog Is Essential to Cerebellar Ventricular Zone Development.” *Proceedings of the National Academy of Sciences* 107 (18) (May 4): 8422–8427. doi:10.1073/pnas.0911838107.
Huang, X, T Ketova, J T Fleming, H Wang, S K Dey, Y Litingtung, and C Chiang. 2009. “Sonic Hedgehog Signaling Regulates a Novel Epithelial Progenitor Domain of the Hindbrain Choroid Plexus.” *Development* 136 (15) (July 10): 2535–2543. doi:10.1242/dev.033795.
Huang, Xi, Tatiana Ketova, Ying LItingtung, and Chin Chiang. 2010. “Isolation, Enrichment, and Maintenance of Medulloblastoma Stem Cells.” *Journal of Visualized Experiments* (43). doi:10.3791/2086.
Huang, Y Z, and L Mei. 2001. “[Neuregulin/ErbB Signal Transduction Pathway in the Development of Nervous System]..” *Sheng Li Ke Xue Jin Zhan [Progress in Physiology]* 32 (3) (July): 197–203.
Hui, C C, D Slusarski, K A Platt, R Holmgren, and A L Joyner. 1994. “Expression of Three Mouse Homologs of the Drosophila Segment Polarity Gene Cubitus Interruptus, Gli, Gli-2, and Gli-3, in Ectoderm- and Mesoderm-Derived Tissues Suggests Multiple Roles During Postimplantation Development.” *Developmental Biology* 162 (2) (April 1): 402–413. doi:10.1006/dbio.1994.1097.
Humke, E W, K V Dorn, L Milenkovic, M P Scott, and R Rohatgi. 2010. “The Output of Hedgehog Signaling Is Controlled by the Dynamic Association Between Suppressor

of Fused and the Gli Proteins." *Genes & Development* 24 (7) (April 1): 670–682. doi:10.1101/gad.1902910.
Hunter, NL, and SM Dymecki. 2007. "Molecularly and Temporally Separable Lineages Form the Hindbrain Roof Plate and Contribute Differentially to the Choroid Plexus." *Development* 134 (19): 3449.
Hyman, JM, AJ Firestone, VM Heine, Y Zhao, CA Ocasio, K Han, M Sun, PG Rack, S Sinha, and JJ Wu. 2009. "Small-Molecule Inhibitors Reveal Multiple Strategies for Hedgehog Pathway Blockade." *Proceedings of the National Academy of Sciences* 106 (33): 14132.
Hynes, M, JA Porter, C Chiang, D Chang, M Tessier-Lavigne, PA Beachy, and A Rosenthal. 1995. "Induction of Midbrain Dopaminergic Neurons by Sonic Hedgehog." *Neuron* 15 (1): 35–44.
Iino, M. 2001. "Glia-Synapse Interaction Through Ca2+-Permeable AMPA Receptors in Bergmann Glia." *Science* 292 (5518) (May 4): 926–929. doi:10.1126/science.1058827.
Ingham, PW, and AP McMahon. 2001. "Hedgehog Signaling in Animal Development: Paradigms and Principles." *Genes & Development* 15 (23): 3059.
Inoki, Ken, Tianqing Zhu, and Kun-Liang Guan. 2003. "TSC2 Mediates Cellular Energy Response to Control Cell Growth and Survival." *Cell* 115 (5): 577–590.
Inouye, M, and U Murakami. 1980. "Temporal and Spatial Patterns of Purkinje Cell Formation in the Mouse Cerebellum.." *The Journal of Comparative Neurology* 194 (3) (December 1): 499–503. doi:10.1002/cne.901940302.
Ito, Masao. 2006. "Cerebellar Circuitry as a Neuronal Machine." *Progress in Neurobiology* 78 (3-5) (February): 272–303. doi:10.1016/j.pneurobio.2006.02.006.
Izzi, Luisa, Martin Lévesque, Steves Morin, Dominique Laniel, Brian C Wilkes, Frédéric Mille, Robert S Krauss, Andrew P McMahon, Benjamin L Allen, and Frédéric Charron. 2011. "Boc and Gas1 Each Form Distinct Shh Receptor Complexes with Ptch1 and Are Required for Shh-Mediated Cell Proliferation." *Developmental Cell* 20 (6) (June): 788–801. doi:10.1016/j.devcel.2011.04.017.
Jacobs, R L, S Lingrell, J R B Dyck, and D E Vance. 2006. "Inhibition of Hepatic Phosphatidylcholine Synthesis by 5-Aminoimidazole-4-Carboxamide-1-Beta-4-Ribofuranoside Is Independent of AMP-Activated Protein Kinase Activation." *Journal of Biological Chemistry* 282 (7) (November 27): 4516–4523. doi:10.1074/jbc.M605702200.
Javaux, F, M F Vincent, D R Wagner, and G Van den Berghe. 1995. "Cell-Type Specificity of Inhibition of Glycolysis by 5-Amino-4-Imidazolecarboxamide Riboside. Lack of Effect in Rabbit Cardiomyocytes and Human Erythrocytes, and Inhibition in FTO-2B Rat Hepatoma Cells.." *The Biochemical Journal* 305: 913–919.
Jensen, P. 2004. "Analysis of Cerebellar Development in Math1 Null Embryos and Chimeras." *Journal of Neuroscience* 24 (9) (March 3): 2202–2211. doi:10.1523/JNEUROSCI.3427-03.2004.
Jeong, J, J Mao, T Tenzen, AH Kottmann, and AP McMahon. 2004. "Hedgehog Signaling in the Neural Crest Cells Regulates the Patterning and Growth of Facial Primordia." *Genes & Development* 18 (8): 937.
Jiang, Jin, and Chi-chung Hui. 2008. "Hedgehog Signaling in Development and Cancer." *Developmental Cell* 15 (6) (December 9): 801–812. doi:10.1016/j.devcel.2008.11.010.
Johnson, RL, AL Rothman, J Xie, LV Goodrich, JW Bare, JM Bonifas, AG Quinn, RM Myers, DR Cox, and EH Epstein Jr. 1996. "Human Homolog of Patched, a Candidate Gene for the Basal Cell Nevus Syndrome." *Science* 272 (5268): 1668.
Jones, David T W, Natalie Jäger, Marcel Kool, Thomas Zichner, Barbara Hutter, Marc

Sultan, Yoon-Jae Cho, et al. 2012. “Dissecting the Genomic Complexity Underlying Medulloblastoma.” *Nature* 488 (7409) (July 25): 100–105. doi:10.1038/nature11284.
Joyner, A L, A Liu, and S Millet. 2000. “Otx2, Gbx2 and Fgf8 Interact to Position and Maintain a Mid-Hindbrain Organizer..” *Current Opinion in Cell Biology* 12 (6) (December): 736–741.
Joyner, A L, W C Skarnes, and J Rossant. 1989. “Production of a Mutation in Mouse en-2 Gene by Homologous Recombination in Embryonic Stem Cells..” *Nature* 338 (6211) (March 9): 153–156. doi:10.1038/338153a0.
Joyner, Alexandra L. 1996. “ Engrailed, Wnt and Pax Genes Regulate Midbrain-Hindbrain Development.” *Trends Genet* 12 (1): 15–20.
Jozwiak, Jaroslaw, Wieslawa Grajkowska, and Pawel Wlodarski. 2007. “Pathogenesis of Medulloblastoma and Current Treatment Outlook.” *Medicinal Research Reviews* 27 (6): 869–890. doi:10.1002/med.20088.
Jørgensen, Sebastian B, Jakob N Nielsen, Jesper B Birk, Grith Skytte Olsen, Benoit Viollet, Fabrizio Andreelli, Peter Schjerling, Sophie Vaulont, D Grahame Hardie, and Bo F Hansen. 2004. “The A2–5′ AMP-Activated Protein Kinase Is a Site 2 Glycogen Synthase Kinase in Skeletal Muscle and Is Responsive to Glucose Loading.” *Diabetes* 53 (12): 3074–3081.
Katerelos, Marina, Stuart J Mudge, David Stapleton, Russell B Auwardt, Scott A Fraser, C-G Chen, Bruce E Kemp, and David A Power. 2010. “5-Aminoimidazole-4-Carboxamide Ribonucleoside and AMP-Activated Protein Kinase Inhibit Signalling Through NF-κB.” *Immunology and Cell Biology* 88 (7) (April 20): 754–760. doi:10.1038/icb.2010.44.
Katoh, Yuriko, and Masaru Katoh. 2006. “WNT Antagonist, SFRP1, Is Hedgehog Signaling Target..” *International Journal of Molecular Medicine* 17 (1) (January): 171–175.
Kemp, B E, D Stapleton, D J Campbell, Z P Chen, S Murthy, Mark Walter, A Gupta, J J Adams, Frosa Katsis, and Bryce van Denderen. 2003. “AMP-Activated Protein Kinase, Super Metabolic Regulator..” *Biochemical Society Transactions* 31 (Pt 1): 162–168.
Kenney, AM, HR Widlund, and DH Rowitch. 2004. “Hedgehog and PI-3 Kinase Signaling Converge on Nmyc1 to Promote Cell Cycle Progression in Cerebellar Neuronal Precursors.” *Development* 131 (1): 217.
Kenney, AM, MD Cole, and DH Rowitch. 2003. “Nmyc Upregulation by Sonic Hedgehog Signaling Promotes Proliferation in Developing Cerebellar Granule Neuron Precursors.” *Development* 130 (1): 15.
Kenney, Anna, and David Rowitch. 2000. “Sonic Hedgehog Promotes G1 Cyclin Expression and Sustained Cell Cycle Progression in Mammalian Neuronal Precursors.” *Molecular and Cellular Biology* 20 (23) (December 1): 9055. doi:10.1128/MCB.20.23.9055-9067.2000.
Kessler, J D, H Hasegawa, S N Brun, B A Emmenegger, Z-J Yang, J W Dutton, F Wang, and R J Wechsler-Reya. 2009. “N-Myc Alters the Fate of Preneoplastic Cells in a Mouse Model of Medulloblastoma.” *Genes & Development* 23 (2) (January 15): 157–170. doi:10.1101/gad.1759909.
Kettenmann, H, and A Verkhratsky. 2011. “[Neuroglia--Living Nerve Glue]..” *Fortschritte Der Neurologie-Psychiatrie* 79 (10) (October): 588–597. doi:10.1055/s-0031-1281704.
Khatib, Ziad A, Hitoshi Matsushime, Marcus Valentine, David N Shapiro, Charles J Sherr, and A Thomas Look. 1993. “Coamplification of the CDK4 Gene with MDM2 and GLI in Human Sarcomas.” *Cancer Research* 53 (22): 5535–5541.
Kim, J, JJ Lee, J Kim, D Gardner, and PA Beachy. 2010. “Arsenic Antagonizes the

Hedgehog Pathway by Preventing Ciliary Accumulation and Reducing Stability of the Gli2 Transcriptional Effector." *Proceedings of the National Academy of Sciences* 107 (30): 13432.

Kim, Jynho, Masaki Kato, and Philip A Beachy. 2009. "Gli2 Trafficking Links Hedgehog-Dependent Activation of Smoothened in the Primary Cilium to Transcriptional Activation in the Nucleus." *Proceedings of the National Academy of Sciences of the United States of America* 106 (51): 21666–21671.

King, Taj D, Ling Song, and Richard S Jope. 2006. "AMP-Activated Protein Kinase (AMPK) Activating Agents Cause Dephosphorylation of Akt and Glycogen Synthase Kinase-3.." *Biochemical Pharmacology* 71 (11) (May 28): 1637–1647. doi:10.1016/j.bcp.2006.03.005.

Knoepfler, Paul S, Pei Feng Cheng, and Robert N Eisenman. 2002. "N-Myc Is Essential During Neurogenesis for the Rapid Expansion of Progenitor Cell Populations and the Inhibition of Neuronal Differentiation.." *Genes & Development* 16 (20) (October 15): 2699–2712. doi:10.1101/gad.1021202.

Ko, H, and J Eggenschwiler. 2011. "Intraflagellar Transport Protein 122 Antagonizes Sonic Hedgehog Signaling and Controls Ciliary Localization of Pathway Components." *Proceedings of the ….*

Koirala, Samir, and Gabriel Corfas. 2010. "Identification of Novel Glial Genes by Single-Cell Transcriptional Profiling of Bergmann Glial Cells From Mouse Cerebellum." Edited by Thomas A Reh. *PLoS ONE* 5 (2) (February 12): e9198. doi:10.1371/journal.pone.0009198.t008.

Komine, Okiru, Mai Nagaoka, Kei Watase, David H Gutmann, Kenji Tanigaki, Tasuku Honjo, Freddy Radtke, Toshiki Saito, Shigeru Chiba, and Kohichi Tanaka. 2007. "The Monolayer Formation of Bergmann Glial Cells Is Regulated by Notch/RBP-J Signaling." *Developmental Biology* 311 (1) (November): 238–250. doi:10.1016/j.ydbio.2007.08.042.

Konnerth, A, I Llano, and C M Armstrong. 1990. "Synaptic Currents in Cerebellar Purkinje Cells.." *Proceedings of the National Academy of Sciences of the United States of America* 87 (7) (April): 2662–2665.

Kool, Marcel, Andrey Korshunov, Marc Remke, David T W Jones, Maria Schlanstein, Paul A Northcott, Yoon-Jae Cho, et al. 2012. "Molecular Subgroups of Medulloblastoma: an International Meta-Analysis of Transcriptome, Genetic Aberrations, and Clinical Data of WNT, SHH, Group 3, and Group 4 Medulloblastomas.." *Acta Neuropathologica* (February 23). doi:10.1007/s00401-012-0958-8.

Kool, Marcel, Jan Koster, Jens Bunt, Nancy E Hasselt, Arjan Lakeman, Peter Van Sluis, Dirk Troost, et al. 2008. "Integrated Genomics Identifies Five Medulloblastoma Subtypes with Distinct Genetic Profiles, Pathway Signatures and Clinicopathological Features." *PLoS ONE* 3 (8) (August 28): e3088.

Kouros-Mehr, Hosein, Seth K Bechis, Euan M Slorach, Laurie E Littlepage, Mikala Egeblad, Andrew J Ewald, Sung-Yun Pai, I-Cheng Ho, and Zena Werb. 2008. "GATA-3 Links Tumor Differentiation and Dissemination in a Luminal Breast Cancer Model.." *Cancer Cell* 13 (2) (February): 141–152. doi:10.1016/j.ccr.2008.01.011.

Kovacs, J J, E J Whalen, R Liu, K Xiao, J Kim, M Chen, J Wang, W Chen, and R J Lefkowitz. 2008. " -Arrestin-Mediated Localization of Smoothened to the Primary Cilium." *Science* 320 (5884) (June 27): 1777–1781. doi:10.1126/science.1157983.

Koziol, Leonard F, Deborah Budding, Nancy Andreasen, Stefano D'Arrigo, Sara Bulgheroni, Hiroshi Imamizu, Masao Ito, et al. 2013. "Consensus Paper: the Cerebellum's Role in Movement and Cognition." *The Cerebellum* (August 31). doi:10.1007/s12311-013-0511-x.

Laderoute, K R, K Amin, J M Calaoagan, M Knapp, T Le, J Orduna, M Foretz, and B Viollet. 2006. “5'-AMP-Activated Protein Kinase (AMPK) Is Induced by Low-Oxygen and Glucose Deprivation Conditions Found in Solid-Tumor Microenvironments.” *Molecular and Cellular Biology* 26 (14) (June 29): 5336–5347. doi:10.1128/MCB.00166-06.

Lai, Karen, Brian K Kaspar, Fred H Gage, and David V Schaffer. 2002. “Sonic Hedgehog Regulates Adult Neural Progenitor Proliferation in Vitro and in Vivo.” *Nature Neuroscience* 6 (1) (December 2): 21–27. doi:10.1038/nn983.

Laine, J, and H Axelrad. 2002. “Extending the Cerebellar Lugaro Cell Class.” *Neuroscience* 115 (2): 363–374.

Landsberg, RL, RB Awatramani, NL Hunter, AF Farago, HJ DiPietrantonio, CI Rodriguez, and SM Dymecki. 2005. “Hindbrain Rhombic Lip Is Comprised of Discrete Progenitor Cell Populations Allocated by Pax6.” *Neuron* 48 (6): 933–947.

Lang, Shih-Shan, Lauren A Beslow, Brandon Gabel, Alex R Judkins, Michael J Fisher, Leslie N Sutton, Phillip B Storm, and Gregory G Heuer. 2011. “Surgical Treatment of Brain Tumors in Infants Younger Than Six Months of Age and Review of the Literature.” *World Neurosurgery* (November). doi:10.1016/j.wneu.2011.09.012.

LARSELL, O. 1947. “The Development of the Cerebellum in Man in Relation to Its Comparative Anatomy..” *The Journal of Comparative Neurology* 87 (2) (October): 85–129.

Lauth, Matthias, Asa Bergström, Takashi Shimokawa, and Rune Toftgård. 2007. “Inhibition of GLI-Mediated Transcription and Tumor Cell Growth by Small-Molecule Antagonists..” *Proceedings of the National Academy of Sciences of the United States of America* 104 (20) (May 15): 8455–8460. doi:10.1073/pnas.0609699104.

Lee, J K, J H Cho, W S Hwang, Y D Lee, D S Reu, and H Suh-Kim. 2000. “Expression of neuroD/BETA2 in Mitotic and Postmitotic Neuronal Cells During the Development of Nervous System..” *Developmental Dynamics : an Official Publication of the American Association of Anatomists* 217 (4) (April): 361–367. doi:10.1002/(SICI)1097-0177(200004)217:4<361::AID-DVDY3>3.0.CO;2-8.

Lee, K J, M Mendelsohn, and T M Jessell. 1998. “Neuronal Patterning by BMPs: a Requirement for GDF7 in the Generation of a Discrete Class of Commissural Interneurons in the Mouse Spinal Cord..” *Genes & Development* 12 (21) (November 1): 3394–3407.

Lee, KJ, P Dietrich, and TM Jessell. 2000. “Genetic Ablation Reveals That the Roof Plate Is Essential for Dorsal Interneuron Specification.” *Nature* 403 (6771): 734–740.

Leis, O, A Eguiara, E Lopez-Arribillaga, M J Alberdi, S Hernandez-Garcia, K Elorriaga, A Pandiella, R Rezola, and A G Martin. 2011. “Sox2 Expression in Breast Tumours and Activation in Breast Cancer Stem Cells.” *Oncogene* 31 (11) (August 8): 1354–1365. doi:10.1038/onc.2011.338.

Leung, C, M Lingbeek, O Shakhova, J Liu, E Tanger, P Saremaslani, M van Lohuizen, and S Marino. 2004. “Bmi1 Is Essential for Cerebellar Development and Is Overexpressed in Human Medulloblastomas.” *Nature* 428 (6980): 337–341.

Leung, J M, T Stanley, J Mathew, P Curling, P Barash, M Salmenpera, J G Reves, M Hollenberg, and D T Mangano. 1994. “An Initial Multicenter, Randomized Controlled Trial on the Safety and Efficacy of Acadesine in Patients Undergoing Coronary Artery Bypass Graft Surgery. SPI Research Group..” *Anesthesia and Analgesia* 78 (3) (March): 420–434.

Lewis, P M, M P Dunn, J A McMahon, M Logan, J F Martin, B St-Jacques, and A P Mcmahon. 2001. “Cholesterol Modification of Sonic Hedgehog Is Required for Long-Range Signaling Activity and Effective Modulation of Signaling by Ptc1..” *Cell* 105 (5) (June 1): 599–612.

Lewis, PM, A Gritli-Linde, R Smeyne, A Kottmann, and AP McMahon. 2004. “Sonic Hedgehog Signaling Is Required for Expansion of Granule Neuron Precursors and Patterning of the Mouse Cerebellum.” *Developmental Biology* 270 (2): 393–410.

Li, Jun, Guangjin Pan, Kai Cui, Yuwen Liu, Shaobin Xu, and Duanqing Pei. 2007. “A Dominant-Negative Form of Mouse SOX2 Induces Trophectoderm Differentiation and Progressive Polyploidy in Mouse Embryonic Stem Cells..” *The Journal of Biological Chemistry* 282 (27) (July 6): 19481–19492. doi:10.1074/jbc.M702056200.

Li, Yina, Huimin Zhang, Ying LItingtung, and Chin Chiang. 2006. “Cholesterol Modification Restricts the Spread of Shh Gradient in the Limb Bud..” *Proceedings of the National Academy of Sciences of the United States of America* 103 (17) (April 25): 6548–6553. doi:10.1073/pnas.0600124103.

Li, Yina, Julie Gordon, Nancy R Manley, Ying LItingtung, and Chin Chiang. 2008. “Bmp4 Is Required for Tracheal Formation: a Novel Mouse Model for Tracheal Agenesis.” *Developmental Biology* 322 (1) (October): 145–155. doi:10.1016/j.ydbio.2008.07.021.

Lindholm, D, E Castrén, P Tsoulfas, R Kolbeck, M da P Berzaghi, A Leingärtner, C P Heisenberg, et al. 1993. “Neurotrophin-3 Induced by Tri-Iodothyronine in Cerebellar Granule Cells Promotes Purkinje Cell Differentiation..” *The Journal of Cell Biology* 122 (2) (July): 443–450.

Lippman, Jocelyn J, Tamar Lordkipanidze, Margaret E Buell, Sung Ok Yoon, and Anna Dunaevsky. 2008. “Morphogenesis and Regulation of Bergmann Glial Processes During Purkinje Cell Dendritic Spine Ensheathment and Synaptogenesis..” *Glia* 56 (13) (October): 1463–1477. doi:10.1002/glia.20712.

Litingtung, Y, and C Chiang. 2000. “Specification of Ventral Neuron Types Is Mediated by an Antagonistic Interaction Between Shh and Gli3..” *Nature Neuroscience* 3 (10) (October): 979–985. doi:10.1038/79916.

Liu, Wei, Timothy M Shaver, Alfred Balasa, M Cecilia Ljungberg, Xiaoling Wang, Shu Wen, Hoang Nguyen, and Ignatia B Van den Veyver. 2012. “Deletion of Porcn in Mice Leads to Multiple Developmental Defects and Models Human Focal Dermal Hypoplasia (Goltz Syndrome).” Edited by Shree Ram Singh. *PLoS ONE* 7 (3) (March 6): e32331. doi:10.1371/journal.pone.0032331.s003.

Lo, Liching, Emma L Dormand, and David J Anderson. 2005. “Late-Emigrating Neural Crest Cells in the Roof Plate Are Restricted to a Sensory Fate by GDF7..” *Proceedings of the National Academy of Sciences of the United States of America* 102 (20) (May 17): 7192–7197. doi:10.1073/pnas.0502581102.

Long, F, X M Zhang, S Karp, Y Yang, and A P Mcmahon. 2001. “Genetic Manipulation of Hedgehog Signaling in the Endochondral Skeleton Reveals a Direct Role in the Regulation of Chondrocyte Proliferation..” *Development* 128 (24) (December): 5099–5108.

Lordkipanidze, Tamar, and Anna Dunaevsky. 2005. “Purkinje Cell Dendrites Grow in Alignment with Bergmann Glia.” *Glia* 51 (3): 229–234. doi:10.1002/glia.20200.

Lorenz, A, M Deutschmann, J Ahlfeld, C Prix, A Koch, R Smits, R Fodde, H A Kretzschmar, and U Schüller. 2011. “Severe Alterations of Cerebellar Cortical Development After Constitutive Activation of Wnt Signaling in Granule Neuron Precursors.” *Molecular and Cellular Biology* 31 (16) (July 27): 3326–3338. doi:10.1128/MCB.05718-11.

Lumsden, A, and R Krumlauf. 1996. “Patterning the Vertebrate Neuraxis..” *Science* 274 (5290) (November 15): 1109–1115.

Ma, H, H Q Li, and X Zhang. 2013. “Cyclopamine, a Naturally Occurring Alkaloid, and Its Analogues May Find Wide Applications in Cancer Therapy..” *Current Topics in Medicinal Chemistry*.

Ma, S, H J Kwon, and Z Huang. 2012. “Ric-8a, a Guanine Nucleotide Exchange Factor for Heterotrimeric G Proteins, Regulates Bergmann Glia-Basement Membrane Adhesion During Cerebellar Foliation.” *Journal of Neuroscience* 32 (43) (October 24): 14979–14993. doi:10.1523/JNEUROSCI.1282-12.2012.

Machold, Rob, and Gord Fishell. 2005. “Math1 Is Expressed in Temporally Discrete Pools of Cerebellar Rhombic-Lip Neural Progenitors..” *Neuron* 48 (1) (October 6): 17–24. doi:10.1016/j.neuron.2005.08.028.

Machold, Robert, Shigemi Hayashi, Michael Rutlin, Mandar D Muzumdar, Susana Nery, Joshua G Corbin, Amel Gritli-Linde, Tammy Dellovade, Jeffery A Porter, and Lee L Rubin. 2003. “Sonic Hedgehog Is Required for Progenitor Cell Maintenance in Telencephalic Stem Cell Niches.” *Neuron* 39 (6): 937–950.

Madisen, Linda, Theresa A Zwingman, Susan M Sunkin, Seung Wook Oh, Hatim A Zariwala, Hong Gu, Lydia L Ng, et al. 2009. “A Robust and High-Throughput Cre Reporting and Characterization System for the Whole Mouse Brain.” *Nature Neuroscience* 13 (1) (December 20): 133–140. doi:10.1038/nn.2467.

Mangano, D T. 1997. “Effects of Acadesine on Myocardial Infarction, Stroke, and Death Following Surgery. a Meta-Analysis of the 5 International Randomized Trials. the Multicenter Study of Perioperative Ischemia (McSPI) Research Group..” *JAMA : the Journal of the American Medical Association* 277 (4) (January): 325–332.

Manto, Mario U, and Patrice Jissendi. 2012. “Cerebellum: Links Between Development, Developmental Disorders and Motor Learning.” *Frontiers in Neuroanatomy* 6. doi:10.3389/fnana.2012.00001.

Mao, J, K L Ligon, E Y Rakhlin, S P Thayer, R T Bronson, D Rowitch, and A P Mcmahon. 2006. “A Novel Somatic Mouse Model to Survey Tumorigenic Potential Applied to the Hedgehog Pathway.” *Cancer Research* 66 (20) (October 15): 10171–10178. doi:10.1158/0008-5472.CAN-06-0657.

Marangos, P J, T Loftus, J Wiesner, T Lowe, E Rossi, C E Browne, and H E Gruber. 1990. “Adenosinergic Modulation of Homocysteine-Induced Seizures in Mice.” *Epilepsia* 31 (3): 239–246.

Maretto, Silvia, Michelangelo Cordenonsi, Sirio Dupont, Paola Braghetta, Vania Broccoli, A Bassim Hassan, Dino Volpin, Giorgio M Bressan, and Stefano Piccolo. 2003. “Mapping Wnt/Beta-Catenin Signaling During Mouse Development and in Colorectal Tumors..” *Proceedings of the National Academy of Sciences of the United States of America* 100 (6) (March 18): 3299–3304. doi:10.1073/pnas.0434590100.

Marigo, V, RL Johnson, A Vortkamp, and CJ Tabin. 1996. “Sonic Hedgehog Differentially Regulates Expression of GLI and GLI3 During Limb Development.” *Dev. Biol* 180 (1): 273–283.

Martin, J L, A L Brown, and A Balkowiec. 2012. “Glia Determine the Course of Brain-Derived Neurotrophic Factor-Mediated Dendritogenesis and Provide a Soluble Inhibitory Cue to Dendritic Growth in the Brainstem.” *Neuroscience* 207 (April): 333–346. doi:10.1016/j.neuroscience.2012.01.013.

Martinez, S, P H Crossley, I Cobos, J L Rubenstein, and G R Martin. 1999. “FGF8 Induces Formation of an Ectopic Isthmic Organizer and Isthmocerebellar Development via a Repressive Effect on Otx2 Expression..” *Development* 126 (6) (March): 1189–1200.

Martínez-Lozada, Zila, Alain M Guillem, Marco Flores-Méndez, Luisa C Hernández-Kelly, Carmelita Vela, Enrique Meza, Rossana C Zepeda, Mario Caba, Angelina Rodríguez, and Arturo Ortega. 2013. “GLAST/EAAT1-Induced Glutamine Release via SNAT3 in Bergmann Glial Cells: Evidence of a Functional and Physical Coupling.” *Journal of Neurochemistry* 125 (4) (March 11): 545–554. doi:10.1111/jnc.12211.

McMahon, Andrew P, and Allan Bradley. 1990. “The Wnt-1 (Int-1) Proto-Oncogene Is Required for Development of a Large Region of the Mouse Brain.” *Cell* 62 (6): 1073–1085.

Meli, Massimiliano, Marzia Pennati, Maria Curto, Maria Grazia Daidone, Janet Plescia, Sam Toba, Dario C Altieri, Nadia Zaffaroni, and Giorgio Colombo. 2006. “Small-Molecule Targeting of Heat Shock Protein 90 Chaperone Function: Rational Identification of a New Anticancer Lead.” *Journal of Medicinal Chemistry* 49 (26) (December): 7721–7730. doi:10.1021/jm060836y.

Metcalfe, C, and F J de Sauvage. 2011. “Hedgehog Fights Back: Mechanisms of Acquired Resistance Against Smoothened Antagonists.” *Cancer Research* 71 (15) (July 28): 5057–5061. doi:10.1158/0008-5472.CAN-11-0923.

Miller-Moslin, Karen, Stefan Peukert, Rishi K Jain, Michael A McEwan, Rajesh Karki, Luis Llamas, Naeem Yusuff, et al. 2009. “1-Amino-4-Benzylphthalazines as Orally Bioavailable Smoothened Antagonists with Antitumor Activity.” *Journal of Medicinal Chemistry* 52 (13) (July 9): 3954–3968. doi:10.1021/jm900309j.

Millet, S, E Bloch-Gallego, A Simeone, and R M Alvarado-Mallart. 1996. “The Caudal Limit of Otx2 Gene Expression as a Marker of the Midbrain/Hindbrain Boundary: a Study Using in Situ Hybridisation and Chick/Quail Homotopic Grafts..” *Development* 122 (12) (December): 3785–3797.

Millonig, J.H., K J Millen, and M E Hatten. 2000. “The Mouse Dreher Gene Lmx1a Controls Formation of the Roof Plate in the Vertebrate CNS.” *Nature* 403 (6771): 764–769.

Miyata, T, K Nakajima, J Aruga, S Takahashi, K Ikenaka, K Mikoshiba, and M Ogawa. 1996. “Distribution of a Reeler Gene-Related Antigen in the Developing Cerebellum: an Immunohistochemical Study with an Allogeneic Antibody CR-50 on Normal and Reeler Mice..” *The Journal of Comparative Neurology* 372 (2) (August 19): 215–228. doi:10.1002/(SICI)1096-9861(19960819)372:2<215::AID-CNE5>3.0.CO;2-6.

Miyata, T, K Nakajima, K Mikoshiba, and M Ogawa. 1997. “Regulation of Purkinje Cell Alignment by Reelin as Revealed with CR-50 Antibody..” *The Journal of Neuroscience : the Official Journal of the Society for Neuroscience* 17 (10) (May 15): 3599–3609.

Miyata, Takaki, Yuichi Ono, Mayumi Okamoto, Makoto Masaoka, Akira Sakakibara, Ayano Kawaguchi, Mitsuhiro Hashimoto, and Masaharu Ogawa. 2010. “Migration, Early Axonogenesis, and Reelin-Dependent Layer-Forming Behavior of Early/Posterior-Born Purkinje Cells in the Developing Mouse Lateral Cerebellum..” *Neural Development* 5: 23. doi:10.1186/1749-8104-5-23.

Monuki, E S, F D Porter, and C A Walsh. 2001. “Patterning of the Dorsal Telencephalon and Cerebral Cortex by a Roof Plate-Lhx2 Pathway..” *Neuron* 32 (4) (November 20): 591–604.

Morales, D, and M E Hatten. 2006. “Molecular Markers of Neuronal Progenitors in the Embryonic Cerebellar Anlage.” *Journal of Neuroscience* 26 (47) (November 22): 12226–12236. doi:10.1523/JNEUROSCI.3493-06.2006.

Mori, Tetsuji, Kohichi Tanaka, Annalisa Buffo, Wolfgang Wurst, Ralf Kühn, and Magdalena Götz. 2006. “Inducible Gene Deletion in Astroglia and Radial Glia-a Valuable Tool for Functional and Lineage Analysis.” *Glia* 54 (1) (July): 21–34. doi:10.1002/glia.20350.

Mulhern, R K. 2005. “Neurocognitive Consequences of Risk-Adapted Therapy for Childhood Medulloblastoma.” *Journal of Clinical Oncology* 23 (24) (July 11): 5511–5519. doi:10.1200/JCO.2005.00.703.

Mullor, J L, M Calleja, J Capdevila, and I Guerrero. 1997. “Hedgehog Activity, Independent of Decapentaplegic, Participates in Wing Disc Patterning..”

Development 124 (6) (March): 1227–1237.
Namgaladze, D, M Kemmerer, A von Knethen, and B Brune. 2013. “AICAR Inhibits PPAR During Monocyte Differentiation to Attenuate Inflammatory Responses to Atherogenic Lipids.” *Cardiovascular Research* 98 (3) (May 17): 479–487. doi:10.1093/cvr/cvt073.
Narkar, Vihang A, Michael Downes, Ruth T Yu, Emi Embler, Yong-Xu Wang, Ester Banayo, Maria M Mihaylova, et al. 2008. “AMPK and PPARδ Agonists Are Exercise Mimetics.” *Cell* 134 (3) (August): 405–415. doi:10.1016/j.cell.2008.06.051.
Nishida, H, and S Okabe. 2007. “Direct Astrocytic Contacts Regulate Local Maturation of Dendritic Spines.” *Journal of Neuroscience* 27 (2) (January 10): 331–340. doi:10.1523/JNEUROSCI.4466-06.2007.
Northcott, P A, A Korshunov, H Witt, T Hielscher, C G Eberhart, S Mack, E Bouffet, et al. 2011. “Medulloblastoma Comprises Four Distinct Molecular Variants.” *Journal of Clinical Oncology* 29 (11) (April 7): 1408–1414. doi:10.1200/JCO.2009.27.4324.
Northcott, Paul A, David T W Jones, Marcel Kool, Giles W Robinson, Richard J Gilbertson, Yoon-Jae Cho, Scott L Pomeroy, et al. 2012. “Medulloblastomics: the End of the Beginning.” *Nature Reviews Cancer* 12 (12) (November 23): 818–834. doi:10.1038/nrc3410.
Northcott, Paul A, Thomas Hielscher, Adrian Dubuc, Stephen Mack, David Shih, Marc Remke, Hani Al-Halabi, et al. 2011. “Pediatric and Adult Sonic Hedgehog Medulloblastomas Are Clinically and Molecularly Distinct.” *Acta Neuropathologica* 122 (2) (June 17): 231–240. doi:10.1007/s00401-011-0846-7.
Nozawa, Yoko Inès, Chuwen Lin, and Pao-Tien Chuang. 2013. “Hedgehog Signaling From the Primary Cilium to the Nucleus: an Emerging Picture of Ciliary Localization, Trafficking and Transduction.” *Current Opinion in Genetics & Development* (May). doi:10.1016/j.gde.2013.04.008.
Oberdick, J, K Schilling, R J Smeyne, J G Corbin, C Bocchiaro, and J I Morgan. 1993. “Control of Segment-Like Patterns of Gene Expression in the Mouse Cerebellum..” *Neuron* 10 (6) (June): 1007–1018.
Oomman, Sowmini, Howard Strahlendorf, Janet Dertien, and Jean Strahlendorf. 2006. “Bergmann Glia Utilize Active Caspase-3 for Differentiation.” *Brain Research* 1078 (1) (March): 19–34. doi:10.1016/j.brainres.2006.01.041.
Packer, R J, A Gajjar, G Vezina, L Rorke-Adams, P C Burger, P L Robertson, L Bayer, et al. 2006. “Phase III Study of Craniospinal Radiation Therapy Followed by Adjuvant Chemotherapy for Newly Diagnosed Average-Risk Medulloblastoma.” *Journal of Clinical Oncology* 24 (25) (August 14): 4202–4208. doi:10.1200/JCO.2006.06.4980.
Palma, V, DA Lim, N Dahmane, P Sanchez, TC Brionne, CD Herzberg, Y Gitton, A Carleton, A Alvarez-Buylla, and AR Altaba. 2005. “Sonic Hedgehog Controls Stem Cell Behavior in the Postnatal and Adult Brain.” *Development* 132 (2): 335.
Pan, Yong, Chunyang Brian Bai, Alexandra L Joyner, and Baolin Wang. 2006. “Sonic Hedgehog Signaling Regulates Gli2 Transcriptional Activity by Suppressing Its Processing and Degradation.” *Molecular and Cellular Biology* 26 (9) (May 1): 3365–3377. doi:10.1128/MCB.26.9.3365-3377.2006.
Parathath, S R, L A Mainwaring, A Fernandez-L, D O Campbell, and A M Kenney. 2008. “Insulin Receptor Substrate 1 Is an Effector of Sonic Hedgehog Mitogenic Signaling in Cerebellar Neural Precursors.” *Development* 135 (19) (August 20): 3291–3300. doi:10.1242/dev.022871.
Pascual, O. 2005. “Astrocytic Purinergic Signaling Coordinates Synaptic Networks.” *Science* 310 (5745) (October 7): 113–116. doi:10.1126/science.1116916.
Perea, G, and A Araque. 2007. “Astrocytes Potentiate Transmitter Release at Single

Hippocampal Synapses." *Science* 317 (5841) (August 24): 1083–1086. doi:10.1126/science.1144640.
Petralia, Ronald S, Ya-Xian Wang, Mark P Mattson, and Pamela J Yao. 2011. "Sonic Hedgehog Distribution Within Mature Hippocampal Neurons.." *Communicative & Integrative Biology* 4 (6) (November 1): 775–777. doi:10.4161/cib.4.6.17832.
Peukert, Stefan, and Karen Miller-Moslin. 2010. "Small-Molecule Inhibitors of the Hedgehog Signaling Pathway as Cancer Therapeutics." *ChemMedChem* 5 (4) (April 6): 500–512. doi:10.1002/cmdc.201000011.
Piper, Michael, Lachlan Harris, Guy Barry, Yee Hsieh Evelyn Heng, Celine Plachez, Richard M Gronostajski, and Linda J Richards. 2011. "Nuclear Factor One X Regulates the Development of Multiple Cellular Populations in the Postnatal Cerebellum." *The Journal of Comparative Neurology* 519 (17) (September 27): 3532–3548. doi:10.1002/cne.22721.
Pons, S, JL Trejo, JR Martinez-Morales, and E Marti. 2001. "Vitronectin Regulates Sonic Hedgehog Activity During Cerebellum Development Through CREB Phosphorylation." *Development* 128 (9): 1481.
Porter, J A, K E Young, and P A Beachy. 1996. "Cholesterol Modification of Hedgehog Signaling Proteins in Animal Development.." *Science* 274 (5285) (October 11): 255–259.
Pöschl, Julia, Daniel Grammel, Mario M Dorostkar, Hans A Kretzschmar, and Ulrich Schüller. 2013. "Constitutive Activation of B-Catenin in Neural Progenitors Results in Disrupted Proliferation and Migration of Neurons Within the Central Nervous System." *Developmental Biology* 374 (2) (February): 319–332. doi:10.1016/j.ydbio.2012.12.001.
Procko, Carl, and Shai Shaham. 2010. "Assisted Morphogenesis: Glial Control of Dendrite Shapes." *Current Opinion in Cell Biology* 22 (5) (October): 560–565. doi:10.1016/j.ceb.2010.07.005.
Proffitt, K D, and D M Virshup. 2012. "Precise Regulation of Porcupine Activity Is Required for Physiological Wnt Signaling." *Journal of Biological Chemistry* 287 (41) (October 5): 34167–34178. doi:10.1074/jbc.M112.381970.
Proffitt, K D, B Madan, Z Ke, V Pendharkar, L Ding, M A Lee, R N Hannoush, and D M Virshup. 2013. "Pharmacological Inhibition of the Wnt Acyltransferase PORCN Prevents Growth of WNT-Driven Mammary Cancer." *Cancer Research* 73 (2) (January 16): 502–507. doi:10.1158/0008-5472.CAN-12-2258.
Pugh, Trevor J, Shyamal Dilhan Weeraratne, Tenley C Archer, Daniel A Pomeranz Krummel, Daniel Auclair, James Bochicchio, Mauricio O Carneiro, et al. 2012. "Medulloblastoma Exome Sequencing Uncovers Subtype-Specific Somatic Mutations." *Nature* 488 (7409) (July 22): 106–110. doi:10.1038/nature11329.
Raffel, Russell H Zurawel Cory Allen Robert Wechsler-Reya Matthew P Scott Corey. 2000. "Evidence That Haploinsufficiency of Ptch Leads to Medulloblastoma in Mice." *Genes, Chromosomes and Cancer* 28 (1): 77–81. doi:10.1002/(SICI)1098-2264(200005)28:1<77::AID-GCC9>3.0.CO;2-Y.
Rakic, P. 1971. "Neuron-Glia Relationship During Granule Cell Migration in Developing Cerebellar Cortex. a Golgi and Electronmicroscopic Study in Macacus Rhesus.." *The Journal of Comparative Neurology* 141 (3) (March): 283–312. doi:10.1002/cne.901410303.
Rakic, Pasko. 2003. "Developmental and Evolutionary Adaptations of Cortical Radial Glia.." *Cerebral Cortex (New York, N.Y. : 1991)* 13 (6) (June): 541–549.
Rao, G, CA Pedone, CM Coffin, EC Holland, and DW Fults. 2003. "C-Myc Enhances Sonic Hedgehog-Induced Medulloblastoma Formation From Nestin-Expressing Neural Progenitors in Mice." *Neoplasia (New York, NY)* 5 (3): 198.

Rao, G, CA Pedone, L Del Valle, K Reiss, EC Holland, and DW Fults. 2004. “Sonic Hedgehog and Insulin-Like Growth Factor Signaling Synergize to Induce Medulloblastoma Formation From Nestin-Expressing Neural Progenitors in Mice.” *Oncogene* 23 (36): 6156–6162.

Rattan, R. 2005. “5-Aminoimidazole-4-Carboxamide-1- -D-Ribofuranoside Inhibits Cancer Cell Proliferation in Vitro and in Vivo via AMP-Activated Protein Kinase.” *Journal of Biological Chemistry* 280 (47) (September 23): 39582–39593. doi:10.1074/jbc.M507443200.

Reichenbach, A, A Siegel, M Rickmann, J R Wolff, D Noone, and S R Robinson. 1995. “Distribution of Bergmann Glial Somata and Processes: Implications for Function..” *Journal Für Hirnforschung* 36 (4): 509–517.

Reifenberger, J, M Wolter, RG Weber, M Megahed, T Ruzicka, P Lichter, and G Reifenberger. 1998. “Missense Mutations in SMOH in Sporadic Basal Cell Carcinomas of the Skin and Primitive Neuroectodermal Tumors of the Central Nervous System.” *Cancer Research* 58 (9): 1798.

Ribi, K, C Relly, M A Landolt, F D Alber, E Boltshauser, and M A Grotzer. 2005. “Outcome of Medulloblastoma in Children: Long-Term Complications and Quality of Life.” *Neuropediatrics* 36 (6) (December): 357–365. doi:10.1055/s-2005-872880.

Rios, I, R Alvarez-Rodríguez, E Martí, and S Pons. 2004. “Bmp2 Antagonizes Sonic Hedgehog-Mediated Proliferation of Cerebellar Granule Neurones Through Smad5 Signalling.” *Development* 131 (13): 3159.

Robarge, Kirk D, Shirley A Brunton, Georgette M Castanedo, Yong Cui, Michael S Dina, Richard Goldsmith, Stephen E Gould, et al. 2009. “GDC-0449—a Potent Inhibitor of the Hedgehog Pathway.” *Bioorganic & Medicinal Chemistry Letters* 19 (19) (October): 5576–5581. doi:10.1016/j.bmcl.2009.08.049.

Roberts, W Mark, Edwin C Douglass, Stephen C Peiper, Peter J Houghton, and A Thomas Look. 1989. “Amplification of the Gli Gene in Childhood Sarcomas.” *Cancer Research* 49 (19): 5407–5413.

Robins, S C, I Stewart, D E McNay, V Taylor, C Giachino, M Goetz, J Ninkovic, et al. 2013. “A-Tanycytes of the Adult Hypothalamic Third Ventricle Include Distinct Populations of FGF-Responsive Neural Progenitors.” *Nature Communications* 4 (June 27). doi:10.1038/ncomms3049.

Robinson, Giles, Matthew Parker, Tanya A Kranenburg, Charles Lu, Xiang Chen, Li Ding, Timothy N Phoenix, et al. 2012. “Novel Mutations Target Distinct Subgroups of Medulloblastoma.” *Nature* 488 (7409) (June 20): 43–48. doi:10.1038/nature11213.

Roessler, E, E Belloni, K Gaudenz, P Jay, P Berta, S W Scherer, L C Tsui, and M Muenke. 1996. “Mutations in the Human Sonic Hedgehog Gene Cause Holoprosencephaly..” *Nature Genetics* 14 (3) (November): 357–360. doi:10.1038/ng1196-357.

Rohatgi, R, and MP Scott. 2007. “Patching the Gaps in Hedgehog Signalling.” *Nature Cell Biology* 9 (9): 1005–1009.

Romer, JT, H Kimura, S Magdaleno, K Sasai, C Fuller, H Baines, M Connelly, CF Stewart, S Gould, and LL Rubin. 2004. “Suppression of the Shh Pathway Using a Small Molecule Inhibitor Eliminates Medulloblastoma in Ptc1+/-P53-/-Mice.” *Cancer Cell* 6 (3): 229–240.

Romer, Justyna, and Tom Curran. 2005. “Targeting Medulloblastoma: Small-Molecule Inhibitors of the Sonic Hedgehog Pathway as Potential Cancer Therapeutics.” *Cancer Research* 65 (12) (June 15): 4975. doi:10.1158/0008-5472.CAN-05-0481.

Roper, Randall J, Laura L Baxter, Nidhi G Saran, Donna K Klinedinst, Philip A Beachy, and Roger H Reeves. 2006. “Defective Cerebellar Response to Mitogenic Hedgehog Signaling in Down [Corrected] Syndrome Mice..” *Proceedings of the National*

Academy of Sciences of the United States of America 103 (5) (January 31): 1452–1456. doi:10.1073/pnas.0510750103.

Roussel, Martine F, and Mary E Hatten. 2011. “Cerebellum Development and Medulloblastoma..” *Current Topics in Developmental Biology* 94: 235–282. doi:10.1016/B978-0-12-380916-2.00008-5.

Rudin, C M. 2012. “Vismodegib.” *Clinical Cancer Research* 18 (12) (June 14): 3218–3222. doi:10.1158/1078-0432.CCR-12-0568.

Rudin, Charles M, Christine L Hann, John Laterra, Robert L Yauch, Christopher A Callahan, Ling Fu, Thomas Holcomb, et al. 2009. “Treatment of Medulloblastoma with Hedgehog Pathway Inhibitor GDC-0449.” *The New England Journal of Medicine* 361 (12) (September 17): 1173–1178. doi:10.1056/NEJMoa0902903.

Ruiz i Altaba, A. 1998. “Combinatorial Gli Gene Function in Floor Plate and Neuronal Inductions by Sonic Hedgehog..” *Development* 125 (12) (June): 2203–2212.

Ryan, K E, and C Chiang. 2012. “Hedgehog Secretion and Signal Transduction in Vertebrates.” *Journal of Biological Chemistry* 287 (22) (May 25): 17905–17913. doi:10.1074/jbc.R112.356006.

Santidrian, A F, D M Gonzalez-Girones, D Iglesias-Serret, L Coll-Mulet, A M Cosialls, M de Frias, C Campas, et al. 2010. “AICAR Induces Apoptosis Independently of AMPK and P53 Through Up-Regulation of the BH3-Only Proteins BIM and NOXA in Chronic Lymphocytic Leukemia Cells.” *Blood* 116 (16) (October 21): 3023–3032. doi:10.1182/blood-2010-05-283960.

Sarnat, H B, and H Alcalá. 1980. “Human Cerebellar Hypoplasia: a Syndrome of Diverse Causes..” *Archives of Neurology* 37 (5) (May): 300–305.

Sasaki, Nobunari, Junko Kurisu, and Mineko Kengaku. 2010. “Sonic Hedgehog Signaling Regulates Actin Cytoskeleton via Tiam1–Rac1 Cascade During Spine Formation.” *Molecular and Cellular Neuroscience* 45 (4) (December): 335–344. doi:10.1016/j.mcn.2010.07.006.

Scales, Suzie J, and Frederic J de Sauvage. 2009. “Mechanisms of Hedgehog Pathway Activation in Cancer and Implications for Therapy.” *Trends in Pharmacological Sciences* 30 (6) (June): 303–312. doi:10.1016/j.tips.2009.03.007.

Schiffmann, S N, B Bernier, and A M Goffinet. 1997. “Reelin mRNA Expression During Mouse Brain Development..” *The European Journal of Neuroscience* 9 (5) (May): 1055–1071.

Schilling, K, M H Dickinson, J A Connor, and J I Morgan. 1991. “Electrical Activity in Cerebellar Cultures Determines Purkinje Cell Dendritic Growth Patterns..” *Neuron* 7 (6) (December): 891–902.

Schmahmann, J D, J Doyon, D McDonald, C Holmes, K Lavoie, A S Hurwitz, N Kabani, A Toga, A Evans, and M Petrides. 1999. “Three-Dimensional MRI Atlas of the Human Cerebellum in Proportional Stereotaxic Space..” *NeuroImage* 10 (3 Pt 1) (September): 233–260. doi:10.1006/nimg.1999.0459.

Schüller, U, M Ruiter, J Herms, and H Kretzschmar. 2008. “Absence of Mutations in the AKT1 Oncogene in Glioblastomas and Medulloblastomas.” *Acta* ….

Schüller, U, VM Heine, J Mao, AT Kho, AK Dillon, YG Han, E Huillard, T Sun, AH Ligon, and Y Qian. 2008. “Acquisition of Granule Neuron Precursor Identity Is a Critical Determinant of Progenitor Cell Competence to Form Shh-Induced Medulloblastoma.” *Cancer Cell* 14 (2): 123–134.

Selvadurai, Hayden J, and John O Mason. 2011. “Wnt/B-Catenin Signalling Is Active in a Highly Dynamic Pattern During Development of the Mouse Cerebellum.” Edited by Cara Gottardi. *PLoS ONE* 6 (8) (August 8): e23012. doi:10.1371/journal.pone.0023012.g006.

Sengupta, Tapas K, Gilles M Leclerc, Ting Hsieh-Kinser, Guy J Leclerc, Inderjit Singh,

and Julio C Barredo. 2007. “Cytotoxic Effect of 5-Aminoimidazole-4-Carboxamide-1-B-4-Ribofuranoside (AICAR) on Childhood Acute Lymphoblastic Leukemia (ALL) Cells: Implication for Targeted Therapy.” *Molecular Cancer* 6 (1): 46. doi:10.1186/1476-4598-6-46.

Sgaier, Sema K, Sandrine Millet, Melissa P Villanueva, Frada Berenshteyn, Christian Song, and Alexandra L Joyner. 2005. “Morphogenetic and Cellular Movements That Shape the Mouse Cerebellum.” *Neuron* 45 (1) (January): 27–40. doi:10.1016/j.neuron.2004.12.021.

Shiga, T, M Ichikawa, and Y Hirata. 1983. “A Golgi Study of Bergmann Glial Cells in Developing Rat Cerebellum..” *Anatomy and Embryology* 167 (2): 191–201.

Shimada, A, C A Mason, and M E Morrison. 1998. “TrkB Signaling Modulates Spine Density and Morphology Independent of Dendrite Structure in Cultured Neonatal Purkinje Cells..” *The Journal of Neuroscience : the Official Journal of the Society for Neuroscience* 18 (21) (November 1): 8559–8570.

Siegelin, Markus D. 2013. “Inhibition of the Mitochondrial Hsp90 Chaperone Network: a Novel, Efficient Treatment Strategy for Cancer?.” *Cancer Letters* 333 (2) (June): 133–146. doi:10.1016/j.canlet.2013.01.045.

Sievers, J, and F W Pehlemann. 1986. “Influences of Meningeal Cells on Brain Development. Findings and Hypothesis..” *Die Naturwissenschaften* 73 (4) (April): 188–194.

Sievers, J, U Mangold, M Berry, C Allen, and H G Schlossberger. 1981. “Experimental Studies on Cerebellar Foliation. I. a Qualitative Morphological Analysis of Cerebellar Fissuration Defects After Neonatal Treatment with 6-OHDA in the Rat..” *The Journal of Comparative Neurology* 203 (4) (December 20): 751–769. doi:10.1002/cne.902030412.

Silbereis, John, Tristan Heintz, Mary Morgan Taylor, Yosif Ganat, Laura R Ment, Angelique Bordey, and Flora Vaccarino. 2010. “Astroglial Cells in the External Granular Layer Are Precursors of Cerebellar Granule Neurons in Neonates.” *Molecular and Cellular Neuroscience* (May 19): 1–12. doi:10.1016/j.mcn.2010.05.001.

Sillitoe, Roy V, and Alexandra L Joyner. 2007. “Morphology, Molecular Codes, and Circuitry Produce the Three-Dimensional Complexity of the Cerebellum..” *Annual Review of Cell and Developmental Biology* 23: 549–577. doi:10.1146/annurev.cellbio.23.090506.123237.

Sommer, I, C Lagenaur, and M Schachner. 1981. “Recognition of Bergmann Glial and Ependymal Cells in the Mouse Nervous System by Monoclonal Antibody..” *The Journal of Cell Biology* 90 (2) (August): 448–458.

Song, X M, M Fiedler, D Galuska, J W Ryder, M Fernström, A V Chibalin, H Wallberg-Henriksson, and J R Zierath. 2002. “5-Aminoimidazole-4-Carboxamide Ribonucleoside Treatment Improves Glucose Homeostasis in Insulin-Resistant Diabetic (Ob/Ob) Mice.” *Diabetologia* 45 (1): 56–65.

Soriano, P. 1999. “Generalized lacZ Expression with the ROSA26 Cre Reporter Strain..” *Nature Genetics* 21 (1) (January): 70–71. doi:10.1038/5007.

Sotelo, C, and I Dusart. 2009. “Intrinsic Versus Extrinsic Determinants During the Development of Purkinje Cell Dendrites.” *Neuroscience* 162 (3) (September): 589–600. doi:10.1016/j.neuroscience.2008.12.035.

Srinivas, S, T Watanabe, C S Lin, C M William, Y Tanabe, T M Jessell, and F Costantini. 2001. “Cre Reporter Strains Produced by Targeted Insertion of EYFP and ECFP Into the ROSA26 Locus..” *BMC Developmental Biology* 1: 4.

Sriwijitkamol, Apiradee, and Nicolas Musi. 2008a. “Advances in the Development of AMPK-Activating Compounds.” doi:10.1517/17460440802365193.

Sriwijitkamol, Apiradee, and Nicolas Musi. 2008b. “Advances in the Development of AMPK-Activating Compounds..” *Expert Opinion on Drug Discovery* 3 (10) (October): 1167–1176. doi:10.1517/17460441.3.10.1167.

Su, R Y, Y Chao, T Y Chen, D Y Huang, and W W Lin. 2007. “5-Aminoimidazole-4-Carboxamide Riboside Sensitizes TRAIL- and TNF -Induced Cytotoxicity in Colon Cancer Cells Through AMP-Activated Protein Kinase Signaling.” *Molecular Cancer Therapeutics* 6 (5) (May 1): 1562–1571. doi:10.1158/1535-7163.MCT-06-0800.

Sudarov, Anamaria, and Alexandra L Joyner. 2007. “Cerebellum Morphogenesis: the Foliation Pattern Is Orchestrated by Multi-Cellular Anchoring Centers..” *Neural Development* 2: 26. doi:10.1186/1749-8104-2-26.

Sullivan, Jane E, Katy J Brocklehurst, Anna E Marley, Frank Carey, David Carling, and Raj K Beri. 1994. “Inhibition of Lipolysis and Lipogenesis in Isolated Rat Adipocytes with AICAR, a Cell-Permeable Activator of AMP-Activated Protein Kinase.” *FEBS Letters* 353 (1): 33–36.

Surzenko, N, T Crowl, A Bachleda, L Langer, and L Pevny. 2013. “SOX2 Maintains the Quiescent Progenitor Cell State of Postnatal Retinal Muller Glia.” *Development* 140 (7) (March 12): 1445–1456. doi:10.1242/dev.071878.

Sutter, R, O Shakhova, H Bhagat, H Behesti, C Sutter, S Penkar, A Santuccione, et al. 2010. “Cerebellar Stem Cells Act as Medulloblastoma-Initiating Cells in a Mouse Model and a Neural Stem Cell Signature Characterizes a Subset of Human Medulloblastomas.” *Oncogene* 29 (12) (January 11): 1845–1856. doi:10.1038/onc.2009.472.

Svärd, Jessica, Karin Heby Henricson, Madelen Persson-Lek, Björn Rozell, Matthias Lauth, Asa Bergström, Johan Ericson, Rune Toftgård, and Stephan Teglund. 2006. “Genetic Elimination of Suppressor of Fused Reveals an Essential Repressor Function in the Mammalian Hedgehog Signaling Pathway.” *Developmental Cell* 10 (2) (February): 187–197. doi:10.1016/j.devcel.2005.12.013.

Swinnen, Johannes V, Annelies Beckers, Koen Brusselmans, Sophie Organe, Joanna Segers, Leen Timmermans, Frank Vanderhoydonc, et al. 2005. “Mimicry of a Cellular Low Energy Status Blocks Tumor Cell Anabolism and Suppresses the Malignant Phenotype..” *Cancer Research* 65 (6) (March 15): 2441–2448. doi:10.1158/0008-5472.CAN-04-3025.

Taipale, J, M K Cooper, T Maiti, and P A Beachy. 2002. “Patched Acts Catalytically to Suppress the Activity of Smoothened.” *Nature* 418 (6900) (August 22): 892. doi:doi:10.1038/nature00989.

Tallman, Martin S, Chadi Nabhan, James H Feusner, and Jacob M Rowe. 2002. “Acute Promyelocytic Leukemia: Evolving Therapeutic Strategies.” *Blood* 99 (3): 759–767.

Tam, Emily W Y. 2013. “Potential Mechanisms of Cerebellar Hypoplasia in Prematurity.” *Neuroradiology* (July 11). doi:10.1007/s00234-013-1230-1.

Taylor, David M, Miranda L Tradewell, Sandra Minotti, and Heather D Durham. 2007. “Characterizing the Role of Hsp90 in Production of Heat Shock Proteins in Motor Neurons Reveals a Suppressive Effect of Wild-Type Hsf1..” *Cell Stress & Chaperones* 12 (2): 151–162.

Taylor, Michael D, Paul A Northcott, Andrey Korshunov, Marc Remke, Yoon-Jae Cho, Steven C Clifford, Charles G Eberhart, et al. 2011. “Molecular Subgroups of Medulloblastoma: the Current Consensus.” *Acta Neuropathologica* (December 2). doi:10.1007/s00401-011-0922-z.

Teglund, Stephan, and Rune Toftgård. 2010. “Hedgehog Beyond Medulloblastoma and Basal Cell Carcinoma.” *Biochimica Et Biophysica Acta (BBA) - Reviews on Cancer* 1805 (2) (April): 181–208. doi:10.1016/j.bbcan.2010.01.003.

Theodoropoulou, S, P E Kolovou, Y Morizane, M Kayama, F Nicolaou, J W Miller, E

Gragoudas, B R Ksander, and D G Vavvas. 2010. “Retinoblastoma Cells Are Inhibited by Aminoimidazole Carboxamide Ribonucleotide (AICAR) Partially Through Activation of AMP-Dependent Kinase.” *The FASEB Journal* 24 (8) (August 1): 2620–2630. doi:10.1096/fj.09-152546.

Theodoropoulou, Sofia, Katarzyna Brodowska, Maki Kayama, Yuki Morizane, Joan W Miller, Evangelos S Gragoudas, and Demetrios G Vavvas. 2013. “Aminoimidazole Carboxamide Ribonucleotide (AICAR) Inhibits the Growth of Retinoblastoma in Vivo by Decreasing Angiogenesis and Inducing Apoptosis.” Edited by Rakesh K Srivastava. *PLoS ONE* 8 (1) (January 3): e52852. doi:10.1371/journal.pone.0052852.g006.

Thibert, C, MA Teillet, F Lapointe, L Mazelin, NM Le Douarin, and P Mehlen. 2003. “Inhibition of Neuroepithelial Patched-Induced Apoptosis by Sonic Hedgehog.” *Science* 301 (5634) (August 8): 843–846. doi:10.1126/science.1085405.

Thomas, W D, J Chen, Y R Gao, B Cheung, J Koach, E Sekyere, M D Norris, et al. 2009. “Patched1 Deletion Increases N-Myc Protein Stability as a Mechanism of Medulloblastoma Initiation and Progression.” *Oncogene* 28 (13) (February 23): 1605–1615. doi:10.1038/onc.2009.3.

Thompson, Margaret C, Christine Fuller, Twala L Hogg, James Dalton, David Finkelstein, Ching C Lau, Murali Chintagumpala, et al. 2006. “Genomics Identifies Medulloblastoma Subgroups That Are Enriched for Specific Genetic Alterations..” *Journal of Clinical Oncology* 24 (12) (April 20): 1924–1931. doi:10.1200/JCO.2005.04.4974.

Towler, M C, and D G Hardie. 2007. “AMP-Activated Protein Kinase in Metabolic Control and Insulin Signaling.” *Circulation Research* 100 (3) (February 16): 328–341. doi:10.1161/01.RES.0000256090.42690.05.

Traiffort, E, D Charytoniuk, L Watroba, H Faure, N Sales, and M Ruat. 1999. “Discrete Localizations of Hedgehog Signalling Components in the Developing and Adult Rat Nervous System..” *The European Journal of Neuroscience* 11 (9) (September): 3199–3214.

Traiffort, Elisabeth, Elodie Angot, and Martial Ruat. 2010. “Sonic Hedgehog Signaling in the Mammalian Brain.” *Journal of Neurochemistry* 113 (3) (May 1): 576–590. doi:10.1111/j.1471-4159.2010.06642.x.

Tremblay, Martin R, André Lescarbeau, Michael J Grogan, Eddy Tan, Grace Lin, Brian C Austad, Lin-Chen Yu, et al. 2009. “Discovery of a Potent and Orally Active Hedgehog Pathway Antagonist (IPI-926).” *Journal of Medicinal Chemistry* 52 (14) (July 23): 4400–4418. doi:10.1021/jm900305z.

Tukachinsky, H, L V Lopez, and A Salic. 2010. “A Mechanism for Vertebrate Hedgehog Signaling: Recruitment to Cilia and Dissociation of SuFu-Gli Protein Complexes.” *The Journal of Cell Biology* 191 (2) (October 18): 415–428. doi:10.1083/jcb.201004108.

Varjosalo, M, and J Taipale. 2008. “Hedgehog: Functions and Mechanisms.” *Genes & Development* 22 (18): 2454.

Velasquez, D A, G Martinez, A Romero, M J Vazquez, K D Boit, I G Dopeso-Reyes, M Lopez, A Vidal, R Nogueiras, and C Dieguez. 2011. “The Central Sirtuin 1/P53 Pathway Is Essential for the Orexigenic Action of Ghrelin.” *Diabetes* 60 (4) (March 29): 1177–1185. doi:10.2337/db10-0802.

Verbich, David, George A Prenosil, Philip K Y Chang, Keith K Murai, and R Anne McKinney. 2012. “Glial Glutamate Transport Modulates Dendritic Spine Head Protrusions in the Hippocampus.” *Glia* 60 (7) (April 4): 1067–1077. doi:10.1002/glia.22335.

Vernadakis, A. 1988. “Neuron-Glia Interrelations..” *International Review of Neurobiology*

30: 149–224.
Vila, G. 2004. “Sonic Hedgehog Regulates CRH Signal Transduction in the Adult Pituitary.” *The FASEB Journal* (November 15). doi:10.1096/fj.04-2138fje.
Vila, G. 2005. “Expression and Function of Sonic Hedgehog Pathway Components in Pituitary Adenomas: Evidence for a Direct Role in Hormone Secretion and Cell Proliferation.” *Journal of Clinical Endocrinology & Metabolism* 90 (12) (December 1): 6687–6694. doi:10.1210/jc.2005-1014.
Vincent, M F, F Bontemps, and G Van den Berghe. 1992. “Inhibition of Glycolysis by 5-Amino-4-Imidazolecarboxamide Riboside in Isolated Rat Hepatocytes..” *The Biochemical Journal* 281: 267–272.
Vogel, MW, K Sunter, and K Herrup. 1989. “Numerical Matching Between Granule and Purkinje Cells in Lurcher Chimeric Mice: a Hypothesis for the Trophic Rescue of Granule Cells From Target-Related Cell Death.” *Journal of Neuroscience* 9 (10) (October 1): 3454.
Wallace, VA. 1999. “Purkinje-Cell-Derived Sonic Hedgehog Regulates Granule Neuron Precursor Cell Proliferation in the Developing Mouse Cerebellum.” *Current Biology* 9 (8): 445–448.
Wang, C, Y Pan, and B Wang. 2010. “Suppressor of Fused and Spop Regulate the Stability, Processing and Function of Gli2 and Gli3 Full-Length Activators but Not Their Repressors.” *Development* 137 (12) (May 25): 2001–2009. doi:10.1242/dev.052126.
Wang, Chong, Huixian Wu, Vsevolod Katritch, Gye Won Han, Xi-Ping Huang, Wei Liu, Fai Yiu Siu, Bryan L Roth, Vadim Cherezov, and Raymond C Stevens. 2013. “Structure of the Human Smoothened Receptor Bound to an Antitumour Agent.” *Nature* 497 (7449) (May 1): 338–343. doi:10.1038/nature12167.
Wang, Hsiang-Ming, Sonya Mehta, Rishipal Bansode, Wei Huang, and Kamal D Mehta. 2008. “AICAR Positively Regulate Glycogen Synthase Activity and LDL Receptor Expression Through Raf-1/MEK/P42/44MAPK/p90RSK/GSK-3 Signaling Cascade.” *Biochemical Pharmacology* 75 (2) (January): 457–467. doi:10.1016/j.bcp.2007.08.028.
Wang, Tian-Yun, Zhong-Min Han, Yu-Rong Chai, and Jun-He Zhang. 2010. “A Mini Review of MAR-Binding Proteins.” *Molecular Biology Reports* (February 22). doi:10.1007/s11033-010-0003-8.
Wang, V Y, and H Y Zoghbi. 2001. “Genetic Regulation of Cerebellar Development.” *Nature Reviews Neuroscience* 2 (7) (July 1): 484–491. doi:10.1038/35081558.
Wang, VY, and HY Zoghbi. 2001. “Genetic Regulation of Cerebellar Development.” *Nature Reviews Neuroscience* 2 (7): 484–491.
Wang, VY, MF Rose, and HY Zoghbi. 2005. “Math1 Expression Redefines the Rhombic Lip Derivatives and Reveals Novel Lineages Within the Brainstem and Cerebellum.” *Neuron* 48 (1): 31–43.
Wang, Xiaohong, Tetsuya Imura, Michael V Sofroniew, and Shinji Fushiki. 2011. “Loss of Adenomatous Polyposis Coli in Bergmann Glia Disrupts Their Unique Architecture and Leads to Cell Nonautonomous Neurodegeneration of Cerebellar Purkinje Neurons..” *Glia* 59 (6) (June): 857–868. doi:10.1002/glia.21154.
Wang, Yanshu, Amir Rattner, Yulian Zhou, John Williams, Philip M Smallwood, and Jeremy Nathans. 2012. “Norrin/Frizzled4 Signaling in Retinal Vascular Development and Blood Brain Barrier Plasticity.” *Cell* 151 (6) (December): 1332–1344. doi:10.1016/j.cell.2012.10.042.
Wang, Yu, Lance Davidow, Anthony C Arvanites, Joel Blanchard, Kelvin Lam, Ke Xu, Vatsal Oza, et al. 2012. “Glucocorticoid Compounds Modify Smoothened Localization and Hedgehog Pathway Activity.” *Chemistry & Biology* 19 (8) (August):

972–982. doi:10.1016/j.chembiol.2012.06.012.
Ward, R J, L Lee, K Graham, T Satkunendran, K Yoshikawa, E Ling, L Harper, et al. 2009. “Multipotent CD15+ Cancer Stem Cells in Patched-1-Deficient Mouse Medulloblastoma.” *Cancer Research* 69 (11) (June 1): 4682–4690. doi:10.1158/0008-5472.CAN-09-0342. http://www.mc.vanderbilt.edu/diglib/.
Wechsler-Reya, RJ, and MP Scott. 1999. “Control of Neuronal Precursor Proliferation in the Cerebellum by Sonic Hedgehog.” *Neuron* 22 (1): 103–114.
Wegner, Michael, and C Claus Stolt. 2005. “From Stem Cells to Neurons and Glia: a Soxist's View of Neural Development.” *TRENDS in Neurosciences* 28 (11) (November): 583–588. doi:10.1016/j.tins.2005.08.008.
Weis, Karsten, Sophie Rambaud, Catherine Lavau, Joop Jansen, Teresa Carvalho, Maria Carmo-Fonseca, Angus Lamond, and Anne Dejean. 1994. “Retinoic Acid Regulates Aberrant Nuclear Localization of PML-RARα in Acute Promyelocytic Leukemia Cells.” *Cell* 76 (2): 345–356.
Weller, Mathias, Nike Krautler, Ned Mantei, Ueli Suter, and Verdon Taylor. 2006. “*Jagged1* Ablation Results in Cerebellar Granule Cell Migration Defects and Depletion of Bergmann Glia.” *Developmental Neuroscience* 28 (1-2): 70–80. doi:10.1159/000090754.
Welte, Michael A. 2004. “Bidirectional Transport Along Microtubules.” *Current Biology : CB* 14 (13) (July 13): R525–37. doi:10.1016/j.cub.2004.06.045.
Wetmore, C, DE Eberhart, and T Curran. 2001. “Loss of P53 but Not ARF Accelerates Medulloblastoma in Mice Heterozygous for Patched.” *Cancer Research* 61 (2): 513.
Wilson, C W, and P-T Chuang. 2010. “Mechanism and Evolution of Cytosolic Hedgehog Signal Transduction.” *Development* 137 (13) (July 1): 2079–2094. doi:10.1242/dev.045021.
Wingate, R J, and M E Hatten. 1999. “The Role of the Rhombic Lip in Avian Cerebellum Development..” *Development* 126 (20) (October): 4395–4404.
Wingate, Richard JT. 2001. “The Rhombic Lip and Early Cerebellar Development.” *Current Opinion in Neurobiology* 11 (1): 82–88.
Woods, A. 2003. “Identification of Phosphorylation Sites in AMP-Activated Protein Kinase (AMPK) for Upstream AMPK Kinases and Study of Their Roles by Site-Directed Mutagenesis.” *Journal of Biological Chemistry* 278 (31) (June 4): 28434–28442. doi:10.1074/jbc.M303946200.
Xie, J, M Murone, S M Luoh, A Ryan, Q Gu, C Zhang, J M Bonifas, et al. 1998. “Activating Smoothened Mutations in Sporadic Basal-Cell Carcinoma.” *Nature* 391 (6662): 90–92. doi:10.1038/34201.
Yalcin, Abdullah, Sucheta Telang, Brian Clem, and Jason Chesney. 2009. “Regulation of Glucose Metabolism by 6-Phosphofructo-2-Kinase/Fructose-2,6-Bisphosphatases in Cancer.” *Experimental and Molecular Pathology* 86 (3) (June): 174–179. doi:10.1016/j.yexmp.2009.01.003.
Yam, Patricia T, Sébastien D Langlois, Steves Morin, and Frédéric Charron. 2009. “Sonic Hedgehog Guides Axons Through a Noncanonical, Src-Family-Kinase-Dependent Signaling Pathway.” *Neuron* 62 (3) (May 14): 349–362. doi:10.1016/j.neuron.2009.03.022.
Yamada, K, M Fukaya, T Shibata, H Kurihara, K Tanaka, Y Inoue, and M Watanabe. 2000. “Dynamic Transformation of Bergmann Glial Fibers Proceeds in Correlation with Dendritic Outgrowth and Synapse Formation of Cerebellar Purkinje Cells..” *The Journal of Comparative Neurology* 418 (1) (February 28): 106–120. doi:10.1002/(SICI)1096-9861(20000228)418:1<106::AID-CNE8>3.0.CO;2-N/asset/8_ftp.pdf?v=1&t=h968d4qo&s=33a3e210756ae9bcd89a4e2e0b1af794908c861f.

Yang, Xiaoming, Qian Shi, Chin-Yu Lai, Chi-Yuan Chen, Emika Ohkoshi, Shuenn-Chen Yang, Chih-Ya Wang, et al. 2012. “Antitumor Agents 295. E-Ring Hydroxylated Antofine and Cryptopleurine Analogues as Antiproliferative Agents: Design, Synthesis, and Mechanistic Studies.” *Journal of Medicinal Chemistry* (July 23): 120723110137001. doi:10.1021/jm3001218.

Yang, ZJ, T Ellis, SL Markant, TA Read, JD Kessler, M Bourboulas, U Schüller, R Machold, G Fishell, and DH Rowitch. 2008. “Medulloblastoma Can Be Initiated by Deletion of Patched in Lineage-Restricted Progenitors or Stem Cells.” *Cancer Cell* 14 (2): 135–145.

Yauch, R L, G J P Dijkgraaf, B Alicke, T Januario, C P Ahn, T Holcomb, K Pujara, et al. 2012. “Smoothened Mutation Confers Resistance to a Hedgehog Pathway Inhibitor in Medulloblastoma.” *The Journal of Cell Biology* 199 (5952) (October 15): 193–197. doi:10.1126/science.1179386. http://www.sciencemag.org/cgi/doi/10.1126/science.1179386.

Yoshimura, Kentaro, Toyoko Kawate, and Sen Takeda. 2010. “Signaling Through the Primary Cilium Affects Glial Cell Survival Under a Stressed Environment.” *Glia* 59 (2) (December 1): 333–344. doi:10.1002/glia.21105.

Yu, T, Y Yaguchi, D Echevarria, S Martinez, and M A Basson. 2011. “Sprouty Genes Prevent Excessive FGF Signalling in Multiple Cell Types Throughout Development of the Cerebellum.” *Development* 138 (14) (June 21): 2957–2968. doi:10.1242/dev.063784.

Yuasa, S. 1996. “Bergmann Glial Development in the Mouse Cerebellum as Revealed by Tenascin Expression..” *Anatomy and Embryology* 194 (3) (September): 223–234.

Yuasa, S, K Kawamura, K Ono, T Yamakuni, and Y Takahashi. 1991. “Development and Migration of Purkinje Cells in the Mouse Cerebellar Primordium..” *Anatomy and Embryology* 184 (3): 195–212.

Yue, Q. 2005. “PTEN Deletion in Bergmann Glia Leads to Premature Differentiation and Affects Laminar Organization.” *Development* 132 (14) (July 15): 3281–3291. doi:10.1242/dev.01891.

Yun, J S, J M Rust, T Ishimaru, and E Diaz. 2007. “A Novel Role of the Mad Family Member Mad3 in Cerebellar Granule Neuron Precursor Proliferation.” *Molecular and Cellular Biology* 27 (23) (November 13): 8178–8189. doi:10.1128/MCB.00656-06.

Zang, Y, L F Yu, T Pang, L P Fang, X Feng, T Q Wen, F J Nan, L Y Feng, and J Li. 2008. “AICAR Induces Astroglial Differentiation of Neural Stem Cells via Activating the JAK/STAT3 Pathway Independently of AMP-Activated Protein Kinase.” *Journal of Biological Chemistry* 283 (10) (January 7): 6201–6208. doi:10.1074/jbc.M708619200.

Zecca, M, K Basler, and G Struhl. 1995. “Sequential Organizing Activities of Engrailed, Hedgehog and Decapentaplegic in the Drosophila Wing..” *Development* 121 (8) (August): 2265–2278.

Zeng, Huiqing, Jinping Jia, and Aimin Liu. 2010. “Coordinated Translocation of Mammalian Gli Proteins and Suppressor of Fused to the Primary Cilium.” Edited by Rafael Linden. *PLoS ONE* 5 (12) (December 29): e15900. doi:10.1371/journal.pone.0015900.s004.

Zervas, Mark, Sandrine Millet, Sohyun Ahn, and Alexandra L Joyner. 2004. “Cell Behaviors and Genetic Lineages of the Mesencephalon and Rhombomere 1..” *Neuron* 43 (3) (August 5): 345–357. doi:10.1016/j.neuron.2004.07.010.

Zhang, S, C Balch, M W Chan, H C Lai, D Matei, J M Schilder, P S Yan, T H-M Huang, and K P Nephew. 2008. “Identification and Characterization of Ovarian Cancer-Initiating Cells From Primary Human Tumors.” *Cancer Research* 68 (11) (June 1): 4311–4320. doi:10.1158/0008-5472.CAN-08-0364.

Zhang, Yan, Baohua Niu, Dongming Yu, Xiangshu Cheng, Bin Liu, and Jinbo Deng. 2010. “Radial Glial Cells and the Lamination of the Cerebellar Cortex.” *Brain Structure and Function* 215 (2) (September 28): 115–122. doi:10.1007/s00429-010-0278-5.

Zhao, H, O Ayrault, F Zindy, JH Kim, and MF Roussel. 2008. “Post-Transcriptional Down-Regulation of Atoh1/Math1 by Bone Morphogenic Proteins Suppresses Medulloblastoma Development.” *Science's STKE* 22 (6): 722.

Zimmerman, L, B Parr, U Lendahl, M Cunningham, R McKay, B Gavin, J Mann, G Vassileva, and A McMahon. 1994. “Independent Regulatory Elements in the Nestin Gene Direct Transgene Expression to Neural Stem Cells or Muscle Precursors..” *Neuron* 12 (1) (January): 11–24.

Zindy, Frederique, Paul S Knoepfler, Suqing Xie, Charles J Sherr, Robert N Eisenman, and Martine F Roussel. 2006. “N-Myc and the Cyclin-Dependent Kinase Inhibitors p18Ink4c and p27Kip1 Coordinately Regulate Cerebellar Development..” *Proceedings of the National Academy of Sciences of the United States of America* 103 (31) (August 1): 11579–11583. doi:10.1073/pnas.0604727103.

Zwerner, J P, J Joo, K L Warner, L Christensen, S Hu-Lieskovan, T J Triche, and W A May. 2007. “The EWS/FLI1 Oncogenic Transcription Factor Deregulates GLI1.” *Oncogene* 27 (23) (December 17): 3282–3291. doi:10.1038/sj.onc.1210991.